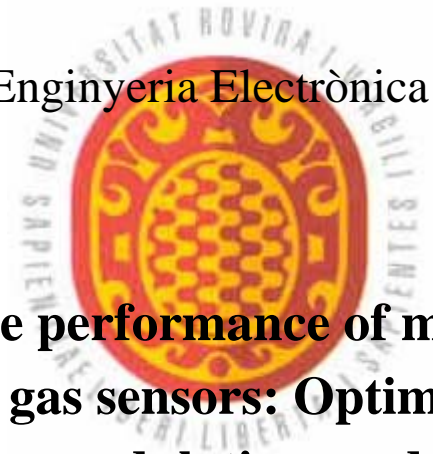




# UNIVERSITAT ROVIRA I VIRGILI

Departament d'Enginyeria Electrònica Elèctrica i  
Automàtica



**Improving the performance of micro-machined  
metal oxide gas sensors: Optimization of the  
temperature modulation mode via pseudo-  
random sequences**

*Doctoral Thesis presented for the qualification of PhD  
by: Alexander Vergara Tinoco*

*Supervisor:  
Dr. Eduard Llobet Valero*

*Date: 25 of July, 2006*

---

UNIVERSITAT ROVIRA I VIRGILI  
IMPROVING THE PERFORMANCE OF MICRO-MACHINED METAL OXIDE GAS SENSORS: OPTIMIZATION OF THE TEMPERATURE MODULATION  
MODE VIA PSEUDORANDOM SEQUENCES.

Alexander Vergara Tinoco

ISN: 978-84-690-7603-3 / DL: T.1219-2007

*Dedicated to*  
*my Parents*  
*Vicente Vergara and Juanita Tinoco*  
*&*  
*my brother and sisters*  
*Berenice, Evelyn and Jaime*

---

UNIVERSITAT ROVIRA I VIRGILI  
IMPROVING THE PERFORMANCE OF MICRO-MACHINED METAL OXIDE GAS SENSORS: OPTIMIZATION OF THE TEMPERATURE MODULATION  
MODE VIA PSEUDORANDOM SEQUENCES.

Alexander Vergara Tinoco

ISN: 978-84-690-7603-3 / DL: T.1219-2007

# CONTENTS

<b>Preface</b>	<b><i>xi</i></b>
<b>Acknowledgements/Agradecimientos.</b>	<b>xii</b>
<b>Abstract.</b>	<b>xv</b>
<b>Resum.</b>	<b>xvii</b>
<b>Resumen.</b>	<b>xix</b>
<b>1. INTRODUCTION.</b>	<b>1</b>
<b>1.1. Introduction.</b>	<b>2</b>
<b>1.2. Thesis Structure.</b>	<b>5</b>
<b>1.3. References.</b>	<b>8</b>
<b>2. STATE OF THE ART</b>	<b>11</b>
<b>2.1. Introduction to the sense of smell.</b>	<b>12</b>
2.1.1. The human olfactory system and odors.	13
2.1.2. The history of electronic noses.	15
2.1.3. Multi-sensors gas analyzer systems.	17
<b>2.2 The selectivity problem of gas sensors.</b>	<b>19</b>
2.2.1. Metal oxide gas sensors.	20
2.2.2. Basic considerations.	23
2.2.3. Developing new materials and technologies.	24
2.2.4. Alternative methods for instrumental analysis of chemical compounds.	28
2.2.5. Pre-treatment methods of gases before sensing.	31
2.2.6. Use of sensor arrays together with techniques of pattern recognition.	33
2.2.7. Use of the dynamic operation mode.	34
<b>2.3. Temperature modulation for selectivity enhancement.</b>	<b>36</b>
<b>2.4. On the optimization of the temperature-modulating signals.</b>	<b>44</b>
2.4.1. Initial methods.	45
2.4.2. Optimization using dynamic models.	45
<b>2.5. Conclusions.</b>	<b>47</b>
<b>2.6. References.</b>	<b>49</b>

<b>3. FEATURE EXTRACTION AND PATTERN RECOGNITION FOR TEMPERATURE-MODULATED GAS SENSORS.</b>	<b>67</b>
<b>3.1. Introduction</b>	<b>68</b>
<b>3.2. Feature extraction methods.</b>	<b>69</b>
3.2.1. Fast Fourier Transform (FFT).	71
3.2.2. Phase space and dynamic moments.	72
<b>3.3. Pattern recognition methods.</b>	<b>73</b>
3.3.1. Principal component analysis (PCA).	75
3.3.2. Partial Least Squares (PLS).	76
3.3.3. Partial Least Squares Discriminant Analysis (PLS-DA).	78
3.3.4. Fuzzy ARTMAP neural network.	78
<b>3.4. Variable selection procedure.</b>	<b>81</b>
<b>3.5. Conclusions.</b>	<b>84</b>
<b>3.6. References.</b>	<b>85</b>
<b>4. GAS/SENSOR SYSTEM IDENTIFICATION</b>	<b>89</b>
<b>4.1. Introduction.</b>	<b>90</b>
<b>4.2. Description of systems: relationship between their input and output.</b>	<b>91</b>
4.2.1. Types of signals.	91
4.2.2. Description of system.	92
<b>4.3. Correlation functions.</b>	<b>94</b>
4.3.1. The correlation function.	95
4.3.2. The Autocorrelation.	96
4.3.3. Cross correlation.	96
<b>4.4. Design and generation of PRBS signals.</b>	<b>97</b>
<b>4.5. Design and generation of MLPRS.</b>	<b>99</b>
<b>4.6. Pseudo Random Sequences (PRS) and systems identification.</b>	<b>102</b>
<b>4.7. Gas/sensor systems identification.</b>	<b>104</b>
<b>4.8. Conclusions.</b>	<b>106</b>
<b>4.9. References.</b>	<b>107</b>

<b>5. EXPERIMENTAL</b>	<b>109</b>
<b>5.1. Introduction.</b>	<b>110</b>
<b>5.2. Fabrication of the micro-hotplate gas sensors used in experiments.</b>	<b>111</b>
5.2.1. Micro-hotplate substrate fabrication.	111
5.2.2. Active layer deposition.	115
<b>5.3. Measurement system layout.</b>	<b>117</b>
<b>5.4. Description of the experiments performed.</b>	<b>123</b>
5.4.1. Experiment 1: PRBS signals to modulate the temperature operation of micro-hotplates gas sensors (preliminary study).	123
5.4.2. Experiment 2: Optimized temperature modulation of micro-hotplate gas sensors using Pseudo Random Binary Sequences (PRBS).	126
5.4.3. Experiment 3: Optimized Temperature Modulation of Metal Oxide Micro-Hotplate Gas Sensors through Multilevel Pseudo Random Sequences.	128
5.4.4. Experiment 4: Qualitative and quantitative gas mixture analysis using temperature-modulated micro-hotplate gas sensors: Selection and validation of the optimal modulating frequencies.	131
<b>5.5. Summary.</b>	<b>134</b>
<b>5.6. References.</b>	<b>136</b>
<b>6. GAS ANALYSIS USING PRBS</b>	<b>139</b>
<b>6.1. Introduction.</b>	<b>140</b>
<b>6.2. Analysis of the data from experiment 1: PRBS signals to modulate the temperature operation of micro-hotplates gas sensors (preliminary study).</b>	<b>141</b>
6.2.1. Estimation of the impulse response.	142
6.2.2. Variable selection procedure.	144
6.2.3. Qualitative and semi-quantitative analysis procedure.	145
<b>6.3. Analysis of the data from experiment 2: Optimized temperature modulation of micro-hotplate gas sensors using Pseudo Random Binary Sequences (PRBS).</b>	<b>147</b>
6.3.1. Steady-state response.	147
6.3.2. Estimation of the impulse response.	148
6.3.3. Variable selection procedure.	151
6.3.4. Qualitative gas analysis.	151
6.3.5. Semi-quantitative gas analysis.	154
<b>6.4. Conclusions.</b>	<b>155</b>
<b>6.5. References.</b>	<b>156</b>

<b>7. GAS ANALYSIS USING MLPRS</b>	<b>157</b>
<b>7.1. Introduction.</b>	<b>159</b>
<b>7.2. Analysis of the data from experiment 3: Optimized Temperature Modulation of Metal Oxide Micro-Hotplate Gas Sensors through Multilevel Pseudo Random Sequences (MLPRS).</b>	<b>160</b>
7.2.1. Estimation of the impulse response and selection of temperature modulating frequencies.	161
7.2.1.1. Estimation of the impulse response.	161
7.2.1.2. Variable selection procedure.	163
7.2.2. Optimization for qualitative gas analysis.	163
7.2.2.1. Identification of the best modulating frequencies.	164
7.2.2.2. Validation of the modulating frequencies.	164
7.2.3. Optimization for quantitative gas analysis.	165
7.2.4. Gas analysis using a sinusoidal temperature modulation.	167
7.2.5. Steady-state response.	170
7.2.6. Gas analysis of metal oxide gas sensors using dynamic moments combined with temperature modulation.	172
7.2.6.1. MLPRS temperature modulation database.	172
7.2.6.2. Multi-sinusoidal modulation database.	175
<b>7.3. Analysis of the data from experiment 4: Qualitative and Quantitative gas mixture analysis using temperature-modulated micro-hotplate gas sensors: Selection and validation of the optimal modulating frequencies.</b>	<b>178</b>
7.3.1. Spectral analysis of the impulse response estimates.	179
7.3.2. Selection of the temperature-modulating frequencies.	181
7.3.3. Optimization for qualitative gas analysis.	181
7.3.4. Optimization for quantitative gas analysis.	184
7.3.5. Gas analysis using multi-sinusoidal temperature modulation.	187
7.3.6. Steady-state response.	193
<b>7.4. Conclusions.</b>	<b>194</b>
<b>7.5. References.</b>	<b>196</b>
<b>8. CONCLUSIONS</b>	<b>197</b>
<b>8.1. Conclusions.</b>	<b>198</b>



<b>9. ANEX: LIST OF PUBLICATIONS</b>	<b>201</b>
<b>9.1. Publications directly derived from this doctoral thesis.</b>	<b>202</b>
<b>9.2. Others related publications.</b>	<b>202</b>
<b>9.3. Conferences.</b>	<b>203</b>
<b>APPENDIX</b>	<b>205</b>
<b>A.1. Introduction.</b>	<b>206</b>
<b>A.2. Continuous flow system: calculating flow values.</b>	<b>206</b>
A.2.1. Example of a calculation.	208
<b>A.3. Electronic board system construction.</b>	<b>209</b>
<b>A.4. Generation algorithm of the modulating signals.</b>	<b>215</b>
A.4.1. Generation algorithm of the PRBS modulating signal.	215
A.4.2. Generation algorithm of the MLPRS modulating signal.	216
A.4.3. Generation code of the multi-sinusoidal modulating signal.	217
<b>A.5. References.</b>	<b>220</b>

UNIVERSITAT ROVIRA I VIRGILI  
IMPROVING THE PERFORMANCE OF MICRO-MACHINED METAL OXIDE GAS SENSORS: OPTIMIZATION OF THE TEMPERATURE MODULATION  
MODE VIA PSEUDORANDOM SEQUENCES.

Alexander Vergara Tinoco

ISN: 978-84-690-7603-3 / DL: T.1219-2007

---

# Preface

---

<i>Preface</i>	<i>xi</i>
<b>Acknowledgements/Agradecimientos.</b>	<b>xii</b>
<b>Abstract.</b>	<b>xv</b>
<b>Resum.</b>	<b>xvii</b>
<b>Resumen.</b>	<b>xix</b>

## Improving the performance of micro-machined metal oxide gas sensors: Optimization of the temperature modulation mode via pseudo-random sequences.

### Acknowledgements/Agradecimientos.

A lo largo de los últimos años he realizado los trabajos de mi tesis doctoral en el Departamento de Ingeniería Electrónica de la Universitat Rovira i Virgili de Tarragona España. En este sitio no solo he formado parte del grupo de microsistemas y nano-tecnología para análisis químicos (MINOS) sino que me he formado e iniciado mis primeros pasos como investigador.

Me gustaría agradecer a todas aquellas personas que han contribuido en la realización de esta tesis Doctoral. En primer lugar quiero agradecer a mi tutor y director de tesis, el Dr. Eduard Llobet Valero, a quien considero un gran ejemplo como profesional, investigador y persona. Le quiero dar las gracias por que siempre me ha brindado su total apoyo, seriedad y responsabilidad; por los conocimientos que me ha transmitido, por los buenos consejos que me ha dado, por la manera especial que ha tenido para dirigir mi tesis doctoral, pero sobre todo por su paciencia y ayuda. Además, le quiero agradecer por las mil y una horas que ha pasado corrigiéndome una y otra vez los escritos que he realizado. De hecho, sin su ayuda esta tesis no habría podido ser escrita. *Moltes gràcies Eduard per haver supervisat les meves primeres passes com a investigador, ha estat un veritable plaer i un honor haver treballat amb tu tots aquests anys.*

Quiero agradecerle al Dr. Jesús Brezmes por los buenos consejos y conocimientos transmitidos, aparte de su ayuda en la realización de mi trabajo durante mi tesis doctoral. Igualmente, agradecer de una manera especial al Dr. Xavier Correig, director de este grupo de investigación, y al Dr. Xavier Vilanova por su ayuda en revisiones de textos y escritos.

Vorrei ringraziare il laboratorio di sensori e microsistemi dell'Università degli studi di Roma "Tor Vergata", dove ho svolto parte del mio lavoro di dottorato. In particolare vorrei ringraziare i professori Corrado Di Natale e Arnaldo D'Amico per avermi offerto la possibilità di lavorare nel loro gruppo ed il Dott. Eugenio Martinelli per i suoi insegnamenti e per la pazienza che ha avuto nei miei riguardi durante la mia permanenza in Italia. Inoltre vorrei ringraziare Emiliano, Sarita ed il loro Mazzoncino Daniele per la loro amicizia ed ospitalità, Andrea Orsini "il Gran Maestro" e la sua famiglia per l'accoglienza e l'affetto che mi hanno dimostrato in questo periodo. Alex Cato "Del Piero" e tutti gli altri amici con i quali abbiamo giocato indimenticabili partite di calcetto e mangiato appetitosi cibi italo-messicani. Ringrazio tutti per avermi fatto sentire come uno del gruppo ed è stato davvero un piacere lavorare con voi. Grazie!!!

Estoy muy agradecido a todas las personas que de algún u otro modo me han ayudado durante el proceso de investigación. En especial al señor Raul Calavia por su amistad además

de su gran ayuda en un sin número de ocasiones en la elaboración de software y circuitería electrónica para el desarrollo de mi trabajo de investigación, así como a los técnicos de la URV.

También quiero dar las gracias a todos mis compañeros y amigos de los laboratorios de la URV que me han apoyado, acompañado y aconsejado durante mi estancia en Tarragona. No voy a nombrarlos a todos, por miedo a dejarme a alguno fuera. Sin embargo quiero detallar algunos momentos especiales que seguro nos habrán marcado mucho y nos dejaran huella para el resto de nuestras vidas. Quiero agradecer a las famosas m&m`s (Mariona & Mariana) por todos los momentos tan especiales que pasamos juntos, esos cafés y conversaciones que hemos compartido, además de esos consejos y regaños que me han dado. A Patineta, por tantas discusiones políticas catalano-españolas y por cambiar mi opinión acerca de los catalanes. *Moltes gràcies per ser tal com ets... simplement Mariona "La Patineta"*. Quiero agradecer también a los otros tres integrantes de la famosa foto "doctores URV Latinoamérica". A Tellita (y tu *Quinua deliciosa*), gracias por tantas y tantas conversaciones durante todo este periodo que compartimos. A Fer, por toda la cocina mexicana que cocinamos juntos para tanta gente y por las cosas que compartimos. A Mauro, por la pizza Italiana y los grandes retos. Gracias a los tres por el tiempo compartido. Gracias a Edgar (y sus patacones), por todo el tiempo que hemos compartido a lo largo del doctorado. Al Dr. Radu "el pijon", quien fue una base e inicio importante en mi tesis. A Edwin "Amigo mío" y esas tardes y fines de semana en la universidad. De manera especial quiero agradecer también a Eliana, con quien he compartido grandes momentos durante este largo y arduo camino del doctorado. *"Vos has sido un gran apoyo para mí, te agradezco todas las enseñanzas que me has transmitido"*. A todos en general les agradezco, ha sido en verdad un placer haber compartido este tiempo de mi vida con todos ustedes.

Por último, pero no por eso menos importante, agradezco y dedico esta tesis doctoral a mis padres Vicente Vergara y Juanita Tinoco, a quien debo lo que soy, mis logros y mis meritos, mis valores, mi dedicación, pero sobre todo la persona que soy. Gracias Papá y Mamá por todo su apoyo. A mis hermanos Berenice, Evelyn y Jaime quienes han sido como unos segundos padres para mí, por todo el apoyo y comprensión que siempre me han brindado. Además, quiero dedicar esta tesis a mis pequeños sobrinos que son motivo de mi alegría, sin olvidar a mis cuñados Martín y Caro quienes también estuvieron presentes en este camino.

Improving the performance of micro-machined metal oxide gas sensors:  
Optimization of the temperature modulation mode via pseudo-random sequences.

Alexander Vergara gratefully acknowledges a pre-doctoral scholarship FI2003 (ref. 1323 U07 E20) from the Autonomous Government of Catalonia. Also my acknowledgements to the Spanish Commission for Science and Technology (CICYT) grant no. TIC2003-06301 and to the Thematic Network in Metabolism and Nutrition ref. C03/08 for funding this work.

I want to express my gratitude to Dr. Isabel Gràcia and Dr. Carles Cané for providing me with the micro-machined substrates and also to Dr. Peter Ivanov and Dr. Mariana Stankova, who deposited the gas-sensitive thick and thin films, respectively. Without this help, the whole PhD thesis would not have been possible.

## Abstract.

One of the major problems in gas sensing systems that use metal oxide devices is the lack of reproducibility, stability and selectivity. In order to tackle these troubles experienced with metal oxide gas sensors, different strategies have been developed in parallel. Some of these are related to the improvement of materials, or the use of sample conditioning and pre-treating methods. Other widely used techniques include taking benefit of the unavoidable partially overlapping sensitivities by using sensor arrays and pattern recognition techniques or the use of dynamic features from the gas sensor response.

In the last years, modulating the working temperature of metal oxide gas sensors has been one of the most used methods to enhance sensor selectivity. This occurs because, since, the sensor response is different at different working temperatures, and therefore, measuring the sensor response at  $n$  different temperatures is, in some cases, similar to the use of an array comprising  $n$  different sensors. This allows for measuring multivariate information from every single sensor and helps in keeping low the dimensionality of the measurement system needed to solve a specific application. Although the good results reported, until now, the selection of the frequencies used to modulate the working temperature remained an empirical process and that is not an accurate method to ensure that the best results are reached for a given application.

In view of this context, the principal objective of this doctoral thesis was to develop a systematic method to determine which are the optimal temperature modulation frequencies to solve a given gas analysis problem. This method, which is borrowed from the field of system identification, has been developed and introduced for the first time in the area of gas sensors. It consists of studying the sensor response to gases when the operating temperature is modulated via maximum-length pseudo-random sequences. Such signals share some properties with white noise and, therefore, can be of help to estimate the linear response of a system with non-linearity (e.g., the impulse response of a sensor-gas system).

The optimization process is conducted by selecting among the spectral components of the impulse response estimates, the few that better help either discriminating or quantifying the target gases of a given gas analysis application. Since spectral components are directly related to modulating frequencies, the selection of spectral components results in the determination of the optimal temperature modulating frequencies.

In the first experiments, pseudo-random binary signals (PRBS) were employed to modulate the working temperature of micro-machined metal oxide gas sensors in a frequency range from 0 up to 112.5 Hz. The upper frequency is slightly higher than the

## Improving the performance of micro-machined metal oxide gas sensors: Optimization of the temperature modulation mode via pseudo-random sequences.

cutoff frequency of the sensor membranes. The outcome of this initial study was that the important modulating frequencies were in the range between 0 and 1 Hz. This is understandable, since the kinetics of reaction and adsorption processes taking place at the sensor surface (i.e., physisorption/chemisorption/ionosorption) are slow and if these are to be altered by the thermal modulation, low frequency modulating signals need to be devised. This explains why low-frequency temperature-modulating signals (i.e. in the mHz range) have been used with micro-hotplate gas sensors, even though the thermal response of their membranes is much faster (typically, near 100 Hz).

In the experiments that followed the first ones, an evolved method to determine the optimal temperature modulating frequencies for micro-hotplate gas sensors was introduced, which was based on the use of maximum length multilevel pseudo-random sequences (MLPRS). Multilevel signals were considered instead of the binary ones because the former can provide a better estimate than the latter of the linear dynamics of a process with non-linearity. And it is well known that temperature-modulated metal oxide gas sensors present non-linearity in their response.

These systematic studies were fully validated by synthesizing multi-sinusoidal signals at the optimal frequencies previously identified using pseudo-random sequences. When the sensors had their operating temperatures modulated by a signal with a frequency content that corresponded to the optimal, the gases and gas mixtures considered could be perfectly discriminated and the building of accurate calibration models to predict gas concentration was found to be possible. In some cases, the validation process was conducted on sensors that had not been used for optimization purposes (e.g. a different sensor array from the same fabrication batch).

Summarizing, the new method developed in this thesis for selecting the optimal modulating frequencies is shown to be consistent and effective. The method applies generally and could be used in any gas analysis problem or extended to other type of sensors (e.g. conducting polymer sensors).

The scientific contributions of this thesis are collected in four journal papers and thirteen conference proceedings.



## Resum.

Un dels majors problemes experimentats pels sistemes de detecció de gasos basats en sensors d'òxids metàl·lics és la seva manca de reproduïbilitat, estabilitat i selectivitat. A fi i a efecte d'intentar resoldre aquest problemes, diferents estratègies han estat desenvolupades en paral·lel. Algunes es relacionen a la millora dels materials i d'altres impliquen el condicionament o el pre-tractament de les mostres. Les més emprades han consistit en aprofitar que els sensors presenten sensibilitats solapades per construir matrius de sensors i emprar tècniques de processament del senyal o bé utilitzar característiques de la resposta dinàmica dels sensors.

En els darrers anys, modular la temperatura de treball del sensors d'òxids metàl·lics s'ha convertit en un dels mètodes més utilitzats per incrementar-ne la selectivitat. Això s'esdevé així donat que la resposta del sensor varia amb la seva temperatura de treball. Per això, en determinats casos, mesurant la resposta d'un sensor a  $n$  temperatures de treball diferents pot ser equivalent a tenir una matriu de  $n$  sensors diferents. Això permet obtenir informació multivariant de cada sensor individualment i ajuda a mantenir baixa la dimensionalitat del sistema de mesura per resoldre una determinada aplicació. Malgrat que molts i bons resultats han estat publicats dins aquest àmbit, la tria de les freqüències emprades en la modulació de la temperatura de treball dels sensor ha consistit fins ara en un procés empíric que no garanteix la obtenció dels millors resultats per una determinada aplicació.

En aquest context, el principal objectiu d'aquesta tesi doctoral ha consistit en desenvolupar un mètode sistemàtic que permeti determinar quines són les freqüències de modulació òptimes que caldria emprar per resoldre un determinat problema d'anàlisi de gasos. Aquest mètode, extret del camp d'identificació de sistemes, ha esta desenvolupat i implementat per primer cop dins l'àmbit dels sensors de gasos. Aquest consisteix en estudiar la resposta dels sensors en presència de gasos mentre la temperatura de treball dels sensors és modulada per un senyal pseudo-aleatori de longitud màxima. Aquest senyals comparteixen algunes propietats amb el soroll blanc, i per tant poden ajudar a estimar la resposta lineal d'un sistema amb no-linealitats (per exemple, la resposta impulsional d'un sistema sensor-gas).

El procés d'optimització es duu a terme mitjançant la selecció entre els components espectrals de les estimacions de la resposta impulsional, d'aquells que millor ajuden bé a discriminar o a quantificar els gasos objectiu dins una aplicació d'anàlisi de gasos donada. Tenint en compte que els components espectrals estan directament relacionats amb les

## Improving the performance of micro-machined metal oxide gas sensors: Optimization of the temperature modulation mode via pseudo-random sequences.

freqüències de modulació, la tria d'uns pocs components espectrals resulta en la determinació de les freqüències òptimes de modulació.

En els primer experiments, senyals binaris pseudo-aleatoris van ser emprats per modular la temperatura de treball de sensors de gasos basats en òxids metàl·lics micro-mecanitzats dins d'un rang comprès entre 0 i 112,5 Hz. La freqüència superior és lleugerament superior a la freqüència de tall de les membranes dels sensors. El resultat principal derivat d'aquest estudi va ser que les freqüències de modulació interessants es trobaven en un rang comprès entre 0 i 1 Hz. Això és comprensible donat que la cinètica de les reaccions i dels processos d'adsorció que es produeixen en la superfície dels sensors són lentes i si aquestes s'han de veure modificades per la modulació tèrmica, llavors caldran senyals de modulació de baixa freqüència. Això explica perquè s'han vingut emprant senyals moduladores de temperatura en el rang dels mHz, malgrat que les membranes d'un dispositiu micromecanitzat presenten respostes tèrmiques molts més ràpides (típicament de l'ordre de 100 Hz).

En els experiments que continuaren els primers, un mètode evolucionat per determinar les freqüències de modulació tèrmica òptimes va ser implementat. Aquest es basa en l'ús de seqüències pseudo-aleatòries multi-nivell de longitud màxima. Els senyals de tipus multi-nivell van ser considerats en substitució dels senyals binaris ja que els primers permeten obtenir una millor estimació que els segons de la dinàmica lineal d'un sistema amb no linealitats. I és ben conegut que els sensors de gasos basats en òxids metàl·lics presenten no linealitat en la seva resposta.

Aquests estudis sistemàtics van ser completament validats mitjançant la síntesi de senyals multi-sinusoidals amb les freqüències prèviament identificades emprant seqüències pseudo-aleatòries. Quan la temperatura de treball dels sensors va ser modulada amb un senyal, el contingut freqüencial del qual era l'òptim, els gasos i les mescles de gasos considerades van poder ser discriminades perfectament i es va mostrar la possibilitat d'obtenir models de calibració acurats per predir la concentració dels gasos. En alguns casos, aquest procés de validació es va portar a terme emprant sensors que no havien estat utilitzats durant el procés d'optimització (per exemple, una agrupació de sensors diferent però del mateix lot de fabricació).

En resum, el nou mètode desenvolupat en aquesta tesi per seleccionar les freqüències de modulació òptimes s'ha mostrat consistent i efectiu. El mètode és d'aplicació general i podria ser emprat en qualsevol problema d'anàlisi de gasos o bé estès a altres tipus de sensors (per exemple sensors polimèrics).

Les contribucions científiques d'aquesta tesi s'han recollit en quatre articles en revistes internacionals i 13 llibres d'actes de conferències.

## Resumen.

Uno de los mayores problemas experimentados en los sistemas de detección de gases basados en dispositivos de óxidos metálicos es su falta de reproducibilidad, estabilidad y selectividad. Con el fin de intentar resolver estos problemas, diferentes estrategias han sido desarrolladas en paralelo. Algunas de ellas se relacionan con la mejora de los materiales y otras implican acondicionamiento o pre-tratamiento de las muestras. Otras estrategias ampliamente empleadas consisten en aprovechar que los sensores presentan sensibilidades solapadas para construir matrices de sensores y emplear técnicas de procesamiento de señal o bien utilizar características de la respuesta dinámica de los sensores.

En los últimos años, modular la temperatura de trabajo de los sensores de óxidos metálicos se ha convertido en uno de los métodos más utilizados para incrementar su selectividad. Esto se debe a, dado que la respuesta del sensor varía con su propia temperatura de trabajo, entonces, en determinados casos, midiendo la respuesta de un sensor a  $n$  temperaturas de trabajo diferentes, es equivalente a tener una matriz de  $n$  sensores diferentes. Esto permite obtener información multivariante de cada sensor individualmente y ayuda a mantener baja la dimensionalidad del sistema de medida para resolver una determinada aplicación. A pesar de los buenos resultados que han sido publicados dentro de este ámbito, la selección de las frecuencias empleadas en la modulación de la temperatura de trabajo de los sensores ha consistido, hasta el momento, en un proceso empírico lo que no garantiza la obtención de los mejores resultados para una determinada aplicación.

En este contexto, el principal objetivo de esta tesis doctoral ha consistido en desarrollar un método sistemático que permita determinar cuales son las frecuencias de modulación óptimas que podrían emplearse para resolver un determinado problema de análisis de gases. Este método, extraído del campo de identificación de sistemas, ha sido desarrollado e implementado por primera vez dentro del ámbito de los sensores de gases. Éste consiste en estudiar la respuesta de los sensores en presencia de gases mientras la temperatura de trabajo de los sensores es modulada mediante una señal pseudo-aleatoria de longitud máxima. Estas señales comparten algunas propiedades con el ruido blanco, y por tanto pueden ayudar a estimar la respuesta lineal de un sistema con no-linealidades (por ejemplo, la respuesta impulsional de un sistema sensor-gas).

El proceso de optimización es llevado a cabo mediante la selección entre las componentes espectrales de las estimaciones de la respuesta impulsional, de aquellas que más ayudan ya sea a discriminar o a cuantificar los gases objetivo dentro de una aplicación de análisis de gases dada. Teniendo en cuenta que las componentes espectrales están directamente

## Improving the performance of micro-machined metal oxide gas sensors: Optimization of the temperature modulation mode via pseudo-random sequences.

relacionadas con las frecuencias de modulación, la selección de unas pocas componentes espectrales resulta en la determinación de las frecuencias óptimas de modulación.

En los primeros experimentos, señales binarias pseudo-aleatorias fueron utilizadas para modular la temperatura de trabajo de los sensores de gases basados en óxidos metálicos micro-mecanizados en un rango comprendido entre 0 a 112.5 Hz. La frecuencia superior es ligeramente mayor a la frecuencia de corte de las membranas de los sensores. El resultado principal derivado de estos estudios fue que las frecuencias de modulación interesantes se encuentran en un rango comprendido entre 0 y 1 Hz. Esto es comprensible dado que la cinética de las reacciones y de los procesos de adsorción que se producen en la superficie del sensor son lentos y si estos se han de alterar mediante la modulación térmica, se habrá de elaborar señales de modulación a bajas frecuencias. Esto explica por que se han venido empleado señales moduladoras de temperatura en el rango de los mHz, a pesar que las membranas de un dispositivo micro-mecanizado presentan respuestas mucho más rápidas (típicamente en el orden de los 100 Hz).

En los experimentos posteriores a los primeros, un método evolucionado para determinar las frecuencias de modulación óptimas de los sensores micro-mecanizados fue implementado, el cual se basa en el uso de secuencias pseudo-aleatorias multi-nivel de longitud máxima (MLPRS). Las señales de tipo multi-nivel fueron consideradas en lugar de las binarias ya que las primeras permiten obtener una mejor estimación que las segundas de la dinámica lineal de un sistema con no linealidades. Y es bien conocido que los sensores de gases basados en óxidos metálicos presentan no-linealidades en su respuesta.

Estos estudios sistemáticos fueron completamente validados mediante la síntesis de señales multi-senoidales con las frecuencias previamente identificadas utilizando secuencias pseudo-aleatorias. Cuando la temperatura de trabajo de los sensores fue modulada por una señal, el contenido frecuencial de la cual es el óptimo, los gases y mezclas de gases considerados pudieron ser discriminados perfectamente y se verificó la posibilidad de obtener modelos de calibración precisos para predecir la concentración de los gases. En algunos casos, estos procesos de validación se llevaron a cabo con sensores que no habían sido utilizados durante el proceso de optimización (por ejemplo, una agrupación de sensores diferentes pero del mismo lote de fabricación).

En resumen, El nuevo método desarrollado in esta tesis para seleccionar las frecuencias de modulación óptimas se a mostrado consistente y efectivo. El método es de aplicación general y podría ser utilizado en cualquier problema de análisis de gases o bien extendido a otro tipo de sensores (por ejemplo sensores poliméricos).

Las contribuciones científicas de esta tesis se han recogido en 4 artículos en revistas internacionales y trece actas de conferencias.

---

# 1.

# Introduction

---

<b>1. INTRODUCTION.</b>	<b>1</b>
<b>1.1. Introduction.</b>	<b>2</b>
<b>1.2. Thesis Structure.</b>	<b>5</b>
<b>1.3. References.</b>	<b>8</b>

## Improving the performance of micro-machined metal oxide gas sensors: Optimization of the temperature modulation mode via pseudo-random sequences.

### 1.1. Introduction.

Human beings have five senses: sight, hearing, touch, taste and smell. These senses are very important because humans act after receiving information from the outside world. The idea to mirror the natural human senses with artificial systems has been a dream of human kind. From this point of view, sensors play an important role in the reproduction/simulation of the five senses or even surpassing them. The sensor is the device that mimics the ability of eye, ear, skin, nose and tongue, in the senses of sight, hearing, touch, smell and taste, respectively.

In the history of sensor development, those corresponding to the receptor parts of sight, hearing and touch, have been developed for many years. By comparison, sensors for simulating the senses of taste and smell have been proposed only recently, in spite of the great demand for these sensors in the food industry and in environmental protection. The sensors for the senses of sight, hearing and touch respond to physical quantities as light, sound waves and pressure (or temperature) respectively and are also called physical sensors. The end target in developing sensors for these parameters may be high sensitivity or selectivity for the physical quantity concerned. On the other hand, many kinds of chemical substances must be assessed at once for smell and taste to be transformed into meaningful quantities to describe these senses. The sensors that play the role of receptors in the senses of smell and taste are the so-called chemical sensors. They are very useful for detecting a specific chemical substance with high selectivity.

In the environment of artificial olfactory system, the big obstacle is how to represent, by understandable mechanisms, the human olfaction system. A key role in this challenge is played by chemical sensors, which have to imitate functional olfactory cells. Figure 1.1 shows a scheme of a typical electronic nose. However, there are many kinds of chemical substances involved in producing smell, and hence it seems really difficult to obtain useful information to discriminate a single chemical species from others.

Although chemical sensors are known since the beginning of XX century, the great advance in the field occurred at the end of the 70's when the technology of materials and microelectronics made possible the advent of solid state sensors.

Solid State Sensors have been conceived as electronic devices able to establish the link between the environment and electronic circuits. Since the beginning of 80's a large number of different chemical sensors have been investigated. The growing interest on chemical sensors comes from the necessity to improve the standard of life quality and an increasing awareness on health problems related to environment pollution, food production, etc.

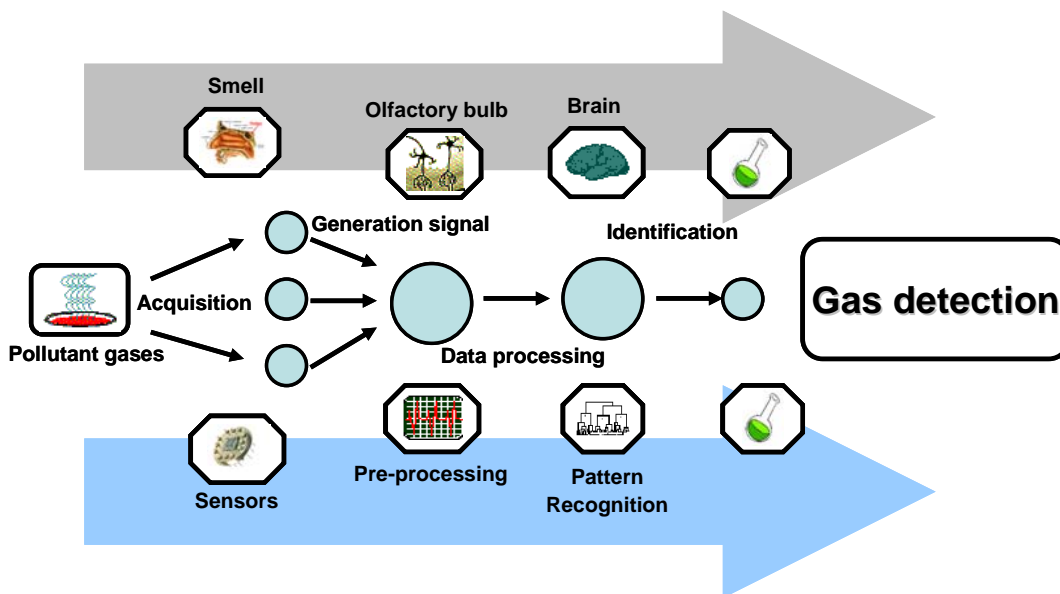


**Figure 1.1:** Comparative scheme between an E-nose and Human nose.

In the last decade, the use of sensor arrays has become customary in the sensor community. Recent developments in chemical sensors have provided simple, but efficient enough strategies suited to environmental applications. Despite the huge number of publications on chemical and biological sensing, not all of the current findings have been developed into commercial devices. This is partly due to the complexity of the environmental matrix, which can cause interference, and partly to the fact that the sensor has to integrate electronics, mechanical design, hardware and software.

In the European Union, as response to the Fifth environment Programme (1992-1999), which was directed to the protection of public health and quality of ambient air, the European Commission published a Directive, the 96/62/CE [1]. The Commission's aim was to establish and define ambient air quality objectives, to monitor air quality in each state member and to obtain the best available set of data on atmospheric pollution. More recently, during the Sixth Environment Action Programme launched by the European Commission [2] one of its main approaches was presented. The principal aim of this Programme is to work very closely with business and consumers to identify solutions for environmental monitoring and control.

A broad spectrum of contaminated gases with wide concentration ranges of target pollutants have to be monitored. All these pollutants are relevant to outdoor and indoor air quality control [3, 4] and are associated to agricultural activities, livestock farming activities

## Improving the performance of micro-machined metal oxide gas sensors: Optimization of the temperature modulation mode via pseudo-random sequences.

and/or petro-chemical industry (toxic or inflammable gases), transport, refrigerating systems and home cookers and boilers. Even though the natural olfactory system is exceptional at detecting and classifying many kinds of odours, most hazardous gases or vapors can only be detected at too high concentrations or just cannot be detected at all. There are some standard methods used for the ambient air determination of some of these compounds in ambient air. These methods are as follows:

The Sulfur dioxide can be analyzed by ultraviolet fluorescence [5]. Nitrogen oxides and ozone are analyzed by the chemiluminescence method [6]. Carbon monoxide and carbon dioxide are analyzed by the non-dispersive infrared spectrophotometric method [7]. Methane, propane and other hydrocarbons are analyzed by flame ionization detection [8]. Benzene and other toxic volatile organic compounds are analyzed by photoionization [8]. Ammonia is reliably detected by Fourier-transform infrared spectroscopy [8]. Suspended particulates are analyzed by the atomic absorption spectrometric method [9]. The methods previously cited involve the use of various techniques and technologies and expensive and bulky equipment.

An alternative, but expensive, method for discriminate and quantifying pollutants gases is known as gas chromatography coupled to mass spectrometry. However, these are laboratory methods that can not produce real time results. Furthermore, the use of this equipment requires highly trained operators. Therefore, for real time analysis of air quality with the purpose of continuously monitoring the emissions of hazardous/offensive gases into the atmosphere, classical analytical methods are not suitable.

Therefore, a need has emerged for developing rugged, reliable, small and inexpensive equipment for air quality monitoring, especially in domestic and transport (e.g. automotive, aircraft) applications. Solid-state gas sensors in general, and semiconductor metal oxides in particular, are a very promising and low cost option for constructing gas analyzers in order to overcome the purpose of monitoring the emissions of toxic species.

Metal oxide based gas sensors have a large number of potential applications in the analysis of single gases and multi-component mixtures. The results obtained using them are very promising and they have been the subject of research for more than twenty years. However, they still suffer important problems associated, especially, to their lack of selectivity and response drift.

In order to tackle the troubles experienced with metal oxide gas sensors presented above, there are several techniques that have been developed and applied, but with limited success. Together with these strategies, in the last years, micro system technology has been applied to develop substrates for integrated metal oxide gas sensor arrays. The use of microsystems technology and, particularly, of conventional silicon micromachining offers all the



advantages that typically characterize integrated circuits, such as low cost, small size and low-power consumption.

In parallel, different strategies have been developed to ameliorate sensor performance. Some are related to the improvement of the sensing films [10, 11] (i.e. use of metal oxides more sensitive to target gases and less responsive to temperature), better control of film microstructure using nanometric oxides, use of new catalysis/dopants and new technologies for material deposition. Other strategies rely on new methods for conditioning and pre-treating gas mixtures such as using catalytic filters that burn out interferent species, separation columns (e.g. chromatographic columns), implementing techniques of selective concentration (e.g. carbon traps or polymer-coated fibres) [12]. Finally, other widely used techniques [13-15] includes partially overlapping sensitivities and pattern recognition techniques, or the use of dynamic features from the sensor response (e.g. A.C. mode [16], concentration modulation [17], and temperature modulation [18]).

## 1.2. Thesis Structure.

The principal aim of this doctoral thesis is to develop a new technique which permits a systematic optimization of the process of frequency selection for modulating the operating temperature of metal oxide gas sensors in view to increase their selectivity. In the last years, modulating the working temperature of metal oxide gas sensors has been one of the most used methods to enhance their selectivity. When the working temperature of a gas sensor is modulated, the kinetics of the gas-sensor interaction is altered and this leads to characteristic response patterns. As the sensor response is different at different working temperatures, measuring the sensor response at  $n$  different temperatures is similar to the use of an array comprising  $n$  different sensors. This allows for measuring multivariate information from every single sensor and helps in keeping low the dimensionality of the measurement system needed to solve a specific application. Although the good results reported, until now, the selection of the frequencies used to modulate the working temperature remains been an empirical process. Because of this, in this thesis we introduce a method, borrowed from the field of system identification, to systematically determine the optimal set of modulating frequencies to solve a given gas analysis application. The method consists of using maximum-length pseudo-random sequences (i.e. either binary or multi level sequences) to modulate the working temperature of metal oxide gas sensors. The structure of the thesis is as follows:

In **Chapter 2** the State of the Art in thermal modulation of gas sensors is presented. This chapter starts by presenting a brief history of electronic nose and multi-sensors gas analyzer

## Improving the performance of micro-machined metal oxide gas sensors: Optimization of the temperature modulation mode via pseudo-random sequences.

systems. Therefrom this chapter continues by presenting the problems caused by the poor selectivity of metal oxide gas sensors, and reviews the different methods proposed by other research groups, which have conducted research in the temperature modulation field, in order to increase sensors selectivity. Additionally, this chapter reviews the feature extraction and pattern recognition methods implemented in the analysis of experimental data from temperature modulated gas sensors. Finally this chapter suggests different optimization strategies used in temperature modulation by different researchers.

**Chapter 3** reviews the different feature extraction and pattern recognition methods implemented in this thesis for analyzing the experimental data. A classical feature extraction method as the Fast Fourier Transform (FFT) was employed, and in this chapter, the analysis of signals and systems by this way, correlation energy and power spectrum are described. The different pattern recognition methods used ranged from linear, non-supervised (PCA) or supervised (PLS) to artificial neural networks, such as Fuzzy ARTMAP. Additionally to these methods, a novel feature extraction method, the so-called phase space (PS) and Dynamic moments (DM), is introduced here and applied to temperature-modulated microhotplate gas sensors [5]. Both techniques (i.e., FFT and DM) are described in this chapter. Finally a method based on data variance analysis for the selection of variables extracted from the feature extraction method is presented.

In **Chapter 4** at first a description and a mathematical definition of a general system is introduced. Furthermore, an introduction to perturbation signals for time and frequency domain system identification is given. Therefrom the ways to obtain the impulse response of a system are mentioned. After this, the generation and application of pseudorandom sequences signals (PRS) of maximum length (either binary or multilevel) is described. This is followed by an explanation on how PRS (binary and/or multilevel) can be used to identify systems and, how the method can be extended to systematically study temperature-modulated gas sensors.

**Chapter 5** describes the sensors used during the experiments performed. Two different types of sensors were used: the first ones were tin oxide gas sensors, while the second ones were tungsten oxide gas sensors. In both cases a microhotplate substrate was employed. The measurement system layout used to perform the experiments and the experimental set-up is described in detail in this chapter. Finally, this chapter describes the different measurements performed during this study.

In **Chapter 6** the experiments 1 and 2 described in **Chapter 5**, are studied and fully analyzed. The first experiment (preliminary study) analysis is twofold: at first the analysis of the thermal response of the gas sensor heating element, in order to obtain the cutoff frequency of the coated membranes and therefrom to determine the clock frequency ( $f_c$ ) and

the length of the PRS signal. Once these parameters are determined, the second part of this experiment is performed.  $\text{NO}_2$  + dry air and pure dry air were measured with  $\text{WO}_3$  and  $\text{SnO}_2$  microhotplate gas sensors while their working temperature was modulated by means of pseudorandom binary sequence (PRBS).

In the second experiment  $\text{NH}_3$ ,  $\text{NO}_2$  and their binary mixtures, diluted in dry air, were measured while the working temperature was modulated by a PRBS. This experiment consists in systematically determining the optimal set of modulation frequencies of the micro-hotplate gas sensors. In both experiments the impulse response estimate is computed. Therefrom the module of the Fast Fourier Transform (FFT) of the impulse response estimate is employed to select the set of optimal spectral components. For this study both, statistical and neural networks pattern recognition methods are used.

**Chapter 7** presents the quantitative and qualitative results for gas analysis of experiments 3 and 4 presented in chapter 5. For experiment 3 similar pollutant gases than in experiment 2 were measured, while during the fourth experiment, pollutant gases like acetaldehyde, ethylene, ammonia, and their binary mixtures were measured. In both experiments the working temperature of the microhotplate gas sensor was modulated by means of MLPRS signals.

The problem envisaged here is the building of calibration models for the quantitative and qualitative analysis of the pollutant species (i.e.,  $\text{NO}_2$ ,  $\text{NH}_3$  and their binary mixtures for experiment 3 and acetaldehyde, ethylene, ammonia and their binary mixtures for experiment 4). In both experiments an estimate of the impulse response is computed and its spectral components are studied. A few selected spectral components correspond to the frequencies that will be used in the qualitative and quantitative analysis of the gases studied. For this, both, linear statistical and neural networks pattern recognition methods are used.

A further validation of these results was envisaged by modulating the working temperature of gas sensors by means of multi-frequency sinusoidal signals. The frequencies within these signals were the ones selected during the training phase in the first part of every one of the experiments presented. A new set of measurements with the same type of pollutant species were performed and analyzed.

Additionally, the results obtained from experiment 3 (i.e., in training phase and validation phase) were compared to the ones obtained by applying the Dynamic Moment's (DM) and Phase Space (PS) feature extraction methods.

Finally **Chapter 8** presents the conclusions derived from the studies performed in this doctoral thesis. The list of publications derived from this thesis is grouped in the *Annex* while supplementary information is presented in the *Appendix*.

Improving the performance of micro-machined metal oxide gas sensors:  
Optimization of the temperature modulation mode via pseudo-random sequences.

### 1.3. References.

- [1] *Council Directive 96/62/CE* “on ambient air quality assessment management”, vol. 27 September 1996.
- [2] <http://europa.eu.int/comm/environment/newprg/index.htm>
- [3] J. S. Garcia Dos Santos Alves and R. Fernandez Patier, “The environmental control of atmospheric pollution. The framework directive and its development. The new European approach.”, *Sensors and Actuators B*, vol. 59, pp. 69-74, 1999.
- [4] T. Oyabu, Y. Matsuura and H. Kimura, “Identification for gaseous indoor air-pollutants using NDV”, *Sensors and Actuators B*, vol. 35-36, pp. 308-311, 1996.
- [5] “Ambient air – Determination of sulphur dioxide – Ultraviolet fluorescence method”, ISO/DIS 10489, *International Organisation for Standardisation*, Geneva.
- [6] “Ambient air – Determination of the mass concentration of nitrogen oxides – Chemiluminescence method”, ISO 7996, *International Organisation for Standardisation*, Geneva, 1985.
- [7] “Ambient air – Determination of carbon monoxide – Non-dispersive infrared spectrometric method”, ISO/DIS 4224, *International Organisation for Standardisation*, Geneva, 2000.
- [8] J. Chou, “Hazardous gas monitors”, *Mc Graw-Hill*, New York, 2000.
- [9] “Air quality – Determination of the PM10 fraction of suspended particulate matter – Reference method and field test procedure to demonstrate reference equivalence of measurement methods”, EN 12341, *European Committee for Standardisation*, Brussels, 1998.
- [10] F. Cosandey, G. Skandan and A. Singhal, “Materials and processing issues in nanostructured semiconductor gas sensors”, *JOM-e*, vol. 52, (10), 2000.
- [11] W. Göpel, “New materials and transducers for chemical sensors”, *Sensors and Actuators B*, vol. 18-19, pp. 1-21, 1994.
- [12] N. Yamazoe, “New approaches for improving semiconductor gas sensors”, *Sensors and Actuators B*, vol. 5, pp. 7-19, 1991.
- [13] C.K. Persaud and G.H. Dodd, *Nature*, vol. 299, pp. 352-355, 1982.

- [14] H.V. Shurmer, J.W. Gardner and P. Corcoran, "Intelligent vapour discrimination using a composite 12-element sensor array", *Sensors and Actuators B*, vol. 1, pp. 256-260, 1990.
- [15] J.W. Gardner, "Detection of vapours and odours from a multi-sensor array using pattern recognition. Part 1: Principal component and cluster analysis", *Sensors and Actuators B*, vol. 4, pp. 109-115, 1991.
- [16] F.J. Gutierrez, L. Arés, J.I. Robla, M.C. Horrillo, I. Sayago and J.A. Agapito, "Properties of polycrystalline gas sensors based on d.c. and a.c. measurements", *Sensors and Actuators B*, vol. 8, pp. 231-235, 1992.
- [17] E. Llobet, J. Brezmes, X. Vilanova, J.E. Sueiras, X. Correig, "Qualitative and quantitative analysis of volatile organic compounds using transient and steady-state responses of a thick-film tin oxide gas sensor array", *Sensors Actuators B*, vol. 41, pp. 13-22, 1997.
- [18] W.M. Sears, K. Colbow and F. Consadori, "General characteristics of thermally cycled tin oxide gas sensors", *Semicond. Sci. Technol.*, vol. 4, pp. 351-359, 1989.

**Improving the performance of micro-machined metal oxide gas sensors:  
Optimization of the temperature modulation mode via pseudo-random sequences.**

This page was left blank intentionally.

---

# 2.

## State of the art

---

<b>2. STATE OF THE ART</b>	<b>11</b>
<b>2.1. Introduction to the sense of smell.</b>	<b>12</b>
2.1.1. The human olfactory system and odors.	13
2.1.2. The history of electronic noses.	15
2.1.3. Multi-sensors gas analyzer systems.	17
<b>2.2 The selectivity problem of gas sensors.</b>	<b>19</b>
2.2.1. Metal oxide gas sensors.	20
2.2.2. Basic considerations.	23
2.2.3. Developing new materials and technologies.	24
2.2.4. Alternative methods for instrumental analysis of chemical compounds.	28
2.2.5. Pre-treatment methods of gases before sensing.	31
2.2.6. Use of sensor arrays together with techniques of pattern recognition.	33
2.2.7. Use of the dynamic operation mode.	34
<b>2.3. Temperature modulation for selectivity enhancement.</b>	<b>36</b>
<b>2.4. On the optimization of the temperature-modulating signals.</b>	<b>44</b>
2.4.1. Initial methods.	45
2.4.2. Optimization using dynamic models.	45
<b>2.5. Conclusions.</b>	<b>47</b>
<b>2.6. References.</b>	<b>49</b>

## Improving the performance of micro-machined metal oxide gas sensors: Optimization of the temperature modulation mode via pseudo-random sequences.

### 2.1. Introduction to the sense of smell.

Humans have five senses: sight, hearing, touch, smell and taste, and these senses are very important because humans act after receiving information coming from the outside world.

These senses can be divided in two main categories: *physical senses* composed by touch, sight and hearing and *chemical senses* by smell and taste. Among the different human senses, chemical senses are understood the least.

The sensors for the senses of sight, hearing and touch respond to physical quantities as light, sound waves and pressure (or temperature) respectively and are also called physical sensors. The end target in developing sensors for these parameters may be high sensitivity or selectivity for the physical quantity concerned, and this can be achieved by, for example, semiconductor technology. On the other hand, many kinds of chemical substances must be assessed at once for smell and taste to be transformed into meaningful quantities to describe these senses. It is still the subject of research what materials can be adequately used to detect chemical substances that produce smell and taste.

Figure 2.1 shows the correspondence between the biological system and the artificial system in process of reception (detection and processing) and taking the appropriate action.

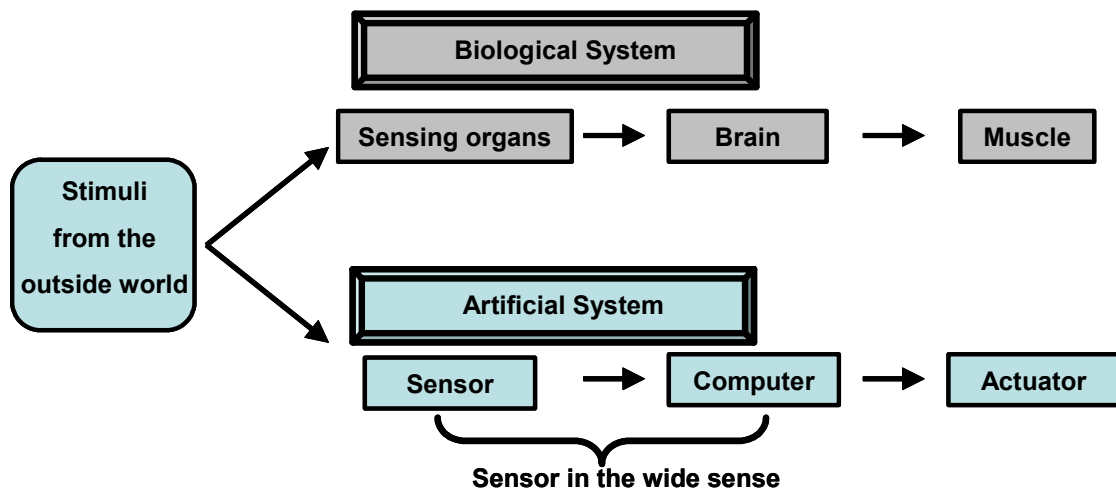


**Figure 2.1:** Correspondence between the biological system and the artificial system in the process of detection, processing and taking action.

The sensor is the device that emulates the ability our sensing organs, (i.e. eye, ear, skin, nose and tongue) in the senses of sight, hearing, touch, smell and taste, respectively.





Improving the performance of micro-machined metal oxide gas sensors:  
 Optimization of the temperature modulation mode via pseudo-random sequences.

These odorant molecules produced are drawn up into nasal cavity and across the olfactory area (epithelium) below the olfactory bulb as is shown in the Figure 2.2 [3, 4]. First there is a thin aqueous mucus layer into which extend the olfactory hairs or cilia from olfactory cells. G-receptor binding proteins are located at the surface of the cilia and act as chemosensory receptors. It is believed that a relatively small number of different receptor proteins ( $\approx 100$ ) exist, so that receptor cells have partially overlapping sensitivities. There are about 100 million olfactory cells (50 million per nostril), which are believed both to amplify the signal and generate secondary messengers. The messengers control ion channels and generate signals that travel down axons from the olfactory nerves to about 5000 glomeruli nodes in the olfactory bulb. These signals are then further processed by about 100 000 mitral cells and then finally sent via a granular cell layer to the brain.

Our understanding of the olfactory process has increased rapidly during the past decade [5] and attempts have been made to model this process [6], but the precise details are still unknown. The performance of the human olfactory system is rather remarkable. The olfactory receptor cells are believed to have a low sensitivity (about ppm), a low specificity and only live on average for about 22 days. Yet the subsequent neural processing enhances sensitivity by about three orders of magnitude, removes drift and provides discrimination between several thousand odors.

**Table 2.1:** Some common simple odors.

Chemical structure	Odor Type	Threshold (ppb in water)
Diacetyl	Off-flavor of beer	500
Trans-2-hexenal	Green leaves	316
Geraniol	rose	290
5-Isopropyl-2-nethylphenol	thyme	86
Limonene	lemons	10
Cis-4-heptenal	off-flavor of white fish	0.04
Octa.1,5-diene-3-one	off-flavor of white butter	0.01
2-Isobutyl-3-methoxypyprazine	Green peppers	0.002
$\alpha$ -Terpinethiol	Grapefruit	0.00002

Odorant molecules are typically hydrophobic and polar with molecular masses of up to about 300 Da. A simple odor is a single molecule and some examples are listed on Table 2.1, together with the type of odor and its olfactory threshold [7]. Actually, most natural smells, like perfumes and flavors are complex mixtures of chemical species and contains hundreds,

if not thousands of constituents. Often, subtle differences in the relative amounts of these constituents determine the smell of the product.

## 2.1.2. The history of electronic noses.

The practical application of the human nose as a smell assessment instrument is severely limited by the fact that our sense of smell is subjective, gets tired easily, and is therefore both expensive and difficult to use. Consequently, there is considerable need for an instrument that could mimic the human sense of smell and be of use in routine industrial applications.

In view of designing an artificial olfactory system or a gas analyzer system, it is fundamental to be aware that olfaction is not an analytical technique. Indeed, it does not provide the composition and the concentration of each volatile compound within an odor, but it gives an overall judgment about a certain sample. For this reason, the attempt to understand how olfaction works and to reproduce electronic tools replacing the human olfactory system still remains a challenge for scientists and engineers.

The basic elements of a generalized electronic instrument to measure odors are shown in Figure 2.3 [8]. First there is an odor delivery system which is designed to transfer the odor from the source material to the sensor chamber. The sensors chamber houses the array of chosen odor sensors, (i.e. metal oxide or conducting polymer chemiresistors, polymer-coated quartz crystal microbalance or surface acoustic wave devices, etc.). Sensor electronics not only convert the chemical signal into an electrical signal but also, usually, amplify and condition it. The signal must be converted into a digital format to be processed by a computer. The computer is programmed to carry out the task and display information about gas classification.

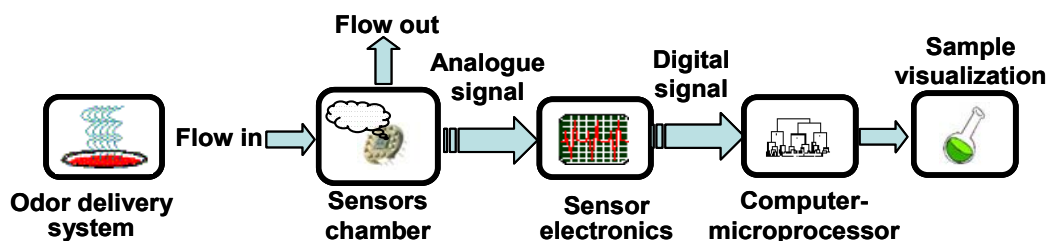


**Figure 2.3:** Block diagram of the basic components of an e-nose instrument. Figure taken from [8].

Indeed, the earliest work on the development of instruments specifically designed to detect odors probably dates back from the end of 1919 and beginning of 1920. In 1920 Zwaardemaker and Hogewind [9] suggested that odors could be detected by measuring the

## Improving the performance of micro-machined metal oxide gas sensors: Optimization of the temperature modulation mode via pseudo-random sequences.

electrical charge developed on a fine spray of water that contained the odorant in solution. However, at that time the lack of a suitable electronic instrumentation prevented them from developing their idea into a useful instrument.

Actually, the first real report of an experimental instrument was published by Hartman and co-workers [10, 11], who described an electrochemical sensor consisting of a polished metal wire microelectrode in contact with the surface of a porous rod saturated with a dilute electrolyte. By using various combinations of metal electrodes, electrolytes and applied potentials, a system of several sensors was made to operate simultaneously. In essence, the sensors used in this work were examples of amperometric electrochemical gas sensors. The instruments they developed comprised an array of eight different electrochemical cells and gave different patterns of response for different odorant samples, although in this work they made no serious attempt to process the patterns which they generated even though computers were becoming available.

At about the same time Moncrieff [12] was working on the same problem but using a different approach. He employed a single thermistor coated with one of a number of different materials, including polyvinyl-chloride, gelatine, and vegetal fat, to monitor odors. He recognized that the coatings he was using were non-specific, and he postulated that if an array of six thermistors with six different coatings were constructed then the resulting instrument would be able to discriminate between a large number of different smells. In 1965 two other groups published early studies of electronic noses. Buck *et al.* [13] made use of the modulation of conductivity, while Dravnieks and Trotter [14] used modulation of the contact of potential to monitor odors. However, the concept of an electronic nose as an intelligent chemical array sensor system for odor classification did not really emerge until nearly 20 years later. This was following the publications by Persaud and Dodd in 1982 [15], who worked at Warwick University in the UK and by Ikegami and co-workers (1985, 1987), working at the Hitachi Research Laboratory in Japan [16, 17]. By this time developments in electronics, sensors, and computing had combined to reach a stage where an electronic nose had become a genuine possibility [18]. The term electronic nose first appeared in the literature around 1988 introduced by Gardner. Then, in 1989, a session of NATO advanced workshop on chemosensory information processing was dedicated to the topic of artificial olfaction [19, 20]. Finally, the first conference dedicated to the topic of electronic noses was held in 1990 [21]. Today the following definition of an electronic nose given by Gardner and Bartlett in 1994 [22] appears to be generally accepted:

*“An electronic nose is an instrument which comprises an array of electronic chemical sensors with partial specificity and an appropriate pattern recognition system, capable or recognizing simple or complex odors.”*

This definition restricts the term electronic nose to those types of sensors array systems that are specifically used to sense odorous molecules in an analogous manner to the human nose. However, the architecture of an electronic nose has much in common with multi-sensor systems designed for the detection and quantification of individual components in a simple gas or vapor mixture [23, 24].

### 2.1.3. Multi-sensors gas analyzer systems.

Artificial olfaction systems are not traditional analytical instruments. Indeed, electronic nose systems do not provide the composition and the concentration of each volatile compound within an odor. As it is well known, the electronic nose is an electronic system that tries to imitate the structure of the human nose, which gives an overall judgment about a certain sample. Therefore, when there is a need to qualitatively and quantitatively analyze a few target species, e.g., some pollutant gases, a different approach is needed. In this case a multi-sensor gas analyzer system should be devised. Multi-sensor gas analyzers are equipped with a an array of gas sensors (e.g. metal oxide, conducting polymer chemoresistors, polymer-coated quartz crystal microbalance, or surface acoustic wave devices, etc.), combined with several feature extraction and pattern recognition methods for the detection, identification, and quantification of specific volatile compounds.

Like in electronic noses, the process of data analysis starts after the sensor signals have been acquired and stored into the computer. The typical steps of *signal preprocessing, dimensionality reduction, prediction, and validation* found with electronic noses also apply to multi-sensor gas analyzers. However, unlike in electronic noses, the system is designed to selectively detect a few target species with quantification capability.

Various research groups have been very active in multi-sensors gas analyzer systems designed to monitor pollutant gases for environmental protection [8, 25-27]. Air pollutants that are due to be monitored, are sulfur dioxide, nitrogen oxides, ozone, carbon monoxide, carbon dioxide, ammonia, benzene, methane, propane, ethanol, lead and suspended particulate. It is well known that all these pollutants are relevant to outdoor and indoor air quality control. According to that, during the last years many authors have developed gas sensors together with new pattern recognition and feature extraction techniques, to integrate gas analyzers, in an attempt to solve environmental issues [28-40]. Some of the studies performed in the most recent years are reviewed in the following paragraphs.

NO<sub>2</sub> and CO were detected and analyzed either by piezoelectric quartz crystal sensors and metal oxide micro-hotplate (MHP) based gas sensors [28-31]. J.-S. Shih and co workers and P. Ivanov et al. studied, with the help of traditional pattern recognition methods, new

## Improving the performance of micro-machined metal oxide gas sensors: Optimization of the temperature modulation mode via pseudo-random sequences.

materials to better detect some pollutant species. The former developed Titanium(IV)/cryptand22 and Zinc(II)/cryptand22-coated piezoelectric (PZ) quartz crystal detection systems with home made computer interfaces for data acquisition. An artificial back propagation neural network (BPN) with a two-channel PZ crystal flow sensor was trained and applied to recognize and distinguish each component ( $\text{NO}_2$  and CO) in a mixed  $\text{NO}_2/\text{CO}$  sample, which showed quite good distinction of the individual species from the mixed gas sample. The quantitative analysis of CO and  $\text{NO}_2$  in pure and mixed CO/ $\text{NO}_2$  were also computed by multivariate linear regression analysis (MLR) in this study. On the other hand the latter reported the use of either reactive magnetron sputtering or screen-printing to deposit tin and tungsten oxide gas sensitive layers onto integrated micro-machined gas sensor arrays. Using PCA and fuzzy ARTMAP neural networks the simultaneous identification and quantification of toxic gases was shown to be possible with good success rate. In addition to developing and studying new materials to improve selectivity in gas analyzers, Manuel Bicego presented a new approach to odor classification and quantification (i.e. low concentration of 2-propanol, acetone and ethanol) using carbon black polymer sensors. The method is based on a similarity representation paradigm. This method proposes to build a new representation space, in which each object is represented by the vector of similarities to other objects in the data set. More information about this novel method can be found in [32-35]. In [36] A.M. Taurino shows the capability of an array of metal oxide gas sensors to perform qualitative and quantitative analysis of the several volatile compounds usually present in the headspace of foods. The qualitative analysis was carried out with two neural network paradigms, RBF and MLP where the last showed a better performance. In the quantitative analysis, a function approximator to discover the concentration value of hexanal in the gas mixtures under consideration was modeled with different versions of RBF and MLP. M Penza in [37] reports a gas analyzer system based on a surface acoustic wave (SAW) multi-gas sensor array for the identification and quantification of volatile organic compounds (VOCs). The gas analyzer system was developed in order to recognize individual components in a binary mixture of methanol and 2-propanol in the range 20-140 and 5-70 ppm respectively. The combination of PCA as data pre-processing technique and the MLP as pattern recognition engine, provides a rapid and accurate recognition and quantification of the species studied. Furthermore, a sensor array system based on an array of 10  $\text{SnO}_2$  sensors on the same substrate with the help of pattern recognition analysis (i.e., PCA and a multi-layer neural network) was developed to recognize various kinds and quantities of VOCs, such as toluene, ethyl alcohol, and acetone by Dae-Sik Lee in [38]. Moreover, René Knake, in [39] demonstrated that it was possible to successfully analyze two mixtures consisting of either three organic electroactive components or of four

inorganic species in the ppm-range. A typical amperometric gas sensor with a high electrode surface was found to be most suitable. The determination of three to four components in mixtures succeeded in the ppm range by using a partial least squares method. Correlation coefficients for these calibrations were good and recoveries mostly acceptable. Additionally, Ya. I. Korenman and co-workers elaborated and presented in [40] a multi-sensor system based on recognition of graphic images (imprints), which gives the possibility to qualitatively and quantitatively analyze low concentrations of nitroethane. The system operates at high speed using an algorithm of image recognition and it is claimed to be simple to operate and easily calibrated.

Other authors [41-47] with the aim of detecting pollutant gases, and estimating their concentrations, have developed novel techniques and methods that can be of great help in the improvement of gas detection and quantification. That is the case of the study of the temperature behavior in gas sensors, since as it is well known, a good selection of the working temperature of gas sensors could result in better accuracy in gas classification and quantification. The method normally consists in the periodical variation of the operating temperature of gas sensors. Indeed, several authors have worked with this strategy and have applied several techniques (e.g. traditional feature extraction techniques like FFT and DWT) to extract features that are important for qualitative and quantitative gas analysis. Then, these features were used as inputs into various pattern recognition methods such as PCA, DFA and fuzzy ARTMAP for discrimination and PLS, RBF or MLP for quantification. By further developing and optimizing the process of temperature modulation, the results of this thesis find their primary application in the field of multi-sensor gas analyzers.

## **2.2 The selectivity problem of gas sensors.**

It is clear that the types of sensors that can be used in electronic nose or gas analyzers need to be responsive to molecules in the gas phase. Many different types of gas sensors are available and many of these have been used in electronic noses or gas analyzers at one time or another. However, at present, commercial instruments are concentrated on two main types of gas sensors –metal oxide and conducting polymer chemoresistors- with more recent works beginning to exploit other types of sensors. Nevertheless, metal oxide gas sensors are a low cost option for constructing gas detectors and electronic nose equipment and they remain the most widely spread. As mentioned before, the analysis of single gases and multi-component mixtures using metal oxide based semiconductor gas sensors has been the subject of research for several years. However, some important problems associated to this approach remain unsolved. This section introduces the problems experienced with metal oxide gas sensors, in

## Improving the performance of micro-machined metal oxide gas sensors: Optimization of the temperature modulation mode via pseudo-random sequences.

particular their lack of selectivity, and reviews methods that have been published in the literature to overcome them. Before, some generalities of metal oxide gas sensors (i.e., fabrication and their sensing mechanism) including a brief history of their development are reviewed.

### 2.2.1. Metal oxide gas sensors.

As was mentioned before, nowadays there is a great interest in using sensing devices to improve the environmental and safety control of toxic gases. Reviewing the history of sensor development it is found that, in 1938 Wagner and Hauffe discovered that atoms and molecules interact with semiconductor surfaces, and influence surface properties such as conductivity and surface potential. The effect of ambient atmosphere upon the electrical conductance of semiconductors was described by Brattain and Bardeen in 1953, Heiland in 1954 and Morrison in 1955. Subsequently, Seiyama and Taguchi in 1962 and 1970, respectively applied this discovery to gas detection by producing the first chemo-resistive semiconductor gas sensors [48]. Many semiconductors, unfortunately, undergo irreversible chemical transformations by forming stable oxide layers. The most suitable semiconductor materials for such sensors are metal oxides, which bind oxygen on their surface in a reversible way.

Chemical reactions, which take place under atmospheric conditions at the surface of the active layer, are of interest since, there is where detection of minor concentrations of potentially dangerous gases occurs.

The main surface reaction that controls the response to gases of semiconducting oxides operating in air (keeping them at temperatures between 300-500°C, to obtain a sufficient reaction rate) involves changes in the concentration of surface oxygen species such as  $O_2^-$  or  $O^-$  (see Figure 2.4).

The formation of such ions by oxygen adsorbed at the gas/solid interface subtracts electrons from the bulk of the solid. The oxygen can be thought of as a trap for electrons from the bulk of the solid. In the case of an *n*-type semiconductor the electrons are drawn from ionized donors via the conduction band, so the charge carrier density at the interface is reduced and a potential barrier to charge transport,  $\Delta G$ , is developed. As the surface charge increases, the ionosorption of further oxygen is limited by the potential barrier that has to be overcome by the electrons in order to reach the surface. The adsorption rate slows down because the charge must be transferred to the adsorbate over the developing surface barrier, and the coverage saturates at a rather low value. At the junctions between the grains of the



solid, the depletion layer and associated potential barrier make high resistance contacts, which dominate the resistance of the solid.

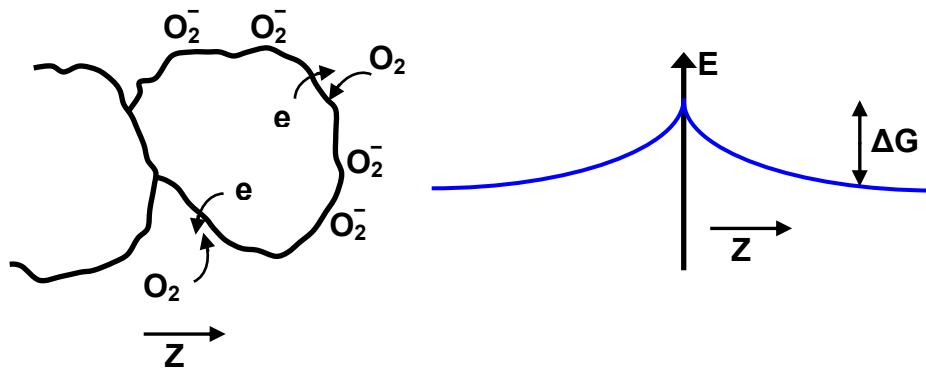


**Figure 2.4:** Charge exchange associated with the chemisorption of oxygen at a semiconductor surface and the potential distribution across a grain junction.

Semiconducting oxides can be used as gas sensitive resistors to monitor in air any gases (reducing or oxidizing gases) which can alter the quantity of charge trapped at the surface.

In the case of a *p*-type oxide, adsorbed oxygen acts as a surface acceptor state, subtracting electrons from the valence band and increasing the charge carrier (hole) concentration at the interface. Any decrease in the surface coverage of oxygen ions, for example caused by reactions such as the one mentioned above, decreases the charge-carrier concentration and hence increases the resistance of the material.

On the basis of reactions such as these, it is expected that responses would take place in the opposite sense to those with reducing gases. A consistent pattern of response type would be as shown in Table 2.2.

**Table 2.2:** Resistance responses expected for reducing and oxidizing gases on *n*-type and *p*-type semiconducting oxides.

Material	Reducing gases	Oxidizing gases
<i>n</i> -type	Resistance falls	Resistance rises
<i>p</i> -type	Resistance rises	Resistance falls

The use of Microsystems technology (MST) to obtain micro-hotplate structures has gained importance in the design of metal oxide sensors with improved performance. Micro-hotplate elements include functionality for measuring and controlling temperature, and

## Improving the performance of micro-machined metal oxide gas sensors: Optimization of the temperature modulation mode via pseudo-random sequences.

measuring the electrical properties of the active films deposited. As their name implies, they are of particular interest because of their ability to examine temperature-dependent phenomena on a micro-scale, and their rapid heating/cooling characteristics have led to the development of low power sensors that can be operated in dynamic temperature programmed modes. Tens or hundreds of micro-hotplates can be integrated within arrays that serve as platforms for efficiently producing and processing performance correlation for sensor materials. The evolution of micromachining as a fabrication technology for chemical sensing has allowed miniaturization to progress with improved fabrication methods. Micromachining of silicon to produce sensor platforms also allows including on-chip circuitry, and it is straightforward to replicate device structures into integrated arrays. Beginning in the early 1990s, the opportunities of silicon micromachining led to the fabrication of new types of micro-hotplate devices and arrays for gas sensing. These devices have been produced both by surface [49] and bulk [50, 51] etching of silicon, and have been used to develop gas micro-sensor prototypes [52]. The ability to locally heat miniature elements has been used both to fabricate micro gas sensors and operate devices in the rapid temperature-programmed mode [53]. Recently, the advantages of micro-hotplates as gas sensor platforms have been widely demonstrated [54-56]. Micro-hotplates contain a built-in heater, thermometer, and sensing film. The devices use conductance changes in the sensing film to detect the presence of adsorbed gas species. Temperature changes may be used to alter the reaction kinetics between the gas and sensor surface. An example of a single element and the multilayer structure used in [56] is illustrated in Figure 2.5.

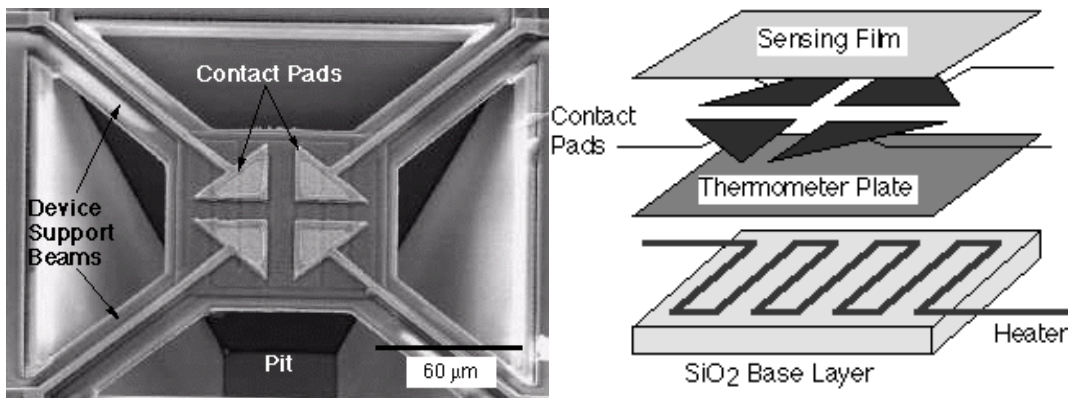


**Figure 2.5:** Micrograph of single micro-hotplate with four arrow-shaped electrodes. Figure extracted from [56].

The micro-hotplate is a multi-layer structure, which has three functional layers: a polysilicon heater, a metal (e.g. Al, Pt or W) thermometer/heat distribution plate, and sensing

film electrical contacts. These layers are separated by insulating layers of a dielectric (e.g.  $\text{SiO}_2$ ). In order to measure the electrical characteristics of the sensing films, the surface electrodes are in direct contact with the sensing film but isolated from the heat distribution layer by the dielectric layers previously mentioned. Maximum device temperatures are largely governed by the types of metallization available at a given foundry. For Al metallization, the maximum temperature is approximately  $500^\circ\text{C}$ , and metal post-processing is needed to produce more acceptable contact between the sensing film and the electrodes. When other metallization, such as W or Ti-W, are available at the foundry, devices can be heated to as high as  $750^\circ\text{C}$ . If the fabrication process does not need to be CMOS compatible, Pt can be used.

### 2.2.2. Basic considerations.

Metal oxide gas sensors are a low cost option for constructing gas alarm monitors, gas analyzers and electronic noses. Metal oxide based semiconductor gas sensors and their usefulness in the analysis of single gases and multi-component mixtures has been the subject of research for more than twenty years. However, some important problems associated to this approach remain unsolved.

It is well known that this kind of sensors suffer from lack of selectivity and response drift [57]. Moreover, they are influenced by water vapor, so changes in the moisture content of the atmosphere being monitored interfere with gas sensing. Nowadays, analytical equipment such as IR spectroscopy, gas chromatography/ mass spectrometry etc., are more used to analyze gases in the laboratory, rather than analyzers based on chemical sensors [58]. However, analytical instruments are very expensive and require highly trained personnel to operate them.

Therefore, the development of less expensive equipment based on chemical sensors in general and on metal oxide gas sensors in particular is still of high interest. This is why several methods to improve their selectivity have been devised. These include:

- A. Developing new materials and technologies
  - Use of new metal oxides more sensitive to target gases and less responsive to temperature or humidity
  - A better control of the film microstructure using nanometric oxides
  - Use of new catalysts/dopants
  - New technologies for depositing gas-sensitive materials onto transducers
- B. Alternative methods for instrumental analysis of chemical compounds

### Improving the performance of micro-machined metal oxide gas sensors: Optimization of the temperature modulation mode via pseudo-random sequences.

- Chromatography-based methods used for the analysis of chemical compounds (e.g. chromatographic columns as a separation step before the sensor chamber)
- C. Pre-treatment methods of gases before sensing
- Catalytic filters
  - Techniques of selective pre-concentration (e.g. carbon traps or polymer-coated fibers)
- D. Use of sensor arrays together with techniques of pattern recognition
- E. Use of the dynamic operation mode
- AC operation mode
  - Modulation of the gas concentration (e.g. step change in gas concentration or flow modulation).
  - Modulation of the sensor operating temperature

Although these techniques are usually applied separately, their simultaneous application should lead to a significant improvement in the selectivity of sensors. In the following subsections some of the findings reported by other researchers in their attempts to improve the selectivity of gas sensors are reviewed.

### 2.2.3. Developing new materials and technologies.

The most studied and used metal oxide is SnO<sub>2</sub>. This material can be sensitized to different gases by selecting an optimal operating temperature for the target gases, by making microstructural modifications or by using dopants and catalysts [59].

However, other metal oxides have been suggested as more appropriate for detecting some gas species. Table 2.3 presents a list of semiconductor oxide materials and their respective targeted response to gases that are relevant for environmental and air quality monitoring. More information of the materials presented in this table can be found in [60, 61].

Different ways to achieve selectivity are either by enhancing gas adsorption or promoting specific chemical reactions via catalytic or electronic effects using bulk dopants, surface modification methods and by the addition of metallic clusters or oxide catalysts [62, 63].

The selectivity of chemical sensors can be strongly influenced by the addition of metal clusters like platinum and palladium. These materials increase the sensor selectivity for reducing gases, e.g. CO [64]. Other studies have shown that gold, combined to metal oxides, has an important application in the catalytic oxidation of CO to CO<sub>2</sub> at room temperature, and function as a selective gas sensor for CO and H<sub>2</sub> [65-69]. Using gold as dopant, including Au-WO<sub>3</sub> for NH<sub>3</sub> detection and Au-In<sub>2</sub>O<sub>3</sub> for ozone and trimethylamine detection can increase the selectivity of metal oxide gas sensors [70]. Penza and co-workers [71] have

shown that the sensitivity and selectivity can be significantly improved by adding thin layers of noble metals such as palladium, platinum or gold on the surface of  $WO_3$  thin films operating at low temperatures. Maekawa and co-workers [72] demonstrated that Au-doped  $WO_3$  sensors had high sensitivity at low concentrations of ammonia gas in dry air.

**Table 2.3:** Semiconductor oxides with targeted selectivity for specific gases.

Oxide type	Detectable gas
$SnO_2$	$H_2, CO, NO_2, H_2S, CH_4$
$WO_3$	$NO_2, NH_3$
$TiO_2$	$H_2, O_2, C_2H_5OH$
$In_2O_3$	$NO_2, O_3$
$Fe_2O_3$	$CO$
$LaFeO_3$	$NO_2, NO_x$
$Cr_{1.8}Ti_{0.2}O_3$	$NH_3$

An alternative strategy to enhance the properties and performance of gas sensors is the use of nano-structured materials because their surface-to-bulk ratio is higher than that of coarse microparticle materials. Nano-structured materials are recognized as essential for achieving high gas sensitivity. Reducing particle size (for range of 5-50 nm), is an alternative but good opportunity to improve the sensitivity of semiconductor gas sensors, information about this can be found in [61, 70, 73].

Numerous deposition schemes have been tested successfully, although only at the laboratory scale. In order to provide the desired oxide composition with specific dopant and the minimum number of processing steps several processing techniques are available.

Basically the deposition techniques available are grouped in two main categories known as: *thin film* deposition processes (i.e. such as sputtering, evaporation, physical vapor deposition – (PVD) and chemical vapor deposition (CVD)), for thickness between 0.005  $\mu m$  and 2  $\mu m$ , and *thick film* deposition processes (i.e. such as screen printing and tape casting) for thickness greater than 10  $\mu m$ . Thermal spaying can be used to deposit coatings of metals, ceramics and cermets that are thicker than  $\sim 50 \mu m$ . Figure 2.6 summarizes the different processing methods used for synthesizing gas sensing films [60]. In the following paragraphs all these techniques are briefly described.

Thin solid films are fabricated by depositing individual atoms on a substrate. Historically Bunsen and Grove, obtained for the first time, thin films in a vacuum system in 1852. Thin

## Improving the performance of micro-machined metal oxide gas sensors: Optimization of the temperature modulation mode via pseudo-random sequences.

films are now widely used. A range of unusual properties can be obtained using this kind of sensors, by means of varying the deposition process, and modifying the film properties during deposition. These can not be obtained in bulk materials.

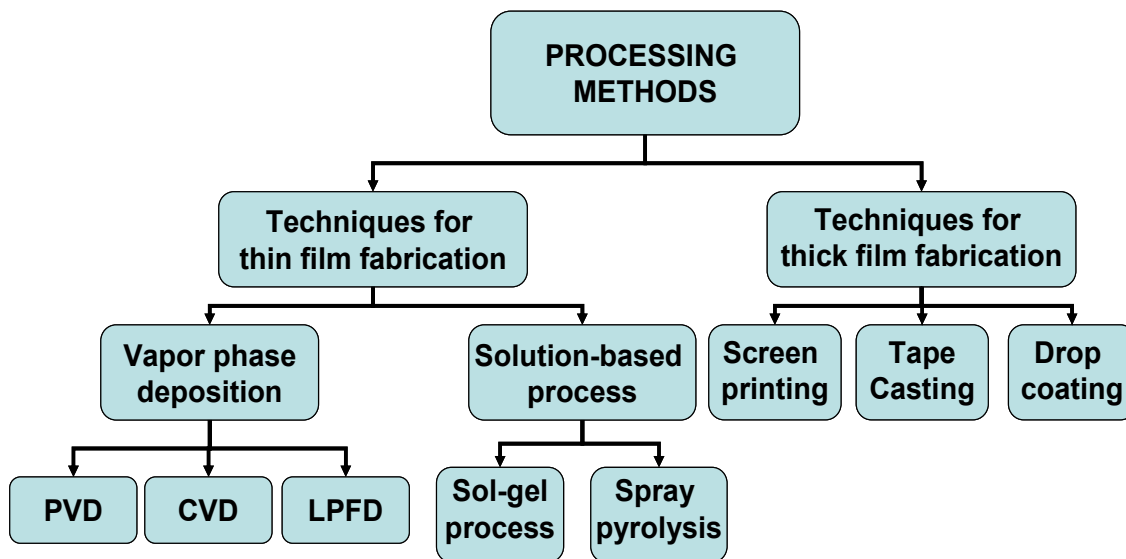


**Figure 2.6:** Processing methods used to fabricate thin and thick films for gas sensing applications.

Indeed, the principal difference between thin-film sensors and those obtained from sintered powder layers is that, in thin films the electric conductivity is modulated in the external region of the layer in contact with the gases, while in sintered layers this modulation is performed in their interior, on the grains whose surface comes into contact with the gases. Nevertheless, in both cases, the main measuring processes are the same: oxygen chemisorption and reaction with the reducing gases.

Thin films are synthesized from atoms or small groups of atoms and are generally  $< 1 \mu\text{m}$  thick. Basically, any thin film deposition process involves three main steps: production of the appropriate atomic, molecular or ionic species; transport of these species to the substrate through a medium; and condensation on the substrate, either directly or via chemical and/or electrochemical reaction. A post-deposition annealing at temperatures higher than the deposition temperature may modify the grain size. It is important to remark that the higher the annealing temperature is, the larger the size of grains will be.

As the same Figure 2.6 shows, there are many chemical and physical methods available for thin-film deposition. In the chemical vapor deposition (CVD) technique, gaseous compound precursors are mixed and heated in a vacuum chamber as they approach the deposition surface. The precursor molecules diffuse to and are adsorbed onto the substrate

surface where they react to form the deposited material. Volatile reaction by-products are then desorbed and transported away. CVD methods provide excellent film-coating conformity over uneven surfaces.

The RF magnetron sputtering (i.e. PVD) consists in bombarding the source material (sputtering target) with magnetically enhanced discharged plasmas. This erodes surface atoms, which travel across a vacuum chamber and condense on the substrate.

Variations of CVD techniques, such as plasma-enhanced (PECVD) [74] and atmospheric-pressure (APCVD) [75], have been used to produce both nano-powders and nano-structured thin films.

Physical vapor deposition (PVD) techniques using either evaporation or a sputter source have also been used extensively [76, 77]. Skandan et al. [78] have used a vapor-phase process to directly deposit, in one step, a nano-structured film of gas sensor material, such as  $\text{SnO}_2$  and  $\text{TiO}_2$ .

The process, called low-pressure flame deposition (LPFD), is based on the combustion flame-chemical-vapor condensation process used to produce oxide nanoparticles with minimal aggregation.

Considerable emphasis is given in developing solution-based thin-film deposition techniques as an economical alternative to the more expensive chemical vapor deposition and reactive sputtering processes. However, the quality of the film produced by vapor deposition processes remains superior.

The sol-gel technique consists of a system going from a liquid sol (colloidal suspension of miniature solid particles in a liquid) to a viscous gel in which the suspended particles are organized in a loose, but definite three-dimensional arrangement. The thin film gel is dried (this process can be repeated several times to achieve the required film thickness) and finally sintered. Gel layers can be formed by spin-coating (the solution is poured onto the substrate surface, which is then spun to expel fluid and create a uniform thickness), by dip-coating (the substrate surface is dipped into the solution) and by spray-coating (the solution is sprayed onto the sensor surface).

Spray pyrolysis, using an atomizing nozzle of  $300\mu\text{m}$ , has recently been used to deposit  $\text{SnO}_2$  films that were 50-300 nm thick. Tin chloride was dissolved in ethanol or deionised water and sprayed at a deposition temperature between 300-550 °C. Mukhopadhyay and co-workers [79] developed a modified chemical solution-based technique, where a thin adherent film of tin sulfide is formed on a ceramic substrate by reacting sodium sulfide and tin chloride. Subsequently, the tin sulfide film was reacted in air to produce  $\text{SnO}_2$ .

Vapor-based processes seem to be the most promising approach. However, new precursors are required for synthesizing multicomponent oxides with specific dopants.

## Improving the performance of micro-machined metal oxide gas sensors: Optimization of the temperature modulation mode via pseudo-random sequences.

On the other hand, with the need to combine different electronic technologies, the existence of thick-film has been justified.

One of the most important thick-film deposition methods is screen-printing, which is similar to that used for ceramics, textiles, etc. A thick-film paste can be formulated to paint or print an active layer onto a substrate [80]. To formulate the paste, finely milled metal oxides or other sensing materials are combined with small amounts of glass frit of a similar size (for adhesion to the substrate), catalysts (if desired), and an organic vehicle to form a printable paste [81, 82]. The particle size of the constituents varies, although for screen printing powders it should be 0.5  $\mu\text{m}$  or less in diameter. The paste is spread on the substrate by means of a screen made from non-rusting steel mesh, polyester or nylon, mounted on a metallic frame. The screen is coated with an ultraviolet-sensitive emulsion. These regions were drawn by photographic methods. The screen is maintained at 0.5 mm from the substrate surface in the screen-printing machine. The paste is pushed through the defined regions by pressure from a spatula. The paste is printed onto a ceramic substrate, typically alumina, dried, and fired at temperatures between 500 and 1000° C for one or more hours. Standard printable thick-film materials for resistive heaters and conductor lines may be applied to the substrate before or after the sensor layer (normally pastes of noble metals like Pt and Au).

Tape casting is a forming technique for producing thick, flat ceramics. The method was originally developed for producing electronic ceramics (insulating substrates and packages and multilayer capacitors). Ceramic slurry is spread evenly onto a flat horizontal surface by means of a 'doctor blade'. Once dry, the flexible 'green tape' is cut, laminated or shaped and sintered. The thickness of the tape is generally in the range 25  $\mu\text{m}$  to 1 mm, but tapes as narrow as 5  $\mu\text{m}$  can be produced.

Another thick film method is drop-coating. A particular thickness can be obtained by varying the number of drops that are deposited. This method is highly dependent on solution viscosity and density. Once the solution is deposited, the solvent evaporates by itself or with the help of gentle firing. Other techniques for thick-film deposition certainly exist, but they are of little interest to this study and, therefore, not discussed.

### **2.2.4. Alternative methods for instrumental analysis of chemical compounds.**

In the last years the use of traditional instrumental techniques together with gas sensors has been proposed. These methods were introduced as a different strategy oriented to increase the resolution and the sensitivity of gas sensors. For example, the Electronic Sensor Technology Company [83, 84] used in its "Znose", in addition to an adsorption/desorption



system, a chromatographic column. In this way, the discrimination between the compounds is realized through the column, to which are applied different temperatures. As a matter of fact, it is a chromatograph in which the detector is substituted by a gas sensor. The principal disadvantage of this system is its cost (about 40 thousand €).

Undeniably, one of the pioneer companies in the electronic nose field is Alpha M.O.S. This company develops electronic nose equipment that is based on mass spectrometry technology or metal oxide gas sensors. One of their equipment is a combination between the MS model (known as Kronos) and the metal oxide model (FOX).

A different company that is working with mass spectrometry based electronic nose technology is HKR Sensorysysteme GmbH. Nowadays, they have two MS based e-nose systems. The first one called MS-Sensor® that uses as mass analyzer a turbo mass Perkin-Elmer. This analyzer incorporates a chemical ionization (CI) and electronic impact (EI) as ionization systems. The second one is called SensiTOF® which uses RElectron Time-Of-Flight (RETOF) technology as mass analyzer.

Smart Nose 300 is another e-nose system based on mass spectrometry, which combines an automatic head space sampler with mass spectrometry fabricated by Balzers instruments Inc. Finally, Agilent technologies develops the HS4440 MS sensor that is the combination between a static head space autosampler like the HP7694 with a mass spectrometer. Some examples of MS based e-nose technology in foodstuffs, medical and other applications can be found [85-88]. Fenaile and co-workers [89] used a MS-based e-nose to classify different unhealthy odors from milk samples. The HP 4440 MS Sensor has been used to identify different origins of olive oil and coffee [90, 91].

A different application within this field of gas analysis, is the correction of signal drift of MS-based sensor by standard gas addition (SGA) [92, 93]. This method consists of introducing a gaseous He-Xe mixture continuously and independently of the carrier gas into the mass spectrometer source. The influence of the SGA signal correction on the discrimination power of the data is evaluated from the analysis of the species by the dynamic headspace coupled to mass spectrometry. SGA afforded a good correction of the main types of drift classically observed in mass spectrometry. A study on the use of different ionization techniques has been conducted by Marsai [94]. Marsai used an Agilent 4440 sensor in order to compare the positive chemical ionization (PCI) using methane or ammonia instead of electronic impact ionization (EI) during the classification of 8 different classes of methane groups. By the fact that chemical ionization is a technique softer than electronic impact ionization (EI) gives an opportunity to have a more selective mass spectrum; so the mathematical model derived is more rugged.

## Improving the performance of micro-machined metal oxide gas sensors: Optimization of the temperature modulation mode via pseudo-random sequences.

The gas chromatograph (GC) is very often combined with a mass spectrometer (GC-MS) for the separation and identification of compounds. After the separation step provided by the chromatographic column, the molecular mass and typical fragmentation of an unknown volatile can be obtained and compared with reference libraries [95, 96]. Infrared spectroscopy using Fourier transform methods can also be combined with a gas chromatograph (GC-FTIR). Due to its ability to differentiate between isomers, it can complement GC-MS [96]. To detect odors, the gas chromatographic separation of volatiles can be combined with sensory analysis of individual peaks, using a split gas-stream GC-technique [95]. In these cases, the injection port of the gas chromatograph is connected to the sensors chamber inside the chromatograph oven.

In the last few years, mass spectrometry-based e-noses (MS e-noses) are becoming an increasingly used alternative to gas sensor-based e-noses in food quality applications [97, 98]. The use of pre-concentration and extraction techniques such as solid-phase micro-extraction (SPME) have improved the sensitivity and reproducibility of MS e-noses [97, 99]. Solid phase microextraction (SPME) is an adsorption/desorption technique, developed in 1990 at the University of Waterloo (Canada) by Arthur and co-workers [100], that eliminates the need for solvents or complicated apparatus for concentrating volatile or nonvolatile compounds in headspace. For high accuracy and precision from SPME, consistency in sampling time and other sampling parameters is more important than full equilibration. By controlling the polarity and thickness of the coating on the fiber, maintaining a consistent sampling time and adjusting extraction parameters, an analyst can ensure highly consistent, quantifiable results from low concentrations of analytes. SPME provides linear results over wide concentrations of analytes [101-104] and is compatible with any packed column capillary gas chromatograph or gas chromatograph-mass spectrometer system. With SPME, the analytes are absorbed from the liquid or gaseous samples onto an absorbent-coated fused-silica fiber, which is part of the syringe needle, for a set time. The fiber is then inserted directly into a GC injection port for thermal desorption [105]. SPME is a solvent-free technique, which is sensitive because of the concentration factor achieved by the fiber and selective because of different coating materials that can be used. One of the advantages of SPME is that it can directly sample the vapor phase in equilibrium with the matrix (headspace - SPME).

E. Llobet and co-workers reported recently for the first time, on the design and use of two e-noses to assess rancidity directly from potato crisps, without any previous oil extraction step. This greatly simplifies sample preparation, avoids unwanted artifacts derived from oil extraction and speeds up the measurement process. The most accurate e-nose is based on SPME-MS [106].

## 2.2.5. Pre-treatment methods of gases before sensing.

Selectively permeable ceramic coatings can be used to increase the selectivity of sensor elements. The selective effect of these membranes is twofold. One mechanism is the specific adsorption of gas molecules at the membrane surface and the other is the size and chemistry dependent-diffusion through the membrane [107]. Additionally, the coating can be used as a protective shield against corrosive components present in the medium.

A deep investigation on the influence of membranes on the properties of coated gas-sensor can be found in [108]. The gas diffusion through the ceramic membrane is species-dependent (i.e., acts as a selective transport barrier) and the cross sensitivities to organic solvents are almost completely eliminated by covering the sensor structure with a porous layer of a refractory ceramic (e.g.  $\text{Al}_2\text{O}_3$  or even  $\text{Ga}_2\text{O}_3$ ). Selectively permeable  $\text{SiO}_2$  and  $\text{Al}_2\text{O}_3$  coatings to customize the selectivity and improve the stability of  $\text{SnO}_2$  conductivity sensors for the detection of organic gases in air were developed by Althainz and co-workers [109]. Park and co-workers [110] proved that depositing a catalytic filter layer over the  $\text{SnO}_2$  sensing element achieved the selectivity to a specific gas. Furthermore, using a  $\text{Nb}_2\text{O}_5$  filter layer, they fabricated hydrocarbon sensors and alcohol sensors with excellent selectivity. Portnoff and co-workers [111] proposed a catalytic filtering technology in which ambient gases must pass through a catalytic filter before reaching the active region of the sensing film in order to achieve selective sensing to combustible gases. They reported that the selectivity could be improved for the more thermochemically stable of the gases by properly selecting and preparing the catalytic material.

Feng and co-workers [112] also suggested that controlling the gas diffusion process, further improvement in selectivity could be achieved because of the difference in the diffusivities of various gases. In their work [113], Schwebel and co-workers shown that Au-dispersion within the membrane could considerably enhance the sensitivity to CO because the reactive solvents were burned and only the more stable CO was allowed to reach the sensor surface. The cross influence of ethanol was almost completely eliminated, with no deterioration on the response behavior of the CO sensor. Know and co-workers [114] reported a highly selective  $\text{C}_3\text{H}_8$  gas sensor by combining the filtering technology using Pd and Pt catalysts and the control of gas diffusion using a  $\text{SiO}_2$  insulating layer.

Dori and co-workers presented a prototype, based on solid state metal oxide gas sensors, suitable for the detection of benzene, toluene and xylene (BTX) compounds in the range of ppb [115]. Their objective was to achieve the same results as with a chromatograph, using a much cheaper system. The system follows a gas chromatographic approach, where a pre-concentration trap and a separation column are used together with a  $\text{SnO}_2$  thin film

## Improving the performance of micro-machined metal oxide gas sensors: Optimization of the temperature modulation mode via pseudo-random sequences.

sensor. Following this approach, benzene, toluene and xylene at very low concentrations (about 3 ppb) in gas mixtures that contained all three compounds, could be detected. A gas-phase chemical analysis system called  $\mu$ ChemLab<sup>TM</sup> was presented by Cernosek in [116]. The system consists of three micro-fabricated components: Firstly, a planar pre-concentrator using a low thermal-mass silicon nitride membrane, secondly, a spiral bulk micromachined gas chromatographic column and finally, an integrated surface acoustic wave (SAW) sensor array detector.

Pre-concentration techniques, like purge and trap or solid phase micro-extraction, can be used to improve the lack of selectivity of the electronic nose instead of the more common non-preconcentrated static headspace.

Purge and trap is one method for extracting and concentrating volatile organic compounds (VOCs). It was originally developed for the analysis of organic volatiles in water samples. Actually, this technique has already been used to improve the overall selectivity. This method was successfully employed as a filter for ethanol [116, 117], i.e. the ethanol contained in the samples was not adsorbed by the porous polymer material and, therefore, was not delivered to the sensors. Consequently, the sensors were not blinded by ethanol content and could respond to other components. The same technique was used by Aishima [118] as a pre-concentration method for coffee aroma with a laboratory-made instrument based on metal oxide sensors.

The analysis of volatile or semi-volatile organic environmental pollutants and many other samples usually begin by concentrating the analytes of interest through various techniques, such as headspace or purge-and-trap. These procedures typically require excessive time and complicated equipment. Seeing that Schaller and co-workers [119] studied for the first time the potential of use of both different techniques; purge and trap and at the same time SPME pre-concentration techniques, coupled to a mass spectroscopy-based electronic nose, presented in the previous subsection. They also compared these two techniques with non-pre-concentrated static headspace. They used these different methods to classify Swiss Emmental cheeses at four different ripening grades. The use of a pre-concentration technique was found to be helpful for this application, because it made possible to extract volatile compounds with higher molecular masses. Of the two systems tested, the SPME was considered by far the best method because of its better repeatability, its simplicity and its compatibility with an auto-sampler.

## **2.2.6. Use of sensor arrays together with techniques of pattern recognition.**

To improve the lack of selectivity experienced with gas sensors, a widely used strategy has been to construct multisensor systems. The success of artificial olfaction and gas analysis depends not only on the development of new sensor technologies, but also on the availability of powerful pattern recognition software.

In the different attempts to measure odors with electronic instruments, the earliest measurements were made in the beginning of the 1950s [8]. Persaud and Dodd [15] were in 1982, the first to use a small array of gas-sensitive metal oxide devices to classify odors. Since then, there has been a steady increase in the number of systems using gas sensor arrays with partially overlapped sensitivity [120-122]. The signals coming from gas sensors encode chemical information about the gas or gas mixture measured. Each sensor in the array defines an axis in a multidimensional space where gases can be represented as points positioned in this space, according to sensor responses. In order to clarify relationships in the multidimensional space of sensor response, pattern recognition use multivariate techniques.

The use of gas sensor arrays in e-nose and gas analyzers has been extensively studied in many different applications fields such as foodstuff, drinks, cosmetics and environmental monitoring [123-125]. Hong and co-workers [126] fabricated and characterized a portable electronic nose system using an oxide semiconductor gas sensor array and a back-propagation artificial neural network as pattern recognition engine. The sensor array consisted in six thick-film gas sensors (Pd-doped  $\text{WO}_3$ , Pt-doped  $\text{SnO}_2$ ,  $\text{TiO}_2\text{-Sb}_2\text{O}_5\text{-Pd}$ -doped  $\text{SnO}_2$ ,  $\text{TiO}_2\text{-Sb}_2\text{O}_5\text{-Pd}$ -doped  $\text{SnO}_2$  + Pd-coated layer,  $\text{Al}_2\text{O}_3$ -doped  $\text{ZnO}$  and PdCl<sub>2</sub>-doped  $\text{SnO}_2$ ). The portable electronic nose system comprised an Intel 80c196kc, an EEPROM that stored the optimized connection weights of the artificial neural network and a liquid crystal display (LCD) for displaying gas concentrations. The system was successfully applied to identify 26 CO/HC car exhaust gas mixtures in the concentration range CO 0 % / HC 0 ppm to CO 7.6 % / HC 400 ppm.

On the other hand, González and co-workers [127] proposed that the classification of different types of commercial vegetable oils could be realized, using an apparatus equipped with an array of six metal oxide semiconductor gas sensors (FOX 2000 Electronic Nose, from Alpha MOS). Llobet and co-workers [128] employed an array of four different inexpensive  $\text{SnO}_2$  gas sensors to analyze the state of ripeness of bananas. Also in reference [129], an olfactory system able to classify fruit samples (peaches, pears and apples) into three different states of ripeness (green, ripe and overripe) is reported. This system is based on a  $\text{SnO}_2$  gas sensor array and neural network pattern recognition techniques.

## Improving the performance of micro-machined metal oxide gas sensors: Optimization of the temperature modulation mode via pseudo-random sequences.

Using an array of commercial gas sensors (TGS 832, TGS 813 and TGS 800) and the discriminant factor analysis (DFA), Sarry and Lumbreras [130] classified CO, forane R134a and their mixtures. Szczurek and co-workers [131] used, with reasonable accuracy, a sensor array of four commercial, tin oxide based, semiconductor gas sensors (TGS 800) and a feed-forward neural network to classify and quantify mixtures of butanol/xylene and butanol/toluene.

The main criticisms to this approach are that the replacement of a single sensor in the array requires a complete retraining of the pattern recognition algorithms and that drift remains a problem that threatens accuracy.

### 2.2.7. Use of the dynamic operation mode.

A different strategy to increase the selectivity of gas sensors consists in operating them in the dynamic mode and characterizing their transient response. In this way new parameters are obtained, which are characteristic of the sensor and gases measured.

Basically the principal methods that have been developed to improve the performance of gas sensor via the dynamic operation mode are:

- AC operation mode
- Modulation of the gas concentration
- Modulation of the sensor operating temperature

The first of the methods, previously mentioned, consists of operating the sensors in AC mode. Measuring in AC mode has some advantages [132]:

- The signal to noise ratio is usually better, because narrow band amplification (either by filters or lock-in techniques) can be implemented and the 1/f noise component is less significant. Thus lower detection limits can be achieved.
- The usual drift effects are reduced as the sensitivity of detection for AC signals is generally more stable than the DC operation point.

Measuring in AC mode at different frequencies has been investigated as a method to dynamically characterize sensors. The plots of the real and imaginary components of the admittance versus frequency provide information about the different parameters that play a role in the sensor conduction mechanism. Gutierrez et al. [133, 134] have found that the peaks that appear in the impedance plots of tin oxide gas sensors in the presence of reducing gases are a function of the nature of the adsorbed species. Amrani et al. [135] have conducted research in the use of AC measurements of conducting polymer sensors in the presence of various chemical species. They showed that for a single sensor element, characteristic patterns can be found over a very wide frequency range.

The second strategy that has been employed is the so-called modulation of the gas concentration. This important approach may lie in the study of the dynamic processes that take place when analyte molecules interact (adsorption/desorption) with the sensor surface. Indeed, this method consists in the controlled modulation of the gas concentration, producing an output signal that contains information on the dynamic adsorption and desorption processes that take place in the sensor surface. Because of this, important information of these processes will be contained in the transient signals that are generated when the controlled modulation of a sensor input parameter is performed. The frequency spectrum of these transient signals should be a source of information containing details on the dynamics of the interaction process and have the potential for analyte identification.

Gouws et al [136] measured and analyzed methanol, toluene, chloroform, tetrahydrofuran, water and benzene using the concentration modulation technique. Quartz crystal microbalance (QCM) gas sensors were used in their study. Testing was performed in an onpurpose-built gas test system using computer-control of a series of mass flow controllers and valves to expose the sensors to controlled concentrations of selected analytes. The resonance frequency of a sensor was measured with resolution of  $\pm 0.5$  Hz at a sampling interval of 1 s by means of an on-purpose-built frequency counter. The concentration modulation was achieved by means of a fast-switching four port valve. Gas concentrations ( $N_2$  gas containing the analyte species and pure  $N_2$  gas) were balanced to prevent pressure transients from occurring on switching. Four modulation cycles (i.e. modulation cycle of 30 and 60 s consisted an adsorption half-cycle followed by a desorption half-cycle) were performed for each analyte.

The transient behavior of gas sensors in response to abrupt changes in the gaseous concentration have been studied and modeled in previous works [137-140]. It has been demonstrated that the study of the dynamic sensor response allows for increasing the selectivity of a sensor array [141-143].

Even though, the controlled modulation of vapor concentration to a QCM gas sensors (among other types of gas sensors) have given excellent results on vapor classification, this strategy requires a difficult gas/gases measurement system and because this, it is difficult to apply and use in practice.

As was mentioned above, many authors have reported strategies based on modulating the analyte concentration [138, 139]. According to this, Brezmes et al [144] introduced for the first time a simple method that, combining simultaneously both effects, analyte concentration modulation and working temperature modulation. This strategy has the potential of increasing the resolving power of metal oxide sensors. Furthermore, its simplicity makes it especially suited for low-cost applications. The approach involves a flow modulation of

## Improving the performance of micro-machined metal oxide gas sensors: Optimization of the temperature modulation mode via pseudo-random sequences.

contaminated air through a sensor chamber. In this manner temperature and concentration modulations are achieved indirectly. By changing flow rate periodically, local differences in the concentration of the species being measured are generated. The gas sensor responses are analyzed by means of the FFT or discrete wavelet transform.

An alternative dynamic strategy to try to overcome the drawbacks experienced with gas sensors in general and metal oxide gas sensors in particular (i.e. poor selectivity, sensor drift and low repeatability) is the so-called modulation of the sensor working temperature. In the last years, modulating the working temperature of metal oxide gas sensors has been one of the most used methods to enhance sensor selectivity. It is well known that when the working temperature of a gas sensor is modulated, the kinetics of the gas-sensor interaction is altered and this leads to characteristic response patterns. As the sensor response is different at different working temperatures, measuring the sensor response at  $n$  different temperatures is similar to the use of an array comprising  $n$  different sensors. This allows for measuring multivariate information from every single sensor and helps in keeping low the dimensionality of the measurement system needed to solve a specific application.

Many authors have introduced different methods to process the multivariate information from temperature modulated micro-hotplate sensors. Since the results obtained using this strategy have been very promising, and the principal aim of this doctoral thesis is the optimization of the selection of temperature modulation frequencies, a review of the state of the art in temperature modulated metal oxide gas sensors is given in the next sub-section.

### **2.3. Temperature modulation for selectivity enhancement.**

In this sub-section, the different strategies of temperature modulation that have been implemented to increase sensor selectivity are revised and discussed.

Early developments did not consist in a proper temperature modulation of the sensor but in its operation at different temperature levels. Clifford [145, 146] appears to be the first researcher to investigate the dynamic change of sensor conductance for individual temperature steps at several different oxygen partial pressures. He used a barrier layer theory [147] to explain the effect of temperature on the sensor response. According to the barrier layer theory, two factors, bulk conductance and the surface concentration of ionosorbed oxygen, change the macroscopic conductance of a  $\text{SnO}_2$  film. Clifford also concluded that selective gas detection could be accomplished using either many sensors at different but fixed temperatures, or by sequential operation of a single sensor at several temperatures. Le Vine [148], Eicker [149] and Owen [150] patented temperature-cycling methods to enhance the selectivity of metal oxide gas sensors to carbon monoxide. CO can be easily oxidized on



the surface of the metal oxide. Therefore, in a first phase, CO is measured when the sensor is operated at a low temperature (e.g. 30 or 150°C), since this measurement is less prone to interference from other gases that are oxidized at higher temperatures (e.g. methane). In a second phase, the temperature of the sensor is significantly raised (e.g. 400 °C) for the surface of the sensor to be purged of adsorbed gases during the low-temperature phase.

The first researchers to use a square wave as the supplying voltage to the sensor heating element were Advani and co-workers [151] in 1983. They measured and compared the values of the sensor conductance at two temperature levels during their thermal cycle, in order to classify and quantify hydrogen sulfide (H<sub>2</sub>S) with a single gas sensor.

Similarly, Lantto and Romppainen [152] developed temperature-cycling methods (i.e. square voltage wave to vary the sensor working temperature between 160 and 380°C) to selectively detect hydrogen sulfide. Like carbon monoxide, hydrogen sulfide can be oxidized at low temperature on the tin oxide surface and this fact is used to discriminate H<sub>2</sub>S from other species such as alkanes and alcohols (but not from CO). Although Lantto [152] mentions that H<sub>2</sub>S concentration plays an important role in the response shape of the temperature-cycled sensor, the selective detection of H<sub>2</sub>S in a wide range of concentrations is not discussed. Bukowiecki and co-workers [153] were the first to introduce a proper temperature modulation of the sensor by testing different modulating waveforms (e.g. triangular, saw-tooth and asymmetrical square waves). Their objective was to discriminate ammonia, methane, hydrogen and carbon monoxide using tin oxide gas sensors. Once again, the stress was put on obtaining different response patterns for the different gases considered, but the problem of changes in the concentration of the gases tested is not addressed.

Sears and co-workers [154] were the first to address the problem of changes in the response of temperature-cycled sensors to variations in the concentration of the gases studied. A square voltage waveform of period equal to 50 s was applied to the heating resistor of a commercially available Taguchi gas sensor [155]. They studied the transient response of the temperature-cycled sensor to propane, carbon monoxide, hydrogen, ethanol and acetone in a wide range of concentrations and found that most of the gases had characteristic peaks both at the initial phase of sensor heating and cooling (see Figure 2.7). The height of these peaks was related to gas concentration and this information was used to define criteria to be used for improving the selectivity of detection. Hirakana and co-workers conducted in [156] a similar study using a step change in the heater voltage of different TGS sensors where they studied the transient conductance during the cooling phase. Once again, they observed peaks that were related to the gas species. In [157, 158] an encapsulation method for the gas sensor is introduced in a way that the flow of gas reaching the sensor is

Improving the performance of micro-machined metal oxide gas sensors:  
 Optimization of the temperature modulation mode via pseudo-random sequences.

restricted (e.g. the gas can only enter during the cooling part of the cycle). This result in an enhanced selectivity among the different gases studied.

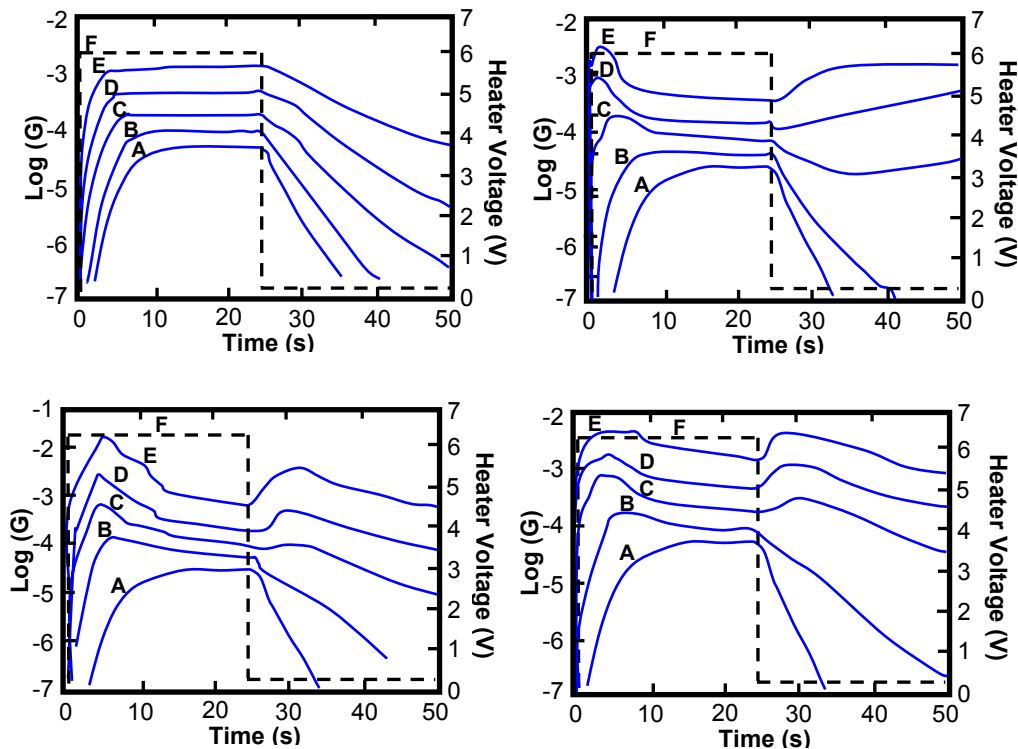


**Figure 2.7:** Logarithm of the conductance (in S) for a tin oxide sensor as a function of cycle time for various concentrations of (from top left, clockwise) propane, carbon monoxide, hydrogen and ethanol: (A) clean air, (B) 10 ppm, (C) 80 ppm, (D) 500 ppm, (E) 5000 ppm, (F) heater voltage. Figure adapted from reference [155].

Sears and co-workers also studied the potential of using a sinusoidal waveform to drive the sensor heating element with respect to increased sensor selectivity [159]. They applied a sinusoidal voltage varying between 0.2 and 7.2 V, with a period between 10 and 200 s, to a tin oxide palladium-doped TGS 812 sensor. They found that both the range of temperature cycling and period of the cycle had a critical effect on the information that could be extracted from the conductance transients in the presence of ethanol, carbon monoxide and propane. Figure 2.8 shows the effects of varying both the maximum temperature and cycle period on the response to ethanol of a tin oxide TGS sensor.

As the maximum temperature increases, two peaks in the conductance curves develop, one on the heating and one on the cooling half-periods of the temperature-modulating signal.

The valley that appears near the maximum temperature represents a loss of response related to reaction rate. Figure 2.8 shows that as the period of the modulating signal increases, more features appear in the conductance transient. If the modulating frequency is too high, the response may not be able to follow these changes either due to the thermal inertia of the substrate or to the slow chemical kinetics of the reactions at the sensor surface.

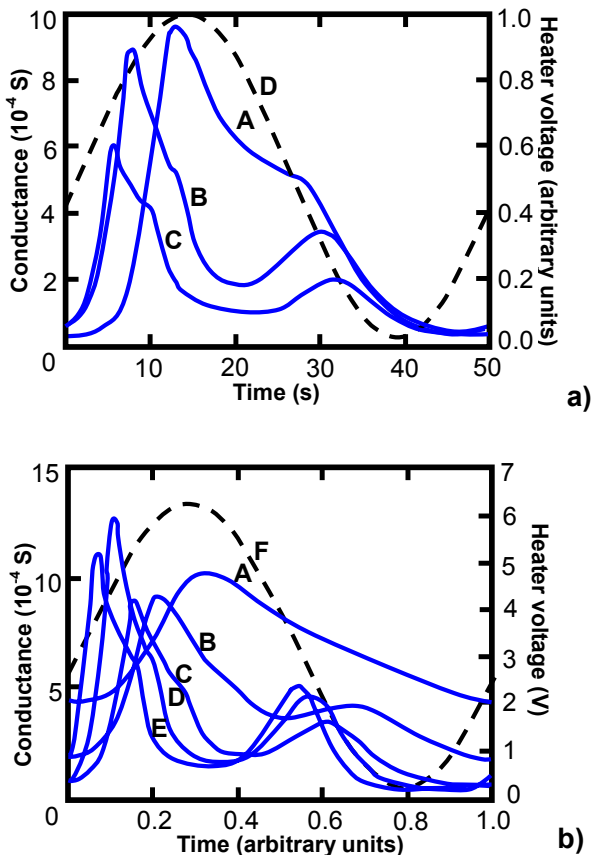


**Figure 2.8:** a) Conductance of a tin oxide sensor as a function of time under a range heater voltages between 5.0 and 7.2 V (i.e. different operating temperatures) in 200 ppm of ethanol. b) Conductance of a tin oxide sensor as a function of relative time with a period between 10 and 200. Figure adapted from [159].

Sears and co-workers [160] were also the first to introduce Fourier transform techniques to extract multi-dimensional information from temperature-cycled gas sensors. They cycled different tin oxide based Taguchi gas sensors by applying a square waveform (between 0 and 5 V) with a period of 50 s to the sensors' heating elements. For each gas and concentration tested, the sensors were allowed to reach a steady-state thermal cycle (usually in two or three

## Improving the performance of micro-machined metal oxide gas sensors: Optimization of the temperature modulation mode via pseudo-random sequences.

cycles), then the conductance transient was sampled (256 data points were taken over a 50 s period). Since different gases gave different conductance shapes under thermal cycling, it was assumed that the fast Fourier transform (FFT) would help in discriminating between the gases. The d.c. component and the first harmonic of the transform were analyzed. The d.c. component is merely an average of the sampled conductance transient and therefore, approximately follows a power-law dependence with gas concentration, which is usual in tin oxide gas sensors.

However, the authors describe a number of serious limitations for their method such as the complexity of calibration (e.g. simple gas mixtures result in involved response patterns) and sensor drift or ambient humidity interference that can significantly affect the d.c. component and first harmonic of the FFT, destroying the discrimination ability.

Seeing previous effects presented, and based on the idea of Sears [160], Nakata and co-workers in a series of articles beginning in 1991 [161-174] published the results of experiments in which they applied a sinusoidal voltage with a frequency of 0.02 – 0.04 Hz to the heater of a tin oxide TGS 813 gas sensor and analyzed the value of the resistance as a function of time. The sensor response was transformed to the frequency domain by applying the FFT. They used various values of the real and imaginary components to discriminate between the gases analyzed. The authors related the values of the high harmonics of the FFT to the characteristics of the molecular structure of the gases. For example, the relative amplitudes of the real part of the first three harmonics increased with chain length for saturated hydrocarbons. In this way it was possible to distinguish the individual responses of the individual gases from the dynamic response of the gas mixture and that is why they claimed that the quantitative discrimination between gas mixtures was enabled by using the higher harmonics of the FFT.

The work of Nakata and co-workers indicates that a quantitative analysis of gas mixtures or the analysis of a gas in the presence of an interfering species would be possible, even using a single temperature-cycled semiconductor gas sensor. However some important aspects as non linearity's presence, sensor drift and noise in gas sensors, remain un-addressed. Furthermore, ceramic sensors deposited on a substrate with high thermal inertia (e.g. TGS sensors) do not seem the best candidate sensors for an effective temperature cycling. Under these conditions extremely low modulating frequencies are used, which results in long, unpractical, measurement times.

With the development of microsystem technology, the availability of micromachined substrates for metal oxide gas sensors implied that sensors had their operating temperature modulated in a more efficient way. Cavicchi and co-workers introduced the use of micromachined tin oxide gas sensors in temperature modulation applications [49, 175-176].

Micromachined devices comprise an inert micro-hotplate substrate with a heating resistor sandwiched between two thin silicon oxide (or silicon nitride) layers and a pair of electrodes on top. Finally, the gas sensitive film is deposited onto the electrodes. The membrane thickness is typically about 1  $\mu\text{m}$  which cause a thermal response in the range of milliseconds, favorably comparable with the thermal response of seconds found in conventional sensors.

Cavicchi and co-workers applied a sequence of temperature pulses of fixed duration and monotonically increasing height to a micromachined sensor. They acquired the sensor conductance between pulses, while the sensor and the sample were approximately at room temperature. This approach is better than using a simple temperature ramp because it avoids masking surface chemical effects (important for gas identification) by thermally activated processes (that cause changes in carrier density or mobility). They tested acetone, formaldehyde, ethanol and methanol while the sensor was under the effect to a train of 100 ms temperature pulses at 8 temperatures ranging from 20 to 370  $^{\circ}\text{C}$ . Response is showed on Figure 2.9, where methanol and ethanol patterns are very similar, while clear differences arise for acetone and formaldehyde patterns. This group has also investigated different pattern recognition techniques to process the response of the temperature-modulated micro-hotplates [177]. The aim was to discriminate acetone, formaldehyde, ethanol and methanol using a single sensor. The signal processing methods used were the Gram-Schmidt approach, the FFT and the Haar wavelet transform [178]. Cavicchi and co-workers [177] selected the Haar function as analyzing wavelet because it was simple and because its shape (i.e., a pulsed signal) seems appropriate for their pulsed temperature modulation. However, the effect of varying the concentration of the different analytes, which is a key factor to determine whether a correct identification of the different species is possible, is not considered in the work presented.

Heiling and co-workers [179] were the first to show that a quantitative analysis of gases was possible with temperature modulated gas sensors. They used a 50 mHz sinusoidal modulating voltage (i.e. modulation ranging from 200 and 420  $^{\circ}\text{C}$ ) and tin oxide micro-hotplate sensors to analyze carbon monoxide and nitrogen dioxide. They used spectral analysis (i.e. the d.c. component, the fundamental frequency component and the first 4 harmonics of the FFT) to extract important information from the sensor transient response. A multilayer perceptron (MLP) neural network was trained and validated to identify and quantify carbon monoxide and nitrogen dioxide. While the gases and gas mixtures could be perfectly discriminated, the quantitative prediction was not so good possibly because of the limited number of measurements available. A similar method but applying a pulsed

## Improving the performance of micro-machined metal oxide gas sensors: Optimization of the temperature modulation mode via pseudo-random sequences.

temperature modulation to discriminate CO in the presence of methane, H<sub>2</sub> and moisture [55] was used by the same group.

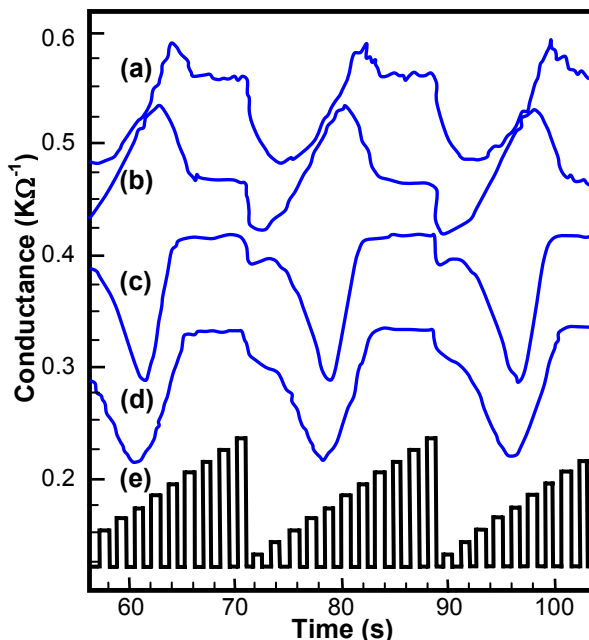


**Figure 2.9:** Conductance of a Pd-doped tin oxide micro-hotplate gas sensor to (a) acetone, (b) formaldehyde, (c) ethanol, (d) methanol during the temperature sequence schematically illustrated in (e). From [176].

Later, Kato and co-workers [180] used the same approach introduced by Heiling in [179] to identify and quantify methanol, ethanol, acetone, diethyl ether, benzene, iso-butane, ammonia and ethylene with promising results. In a similar application, (i.e., the detection of CH<sub>4</sub> and CO in domestic premises) S. Marco and co-workers [181] developed an intelligent detector based on micromachined metal oxide gas sensors. A triangular waveform was applied to modulate the operating temperature of the sensors and the FFT was used to extract features (first eight harmonics) from the response transients. Linear cluster analysis and the SOM neural network were the methods selected to perform data analysis. The system intelligence (i.e., FFT, SOM neural networks and classification algorithms) was implemented on a DSP platform that allows a real-time implementation of the algorithms.

More recently, Llobet and co-workers [182-185] studied the use of alternative feature extraction and pattern recognition methods applied to micromachined and non-micromachined SnO<sub>2</sub> and WO<sub>3</sub> based gas sensors to perform accurate qualitative and quantitative analysis of gases and mixtures (i.e. CO and NO<sub>2</sub> and different concentrations).

The FFT and the DWT were used to extract features from the response of the temperature modulated sensors. These methods were coupled with principal component analysis (PCA) to classify the response patterns. When a SnO<sub>2</sub> micro-hotplate gas sensor was used [182], its operating temperature was modulated between 200 and 420 °C by applying a 50 mHz sinusoidal signal to the heater. The FFT was computed and the d.c. component and the first 5 harmonics were extracted. The DWT was computed on a single period of the response signal using the 4th order Daubechies (db4) as analyzing wavelet. PCA was the pattern recognition method chosen to classify the different gases and gas mixtures analyzed, and the DWT led to a better separation than FFT. Principal component regression (PCR) and partial least square (PLS) were used to build regression models. As PCR and PLS are linear regression methods, failed to accurately predict the concentration of CO and NO<sub>2</sub>. Therefore, MLP networks (i.e., a non-linear method) were used to simultaneously identify and quantify the gas mixtures analyzed. A 10-fold bootstrap cross-validation technique was used to obtain better estimates of the quantification performance of the network.

The effects produced by the presence of humidity (i.e.0 and 50% R.H) on the discrimination of CO and NO<sub>2</sub> at different concentration with a single resistive gas sensor working under the temperature modulation mode was analyzed in [186] by the same authors. The species were classified with a success rate of 91.1 % and 87.5 % (at 0 and 50 % of RH respectively) using a RBF neural network. That means that temperature modulation help fighting moisture interference.

More recently, Gardner and co-workers [187, 188] introduced a support vector machine (SVM) as an alternative pattern recognition method for temperature modulated sensors to identify and predict the concentration of CO and NO<sub>2</sub>. The gas sensor working temperature was modulated by a sinusoidal voltage, and features from the response transients were extracted by the DWT using the Daubechies family as analyzing wavelet. SVM can be used to classify data into different groups. The same author found that using a reduced set of 10 wavelet coefficients extracted from the response transients and a SVM, the concentrations of CO and NO<sub>2</sub> could be predicted with an error lower than 5%.

Maziarz and co-workers in [189] suggested the use of fuzzy logic to process the dynamic response of a temperature modulated semiconductor gas sensor. The idea of using fuzzy logic to quantify gases was first introduced by Yea and co-workers [190] where, in their method, the steady-state sensor signal was the only input to the fuzzy system. Now Maziarz applied a 40 mHz sinusoidal voltage (i.e. range of temperature change near 100 °C) to the heating element of a thin Sb-doped SnO<sub>2</sub> gas sensor. Ethanol diluted in air was measured at concentrations varying from 0 to 450 ppm with 30 ppm steps, and each concentration was measured at different relative humidities (10, 25, 50, 75 and 100 %). Features from the

## Improving the performance of micro-machined metal oxide gas sensors: Optimization of the temperature modulation mode via pseudo-random sequences.

sensor responses in the presence of ethanol and humidity were extracted by the FFT. The d.c. component and the first three harmonics were retained for further processing by a fuzzy model based on Tagaki-Sugeno-Kang (TSK) theory [191]. The complete dataset was split in training and validation sets. For measurements in the test set, the RMS error in the prediction of ethanol concentration was below 11.5%. This error can be considered as moderate considering that relative humidity varied in a wide range (between 10 and 100%).

A. Gramm and co-workers [192, 193] used two temperature cycled metal oxide sensors and hierarchical classification (i.e., decision trees) to identify six organic solvents (benzene, isopentane, diethyl ether, methyl 4-butyl ether, propylene oxide and methyl alcohol) while relative humidity varied between 30 and 70 %. Features from the sensor transients were extracted by the FFT, the DWT and by direct generation of secondary features that were descriptive of the transients such as the slope after a temperature change, mean value at a constant temperature set point, etc. Therefore, not all classes are separated in one step but subgroups are defined which are further discriminated by using different approaches.

R. Gutierrez-Osuna and co-workers [194] investigated the use of a staircase waveform (i.e., a series of step inputs at increasing voltage levels) applied to the sensor heating element, and evaluated four different transient analysis techniques (Pade-Z-transform, mutiexponential transient spectroscopy (METS), window time slicing (WTS) and ridge regression) on the basis of their ability to extract response features that improve sensor selectivity.

## **2.4. On the optimization of the temperature-modulating signals.**

Although the results reached are very promising, in most of the works cited above the selection of the waveform and frequencies used to modulate sensor temperature has been conducted in a non-systematic way. Since this selection is based in a trial and error procedure, there is no way to ensure that the optimal modulation frequencies were chosen for a given application. That is why, in this thesis we introduce a method, borrowed from the field of system identification, to systematically study the effect of modulation frequencies in the discrimination and quantification ability of metal oxide based micro-hotplate gas sensors. Using this method, the optimal set of modulating frequencies can be determined for a given gas analysis application. Some authors have addressed this problem by suggesting different optimization strategies.



### 2.4.1. Initial methods.

A. Fort and co-workers [195, 196] used temperature modulated metal oxide gas sensors (using a pure sinusoidal signal) to show that the selection of the signal frequency was of paramount importance for gas identification. If the temperature of the sensors is varied fast in comparison with the chemical response time, the sensor resistance varies as a function of temperature with an exponential law (characteristic of metal oxides). In such case the response shape has only a slight dependence on the chemical environment. On the other hand, when the operating temperature varies slowly compared to chemical response time, the response profile is given by a series of quasi-stationary chemical responses. The best discrimination among the species studied (vapors from water solutions containing ethanol and other volatile organic compounds) was obtained by selecting a temperature profile with a period near the chemical response time of the sensor. These results suggest that the effectiveness of the temperature modulation analysis depends on the period of the sine wave that must be chosen in agreement to the chemical reaction rate of each sensor. Similar results were found by other authors using different temperature modulation signals such as pulse, trapezoid, triangular and saw-tooth [197, 198]. By checking different modulation frequencies (50, 30, 40 and 20 mHz), Huang and co-workers showed in [198] that as the modulating frequency was lowered down to 20 mHz, specific response patterns developed.

### 2.4.2. Optimization using dynamic models.

Despite all this above cited attempts, one question remains unanswered: given a metal oxide gas sensor, how does one select the best temperature profile for fast and reliable discrimination of chemical species? Cavicchi and co-workers [199] developed a method to optimize temperature-programmed sensing with micro-hotplate gas sensors. In temperature programmed sensing, a sequence of pulses of increasing amplitudes is input to the heating element of the micro-hotplate and sensor resistance is acquired at room temperature (i.e., between two consecutive pulses). The objective was to optimize the sequence by adapting pulse amplitude, pulse duration, delay between two consecutive pulses and number of pulses in a cycle to better discriminate between ethanol and methanol vapors. In a first step, black-box dynamic models based on input-output data were developed for predicting sensor responses in the presence of ethanol and methanol for a given temperature profile. Among the different dynamic modeling methods studied, the wavelet network method was the most accurate. The wavelet network (WNET) combines the multi-resolution feature of the wavelet transform with neural networks (one hidden layer). Such a network is able to approximate

Improving the performance of micro-machined metal oxide gas sensors:  
 Optimization of the temperature modulation mode via pseudo-random sequences.

any function to an arbitrary accuracy [200]. In this particular case, the Mexican hat wavelet was used as analyzing wavelet and coefficients from the first four scales were selected by stepwise selection to form the initial model structure.

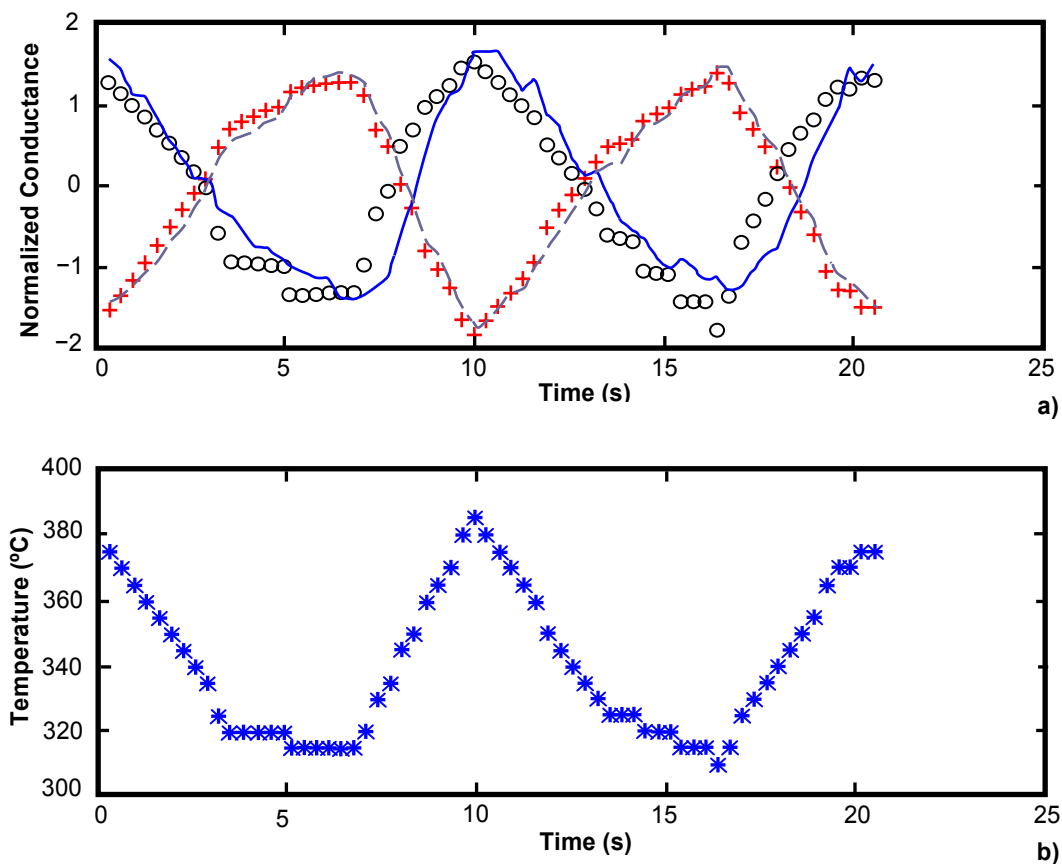


**Figure 2.10:** (a) Actual experiments in methanol (solid line) and ethanol (dashed line) gases, model predictions are shown by circles for methanol and plus for ethanol models; (b) the optimum temperature profile derived from the off-line optimization process. Figure adapted from ref. [199].

This initial model was further trained to set parameter values of the neural network. The predictive models of ethanol and methanol were used in an off-line optimization scheme, where an optimal temperature profile for vapor discrimination was computed and validated. Given a temperature profile  $u$ ,  $y^{\text{MeOH}}$  and  $y^{\text{EtOH}}$  are the conductance responses predicted by the WNET models for methanol and ethanol, respectively. Since the predicted responses for each gas are functional mappings that depend on the temperature profile  $u$ , the optimization

can be formulated as finding  $u$  that maximizes the distance between  $y^{\text{MeOH}}$  and  $y^{\text{EtOH}}$ . The metric used to quantify this distance is the normalized sum of squared differences (NSSD) between two response curves:

$$\text{NSSD} = \sum_{i=1}^n \left( y_i^{\text{MeOH}} - y_i^{\text{EtOH}} \right)^2 / n \quad (2.1)$$

where  $n$  is the number of temperature pulses in a cycle.

The search space for the optimal temperature profile is over a limited subset of realizable temperature pulses (e.g., lower and upper limits are chosen based on the sensor structure) and under the constraint that two consecutive pulses cannot differ in more than 40°C (to avoid drastic changes in the surface). Figure 2.10 shows the optimal temperature profile to discriminate ethanol and methanol that was computed and validated through experimental measurements. This temperature profile produces methanol and ethanol responses that are out of phase (i.e., easy to discriminate). Although this methodology is systematic and should be extensible to other analytes, its application to the qualitative and quantitative analysis of multi-component mixtures is not straightforward. The fact that the method relies in the building of good predictive response models complicates the optimization process for multi-gas, concentration variant environments.

## 2.5. Conclusions.

This section summarizes what has been revised in this chapter and puts the stress on some important issues that still remain unsolved in the field of temperature modulated gas sensors. These issues are expected to continue deserving the interest of the research community during the next years.

This chapter begins with a brief introduction to the sense of smell. A comparison between humans and artificial systems are exposed in Section 2.1. On the other hand the history of electronic nose is included in Section 2.2.1, while in Section 2.1.3 a brief overview of multi-sensors gas analyzer systems are briefly described.

Furthermore this chapter (Section 2.2) reviews the various strategies used by different research groups in order to enhance the selectivity of metal oxide gas sensors. These include the improvement of the sensitive material (Section 2.2.2), alternative methods for the analysis of chemical compounds and new methods of conditioning and pretreatment of gas mixtures before sensing (Section 2.2.3 and 2.2.4 respectively), the use of sensor arrays

## Improving the performance of micro-machined metal oxide gas sensors: Optimization of the temperature modulation mode via pseudo-random sequences.

together with techniques of pattern recognition (Section 2.2.5), and measurements performed in the dynamic operation mode (Section 2.2.6).

Additionally a review of the temperature modulation for selective enhancement in gas sensors is presented in Section 2.3. Therein were reviewed from early works of temperature modulation (applied to TGS commercial gas sensors) until the most recently ones where temperature modulation is applied to micromachined gas sensors, which have membranes with thermal responses in the range of milliseconds, seem more appropriate for being operated in this operation mode. Furthermore, different methods to extract and process features from temperature modulated gas sensors (e.g. window time slicing, frequency domain methods like Fourier transform and mixed methods like discrete wavelet transform) have been introduced in this section.

Finally, it is important to mention that, although the results obtained by temperature modulation of metal oxide gas sensors, and the methods and techniques discussed above, have been very promising, the use of modulating frequencies still remains an empirical method. That is why, in this thesis a method, borrowed from the field of system identification, to systematically study the effect of modulation frequencies in the discrimination and quantification ability of metal oxide based micro-hotplate gas sensors was introduced. Using this method, the selection of the optimal set of modulating frequencies is ensured and can be determined for a given gas analysis application. Some authors have addressed before this problem by suggesting different optimization strategies. Section 2.4 summarizes these strategies.

## 2.6. References.

- [1] R. Axel, "The molecular logic smell", *Sci. Am.*, vol. 273, pp.154-159, 1995.
- [2] Kandel E. R., Schwartz, J. H. & Jessell T. M., "*Principios de neurociencia*", Capítulo 32: Olfato y gusto: los sentidos químicos, pp. 625-647, McGrawHill: Madrid, 2001.
- [3] J. E. Moore, J. W. Johnston and M. Rubin, "The stereochemical theory of odour", *Sci. Am.*, vol. 210, pp. 42-49, 1964.
- [4] J. S. Kauer, "Contributions of topography and parallel processing to odour coding in the vertebrate olfactory pathway", *Trends Neuroscience*, vol. 14, pp. 79-85, 1991.
- [5] D. schild (ed.), "Chemosensory information processing", NATO ASI series H: cell biology, vol. 39, Springer, Berlin, 1990.
- [6] M. Meredith, "Neural circuit computation: complex patterns in the olfactory bulb", *Brain Res. Bull.*, vol. 29, pp. 111-117, 1992.
- [7] G.H. Dodd, P. N. Bartlett and J. W. Gardner, "Odours – The stimulus for an electronic nose", in J. W. Gardner and P. N. Bartlett (eds.), "*Sensors and Sensory for an Electronic Nose*", NATO ASI Series E: Applied Sciences, Vol. 212, Kluwer, Dordrecht, Ch., vol. 1, 1992.
- [8] J. W. Gardner, P. N. Bartlett, "*Electronic noses principles and applications*", Oxford University press, 1999.
- [9] H. Zwaardemaker, F. Hogewind, "On spray-electricity for an waterfall- electricity", *Proc. Acad. Sci. Amst.*, vol. 22, pp. 429. 437, 1920.
- [10] J. D. Hartman, "A possible objective method for the rapid estimation of flavors in vegetables", *Proc. Am. Soc. Hort. Sci.*, vol. 64, pp. 335, 1954.
- [11] W. F. Wilkens and J. D. Hartman, "An electronic analogue for the olfactory process", *Ann. NY Acad. Sci.*, vol. 116, pp. 608-612, 1964.
- [12] R. W. Moncrieff, "An instrument for measuring and classifying odours", *J. Appl. Physiol.*, vol. 16, pp. 742, 1961.
- [13] T. M. Buck, F. G. Allen and M. Dalton, "Detection of chemical species by surface effects on metals and semiconductors", in T. Bregman and A. Dravenieks (eds.), "*Surface Effects in detection*", Spartan Books Inc., USA, 1965.

Improving the performance of micro-machined metal oxide gas sensors:  
Optimization of the temperature modulation mode via pseudo-random sequences.

- [14] A. Dravenieks, and P. J. Trotter, "Polar vapour detection based on thermal modulation of contact potentials", J. Sci. Instrum., vol. 42, pp. 624, 1965.
- [15] K. Persaud and G. H. Dodd, "Analysis of discrimination mechanisms of the mammalian olfactory system using a model nose", Nature, vol. 299, pp. 352-355, 1982.
- [16] A. Ikegami and M. Kaneyasu, "Olfactory detection using integrated sensors", Proc. 3<sup>rd</sup> Int. Conf. Solid.State Sensors and Actuators (Transducers'85), Philadelphia, PA, USA, 7-11, pp. 136-139, June 1985.
- [17] M. Kaneyasu, A. Ikegami, H. Arima and S. Iwanga, "Smell identification using thick-film hybrid gas sensors", IEEE Trans. Components, Hybrids Mnufact. Technol., CHMT., vol. 10, 1987.
- [18] J. W. Gardner, "Pattern recognition in the Warwick Electronic Nose", 8<sup>th</sup> Int. Congress of European Chemoreception Research Organisation, University of Warwick, UK, July 1987.
- [19] D. Schild (ed.), "Chemosensory Information Processing", NATO ASI Series H: Cell Biology, vol. 39, Springer, Berlin, 1990.
- [20] J. W. Gardner, P. N. Bartlett, G. H. Dodd and H. V. Shurmer, "The design of an artificial olfactory system", In D. Schild (ed.), "*Chemosensory Information Processing*", NATO ASI series H: Cell Biology, vol. 39, Spronger, Berlin, pp. 131-173, 1990.
- [21] NATO Advance Research Workshop, Reykjavik, Iceland, August 1991, J. W. Gardner and P. N. Martlett (eds), Sensors and Sensory Systems for an Electronic Nose, NATO ASI Series E: Applied Sciences, vol. 212, Kliwer, Dordrecht, 1992.
- [22] J. W. Gardner, P. N. Bartlett, "A brief history of electronic noses", Sensors and Actuators B, vol. 18-19, pp. 211-220, 1994.
- [23] J. W. Gardner, P. N. Bartlett, "Pattern recognition in gas sensing", In Adam Hilger, Bristol, "*Techniques and mechanisms in gas sensing*" (ed. P. Moseley, J. Norris, and D. Williams), pp. 347-380, 1991.
- [24] S. Vaihinger, and W. Göpel, "Multicomponent analysis in chemical sensing", VCH Weinheim, Sensor: a comprehensive Study: Vol. 2/3, chemical sensors (ed. W. Göpel, T. A. Jones, M. Kleitz, I. Lundström, and T. Seiyama), pp. 191-237.
- [25] F. Davide , C. Di Natale, A. D'Amico, "Redundancy in sensors arrays", Sensors and Actuators A, vol. 37-38, pp. 296-300, 1993.

- [26] B. Borrounet, T. Talou, A. Gaset, "Application of multigas sensor device in the meat industry for boat-taint detection", *Sensors and Actuators B*, vol. 26-27, pp. 250-254, 1995.
- [27] M. Schweizer-Berberich, S.-Vaihinger, W. Göpel, "Characterization of food freshness with sensors arrays", *Sensors and Actuators B*, vol. 18-19, pp. 282-290, 1994.
- [28] J.-S. Shih, A. I. Popov, "K-39 and C-13 NMR studies of potassium, cryptates in nonaqueous solution", *Inorg. Chem.*, vol. 19, pp. 1689, 1980.
- [29] J.-S. Shih, "Applications of macrocyclic polyethers in analytical sensors and ion separation", *J. Chin.Chem. Soc.*, vol. 41, pp. 309-314, 1998.
- [30] C.-W. Kuo, J.-S. Shih, "Cryptan/metal ion coated piezoelectric quartz crystal sensors with artificial back propagation neural networks analysis for nitrogen dioxide and carbon monoxide", *Sensors and Actuators B*, vol. 106, pp. 468-476, 2005.
- [31] P. Ivanov, M. Stankova, E. Llobet, X. Vilanova, J. Brezmes, I. Gràcia, C. Cané, J. Calderer and X. Correig, "Nanoparticle metal-oxide films for micro-hotplate-based gas sensor systems", *IEEE Sensors Journal*, vol. 5, (5), pp. 798-809, October 2005.
- [32] Manuele Bicego, G. Tessari, G. Tecchiolli, M. Bettinelli, "A comparative analysis of basic pattern recognition techniques for the development of small size electronic nose", *Sensors and Actuators B*, vol. 85, (1-2), pp. 137-144, 2002.
- [33] Manuele Bicego, V. Murino, M. Figueiredo, "Similarity-based classification of sequences using hidden Markov models", *Pattern Recog.*, vol. 37, (12), pp. 2281-2291, 2004.
- [34] Manuele Bicego, V. Murino, M. Figueiredo, "Similarity-based clustering of sequences using hidden Markov models", in: P. Perner, A. Rosenfeld (Eds.), *Machine Learning and Data Mining in Pattern Recognition*, vol. LNAI2734, Springer, pp. 86-95, 2003.
- [35] Manuele Bicego, "Odor classification using similarity-based representation", *Sensors and Actuators B*, vol. 110, pp. 225-230, 2005.
- [36] A.M. Taurino, C. Distanto, P. Siciliano, L. Vasanelli, "Quantitative and qualitative analysis of VOCs mixtures by means of a microsensor array and different evaluation methods", *Sensors and Actuators B*, vol. 93, pp. 117-125, 2003.
- [37] M. Penza, G. Cassano, "Application of principal component analysis and artificial neural networks to recognize the individual VOCs of methanol/2-propanol in a binary

Improving the performance of micro-machined metal oxide gas sensors:  
Optimization of the temperature modulation mode via pseudo-random sequences.

- mixture by SAW multi-sensor array”, *Sensors and Actuators B*, vol. 89, pp. 269-284, 2003.
- [38] Dae-Sik Lee, Jong-Kyong Jung, Jun-Woo Lim, Jeung-Soo Huh, Duk-Dong Lee, “Recognition of volatile compounds using SnO<sub>2</sub> sensor array and pattern recognition analysis”, *Sensors and Actuators B*, vol. 77, pp. 228-236, 2001.
- [39] René Knake, Renato Guchardi, Peter C. Hauser, “Quantitative analysis of gas mixtures by voltammetric sensing”, *Analytica Chimica Acta*, vol. 475, pp. 17-25, 2003.
- [40] Ya. I. Korenman, A. V. Kalach, “Application of multi-sensor system for determination of nitroethane in the air”, *Sensors and Actuators B*, vol. 88, pp. 334-336, 2003.
- [41] A. Burrelli, A. Fort, S. Rocchi, B. Serrano Santos, N. Ulivieri and V. Vignoli, “Temperature profile investigation of SnO<sub>2</sub> sensors for CO detection enhancement”, *IEEE transactions on instrumentation and measurement*, vol. 54, (1), pp. 79-86, February 2005.
- [42] Xingjiu Huang, Lianchao Wang, Yufeng Sun, Fanli Meng, Jinhui Liu, “Quantitative analysis of pesticide residue based on the dynamic response of a single SnO<sub>2</sub> gas sensor”, *Sensors and Actuators B*, vol. 99, pp. 330-335, 2004.
- [43] R. Ionescu, A. Hoel, C. G. Granqvist, E. Llobet, P. Heszler, “Ethanol and H<sub>2</sub>S gas detection in air and in reducing and oxidizing ambience: application of pattern recognition to analyse the output from temperature modulated nanoparticle WO<sub>3</sub> gas sensor”, *Sensors and Actuator B*, vol. 104, pp. 124-131, 2005.
- [44] R. Ionescu, A. Hoel, C. G. Granqvist, E. Llobet, P. Heszler, “Low level detection of ethanol and H<sub>2</sub>S with temperature modulated WO<sub>3</sub> nanoparticle gas sensors”, *Sensors and Actuator B*, vol. 104, pp. 132-139, 2005.
- [45] Andrew P. Lee, Brian J. Reedy, “Temperature modulation in semiconductor gas sensing”, *Sensors and Actuators B*, vol. 60, pp. 35-42, 1999.
- [46] Osvaldo L. Figueroa, Chonghoon Lee, Sheikh A. Akbar, Nicholas F. Szabo, Joseph A. Trimboli, Prabir K. Dutta, Naoto Sawaki, Ahmed A. Soliman, Henk Verweij, “Temperature-controlled CO, CO<sub>2</sub> and NO<sub>x</sub> sensing in a diesel engine exhaust stream”, *Sensors and Actuators B*, vol. 107, pp. 839-848, 2005.
- [47] H. Ding, H. Ge, J. Liu, “High performance of gas identification by wavelet transform based fast feature extraction from temperature modulated semiconductor gas sensor”, *Sensors and Actuator B*, vol. 107, pp. 749-755, 2005.



- [48] Figaro Gas Sensor Company, “*Gas sensor catalogue and technical information*”, 2000.
- [49] J. S. Suehle, R. E. Cavicchi, M. Gaitan, S. Semancik, “Tin oxide gas sensor fabricated using CMOS micro-hotplates and in situ processing”, *IEEE Electr. Dev. Lett.*, vol. 14, pp. 118-120, 1993.
- [50] N. Najafi, K. D. Wise, R. Merchange, J. W. Schwank, “An integrated multi-element ultrathin film gas analyzer”, *Proceedings of the 1992 Workshop on Sensors and Actuators*, Hilton Head, pp. 19-22, 1992.
- [51] N. Najafi, K. D. Wise, J. W. Schwank, “A micromachined ultra-thin-film gas detector”, *IEEE Transaction on Electron Devices*, vol. 41, pp. 1770-1777, 1994.
- [52] S. Semancik, R. Cavicchi, M. Gaitan, J. Suehle, “Temperature-controlled, micromachined arrays for chemical sensor fabrication and operation”, *US Patent no. 5345213*, 1994.
- [53] S. Semancik, R. E. Cavicchi, “Kinetically-controlled chemical sensing using micromachined structures”, *Accounts of Chemical Research*, vol. 31, pp. 279-287, 1998.
- [54] G. Faglia, E. Comini, A. Cristalli, G. Sberveglieri, L. Dori, “Very low power consumption micromachined CO sensors”, *Sensors and Actuators B*, vol. 55, pp. 140-146, 1999.
- [55] M. Schweizer-Berberich, M. Zdralek, U. Weimar, W. Göpel, T. Viard, D. Martinez, A. Seube, A. Peyre-Lavigne, “Pulsed mode of operation and artificial neural network evaluation for improving the CO selectivity of SnO<sub>2</sub> gas sensors”, *Sensors and Actuators B*, vol. 65, pp. 91-93, 2000.
- [56] S. Semancik, R. E. Cavicchi, M. C. Wheeler, J. E. Tiffany, G. E. Poirier, R. M. Walton, J. S. Suehle, B. Panchapakesan, D. L. DeVoe, “Microhotplate platforms for chemical sensor research”, *Sensors and Actuators B*, vol. 77, pp. 579-591, 2001.
- [57] P. Moseley and B. Tofield, “Solid state gas sensors”, *Adam Hilger*, Bristol, U.K., 1987.
- [58] P.T. Moseley, A.M. Stoneham and D.E. Williams, “Techniques and mechanisms in gas sensing”, *Adam Hilger*, Bristol, U.K., 1991.
- [59] G. Sberveglieri, “Recent developments in semiconducting thin-film gas sensors”, *Sensors and Actuators B*, vol. 23, pp. 102-109, 1995.

Improving the performance of micro-machined metal oxide gas sensors:  
Optimization of the temperature modulation mode via pseudo-random sequences.

- [60] F. Cosandey, G. Skandan and A. Singhal, "Materials and processing issues in nanostructured semiconductor gas sensors", JOM-e, vol. 52, (10), 2000.
- [61] C. Xu, J. Tamaki, N. Miura and N. Yamazoe, "Grain size effects on gas sensitivity of porous SnO<sub>2</sub>-based elements", Sensors and Actuators B, vol. 3, (2), pp. 147-155, 1991.
- [62] W. Göpel, "New materials and transducers for chemical sensors", Sensors and Actuators B, vol. 18-19, pp. 1-21, 1994.
- [63] V. Demarne and R. Sanjines, "Gas sensors principles, operation and development", Kluwer Academic, ed. G. Sberveglieri, Dordrecht, the Netherlands, pp. 89-116, 1992.
- [64] D. Hohl, "The role of noble metals in the chemistry of solid-state gas sensors", Sensors and Actuators B, vol. 1, pp. 158-165, 1990.
- [65] M. Haruta, "Size- and support-dependency in the catalysis of gold", Catalysis Today, vol. 36, pp. 153-166, 1997.
- [66] M. Valden, X. Lai and D.W. Goodman, "Onset of catalysis activity of gold clusters on titania with the appearance of nonmetallic properties", Science, vol. 281, pp. 1647-1650, 1998.
- [67] S.D. Lin, M. Bollinger and M.A. Vannice, "Low temperature CO oxidation over Au/TiO<sub>2</sub> and Au/SiO<sub>2</sub> catalysts", Catalysis Letters, vol. 17, pp. 245-262, 1993.
- [68] M. Haruta, S. Tsubota, T. Kobayashi, H. Kageyama, J.M. Genet and B. Delmon, "Low-temperature oxidation of CO over gold supported on TiO<sub>2</sub>,  $\alpha$ -Fe<sub>2</sub>O<sub>3</sub> and Co<sub>3</sub>O<sub>4</sub>", Journal of Catalysis, vol. 144, pp. 175-192, 1993.
- [69] H.M. Lin, C.M. Hsu, N.Y. Yang, P.Y. Lee and C.C. Yang, "Nanocrystalline WO<sub>3</sub>-based H<sub>2</sub>S sensors", Sensors and Actuators B, vol. 22, pp. 63-68, 1994.
- [70] Y. Shimizu and M. Egashira, "Basic aspects and challenges of semiconductor gas sensors", MRS Bulletin, pp. 18-24, June 1999.
- [71] M. Penza, C. Martucci and G. Cassano, "NO<sub>x</sub> gas sensing characteristics of WO<sub>3</sub> thin films activated by noble metals (Pd, Pt, Au) layers", Sensors and Actuators B, vol. 50, pp. 52-59, 1998.
- [72] T. Maekawa, J. Tamaki, N. Miura and N. Yamazoe, "Gold-loaded tungsten oxide sensor for detection of ammonia in air", Chem. Lett., vol. 2, pp. 639-642, 1992.
- [73] N. Yamazoe, "New approaches for improving semiconductor gas sensors", Sensors and Actuators B, vol. 5, pp. 7-19, 1991.

- [74] Y. Lin et al., "Structural and gas sensing properties of nanometre tin oxide prepared by PECVD", *Journal of Materials Science: Materials in Electronics*, vol. 7, pp. 179-282, 1996.
- [75] C.C. Chai, J. Pong and B.P. Yan, "Preparation and gas sensing properties of alpha-Fe<sub>2</sub>O<sub>3</sub> thin films", *J. Electronic Materials*, vol. 24, pp. 799-804, 1995.
- [76] F. Edelman et al., "E-gun sputtered and reactive ion sputtered TiO<sub>2</sub> thin films for gas sensors", *Inst. Electron Technol.*, vol. 33, pp. 89-107, 2000.
- [77] M. Ferroni, D. Boscarino, E. Comini, D. Gnani, V. Guidi, G. Martinelli, P. Nelli, V. Rigato and G. Sberveglieri, "Nanosized thin films of tungsten-titanium mixed oxides as gas sensors", *Sensors and Actuators B*, vol. 58, pp. 289-294, 1999.
- [78] G. Skandan, N. Glumac, Y.J. Chen, F. Cosandey, E. Heims and B.H. Kear, "Low-pressure flame deposition of nanostructured oxide films", *Journal of the American Ceramic Society*, vol. 81, (10), pp. 2753-2756, 1998.
- [79] A.K. Mukhopaghyay, P. Mitra, A.P. Chatterjee, H.S. Maiti, "A new method of preparing tin dioxide thin film sensors", *Journal of Materials Science Letters*, vol. 17, (8), pp. 625-627, 1998.
- [80] N. M. White, J. D. Turner, "Thick-film sensors: past, present and future, *Measurement Science and Technology*", vol. 8, pp. 1-20, 1997.
- [81] G. Martinelli, M.C. Carotta, M. Ferroni, Y. Sadaoka and E. Traversa, "Screen-printed perovskite-type thick films as gas sensors for environmental monitoring", *Sensors and Actuators B*, vol. 55, (2-3), pp. 99-110, 1999.
- [82] G. Martinelli, M.C. Carotta, E. Traversa and G. Ghiotti, "Thick-film gas sensors based on nano-sized semiconducting oxide powders", *MRS Bulletin*, pp. 30-35, June 1999.
- [83] <http://www.znose.com>
- [84] E.J. Staples, "An electronic nose containing 500 orthogonal sensors with pattern recognition based upon Vaporprints", *Proceedings ISOEN'99*, pp. 42-44, 1999.
- [85] [www.gerstel.de/](http://www.gerstel.de/)
- [86] [www.alpha-mos.com/](http://www.alpha-mos.com/)
- [87] [ww.hkr-sensor.de/start](http://www.hkr-sensor.de/start).
- [88] <http://www.smartnose.com/>

Improving the performance of micro-machined metal oxide gas sensors:  
Optimization of the temperature modulation mode via pseudo-random sequences.

- [89] Fenaille, F.; Visani, P.; Fumeaux, R.; Milo, C.; Guy, P. A.; “Comparison of Mass Spectrometry-Based Electronic Nose and Solid Phase MicroExtraction Gas Chromatography-Mass Spectrometry Technique to Assess Infant Formula Oxidation”, *J. Agric. Food Chem.*, vol. 51, (9), pp. 2790-2796, 2003.
- [90] Marcos Lorenzo. I, Pérez Pavón, J.L, Fernández Laespada M.E., García Pinto, C., Moreno Cordero, B., Henriques, L. R, Peres, M.F, Simões M.P, Lopes P.S, “Application of headspace-mass spectrometry for differentiating sources of olive oil”, *Anal Bional Chem.*, vol. 374, pp. 1205-1211, 2002.
- [91] Dirinck, I. Van Leuven, P. Dirinck, Arn C. Heiden, Carlos Gil, “Coffee Aroma Analysis Using a Mass Spectrometry-based Electronic nose”, *Proceedings of the Ninth International Symposium on Olfaction and Electronic Nose-ISOEN’02, Rome, 2002.*
- [92] Christophe Pérès, Frédéric Begnaud and Jean-Louis Berdagué, *Standard Gas Addition: A Calibration Method for Handling Temporal Drifts of Mass Spectrometry-Based Sensors*, *Anal. Chem.*, vol. 74, pp. 2279-2283, 2002.
- [93] José Luis Pérez Pavón, Miguel del Nogal Sánchez, Carmelo García Pinto, Ma Esther Fernández Laespada, and Bernardo Moreno Cordero, “Calibration Transfer for Solving the Signal Instability in Quantitative Headspace-Mass Spectrometry”, *Anal. Chem.*, vol. 75, pp. 6361-6367, 2003.
- [94] *Flavor, Fragrance and Odor Análisis*, ed *Ray Marsili*, Marcel Dekker, Inc., New York, 2002.
- [95] T. Börjesson, U. Stöllman and J. Schnürer, “Off-odours compounds produced by moulds on oatmeal agar. Identification and relations to other growth characteristics”, *J. Agric. Food Chem.*, vol. 41, pp. 2104-2111, 1993.
- [96] T.O. Larsen and J.C. Frisvad, “A simple method for collection of volatile metabolites from fungi based on diffusive sampling from petridishes”, *J. Microbiol. Meth.*, vol. 19, pp. 297-305, 1994.
- [97] R. Marsili, *Flavor, Fragrance and Odor Analysis*, Marcel Dekker, Inc., New York, 2002.
- [98] R.T. Marsili, “SPME-MS-MVA as an Electronic Nose for the Study of Off-Flavors in Milk”, *Journal of Agricultural and Food Chemistry*, vol. 47, pp. 648-654, 1999.
- [99] E. Schaller, S. Zenhäusern, T. Zesiger, J.O. Bosset, F. Escher, “Use of pre-concentration techniques applied to a MS-based Electronic Nose”, *Analysis*, vol. 28, pp. 743-749, 2000.

- [100] C.L. Arthur and J. Pawliszyn, "Solid phase microextraction with thermal desorption using fused silica optical fiber", *Anal. Chem.*, vol. 62, pp. 2145-2148, 1990.
- [101] C.L. Arthur, D.W. Potter, K.D. Buchholz, S. Motlagh and J. Pawliszyn, *LC-GC*, vol. 10, (9), pp. 656-661, 1992.
- [102] C.L. Arthur, L.M. Killam, S. Motlagh, M. Lim, D.W. Potter and J. Pawliszyn, "Analysis of substituted benzene compounds in groundwater using solid-phase microextraction", *Environmental Science & Technology*, vol. 26, (5), pp. 979-983, 1992.
- [103] C.L. Arthur, K. Pratt, S. Motlagh and J. Pawliszyn, "Journal of High Resolution Chromatography", vol. 15, pp. 741-744, 1992.
- [104] C.L. Arthur, L. Killam, K. Buchholtz, D. Potter, M. Chai, Z. Zhang and J. Pawliszyn, *Environmental Lab*, pp. 10-14, Dec. 1992 / Jan. 1993.
- [105] J. Chen and J. Pawliszyn, "Solid phase microextraction coupled to high performance liquid chromatography", *Anal. Chem.*, vol. 67, pp. 2530-2533, 1995.
- [106] M. Vinaixa, A. Vergara, C. Duran, E. Llobet, C. Badia, J. Brezmes, X. Vilanova, X. Correig, "Fast detection of rancidity in potato crisps using e-noses based on mass spectrometry or gas sensors", *Sensors and Actuators B*, vol. 106, pp. 67-75, 2005.
- [107] R.J.R. Uhlhorn and A.J. Burggraaf, "Gas separation with inorganic membranes", in R.R. Bhave (ed.), "*Inorganic Membranes: Synthesis Characteristics and Applications*", Van Nostrand Reinhold, New York, U.S.A., pp. 155, 1991.
- [108] P. Althainz, A. Dahlke, J. Goschnick and H.J. Ache, "Low temperature deposition of glass membranes for gas sensors", *Thin Solid Films*, vol. 241, pp. 344-347, 1994.
- [109] P. Althainz, A. Dahlke, J. Goschnick and H.J. Ache, "Low temperature deposition of glass membranes for gas sensors", *Thin Solid Films*, vol. 241, pp. 344-347, 1994.
- [110] C.O. Park, S.A. Akbar, J. Hwang, "Selective gas detection with catalytic filter", *Materials Chemistry and Physics*, vol. 73, (1-3), pp. 56-60, 2002.
- [111] M.A. Portnoff, R.G. Grace, A.M. Guzman, P.D. Runco and L.N. Yannopoulos, "Enhancement of MOS gas sensor selectivity by on-chip catalytic filtering", *Technical Digest of the 3rd International Meeting on Chemical Sensors*, Cleveland, U.S.A., pp. 96-97, September 24-26, 1990.

Improving the performance of micro-machined metal oxide gas sensors:  
Optimization of the temperature modulation mode via pseudo-random sequences.

- [112] C.D. Feng, Y. Shimizu and M. Egashira, "Effect of gas diffusion process on sensing properties of SnO<sub>2</sub> thin film sensors in a SiO<sub>2</sub>/SnO<sub>2</sub> layer-built structure fabricated by sol-gel process", J. Electrochem. Soc., vol. 141, (1), pp. 220-225, 1994.
- [113] T. Schwebel, M. Fleischer and H. Meixner, "CO-Sensor for domestic use on high temperature stable Ga<sub>2</sub>O<sub>3</sub> thin films", IEEE Transducers '97 on Solid-State Sensors and Actuators, Chicago, U.S.A., pp. 547-550, 1997.
- [114] C.H. Kwon, D.H. Yun, H.K. Hong, S.R. Kim, K. Lee, H.Y. Lim and K.H. Yoon, "Multi-layered thick-film gas sensor array for selective sensing by catalytic filtering technology", Sensors and Actuators B, vol. 65, pp. 327-330, 2000.
- [115] L. Dori, S. Nicoletti and I. Elmi, "A gas chromatographic-like system for the separation and monitoring of benzene, toluene and xylene compounds at the ppb level using solid state metal oxide gas sensors", Sensors and Materials Journal, vol. 12, (3), pp.163-174, 2000.
- [116] T. Aishima, "Discrimination of liquor aromas by pattern recognition analysis of responses from a gas sensor array", Anal. Chim. Acta, vol. 243, pp. 287-292, 1991.
- [117] E. Privat, S. Roussel, P. Grenier, V. Bellon-Maurel, Sci. Aliments, vol. 18, (5), pp. 459-470, 1998.
- [118] T. Aishima, "Aroma discrimination by pattern recognition analysis of responses from semiconductor gas sensor array", Journal of Agricultural and Food Chem., vol. 39, (4), pp. 752-756, 1991.
- [119] E. Schaller, S. Zenhäusern, T. Zesiger, J.O. Bosset and F. Escher, "Use of preconcentration techniques applied to a MS-based electronic nose", Analysis, vol. 28, pp. 743-749, 2000.
- [120] J.W. Gardner, "Detection of vapours and odours from a multi-sensor array using pattern recognition. Part 1: Principal component and cluster analysis", Sensors and Actuators B, vol. 4, pp. 109-115, 1991.
- [121] D. Kohl, "The role of noble metals in the chemistry of solid-state gas sensors", Sensors and Actuators B, vol. 1, pp. 158-164, 1990.
- [122] H.V. Shurmer, J.W. Gardner and P. Carcoran, "Intelligent vapour discrimination using a composite 12-element sensor array", Sensors and Actuators B, vol. 1, pp. 256-260, 1990.

- [123] J.W. Gardner and P.N. Bartlett, "Monitoring of fish freshness using tin oxide sensors", in *Sensors and Sensory Systems for an Electronic Nose*, Kluwer Academic Publishing, pp. 257-272, 1992.
- [124] H. Nanto, K. Kondo, M. Habara, Y. Douguchi, R.I. Waite and H. Nakazumi, "Identification of aroma from alcohols using a Japanese-lacquer-film-coated quartz resonator gas sensor in conjunction with pattern recognition analysis", *Sensors and Actuators B*, vol. 35-36, pp. 183-186, 1996.
- [125] T. Nakamoto, S. Sasaki, A. Fukuda and T. Moriizumi, "Selection method of sensing membranes in odour-sensing system", *Sensors and Materials*, vol. 4, pp. 111-119, 1992.
- [126] H.K. Hong, C.H. Kwon, S.R. Kim, D.H. Yun, K. Lee and Y.K. Sung, "Portable electronic nose system with gas sensor array and artificial neural network", *Sensors and Actuators B*, vol. 66, pp. 49-52, 2000.
- [127] Y. González Martín, J.L. Pérez Pavón, B. Moreno Cordero and C. García Pinto, "Classification of vegetable oils by linear discriminant analysis of Electronic Nose data", *Analytica Chimica Acta*, vol. 384, pp. 83-94, 1999.
- [128] E. Llobet, E.L. Hines, J.W. Gardner and S. Franco, "Non-destructive banana ripeness determination using a neural network-based electronic nose", *Meas. Sci. Technol.*, vol. 10, pp. 538-548, 1999.
- [129] J. Brezmes, E. Llobet, X. Vilanova, G. Saiz and X. Correig, "Fruit ripeness monitoring using an Electronic Nose", *Sensors and Actuators B*, vol. 69, pp. 223-229, 2000.
- [130] F. Sarry and M. Lumberras, "Discrimination of carbon dioxide and fluorocarbon using semiconductor gas sensors", *Sensors and Actuators B*, vol. 67, pp. 258-264, 2000.
- [131] A. Szczurek, P.M. Szczówka and B.P. Licznarski, "Application of sensor array and neural networks for quantification of organic solvent vapours in air", *Sensors and Actuators B*, vol. 58, pp. 427-432, 1999.
- [132] P. Aigner, F. Auerbach, P. Huber, R. Müller and G. Scheller, "Sinusoidal temperature modulation of the Si-Planar-Pellistor", *Sensors and Actuators B*, vol. 18-19, pp. 143-147, 1994.
- [133] F.J. Gutierrez, L. Arés, M.C. Horrillo, I. Sayago, J.A. Agapito and L. López, "Use of complex impedance spectroscopy in chemical sensor characterisation", *Sensors and Actuators B*, vol. 4, pp. 359-363, 1991.

Improving the performance of micro-machined metal oxide gas sensors:  
Optimization of the temperature modulation mode via pseudo-random sequences.

- [134] F.J. Gutierrez, L. Arés, J.I. Robla, M.C. Horrillo, I. Sayago and J.A. Agapito, "Properties of polycrystalline gas sensors based on d.c. and a.c. measurements", *Sensors and Actuators B*, vol. 8, pp. 231-235, 1992.
- [135] H. Amrani, P. Payne and K. Persaud, "Multi-frequency measurements of organic conducting polymers for sensing of gases and vapours", *Sensors and Actuators B*, vol. 33, pp. 137-141, 1996.
- [136] G. J. Gouws, D. J. Gouws, Analyte identification using concentration modulation and wavelet analysis of QVM sensors, *Sensors and Actuators B*, vol. 91, pp. 326-332, 2003.
- [137] X. Vilanova, E. Llobet, R. Alcubilla, J.E. Sueiras and X. Correig, "Analysis of the conductance transient in thick-film tin oxide gas sensors", *Sensors and Actuators B*, vol. 31, pp. 175-180, 1996.
- [138] E. Llobet, X. Vilanova, J. Brezmes, R. Alcubilla, J. Calderer, J.E. Sueiras and X. Correig, "Conductance transient analysis of thick-film tin oxide gas sensors under succesive gas injection steps", *Meas. Sci. Technol.*, vol. 8, (10), pp. 1133-1138, 1997.
- [139] E. Llobet, X. Vilanova, J. Brezmes, J.E. Sueiras and X. Correig, "Transient response of thick-film tin oxide gas sensors to multicomponent gas mixtures", *Sensors and Actuators B*, vol. 47, pp. 104-112, 1998.
- [140] E. Llobet, X. Vilanova, J. Brezmes, J.E. Sueiras, R. Alcubilla and X. Correig, "Model for the steady-state and transient behaviour of thick-film tin oxide gas sensors in the presence of gas mixtures", *Journal of the Electrochemical Society*, vol. 145, (5), pp. 1772-1779, 1998.
- [141] E. Llobet, J. Brezmes, X. Vilanova, J.E. Sueiras and X. Correig, "Qualitative and quantitative analysis of volatile organic compounds using transient and steady-state responses of a thick-film tin oxide gas sensor array", *Sensors and Actuators B*, vol. 41, pp. 13-22, 1997.
- [142] E. Llobet, J. Brezmes, X. Vilanova, L. Fondevila and X. Correig, "Quantitative vapour analysis using the transient response of non-selective thick-film tin oxide gas sensors", *Tech. Digest of 9th Int. Conf. on Sensors and Actuators, Transducers'97*, vol. 2, pp. 971-974, Chicago, IL, U.S.A., 1997.
- [143] E. Llobet, "Selectivity enhancement of metal oxide semiconductor chemical sensors through the study of their transient response to a step-change in gas concentration", *Doctoral Thesis, Universitat Politècnica de Catalunya, Barcelona*, 1997.



- [144] C. Duran, J. Brezmes, E. Llobet, X. Vilanova, and X. Correig, "Enhancing sensor selectivity through flow modulation", book of abstracts of the IEEE sensors 2005: the 4th IEEE conference on sensors, California USA, pp. 428-431, 2005.
- [145] P. K. Clifford, D. T. Tuma, "Characteristics of semiconductor gas sensor II, Transient response to temperature change", *Sensor and Actuators B*, vol. 3, pp. 233-254, 1982-1983.
- [146] P. K. Clifford, "Mechanisms of gas detection of metal oxide surface", PhD thesis, Carnegie-Mellon University, 1981.
- [147] S. R. Morrison, "Chemical Physics of surfaces", Plenum Press, New York, 1990.
- [148] H. D. Le Vine, "Method and apparatus for operating a gas sensor", US Patent 3,906,473, 1975.
- [149] H. Eicker, "Method and apparatus for determining the concentration of one gaseous component in a mixture of gases", US Patent, 4,012,692, 1977.
- [150] L. J. Owen, "Gas monitors", US Patent, 4,185,491, 1980.
- [151] G. N. Advani, R. Beard, L. Nanis, "Gas measurement method", US Patent, 4,399,684 1983.
- [152] V. Lantto, P. Romppainen, "Response of some SnO<sub>2</sub> gas sensors to H<sub>2</sub>S after quick cooling", *J. Electrochem. Soc.*, vol. 135, pp. 2550-2556, 1988.
- [153] S. Bukowiecki, G. Pfister, A. Reis, A.P. Troup and H.P. Ulli, "Gas or vapor alarm system including scanning gas sensors", US Pat. 4567475, January 28, 1986.
- [154] W.M. Sears, K. Colbow and F. Consadori, "Algorithms to improve the selectivity of thermally cycled tin oxide gas sensors", *Sensors and Actuators B*, vol. 19, pp. 333-349, 1989.
- [155] Semiconductor Gas Sensors, "Technical Information from Figaro Engineering Inc"., Japan.
- [156] Y Hiranaka, T. Abe, H. Murata, "Gas-dependent response in the temperature transient of SnO<sub>2</sub> gas sensors", *Sensors Actuators B*, vol. 9, pp. 177-182, 1992.
- [157] W. M. Sears, K. Colbow, F. Consadori, "A restricted flow thermally cycled gas sensor", *Sensors Actuators B*, vol. 1, pp. 62-67, 1990.

Improving the performance of micro-machined metal oxide gas sensors:  
Optimization of the temperature modulation mode via pseudo-random sequences.

- [158] W. M. Sears, K. Colbow, R. Slamka, F. Consadori, "Surface adsorption and gas consumption in restricted flow thermally driven gas sensors", *Semicond. Sci. Technol.*, vol. 5, pp. 45-53, 1990.
- [159] W. M. Sears, K. Colbow, F. Consadori, "General characteristics of thermally cycled tin oxide gas sensors", *Semicond. Sci. Technol.*, vol. 4, pp. 351-359, 1989.
- [160] W. M. Sears, K. Colbow, R. Slamka, F. Consadori, "Selective thermally cycled gas sensing using fast Fourier transform techniques", *Sensors Actuators B*, vol. 2, pp. 283-289, 1990.
- [161] S. Nakata, K. Takemura, N. Ojima, T. Hiratani, S. Yamabe, "Mechanism of nonlinear responses of a semiconductor gas sensor", *Instrum. Sci. Technol.*, vol. 28, pp. 241-251, 2000.
- [162] S. Nakata, K. Takemura and K. Neya, "Non-linear dynamic responses of a semiconductor gas sensor: Evaluation of kinetic parameters and competition effect on the sensor response", *Sensors Actuators B*, vol. 76, pp. 436-441, 2001.
- [163] S. Nakata, H. Nakamura, K. Yoshikawa, "New strategy for the development of a gas sensor based on the dynamic characteristics: principle and preliminary experiment", *Sensors Actuators B*, vol. 8, pp. 187-189, 1992.
- [164] Y. Kato, K. Yoshikawa, "Chemical sensing based on the informational source of nonlinear dynamics", *IJCNN '93-Nagoya. Proceedings of 1993 International Joint Conference on Neural Networks*, vol. 1, pp 1019-1022, October 25-29, 1993.
- [165] S. Nakata, S. Akakabe, M. Nakasuji, K. Yoshikawa, "Gas sensing based on a nonlinear response: Discrimination between hydrocarbons and quantification of individual components in a gas mixture", *Anal. Chem.*, vol. 68, pp. 2067-2072, 1996.
- [166] Y. Kato, K. Yoshikawa, M. Kitora, "Temperature-dependent dynamic response enables the qualification and quantification of gases by a single sensor", *Sensors Actuators B*, vol. 40, pp. 33-37, 1997.
- [167] S. Nakata, E. Ozaki, N. Ojima, "Gas sensing based on the dynamic nonlinear responses of a semiconductor gas sensor: dependence on the range and frequency of a cyclic temperature change", *Anal. Chim. Acta*, vol. 361, pp. 93-100, 1998.
- [168] S. Nakata, N. Ojima, M. Nakasuji, M. Kitora, "Characteristic nonlinear responses for gas species on the surface of different semiconductor gas sensors", *Appl. Surf. Sci.*, vol. 135, pp. 285-292, 1998.

- [169] S. Nakata, N. Ojima, "Detection of a sample gas in the presence of an interferant gas based on a nonlinear dynamic response", *Sensors Actuators B*, vol. 56, pp. 79-84, 1999.
- [170] S. Nakata, T. Nakamura, K. Kato, Y. Kato, K. Yoshikawa, Discrimination and quantification of flammable gases with a SnO<sub>2</sub> sniffing sensor, *Analyst*, vol. 125, pp. 517-522, 2000.
- [171] S. Nakata, K. Neya, K. Takemura, "Non-linear dynamic response of a semiconductor gas sensor – Competition effect on the sensor responses to gaseous mixtures", *Thin Solid Films*, vol. 391, pp. 293-298, 2001.
- [172] S. Nakata, K. Takemura, K. Neya, "Chemical sensor based on nonlinearity: Principle and application", *Analytical Sciences*, vol. 17, pp. 365-373, 2001.
- [173] S. Nakata, K. Neya, T. Hashimoto, "A semiconductor gas sensor based on nonlinearity: Utilization of the effect of competition on the sensor responses to gaseous mixtures", *Electroanalysis*, vol. 14, (13), pp. 881-887, 2002.
- [174] S. Nakata, T. Hashimoto, H. Okunishi, "Evaluation of the responses of a semiconductor gas sensor to gaseous mixtures under the application of temperature modulation", *Analyst*, vol. 127, pp. 1642-1648, 2002.
- [175] R.E. Cavicchi, J. S. Suehle, K. G. Kreider, M. Gaitan, P. Chaparala, "Fast temperature programmed sensing for micro-hotplate gas sensors", *IEEE Electron Device Lett.*, vol. 16, pp. 286-288, 1995.
- [176] R.E. Cavicchi, J. S. Suehle, K. G. Kreider, M. Gaitan, P. Chaparala, "Optimized temperature-pulse sequences for the enhancement of chemically specific response patterns from micro-hotplate gas sensors", *Sensors Actuators B*, vol. 33, pp. 142-146, 1996.
- [177] L. Ratton, T. Kunt, T. McAvoy, T. Fuja, R. Cavicchi, S. Semancik, "A comparative study of signal processing techniques for clustering microsensor data (a first step towards an artificial nose)", *Sensors Actuators B*, vol. 41, pp. 105-120, 1997.
- [178] A. B. Carlson, "Communications Systems", 3rd Edition, McGraw Hill, Singapore, 1986.
- [179] A. Heilig, N. Bârsan, U. Weimar, M. Schweizer-Berberich, J.W. Gardner, W. Göpel, "Gas identification by modulating temperatures of SnO<sub>2</sub>-based thick-film sensors", *Sensors Actuators B*, vol. 43, pp. 45-51, 1997.

Improving the performance of micro-machined metal oxide gas sensors:  
Optimization of the temperature modulation mode via pseudo-random sequences.

- [180] K. Kato, Y. Kato, K. Takamatsu, T. Udaka, T. Nakahara, Y. Matsuura, K. Yoshikawa, "Toward the realization of an intelligent gas sensing system utilizing a non-linear dynamic response", *Sensors and Actuators B*, vol. 71, pp. 192-196, 2000.
- [181] A. Ortega, S. Marco, A. Perera, T. Sundic, A. Pardo, J. Samitier, "An intelligent detector based on temperature modulation of a gas sensor with a digital signal processor", *Sensors and Actuators B*, vol. 78, pp. 32-39, 2001.
- [182] E. Llobet, R. Ionescu, S. Al-Khalifa, J. Brezmes, X. Vilanova, X. Correig, N. Bârsan and J.W. Gardner, "Multicomponent gas mixture analysis using a single tin oxide sensor and dynamic pattern recognition", *IEEE Sensors Journal*, vol. 1, pp. 207-213, 2001.
- [183] R. Ionescu, E. Llobet, "Wavelet transform-based fast feature extraction from temperature modulated semiconductor gas sensors", *Sensors and Actuators B*, vol. 81, pp. 289-295, 2002.
- [184] R. Ionescu, E. Llobet, X. Vilanova, J. Brezmes, J.E. Suerias, J. Calderer, X. Correig, "Quantitative analysis of NO<sub>2</sub> in the presence of CO using a single tungsten oxide semiconductor sensor and dynamic signal processing", *Analyst*, vol. 127, pp. 1237-1246, 2002.
- [185] E. Llobet, J. Brezmes, R. Ionescu, X. Vilanova, S. Al-Khalifa, J. W. Gardner, N. Bârsan, X. Correig, "Wavelet Transform and Fuzzy ARTMAP Based Pattern Recognition for Fast Gas Identification Using a Micro-Hotplate Gas Sensor", *Sensors and Actuators B*, vol. 83, (1-3), pp. 238-244, 2002.
- [186] R. Ionescu, E. Llobet, J. Brezmes, X. Vilanova, X. Correig, "Dealing with humidity in the qualitative analysis of CO and NO<sub>2</sub> using a WO<sub>3</sub> sensor and dynamic signal processing", *Sensors and Actuators B*, vol. 95, pp. 177-182, 2003.
- [187] S. Al-Khalifa, S. Maldonado-Bascón, J.W. Gardner, "Identification of CO and NO<sub>2</sub> using a thermally resistive microsensor and support vector machine", *IEE Proc.-Sci. Meas. Technol.*, vol. 150, pp. 11-14, 2003.
- [188] C.J.C. Burges, "A tutorial on support vector machines for pattern recognition", *Data Min. Knowl. Discov.*, vol. 2, pp. 121-167, 1998.
- [189] W. Maziarz, P. Potempa, A. Sutor, T. Pisarkiewicz, "Dynamic response of a semiconductor gas sensor analysed with the help of fuzzy logic", *Thin Solid Films*, vol. 436, pp. 127-131, 2003.

- [190] B. Yea, T. Osaki, K. Sugahara, R. Konishi, "The concentration estimation of inflammable gases with a semiconductor gas sensor utilizing neural networks and fuzzy inference", *Sensors and Actuators B*, vol. 41, pp. 121-129, 1997.
- [191] R.R. Yager, D.P. Filev, "Essentials of Fuzzy Modeling and Control", John Wiley and Sons, New York, 1994.
- [192] A. Schütze, A. Gramm, T. Rühl, "Identification of organic solvents by a virtual multisensor system with hierarchical classification", *IEEE Sensors 2002*, Orlando, USA, vol. 1, pp. 382-387, 2002.
- [193] A. Gramm, A. Schütze, "High performance vapor identification with a two sensor array using temperature cycling and pattern classification", *Sensors and Actuators B*, vol. 95, pp. 58-65, 2003.
- [194] R. Gutierrez-Osuna, A. Gutierrez-Galvez, N. Powar, "Transient response analysis for temperature-modulated chemoresistors", *Sensors and Actuators B*, vol. 93, pp. 57-66, 2003.
- [195] A. Fort, M. Gregorkiewitz, M. Machetti, S. Rocchi, B. Serrano, L. Tondi, N. Ulivieri, V. Vignoli, G. Faglia, E. Comini, "Selectivity enhancement of SnO<sub>2</sub> sensors by means of operating temperature modulation", *Thin Solid Films*, vol. 418, (1), pp. 2-8, 2002.
- [196] A. Fort, M. Machetti, S. Rocchi, B. Serrano, L. Tondi, N. Ulivieri, V. Vignoli, G. Sberveglieri, "Tin oxide gas sensing: comparison among different measurement techniques for gas mixture classification", *IEEE Transactions on Instrumentation and Measurement*, vol. 52, (3), pp. 921-926, 2003.
- [197] N.H. Choi, C.H. Shim, K.D. Song, D.S. Lee, J. S. Huh, D.D. Lee, "Classification of workplace gases using temperature modulation of two SnO<sub>2</sub> sensing films on substrate", *Sensors Actuators B*, vol. 86, pp. 251-258, 2002.
- [198] X. Huang, J. Liu, D. Shao, Z. Pi, Z. Yu, "Rectangular mode of operation for detecting pesticide residue by using a single SnO<sub>2</sub>-based gas sensor" *Sensors Actuators B*, vol. 96, pp. 630-635, 2003.
- [199] T.A. Kunt, T.J. McAvoy, R.E. Cavicchi, S. Semancik, "Optimization of temperature programmed sensing for gas identification using micro-hotplate sensors", *Sensors Actuators B*, vol. 53, pp. 24-43, 1998.
- [200] Q. Zhang, A. Benveniste, "Wavelet networks", *IEEE Transactions on Neural Networks*, vol. 3, (6) pp. 889-898, 1992.

Improving the performance of micro-machined metal oxide gas sensors:  
Optimization of the temperature modulation mode via pseudo-random sequences.

This page was left blank intentionally.

---

# 3.

# Feature extraction and pattern recognition for temperature-modulated gas sensors

---

<b>3. FEATURE EXTRACTION AND PATTERN RECOGNITION FOR TEMPERATURE-MODULATED GAS SENSORS.</b>	<b>67</b>
<b>3.1. Introduction</b>	<b>68</b>
<b>3.2. Feature extraction methods.</b>	<b>69</b>
3.2.1. Fast Fourier Transform (FFT).	71
3.2.2. Phase space and dynamic moments.	72
<b>3.3. Pattern recognition methods.</b>	<b>73</b>
3.3.1. Principal component analysis (PCA).	75
3.3.2. Partial Least Squares (PLS).	76
3.3.3. Partial Least Squares Discriminant Analysis (PLS-DA).	78
3.3.4. Fuzzy ARTMAP neural network.	78
<b>3.4. Variable selection procedure.</b>	<b>81</b>
<b>3.5. Conclusions.</b>	<b>84</b>
<b>3.6. References.</b>	<b>85</b>

## Improving the performance of micro-machined metal oxide gas sensors: Optimization of the temperature modulation mode via pseudo-random sequences.

### 3.1. Introduction.

In the last decade, the use of gas sensor arrays with partially overlapped sensitivity has become a strategy largely widespread among the sensor community. This solution, matched with a proper multivariate data analysis, made possible the use of non-selective sensors in many practical applications. Indeed, combining appropriate feature extraction techniques with suitable data analysis procedures it is possible to improve the system performance and counteract disturbances such as noise or drift.

A considerable number of feature extraction and pattern recognition methods have been introduced and applied to analyze the response of sensor arrays.

An in-depth and comprehensive review of all existing methods is beyond the scope of this chapter. Instead, after a brief introduction where some general aspects shared by the different feature extraction and pattern recognition methods are discussed, the chapter focuses on the different methods employed in this thesis. Therefore, the different methods employed to extract important features from the responses of temperature-modulated gas sensors and the pattern recognition algorithms implemented to recognize and quantify the gases and their mixtures studied will be discussed.

Additionally, the two feature extraction methods used are the Fast Fourier Transform (FFT) and the phase space (PS) + dynamic moments (DM). The FFT has been by far the most commonly used feature extraction method in the field of temperature modulated gas sensors [1–4]. Additionally to this method, a novel feature extraction method, performed the so-called phase space (PS) and Dynamic moments (DM), is introduced here and applied to temperature-modulated microhotplate gas sensors [5]. Both techniques (i.e., FFT and DM) are described in this chapter.

On the other hand, the different pattern recognition methods used in the analysis of the experimental data sets are described. Principal component analysis (PCA), partial least squares (PLS), and PLS-DA are within the conventional statistical pattern recognition techniques. A fuzzy ARTMAP neural network is alternatively used as classifier.

Finally a method based on data variance analysis for the selection of variables extracted from the feature extraction method is presented.



## 3.2. Feature extraction methods.

Considering a system governed by  $L$  independent variables  $x_1, x_2, \dots, x_L$ . The system is always represented by an  $L$ -dimensional vector  $x = [x_1 x_2 \dots x_L]^T$  spanning a subspace  $S \in \mathfrak{R}^L$ . These parameters characterize the evolution of the system.

Generally, the intrinsic dimension  $L$  of the system is unknown. It is possible to obtain an observation of the physical system measuring the evolution of a number  $D$  of variables. The feature extraction is then defined as the operation that extracts a number of synthetic descriptors (features) from the evolution of the  $D$  variables in order to represent as much as possible the state of the system. Therefore, considering an observed variable, the process of feature extraction is defined by the following expression:

$$M \xrightarrow{g} F \tag{3.1}$$

$$M \in \mathfrak{R}^m; F \in \mathfrak{R}^n \therefore m \gg n$$

where  $M$  is the space of the observed variables,  $F$  the feature space and  $g$  are the mapping function between the spaces. This operation can be represented as a projection from the space  $M$  into a space  $F$  of lower dimensions.

Indeed, the goal of feature extraction is to find a low-dimensional mapping  $g$  that preserves most of the information in the original feature vector  $x$  [6, 7], and its importance can be resumed in the following points:

- The feature extraction depends from the system under study and by the parameter that rules this phenomenon.
- Not always more features leads to better performance.
- A good feature extraction is an operation that increases the signal to noise ratio, where signal is the discriminating information of the feature.
- Whereas a large number of different features is necessary, a pre-processing is requested to maintain a good system accuracy.

In pattern recognition, a “feature” is any direct or derived measurement of the entities to be classified that helps differentiate between classes. In chemical sensor arrays, the individual measurements are the entities that have to be assigned to classes, and a measurement is a sequence of temporal ordered sensor signals taken during the exposure of the sensor to the sample. Subsequently, the feature extraction for chemical sensors consists in the determination, out of a stream of sensor signals, of a number of synthetic parameters that can, as much as possible, represent the whole sensor experience and contains those kinds

## Improving the performance of micro-machined metal oxide gas sensors: Optimization of the temperature modulation mode via pseudo-random sequences.

of information related to the classification objective. Feature extraction is of fundamental importance because the sensor features are then utilized in any successive elaboration in order to produce the output of the sensor system in terms of estimation of the measured quantities.

In order to define the feature extraction procedure it is necessary to consider that the adaptation of the output signal of a chemical sensor to the variation of the concentration of gases at which it is exposed occurs with a certain dynamics. The not easy handling of gas concentration complicates the investigation of the dynamic of the sensor response. General sensor response models, based on the assumption of a very rapid concentration transition from two steady states, result in exponential behaviors.

The straightforward solution of the feature extraction problem disregards the dynamic transitions considering only the signal shift between two stationary states before the application of gas stimuli and during the exposure to gas after the transitory phase. This quantity has a straightforward meaning being related to the equilibrium conditions established between analyte molecules in gas phase and those interacting with the sensor. Although the straight chemical and physical meaning of the steady state signal shift, it is worth to investigate if the dynamic properties can provide features with extended information content.

For example, it is widely known that by modulating the operating temperature of metal-oxide gas sensors (because of the temperature-selectivity dependence of these devices), their information content can be improved obtaining their dynamic response during the exposure to target gases [8]. Several authors have studied both, temperature cycling and temperature transient (i.e., thermal modulation) in order to improve the selectivity of gas sensors [9-16]. Most authors transform the sensor response into the frequency domain by means of the Fast Fourier Transform (FFT), and use the coefficients to discriminate and quantify the species to be measured by pattern recognition approaches. Although the FFT is perhaps the most commonly used feature extraction method in the field of temperature modulated gas sensors [1-4], wavelet analysis provides an alternative way of breaking a signal down to its constituent parts that are quite informative for discrimination and quantification tasks [17]. Other techniques as Pade-Z-transform [18], multi-exponential transient spectroscopy (METS) [19], window time slicing (WTS) [20], and ridge regression curve fitting (RRCF) techniques, have been alternative techniques used to analyze the transient response of gas sensors while their operating temperature is modulated. However, remembering that this doctoral thesis is aimed at optimizing the temperature modulation of micro-hotplate gas sensors (and not the feature extraction step), the absolute value of the Fast Fourier Transform (FFT) is used as feature extraction method. Additionally, a novel feature extraction method

called Dynamic Moments (DM) and Phase Space (PS) is used. The usefulness of the method is assessed by analyzing the transient response of metal oxide gas sensors to a thermal modulation [5]. In this case, DM and PS methods give the opportunity to use novel features that describe sensor trajectories while adsorption and reaction kinetics are altered by the temperature modulation. Both methods are described in the following sub-sections.

### 3.2.1. Fast Fourier Transform (FFT).

Fourier's representation of functions as a superposition of sines and cosines has become ubiquitous for the analysis and treatment of communication signals and systems.

The Fourier Transform (FT) usefulness lies in its ability to analyze a signal in the time domain for its frequency content. The transform works by first translating a function in the time domain into a function in the frequency domain. The signal can then be analyzed for its frequency content because the Fourier coefficients of the transformed function represent the contribution of each sine and cosine function at each frequency.

The Discrete Fourier Transform (DFT) estimates the Fourier Transform of a function from a finite number of its sampled points. The sample points are supposed to be typical of what the signal looks like at all other times.

The Short Time Fourier Transform (STFT) is one solution to the problem of better representing non-periodic signals. The STFT can be used to give information about signals simultaneously in the time domain and in the frequency domain. With the STFT, the input signal is chopped up into sections, and each section is analyzed for its frequency content separately.

To approximate a function by samples, and to approximate the Fourier integral by the Discrete Fourier Transform, requires applying a matrix whose order is the number sample points  $n$ . The number of arithmetic operations required ( $2^n$ ) can be reduced to  $n \log n$  when applying the Fast Fourier Transform. The FFT can be used only when the samples are uniformly spaced.

When a continuous-time signal such as the sensor response has been sampled at a uniform rate, the resulting sample values may be treated as a discrete-time signal and processed using the FFT.

For a response sequence  $r$  of length  $n$ , the Discrete Fourier Transform is a vector  $R$  of length  $n$ , whose elements are defined as follows:

$$R(k) = \sum_{p=0}^{n-1} r(p) e^{-j2\pi kp/n} \quad (3.2)$$

### Improving the performance of micro-machined metal oxide gas sensors: Optimization of the temperature modulation mode via pseudo-random sequences.

where  $k = 0, 1, \dots, n-1$ .

When the continuous-time sensor response has been sampled every  $\tau_s$  seconds over a finite time interval  $0 \leq t \leq \tau_0$ , the observation interval and sampling rate are chosen such that  $\tau_0 = n\tau_s$ . Then,  $f_s/2$  (where  $f_s = 1/\tau_s$ ) represents the highest observation frequency, since higher frequencies would exceed the Nyquist rate and would be subject to aliasing, and  $f_0$  (where  $f_0 = 1/\tau_0$ ) represents the lower observable frequency (aside from a DC component), since any lower frequency would not go through a complete period in  $\tau_0$  seconds [21].

### 3.2.2. Phase space and dynamic moments.

The nature of the sensing mechanisms ruling of chemical sensors is still far from full comprehension. The extraction of features from the response of chemical sensors consists in the selection of some characteristics of their temporal response sequence, which results from the interaction between sensors and the compounds to be detected. The extracted features are then input to pattern recognition systems. From a general point of view, a chemical sensor can be considered as a dynamic system whose response signal temporally evolves following, with its proper dynamics, the concentration of the analytes. Therefore, any of the currently available tools usually employed to study the properties of dynamic systems may be employed [22].

The Phase Space (PS) is a central concept in the analysis of dynamic systems. Given a system whose state is completely described by  $n$  scalar variables, different states correspond to different points in a  $n$ -dimension vector space defined by an orthonormal basis where each direction correspond to one of the scalar variables. The fundamental property of the PS is the correspondence between each point and the instantaneous state of the system. A generic PS can be defined considering the Taken's Embedding theorem [23]. Given an observable quantity  $s(t)$  and defining a time lag  $\tau$ , the space coordinates are:

$$\left[ s(t) \ s(t + \tau) \dots s(t + (k - 1)\tau) \right] \quad (3.3)$$

The time evolution of  $s(t)$  results in a trajectory containing the dynamic properties of the system. Trajectories assume a large variety of shapes depending on the nature of the phenomena. Neglecting the scale effects, the shapes of the trajectories are expected to be associated to the properties of the phenomena. From this point of view, it is interesting to define some morphological descriptors able to encode the shape of the trajectories. These morphological descriptors can then be used to obtain information about the system dynamics.

Here, sets of morphological descriptors representing the parameters analogous to the second moments of the area of a geometrical figure in a 2-D space are considered. These quantities are sometimes called Dynamic Moments (DM) [24, 25]. They are calculated considering both the coordinates and bisectors of the Phase Space:

$$MD2 = \frac{1}{n} \sum_{i=0}^n x_i y_i \quad (3.4)$$

$$MD3_{PB} = \frac{\sqrt{2}}{2n} \sum_{i=0}^n (x_i^2 y_i - x_i y_i^2) \quad (3.5)$$

$$MD3_{SB} = \frac{\sqrt{2}}{2n} \sum_{i=0}^n [2x_i^3 + 3(x_i^2 y_i - x_i y_i^2)] \quad (3.6)$$

$$MD3_x = \frac{1}{2n} \sum_{i=0}^n (x_i^3 - 3x_i y_i^2) \quad (3.7)$$

$$MD3_y = \frac{1}{2n} \sum_{i=0}^n (x_i^3 - 3x_i^2 y_i) \quad (3.8)$$

where  $PB$  and  $SB$  are principal and secondary bisectors,  $x$  and  $y$  are the PS axis. Each of the moments describes the different morphological features of the trajectory, so that the collective use of more than one moment is required for an exhaustive description. It is also important to emphasize that the moments' value depends on the time lag generating the PS. In [26, 27] the first attempts to introduce the PS and DM to represent the temporal evolution of chemical sensor signals (QCM) was presented.

Finally, it is important to remark that in order to apply the DM to gas sensors, a transient operating mode of the sensors needs to be considered. For example the adsorption/desorption phenomena when gas sensors are abruptly exposed to a gas concentration or the alteration of adsorption/desorption and reaction kinetics caused by a periodic temperature modulation.

### 3.3. Pattern recognition methods.

The problem of analyzing the data generated by a gas sensor array is basically one of determining the underlying relationships between one set of independent variables (i.e., the output from an array of  $n$  sensors) and another set of dependent variables (i.e., odor class and component concentrations). The methods employed may be either an unsupervised one that

Improving the performance of micro-machined metal oxide gas sensors:  
 Optimization of the temperature modulation mode via pseudo-random sequences.

seeks to determine between unknown odor vectors or, alternatively, it may be a supervised one in the sense that unknown odor vectors are analyzed using relationship found a priori from a set of known odor vectors used in an initial calibration, learning or training stage [28]. Data processing, at the same time can be sub-divided in two main approaches. The former, is statistical and in some ways is the more general and logical. This statistical approach is sometimes referred to as parametric in that it assumes that the data can be described by a probability density function (pdf), such as a multinormal distribution. The latter approach seeks to solve multivariate problems in a manner similar to the human cognitive process by using a biologically inspired neural construct and rules based upon human reasoning. This non-parametric approach to multivariate data analysis has led to the fields of artificial neural networks [29].

Table 3.1 lists the main qualitative and quantitative pattern recognition methods commonly used in gas sensor response data analysis, where their principal characteristics are summarized.

**Table 3.1:** Classification scheme for pattern recognition (PARC) systems.

PARC	Learning	Linear	Parametric	Application	Comments
PCA	non-sup.	yes	no	Feature extraction/ classification of unknown species	Data separated on basis of variance
DFA	supervised	yes	yes	Classification of known set of calibrants	Classifies species using assumptions about multivariate normality
PCR	supervised	yes	yes	Classification and quantitative mixture analysis	PCR: data separated on basis of variance
PLS PLS-DA	supervised	yes	yes		
MLP	supervised	no	no	Classification and quantitative mixture analysis	Artificial neural networks are opaque in nature
RBF	supervised	no	no	Classification and quantitative mixture analysis	Trained in two phases
Fuzzy ARTMAP	supervised	no	no	Classification and quantitative mixture analysis	Allows for subjective classification

However, in this sub-section a detailed description of both, statistical and neural networks pattern recognition techniques used in this doctoral thesis to quantitatively and qualitatively analyze the gas sensor response data is given. Among the statistical pattern recognition approaches the Principal Component Analysis (PCA) is used as an unsupervised technique but also as a standard pre-processing technique. Partial Least Squares (PLS), on the other hand, is used to build regression models for quantitative analysis and PLS-Discriminant Analysis (PLS-DA) is applied in the case of classification problems when the Dynamic Moments (DM) and Phase Space (PS) are used as feature extraction method. Additionally, qualitative gas analysis is also envisaged using neural networks by building fuzzy ARTMAP classifiers. Fuzzy ARTMAP is implemented using functions from MATLAB developed by J. Brezmes [30].

### 3.3.1. Principal component analysis (PCA).

Principal Component Analysis (PCA) is a linear and unsupervised pattern recognition method widely used to discriminate the response of a gas sensor to simple and complex odors [31, 32]. It is based on the Karhunen-Love expansion, which yields qualitative results.

The most frequent application of PCA is in cases where the sensor response matrix,  $R$ , is expected to contain variables with some degree of collinearity. This collinearity means that  $R$  will have some dominating types of variability that carry most of the available information.

The objective of PCA is to express the information in the variables of  $R = \{r_k, k = 1, 2, \dots, K\}$  ( $K$  is the number of columns in the response matrix) by a lower number of variables  $P = \{p_1, p_2, \dots, p_n\}$  ( $n < K$ ) often called principal components (PCs). The PCs are chosen to contain the maximum data variance and to be orthogonal. This technique allows visualizing, in two or three dimensions, a multidimensional datasets for a preliminary data exploration to study the intrinsic capability of the system to discriminate the data in clusters.

The response matrix is decomposed into a product of two matrices (scores and loadings). While the loadings matrix,  $L$ , contains the contribution of the original response vectors to the new response vectors or PCs, the score matrix contains the response vectors projected onto the space defined by the PCs. More formally, the first PC loading  $l_1$  is defined as the normalized vector (its norm = 1) that maximizes the scalar  $l_1^t R^t R l_1 = p_1^t p_1$  (where  $t$  means transpose). The second PC loading  $l_2$  is defined as the vector maximizing  $l_2^t R^t R l_2 = p_2^t p_2$  under the constraint that  $p_1$  and  $p_2$  are orthogonal. The procedure continues this way under the constraint that the scores of the new factors are uncorrelated orthogonal with those of the previous factors.

Improving the performance of micro-machined metal oxide gas sensors:  
 Optimization of the temperature modulation mode via pseudo-random sequences.

Finally, an interesting property of PCA is that  $L$  can be found by least squares fitting of  $R$  to  $P$ , in the same way as  $P$  can be found by least squares fitting of  $R$  to  $L$ . We have:

$$L^t = (P^t P)^{-1} P^t R \tag{3.9}$$

$$P = RL(L^t L)^{-1} = RL, \text{ since } (L^t L)^{-1} = I \tag{3.10}$$

### 3.3.2. Partial Least Squares (PLS).

Partial Least Squares (PLS) regression is a data analysis technique that combines characteristics from principal component analysis (PCA) and multiple regression (MLR). It is mostly useful when we need to predict a set of dependent variables from a large set of independent variables (predictors). It originated in social sciences but became popular in chemometrics due in part to the work developed by Svante Wold, [33]. Let us then consider  $M$  observations described by  $K$  dependent variables are stored in a  $M \times K$  matrix denoted  $Y$ , the values of  $J$  predictors collected on these  $M$  observations are collected in the  $M \times J$  matrix  $X$ .

The goal of PLS regression is to predict  $Y$  from  $X$  and to describe their common structure. When  $Y$  is a vector and  $X$  is full rank, this goal could be accomplished using ordinary multiple regression [34]. When the number of predictors is large compared to the number of observations,  $X$  can be singular and the regression approach is no feasible (i.e., because of multi-collinearity). Several approaches have been developed to solve this problem. One approach is to eliminate some predictors (trying to avoid the multi-collinearity) another one, called principal component regression, is to perform a principal component analysis (PCA) of the  $X$  matrix and then use the PCs of  $X$  as regressors on  $Y$ . The orthogonality of the principal components eliminates the multi-collinearity problem. But, the problem of choosing an optimum subset of predictors remains. As example, the choice of the first PCs of  $X$  can not be relevant to find a correlation with the variables  $Y$ .

Instead, PLS regression finds components from  $X$  that are relevant for  $Y$ . In particular, PLS regression searches for a set of components, called latent vectors, that achieves a simultaneous decomposition of  $X$  and  $Y$  with the restriction that these components explain as much as possible the covariance between  $X$  and  $Y$ . Then PLS algorithm searches the subset of  $X$  that show the maximum correlation with  $Y$ .

PLS regression decomposes both  $X$  and  $Y$  as a product of a common set of orthogonal factors and a set of specific loadings. So, the  $X$  matrix is decomposed in the following way:

$$X = TP^t + E \text{ with } TT^t = I \tag{3.11}$$



with  $I$  the identity matrix, by analogy with PCA  $T$  is called the score matrix,  $P$  the loading matrix,  $E$  the residuals matrix. It is worth to note that in PLS regression the loadings are not orthogonal contrary to PCA where the loadings are orthogonal. In the same way,  $Y$  is decomposed as:

$$Y = UC^T + G \text{ with } CC^T = I \tag{3.12}$$

where  $U$  is called the score matrix,  $C$  the loading matrix and  $G$  the residuals matrix. It is possible to estimate  $Y$  with

$$\hat{Y} = TC^T + F \tag{3.13}$$

where  $F$  is the residuals matrix.

Taking into account the eq. (3.11), the eq (3.12) ca be written as

$$Y = XWC^T + F = XB + F \tag{3.14}$$

$$B = WC^T$$

where  $W$  is found with the relation  $T = WX$ .

The matrixes  $T$  and  $C$  have to find maximizing the covariance between  $X$  and  $Y$ . More details about the PLS algorithm can be found in ref [33].

It is worth to remark that PLS is a projection method. Then, this technique can be seen as a projection of the  $X$ -matrix down on a  $K$ -dimensional plane in such way that the coordinates of the projection ( $t_a \ a = 1, \dots, K$  given by the matrix  $T$ ) are good predictors of  $Y$ . The prediction error of the model is strongly dependent by the number of variables (features) and by the number of measures. In the case of small dataset, in order to have realistic error estimation, a cross validation technique is applied. The number of latent variables that minimizes the prediction error in the validation phase is used to build a model for the subsequent test phase.

Several cross-validation techniques have been introduced but here the Leave-one-out cross-validations is considered and implemented. Since the number of samples is rather low, the prediction error rate is computed using cross-validation by blocks or a leave-one-out cross-validation. In this approach, the data set is divided into  $k$  subsets: the calibration is carried out on  $(k-1)$  blocks, and the prediction is made on the samples belonging to the  $k$ th subset. This is repeated  $k$  times with block permutation, in order to predict all the samples. The cross-validation is called leave-one-out cross-validation where each subset is composed of only one sample: in this case, there are as many subsets and models as samples ( $k = n$ ).

The root mean square error of cross validation (RMSECV) versus the number of latent variables is computed in order to give a generalization of the prediction error of the model, according to the definition:

Improving the performance of micro-machined metal oxide gas sensors:  
 Optimization of the temperature modulation mode via pseudo-random sequences.

$$RMSECV = \sqrt{\frac{\sum_{i=1}^n (Y_i - y_i)^2}{n}} \quad (3.15)$$

where  $Y_i$  is the actual concentration value and  $y_i$  the model prediction.

### 3.3.3. Partial Least Squares Discriminant Analysis (PLS-DA).

PLS regression is not perfectly suited to pattern recognition problems, i.e. for classification purposes. However, this technique can be adapted for classification, giving rise to the PLS-DA method.

PLS-DA is carried out using an exclusive binary coding scheme with one bit per class, providing a triplet {a; b; c} if one wants to discriminate between three classes. Each number represents a “membership value” for each class, e.g., a response encoded {0; 1; 0} means that the sample belongs to class 2. During the calibration process, the PLS-DA method is trained to compute the three “membership values”, one for each class; the sample is then assigned to the class showing the highest membership value. Leave-one-out cross-validation was used to compare the performance of the various models. The prediction results are displayed in a confusion matrix, presenting the number of samples assigned to each class. So the classification rate of the system is given by the following relation

$$C_R (\%) = 100 \times \left( \frac{M_{Samples}}{TOT_{Samples}} \right) \quad (3.16)$$

where  $M_{Samples}$  is the number of samples correctly classified and  $TOT_{Samples}$  the total number of samples.

### 3.3.4. Fuzzy ARTMAP neural network.

Artificial Neural Networks (ANN) are highly parallel mathematical constructs that have been inspired by our understanding of the biological nervous system. It is well known that ANN consist of a lattice of information processing elements called *neurons*, which are connected together in a certain way. The strengths of these connections are called weights and are determined either during a training phase (or learning phase) for supervised ANN, or by an algorithm for unsupervised ANN. There are many different types of ANN that have been applied to solve gas identification problems. These are mainly single layer competitive ANN such as Kohonen’s self organizing map, multilayer neural networks, such as the

ubiquitous back-propagation trained multilayer perceptron (MLP) or networks based on adaptive resonance theory (ART) and fuzzy methods [35]. Indeed, the network considered in this doctoral thesis for discrimination purposes is the so-called Fuzzy ARTMAP ANN. This ANN is a supervised version of the Fuzzy ART network.

Fuzzy ART, which is a fuzzy version of the ART2 network, is formed by two major subsystems: the attentional subsystem and the orienting subsystem (Figure 3.1).

Two interconnected layers of neurons F1 and F2, which are fully connected both bottom-up and top-down, comprise the attentional subsystem. The links between F1 and F2 are called adaptive filters where the weights represent the long-term memory (LTM) as they remain in the network for an extended period.

The application of a single input vector leads to patterns of neural activity in both layers F1 and F2. These patterns are known as the short term memory (STM).

The activity in F2 nodes reinforces the activity in F1 nodes due to top-down connections. The interchange of bottom-up and top-down information leads to a resonance in neural activity. As a result, critical features in F1 are reinforced and have the greatest activity.

The orienting subsystem is responsible for generating a reset signal to F2 when the bottom-up input pattern and top-down template pattern mismatch at F1, according to a vigilance criterion. In other words, once it has detected that the input pattern is novel, the orienting subsystem must prevent the previously organized category neurons in F2 from learning this pattern, via a reset signal. Otherwise, the category will become increasingly non-specific. When a mismatch is detected, the network adapts its structure by immediately storing the novelty in additional weights.

The vigilance criterion is set by the value of the vigilance parameter. A high value of the vigilance parameter means that only a slight mismatch will be tolerated before a reset signal is emitted. On the other hand, a small value (low vigilance) means that large mismatch will be tolerated.

After the resonance check, if a pattern match is detected according to the vigilance parameter, the network changes the weights of the winning node. The Fuzzy ART network stores a weighted part of the present input vector in the LTM, just as any other neural network does.

Fuzzy ARTMAP, in its most general form, includes two Fuzzy ART modules (ART<sub>a</sub> and ART<sub>b</sub>), which F2 layers are linked by an inter-ART associative memory referred to as 'match tracking system'.

Improving the performance of micro-machined metal oxide gas sensors:  
 Optimization of the temperature modulation mode via pseudo-random sequences.

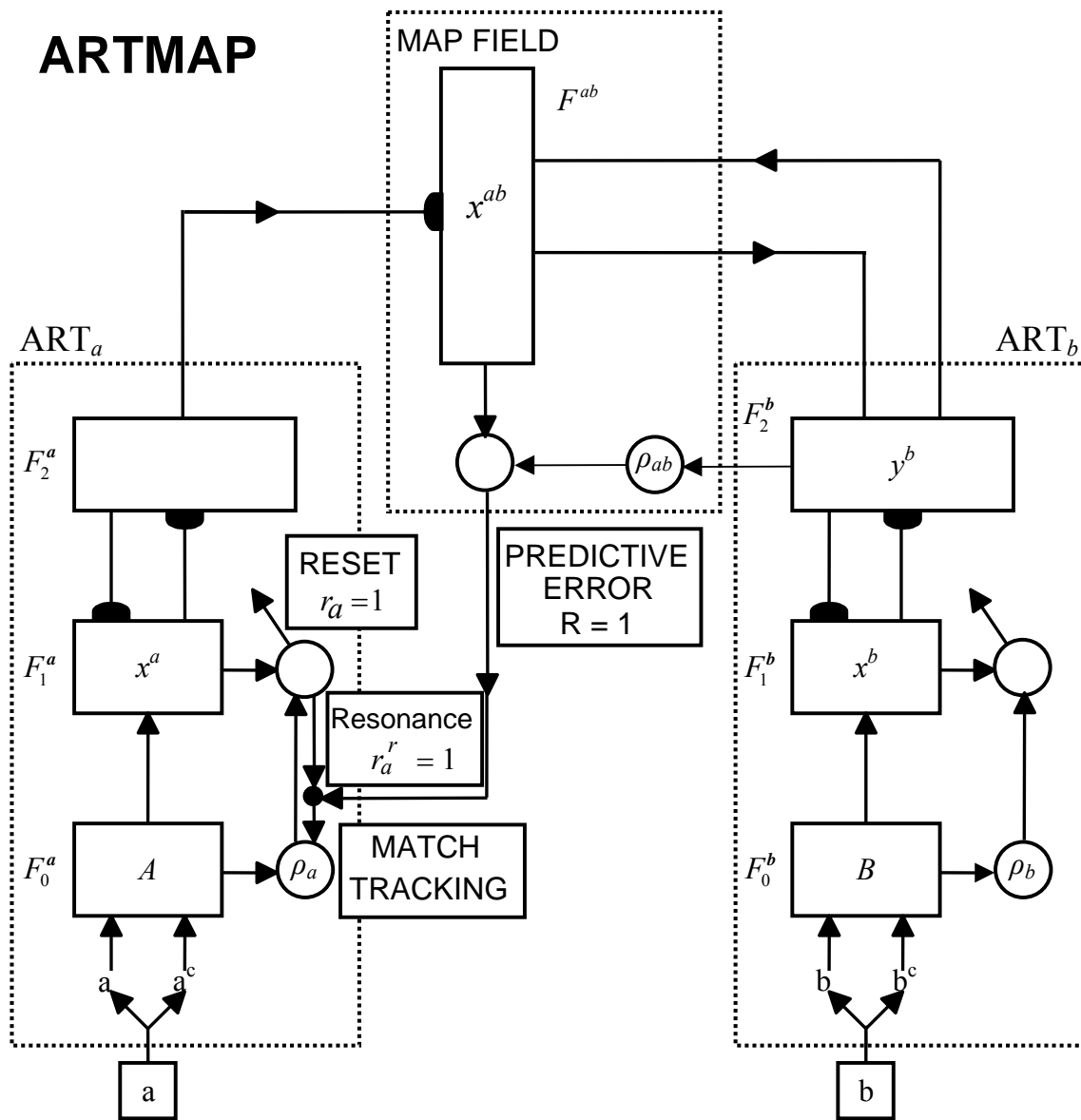


**Figure 3.1:** The structure of the Fuzzy ARTMAP neural network.

During supervised learning  $ART_a$  receives a stream of input patterns  $\{a\}$  and  $ART_b$  also receives a stream of patterns  $\{b\}$ , where  $b$  is the correct prediction given  $a$ . When a prediction by  $ART_a$  is not confirmed by  $ART_b$ , inhibition of the inter-ART associative

memory activates a match tracking process. This increases  $ART_a$  vigilance by the minimum amount needed for the system either to activate an  $ART_a$  category that matches the  $ART_b$  category or to learn a new  $ART_a$  category.

An in-depth review of this architecture can be found in [36-38].

### 3.4. Variable selection procedure.

Once the feature extraction methods have been applied to the gas sensor transient response (because of the temperature modulation) a simple variable selection procedure is needed to be implemented in order to select a short number of features (i.e., the ones more representative of the problem) among the total number of variables extracted.

A criterion was defined to rate the resolution power of each variable selected. For gas identification purposes, the measurements were grouped in as many categories as pollutant species are (i.e. single species or their mixtures). In a similar way for quantification purposes, one specific model per species or gas-mixture was built. Therefore, for every quantification model, the measurements were grouped in as many categories as gas or gas mixture concentrations were measured.

For each set of variable selected, intra-group and between-group variances were computed:

An intra-group variance was defined as the variance of the set of features or variable extracted considered within a given group of measurements. Two examples of intra-group variances are as follows: the variance of a spectral component within the measurements of a pollutant gas, no matter the concentration (case of gas identification) or the variance within the measurement of a given concentration of pollutant specie (case of quantification). The intra-group variance of a variable set  $j$ , can be defined as:

$$\sigma_{\text{intra},j}^2 = \frac{\sum_{i=1}^n (N_{ji} - \mu_j)^2}{n-1} \quad (3.17)$$

where  $n$  is the number of measurements within the group,  $N_{ji}$  is the value of variable set  $j$  for measurement  $i$  and  $\mu_j$  is the mean of variable set  $j$  over the measurements within the group. A schematic of how intra-group variance is calculated is shown in Figure 3.2.

Improving the performance of micro-machined metal oxide gas sensors:  
 Optimization of the temperature modulation mode via pseudo-random sequences.

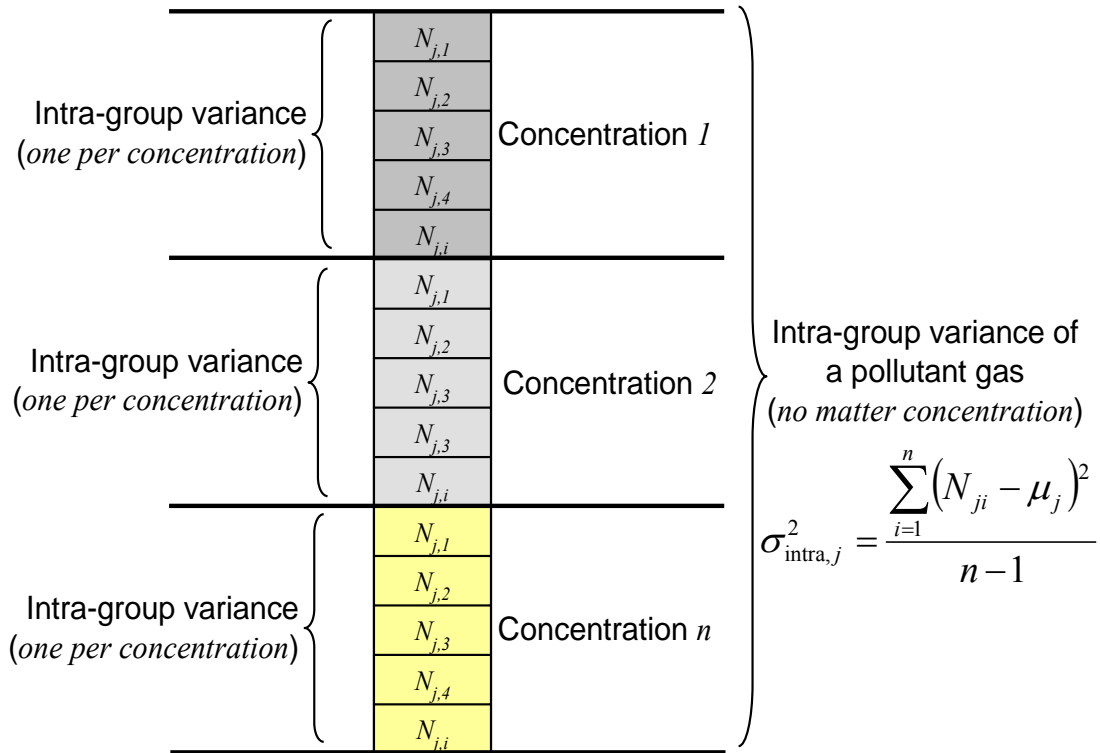


**Figure 3.2:** Intra-group variance: Case of gas identification (no matter concentration): all measurements in the figure belong to the same class (see right). Case of gas quantification: 3 classes exist and an intra-variance is computed per gas concentration (see left).

In a similar way, for every variable set, a between-group variance was defined as the variance within the category means (*centroids*). Therefore, the between-group variance can be defined as:

$$\sigma_{\text{be},j}^2 = \frac{\sum_{i=1}^d (\mu_{ji} - \bar{\mu}_j)^2}{d - 1} \tag{3.18}$$

where  $\mu_{ji}$  is the mean of variable set  $j$  over the measurements within group  $i$ ,  $d$  is the number of different groups and  $\bar{\mu}_j$  is the mean over the  $\mu_{ji}$ . Figure 3.3 shows a schematic of this between-group variance.

Feature extraction and pattern recognition for temperature-modulated gas sensors.

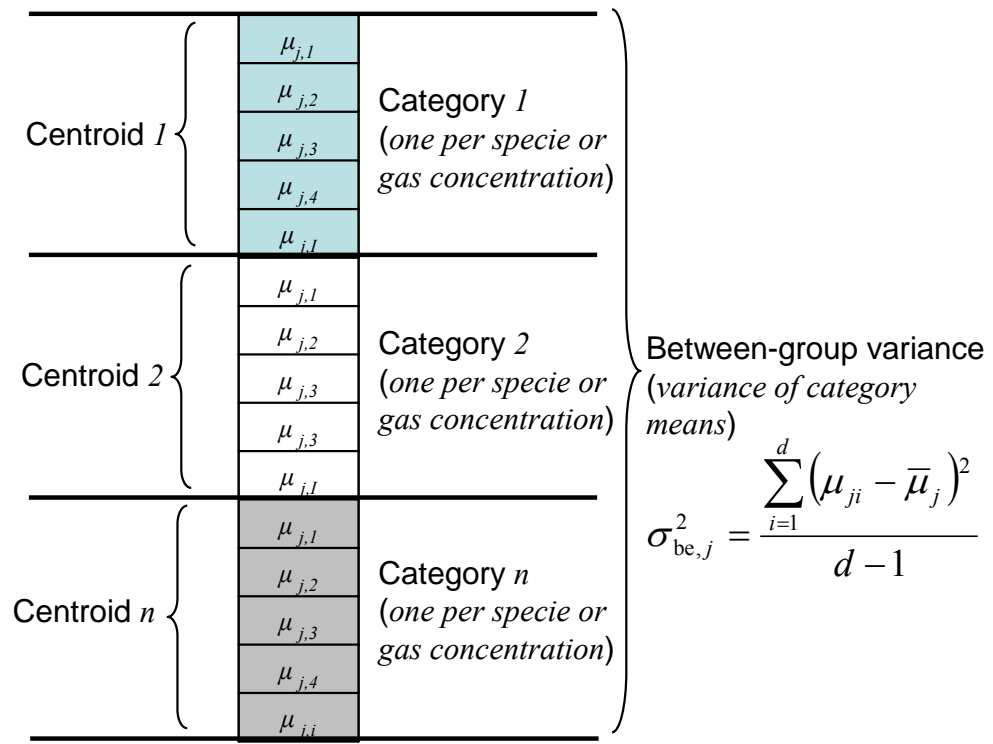


**Figure 3.3:** Between-group variance: each category is per species or gas concentration.

Finally, a figure of merit for the resolution power,  $RP$ , of a spectral component was defined as the ratio:

$$RP_j = \frac{\sigma_{be,j}^2}{\sigma_{intra,j}^2} \quad (3.19)$$

The higher the figure of merit defined in equation 3.19 is, the more important is the spectral component considered to correctly discriminate or quantify gases.

Finally, a small set of spectral components, which comprises those that have the higher figure of merit, is selected. These spectral components correspond to the temperature-modulating frequencies that lead to a better discrimination or quantification of the gases studied.

## Improving the performance of micro-machined metal oxide gas sensors: Optimization of the temperature modulation mode via pseudo-random sequences.

### 3.5. Conclusions.

This chapter presents the different feature extraction and pattern recognition methods employed in the analysis of the experimental data set reported during the experimental set-up in Chapter 5.

Originally, the sensor transient responses were decomposed and converted to the frequency domain by the Fast Fourier Transform (FFT) feature extraction method, which are presented in Section 3.2.1. It is well known that the FFT has been by far the most commonly method used in the field of temperature modulated gas sensors. In this case in particular, the FFT was used as feature extraction method in the sense to obtain the more important characteristics of the phenomenon under study. Therefore, the FFT is computed to obtain the features of the gas sensors transient response. These variables extracted set are then undergone to a variable selection process in order to select the optimal ones for the determined gas application purpose.

Additionally, in this doctoral thesis, a novel feature extraction method called Dynamic Moments (DM) and Phase Space (PS) was used to extract features from the response of micro-hotplate gas sensors. The data resulting from the decomposition of the original sensor signals are then input into different pattern recognition algorithms in order to classify and quantify the gases measured in the experiments. The pattern recognition methods employed in this study were presented in sub-section 3.3.

This chapter ends with the variable selection procedure of the set of features extracted by the FFT (that are the input of the different pattern recognition methods).



### 3.6. References.

- [1] S.W. Wlodek, K. Colbow and F. Consadori, "Signal-shape analysis of a thermally cycled tin-oxide gas sensor", *Sensors and Actuators B*, vol. 3, pp. 63-68, 1991.
- [2] R.E. Cavicchi, J.E. Suehle, K.G. Kreider, M. Gaitan and P. Chaparala, "Optimised temperature-pulse sequences for the enhancement of chemically specific response patterns from micro-hotplate gas sensors", *Sensors and Actuators B*, vol. 33, pp. 142-146, 1996.
- [3] A. Heilig, N. Bârsan, U. Weimar, M. Sweizer-Berberich, J.W. Gardner and W. Göpel, "Gas identification by modulating temperatures of SnO<sub>2</sub>-based thick film sensors", *Sensors and Actuators B*, vol. 43, pp. 45-51, 1997.
- [4] S. Nakata, T. Nakamura, K. Kato and K. Yoshikawa, "Discrimination and quantification of flammable gases with a SnO<sub>2</sub> sniffing sensor", *The Analyst*, vol. 125, pp. 517-522, 2000.
- [5] A. Vergara, E. Llobet, E. Martinelli, C. Di Natale, A D'Amico, X. Correig, "Feature extraction of metal oxide gas sensors using dynamic moments", *Sensors and Actuators B*, in press, 2006.
- [6] R. Gutierrez-Osuna, "Pattern Analysis for Machine Olfaction: A Review", *IEEE Sensors Journal*, vol. 2, (3), 2002.
- [7] T. Masters, "*Advanced Algorithms for Neural Networks*", New York: Wiley, 1995.
- [8] A. P. Lee, B. J. Reedy, "Temperature modulation in semiconductor gas sensing", *Sensors and Actuators B*, vol. 60, pp. 35-42, 1999.
- [9] W. M. Sears, K. Colbow, F. Consadori, "General characteristics of thermally cycled tin oxide gas sensors", *Semicond. Sci. Technol.*, vol. 4, pp. 351- 359, 1989.
- [10] W. M. Sears, K. Colbow, F. Consadori, "Algorithms to improve the selectivity of thermally cycled tin oxide gas sensors", *Sensors and Actuators B*, vol. 19, pp. 333-349, 1989.
- [11] S. Nakata, Y. Kaneda, H. Nakamura, K. Yoshikahua, "Detection and quantification of CO gas based on the dynamic response of a ceramic sensor", *Chem., Lett.*, pp. 1505-1508, 1991.

Improving the performance of micro-machined metal oxide gas sensors:  
Optimization of the temperature modulation mode via pseudo-random sequences.

- [12] S. Nakata, H. Nakamura, K. Yoshikahua, "New strategy for the development of a gas sensor based on the dynamic characteristic principle and preliminary experiment", *Sensors and Actuators B*, vol. 8, pp. 187-189, 1992.
- [13] S. Nakata, S. Akakabe, M. Nakasuji, K. Yoshikahua, "Gas sensing based on a non-linear response: discrimination between hydrocarbons and quantification of individual components in a gas mixture", *Anal. Chem.*, vol. 68, pp. 2067-2072, 1996.
- [14] S. Nakata, K. Yoshikahua, "Non-linear dynamics in chemical assembly", *Trends Chem. Phys.*, vol. 4, pp. 23-58, 1996.
- [15] S. Nakata, E. Ozaki, N. Ojima, "Gas sensing based on the dynamic non-linear response of a semiconductor gas sensor: dependence on the range and frequency of a cycle temperature change", *Anal. Chim. Acta*, vol. 361, pp. 93-100, 1998.
- [16] A. Heiling, N. Barsan, U. Weimar, M. Schweizer-Berberich, J. W. Gardner, W. Gopel, "Gas identification by modulating temperatures of SnO<sub>2</sub>-based thick film sensors", *Sensors and Actuators B*, vol. 43, pp. 45-51, 1997.
- [17] E. Llobet, R. Ionescu, S. Al-khalifa, J. Brezmes, X. Vilanova, X. Correig, N. Barsan, J. W. Gardner, "Multi-component gas mixture analysis using a single tin oxide sensor and dynamic pattern recognition", *IEEE Sensors Journal*, vol. 1, (3), pp. 207-213, 2001.
- [18] E. Yeramian. P. Claverie, "Analysis of multi-exponential functions without a hypothesis as to the number of components", *Nature*, vol. 326, pp. 169-1174, 1987.
- [19] S. Marco, J. Samitier, J. R. Morante, "A novel time domain method to analyze multi-component exponential transients", *Meas. Sci., Technol.*, vol. 6, pp. 135-142, 1995.
- [20] B. G. Kermani, "On using neural networks and genetic algorithms to optimize the performance of an electronic nose", PhD. Dissertation, North Carolina State University, Raleigh, NC, 1995.
- [21] A.V. Openheim and K.W. Schafer, "*Discrete-time signal processing*", *Englewood Cliffs, Prentice Hall*, N.J., U.S.A., 1989.
- [22] L. Ljung, T. Glad, "*Modelling of dynamic systems*", Prentice Hall, Englewood Cliffs, NJ, 1994.
- [23] F. Takens, "Detecting strange attractors in turbulence", in: D. Rand, L.S. Young (Eds.), "*Dynamical Systems and Turbulence*", Warwick, pp. 366-381, 1980.

- [24] A. Fichera, C. Losenno, A. Pagano, "Clustering of chaotic dynamics of a lean gas-turbine combustor", *Appl. Energy*, vol. 69, pp. 101-117, 2001.
- [25] M Annunziato, H.D.I. Abarbanel, "Non linear dynamics for classification of multiple flow regimes", in: *Proceedings of the International Conference on Soft Computing, SOCO*, Genoa, 1999.
- [26] E. Martinelli, C. Falconi, C. Di Natale, A. D'amico, "Feature extraction of chemical sensors in phase space", *Sensors and Actuators B*, vol. 95, pp. 132-139, 2003.
- [27] E. Martinelli, G. Pennazza, C. Di Natale, A. D'amico, "Chemical sensors clustering with the dynamic moments approach", *Sensors and Actuators B*, vol. 101, pp. 346-352, 2004.
- [28] J. W. Gardner, P. N. Bartlett, "Electronic noses principles and applications", *Oxford science publications*, Oxford university press.
- [29] D. E. Rumelhart, J. L. McClelland, "*Parallel distributed processing*". MIT Press, Cambridge, MA, USA.
- [30] J. Brezmes, "Fuzzy ART and Fuzzy ARTMAP neural networks using MATLAB", Dept. of Electronic Engineering, URV, Tarragona, Spain, 1999.
- [31] H. Abe, T. Y. Yoshimura, S. Kanaya, Y. Takahashi, Y. Miyashita, S. Sasaki, "Automated odor-sensing system based on plural semiconductor gas sensors and computerised pattern recognition techniques", *Anal Chim Acta*, vol. 194, pp. 1-9, 1987.
- [32] M. Holmberg, F. Winquist, I. Lundström, J. W. Gardner, E. L. Hines, "Identification of paper quality using a hybrid electronic nose", *Sensors and Actuator B*, vol. 26-27, pp. 246-249, 1995.
- [33] F. Wold, "Festschriftjerzyneyman", Wiley, New York, 1966.
- [34] J. W. Gardner, E. L. Hines, "Pattern analysis techniques", in "*Handbook of biosensors and electronic noses*", (ed. E. Kress-Rogers), Chapter 27. CRC Press USA, 1996.
- [35] L. A. Zadeh, "Fuzzy logic and its applications", Academic Press New York, 1965.
- [36] G. Carpenter, S. Grossberg, N. Markuzon, J. Reynolds and D. Rosen, "Fuzzy ARTMAP: A neural network architecture for incremental supervised learning of analog multidimensional maps", *IEEE Trans. Neural Networks*, vol. 3, (5), pp. 698-713, 1992.

Improving the performance of micro-machined metal oxide gas sensors:  
Optimization of the temperature modulation mode via pseudo-random sequences.

- [37] G. Carpenter, S. Grossberg and J. Reynolds, "A fuzzy ARTMAP nanoparametric probability estimator for nonstationary pattern recognition problems", IEEE Trans. Neural Networks, vol. 6, (6), pp. 1330-1336, 1995.
- [38] R. Ionescu, E. Llobet, X. Vilanova, J. Brezmes, J.E. Suerias, J. Calderer, X. Correig, "Quantitative analysis of NO<sub>2</sub> in the presence of CO using a single tungsten oxide semiconductor sensor and dynamic signal processing", Analyst, vol. 127, pp. 1237-1246, 2002.

---

# 4.

# Gas/sensor system identification

---

<b>4. GAS/SENSOR SYSTEM IDENTIFICATION</b>	<b>89</b>
<b>4.1. Introduction.</b>	<b>90</b>
<b>4.2. Description of systems: relationship between their input and output.</b>	<b>91</b>
4.2.1. Types of signals.	91
4.2.2. Description of system.	92
<b>4.3. Correlation functions.</b>	<b>94</b>
4.3.1. The correlation function.	95
4.3.2. The Autocorrelation.	96
4.3.3. Cross correlation.	96
<b>4.4. Design and generation of PRBS signals.</b>	<b>97</b>
<b>4.5. Design and generation of MLPRS.</b>	<b>99</b>
<b>4.6. Pseudo Random Sequences (PRS) and systems identification.</b>	<b>102</b>
<b>4.7. Gas/sensor systems identification.</b>	<b>104</b>
<b>4.8. Conclusions.</b>	<b>106</b>
<b>4.9. References.</b>	<b>107</b>

## Improving the performance of micro-machined metal oxide gas sensors: Optimization of the temperature modulation mode via pseudo-random sequences.

### 4.1. Introduction.

It is always best to begin at the beginning. Since this chapter is about signals, systems, and how they can be identified, the first question to answer is, what are they? Any time-varying physical phenomenon which is intended to convey information is a signal. Examples of signals are the human voice, a dog bark, a lion's roar, smoke signals, drums, sign language, Morse code, and traffic signals. Examples of high-speed signals are the voltages on telephone wires, the electric fields emanating from radio or television transmitters, and variations of light intensity in an optical fiber on a telephone or computer network. Noise, is sometimes called random signal, is like a signal in that it is a time-varying physical phenomenon, but unlike a signal it usually does not carry useful information and is almost considered undesirable.

Signals are processed or operated on by systems. When one or more excitation signals are applied at one or more system inputs, the system produces one or more response signals at its outputs (see Figure 4.1). In a communication system, a transmitter is a device that produces a signal and a receiver is a device which acquires the signal. A channel is the path a signal and/or noise take from a transmitter and/or noise source to a receiver. The transmitter, channel and receiver are all systems, which are components or sub-systems of the overall system. Other types of systems also process signals which are analyzed using signal analysis. Some systems are readily analyzed in detail, some others can be analyzed approximately, but some are so complicated or difficult to measure that are hardly known enough to understand or control them.

In this particular case a gas-sensor pair is considered as a system where, on the one side, the temperature stimulation or excitation to the heating element and the pollutant gas to be measured are the inputs, and on the other side, the sensor operating temperature and the sensor response to the pollutant are the outputs of the system. This chapter is divided as follows: a mathematical definition of a general system is described in section 4.2. Therefrom the ways to obtain the impulse response of a system are mentioned in section 4.3. In section 4.4 the generation of maximum length based pseudo random sequences signals (PRS) (either binary or multilevel) to study a system is presented. Furthermore, the use of these kinds of signals in the identification of systems is presented in section 4.5. Section 4.6 analyzes for the first time a gas sensor pair as a system. PRS signals are used to identify, optimize and select the best frequencies to modulate the working temperature of a micro-hotplate gas sensor system. Finally, section 4.7 presents the conclusion derived from these descriptions.

## 4.2. Description of systems: relationship between their input and output.

The words signal and system were defined very generally in the introduction of this chapter but their definition is broader than that. On the one hand there are several broad classifications of signals: Continuous- time, discrete-time, continuous-value, discrete value, random and non random. All of them are reviewed here below. On the other hand the term system is so broad and abstract that it is difficult to define; actually a system can be almost anything. The term system is also defined in the following paragraphs. More information about signals and systems are found in [1, 2].

### 4.2.1. Types of signals.

In signals and systems analysis, signals are described by mathematical functions. The signal is the actual physical phenomenon which carries information, and the function is a mathematical description of the signal.

A **continuous-time** signal is one which is defined at every instant of time over the time interval. Another common name for a continuous-time signal is an analog signal. The name analog comes from the fact that in many systems the variation of the analog signal with time is analogous to some physical phenomenon, which is being measured or monitored.

The process of **sampling** the signal is to take values from it at discrete points in time and then to use only the samples to represent the original continuous-time signal. The set of samples taken from a continuous-time signal is one example of a **discrete-time** signal. A discrete-time signal can also be created by an inherently discrete time system which produces signals values only at discrete times. A discrete-time signal has defined values only at discrete points in time and not between them.

A **continuous-value** signal is one which may have a value anywhere within a continuum of allowed values. The continuum may have a finite or infinite extent. A continuum is a set of values with no “space” between allowed values; two allowed values can be arbitrary close together. The set of real numbers is a continuum with infinite extent. The set of real numbers between zero and one is a continuum with finite extent. Each of these examples is a set with infinitely many members.

A **discrete-value** signal can only have values taken from a discrete set of values. A discrete set of values is a set for which there is a finite space between allowed values. Discrete-time signals are usually transmitted as digital signals. The term digital signal

## Improving the performance of micro-machined metal oxide gas sensors:

### Optimization of the temperature modulation mode via pseudo-random sequences.

applies to the transmission of a sequence of values of a discrete time signal in the form of digits in some encoded form (usually binary). The term digital is some times used loosely to refer a discrete-value signal which only has two possible values.

A **random signal** is one whose values cannot be predicted exactly and cannot be described by any mathematical function. A non-random signal, which is also called a deterministic signal, is one that can be mathematically described, at least approximately. As previously stated, a common name for a random signal is noise.

### 4.2.2. Description of system.

One way to define a system is as anything that performs a function. That is, it operates on something and produces something else. Another way to define a system is as anything that responds when stimulated or excited. A system can be an electrical system, a mechanical system, a biological system, a computer system, an economical system, a political system, etc. Some systems can be thoroughly and completely analyzed through mathematics. Others may be so complicated that mathematical analysis is extremely difficult. And still others are just not well understood because the difficulty in measuring their characteristics. Although the definition of a system is very broad, in electronics the term system usually refers to something that is excited by certain signals and responds with other signals.

Although systems can be of many different kinds, they have some features in common. A system operates in signals at one or more inputs to produce signals at one or more outputs. In system analysis it is very useful to represent systems by block diagrams. Actually, the form of the system to be considered in this chapter is shown in Figure 4.1. The input signal  $x(t)$  produces a system response signal  $y(t)$ . In many experimental situations,  $x(t)$  and  $y(t)$  are perturbations around steady-state input and output levels, and in these situations, the terms 'input' and 'output' will be taken to refer to deviations from the steady-state operating levels. There may be noise in the system and /or in the measuring device and this is commonly represented by a noise signal  $n(t)$  added to the system output  $y(t)$  to give the measurable output signal  $z(t)$ , so that

$$z(t) = y(t) + n(t) \tag{4.1}$$

The system is assumed to be linear, so that the principle of superposition applies. This means that if  $x_1(t)$  produces a response  $y_1(t)$ ,  $x_2(t)$  produces a response  $y_2(t)$  and so on, then the sum  $[x_1(t) + x_2(t) + \dots]$  produces a response  $[y_1(t) + y_2(t) + \dots]$ .



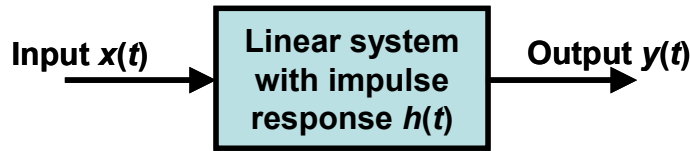


**Figure 4.1:** Block diagram of a linear system.

There is a systematic method to find how linear systems respond to excitations or inputs. This systematic method is called convolution. The convolution technique for finding the response of a linear system is based on a simple idea. The system response  $y(t)$  is given by an integral of weighted inputs which have occurred in the past. The past values of input are multiplied by a function  $h(t)$ , called the weighting function of the system and the mathematical equation describing the relationship is:

$$y(t) = \int_0^{\infty} h(\lambda)x(t - \lambda)d\lambda \quad (4.2)$$

where  $\lambda$  is a time variable. If the characteristics of the system do not change with time, then the weighting function is also equal to the unit impulse response of the system. This is the response  $y(t)$  to an input  $x(t) = \delta(t)$ , where  $\delta(t)$ , the Dirac delta distribution centered at  $t = 0$ , is a distribution of height which tends to infinity and duration which tends to zero such that (height  $\times$  duration) = 1. This equation (4.2) is the so-called convolution.

In a practical situation, inputs which have occurred at times greater than  $T_S$  in the past have negligible effect on the present output of the system so the previous equation may be modified to:

$$y(t) = \int_0^{T_S} h(\lambda)x(t - \lambda)d\lambda \quad (4.3)$$

the  $T_S$  is called the setting time of the system. Combining equation (4.1) and 4.3, the measurable output is given by:

$$z(t) = \int_0^{T_S} h(\lambda)x(t - \lambda)d\lambda + n(t) \quad (4.4)$$

All equations and techniques shown until now are destined for finding the response of continuous-time systems. So, on the other hand the convolution technique for finding the response of a discrete-time linear system is based on a simple idea. No matter how complicated an excitation signal is, it is simply a sequence of discrete-time impulses. To find the response of a linear system, it is necessary to find the response of the system to one impulse at a time, all those responses to form the actual overall response. The responses to those impulses all have the same functional form except that shifted in time. Therefore, if a

Improving the performance of micro-machined metal oxide gas sensors:  
Optimization of the temperature modulation mode via pseudo-random sequences.

response of a linear system to a unit impulse excitation occurring at time  $n = 0$  is obtained, the response to any other excitation can be easily found. Therefore, the use of the convolution technique begins with the assumption that the response of the system to a unit impulse excitation occurring at time  $n = 0$  has already been found, and it is called the impulse response  $h[n]$ .

Therefore, since the response of the system to a single unit impulse occurring at discrete time  $n = 0$  is known, by means of the convolution of the impulse response  $h[n]$  of the system and the input  $x[n]$ , the output of the system  $y[t]$  can be found by the convolution expression as in the case of continuous-time systems. So, the discrete equivalent for equations (4.3) and (4.4) (convolution expressions) respectively are shown as follows:

$$y[n] = \sum_{m=0}^L h[n]x[n-m] \tag{4.5}$$

$$z[n] = \sum_{m=0}^L h[n]x[n-m] + n[n] \tag{4.6}$$

where the time  $T_s$  is now denoted by  $L$ .

In theory equation (4.4) or its discrete equivalent (4.6), could be solved to give an estimate of the system weighting function from almost any input-output records.

### 4.3. Correlation functions.

In signals and systems analysis the characteristics of individual signals are, of course, important, but often the relationships between signals are just as important. Relationships between signals often indicate whether the physical phenomena which caused the signals are related or whether one signal is a modified version of the other. The relationship between two signals in a system can be used to measure system's characteristics. But the question is how to determine whether two signals are correlated? The natural answer is to simply look at them and try to detect any similarity between them. However it is necessary to precisely and quantitatively indicate the correlation between signals in a mathematical way. In this section we will explore the mathematical techniques of comparing two signals. These comparison methods can be applied to all kinds of signals, continuous-time and discrete-time, deterministic and random.

### 4.3.1. The correlation function.

The correlation is useful as a visualization tool, but it would be nice to have a precise mathematical way of expressing the relationship between two signals. Correlation is the mathematical technique which indicates whether two signals are related and in a precise quantitative way how much they are related.

The mathematical calculation of correlation is based in an analysis of whether two signals tend to move together. That is, if one signal moves in a positive direction and the other signal also moves in a positive direction at the same time, they are correlated, at least for that time. The same is true if both signals move in a negative direction together. If, over a long period of time, the signals tend to move in the same direction at the same time, they are positively correlated. On the other hand, if over a long period of time, two signals tend to move in opposite direction at the same time, they are also correlated, but in a negative sense. On the contrary, if, over a long period of time, the two signals tends to move in the same direction about half the time and in opposite directions the other half of the time, they are said to be uncorrelated.

The mathematical definition of correlation depends on the type of signals being analyzed. For two continuous time energy signals  $x(t)$  and  $y(t)$ , correlation is defined by  $\int_{-\infty}^{\infty} x(t)y^*(t)dt$ . For two discrete time energy signals  $x[n]$  and  $y[n]$ , correlation is defined by  $\sum_{n=-\infty}^{\infty} x[n]y^*[n]$ . It is more common in signal and system analysis to refer to the correlation function instead of just the correlation. The correlation function is a mathematical expression of how correlated two signals are as a function of how much one of them is shifted. The correlation between two functions is a single number. The correlation function between two functions is itself a function, a function of the shift amount. The mathematical definition of the correlation function  $R_{xy}$  between two continuous time energy signals  $x(t)$  and  $y(t)$  is

$$R_{xy}(\tau) = \int_{-\infty}^{\infty} x(t)y^*(t + \tau)dt = \int_{-\infty}^{\infty} x(t - \tau)y^*(t)dt \quad (4.7)$$

or, if two signals  $x(t)$  and  $y(t)$  are real,

$$R_{xy}(\tau) = \int_{-\infty}^{\infty} x(t)y(t + \tau)dt = \int_{-\infty}^{\infty} x(t - \tau)y(t)dt \quad (4.8)$$

For discrete time energy signals,

$$R_{xy}[m] = \sum_{n=-\infty}^{\infty} x[n]y^*[n + m] = \sum_{n=-\infty}^{\infty} x[n - m]y^*[n] \quad (4.9)$$

or, if both signals  $x[n]$  and  $y[n]$ , are real,

Improving the performance of micro-machined metal oxide gas sensors:  
 Optimization of the temperature modulation mode via pseudo-random sequences.

$$R_{xy}[m] = \sum_{n=-\infty}^{\infty} x[n]y[n+m] = \sum_{n=-\infty}^{\infty} x[n-m]y[n] \quad (4.10)$$

where \* indicates the complex conjugated of the signal  $y(t)$  and  $y[n]$ .

### 4.3.2. The Autocorrelation.

A very important case of the correlation function is the correlation of a function with itself. This type of correlation function is called autocorrelation function. If  $x(t)$  is an energy signal, its autocorrelation is

$$R_{xx}(\tau) = \int_{-\infty}^{\infty} x(t)x(t+\tau)dt \quad \text{or} \quad R_{xx}[m] = \sum_{n=-\infty}^{\infty} x[n]x[n+m] \quad (4.11)$$

At a shift of zero that becomes

$$R_{xx}(0) = \int_{-\infty}^{\infty} x^2(t)dt \quad \text{or} \quad R_{xx}[0] = \sum_{n=-\infty}^{\infty} x^2[n] \quad (4.12)$$

which is the total energy of the signal.

The autocorrelation depends on the choice of the shift amount, so we cannot say what the autocorrelation function looks like until we know what function is. But we can say that the value of the autocorrelation can never be higher than it is at zero shift. That is

$$R_{xx}(0) \geq R_{xx}(\tau) \quad \text{or} \quad R_{xx}[0] \geq R_{xx}[m] \quad (4.13)$$

because at a zero shift, the correlation with itself is obviously as large as it can get since the shifted and unshifted versions coincide.

### 4.3.3. Cross-correlation.

A common term for the correlation function between two different signals is cross correlation to distinguish it from autocorrelation. Autocorrelation is simply a special case of the cross-correlation function. Cross correlation is more general than autocorrelation, so the properties are not as numerous, but there is one property that is sometimes useful,

$$R_{xx}(\tau) = R_{xx}(-\tau) \quad \text{or} \quad R_{xx}[m] = R_{xx}[-m] \quad (4.14)$$

Notice that when  $y(t) = x(t)$  or  $y[n] = x[n]$  this property reduces to the property of autocorrelation functions that they are even functions of shift.

## 4.4. Design and generation of PRBS signals.

One of the most useful types of periodic signal for process identification is the pseudo-random binary sequence (PRBS) [3 - 5], which has the following properties:

- The signal has two levels (e.g. 0 or 1), and it can switch from the one level to the other only at certain event points  $t = 0, \Delta t, 2\Delta t$ , etc. Therefore, since the signal changes level at *predetermined* event points, the PRBS is deterministic and experiments performed using this signal are repeatable.
- The PRBS is periodic with period  $T = L\Delta t$ , where  $L$  is an odd integer. The most commonly used PRBS signals are based upon maximum-length sequences (MLS) of length  $L = (2^n - 1)$  where  $n$  is the order of the sequence. The reason why PRBS are so popular is that they can be readily generated using a feedback shift register circuit and simple XOR logic gates. The number of shift registers employed is the order,  $n$ , of the sequence [6].
- In any one period, there are  $\frac{1}{2}(L+1)$  intervals when the signal is at one level and  $\frac{1}{2}(L-1)$  intervals when it is the other.

These properties imply that a PRBS shares some properties with white noise but having the advantage of being repeatable.

A PRBS of length  $L = 2^n - 1$  is generated by an  $n$ -stage shift register ( $n > 1$ ) with an OR-exclusive logic gate feedback to the first stage. The XOR gate performs an modulo 2 addition, and the logic values are given by:

$$1 \oplus 1 = 0 \oplus 0 = 0$$

$$1 \oplus 0 = 0 \oplus 1 = 1$$

Such a circuit goes through a set of states and eventually repeats itself after  $2^n - 1$  clock pulses, where  $n$  is an integer  $> 1$ . Figure 4.2 shows an example of a shift register circuit that generates a sequence of length  $L=7$  (a) and a sample of a 7-length PRBS signal (b). The algorithm of generation of the PRBS signal in MATLAB environment is shown in appendix A. The shift register can be started with any binary number excepted 0, 0, 0 (which would give a sequence of length unity). In Table 4.1 the register started (arbitrarily) with 0, 0, 1 and it is seen that this number reappears after  $2^3 - 1$  clock pulses (feedback are from stages 1 and 3). Each binary number from 0 0 1 to 1 1 1 appears as the register contents exactly once during the cycle. This is a general result for all binary  $m$ -sequences: each binary number form 1 to  $2^n - 1$  appears in the sequences exactly once.

Improving the performance of micro-machined metal oxide gas sensors:  
 Optimization of the temperature modulation mode via pseudo-random sequences.

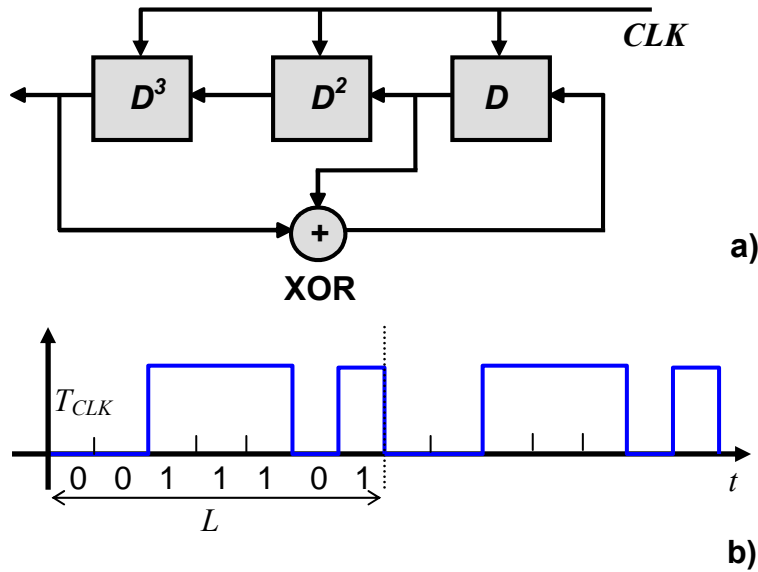


**Figure 4.2:** Shift register circuit used to generate a PRBS of length  $L = 7$  (a) and 2 periods of a sequence generated (b). CLK is the clock signal and  $T_{CLK}$  is the clock period.

A shift register with the appropriate connections to generate a PRBS has a characteristic equation in the delays,  $D$ , (introduced by each stage of the shift register) according to a primitive binary polynomial (modulo 2). A list of primitive polynomials can be found in [7, 8].

**Table 4.1:** PRBS from a 3-stage shift register with feedback connections corresponding to a primitive polynomial (modulo 2).

Number of clock pulses	Shift register stage		
	1	2	3
1	0	0	1
2	1	0	0
3	1	1	0
4	1	1	1
5	0	1	1
6	1	0	1
7	0	1	0
8	0	0	1

If the polynomial  $p(x) = p_0x^n + p_1x^{n-1} + \dots + p_{n-1}x + p_n$  is a primitive polynomial (modulo 2), then the characteristic equation in the delays,  $D$ , introduced by a shift register of length  $n$  is [9]:

$$p_0D^n + p_1D^{n-1} + \dots + p_{n-1}D + p_n = 0, \text{ modulo } 2 \quad (4.15)$$

Therefore,

$$p_nX = -p_0D^nX - p_1D^{n-1}X - \dots - p_{n-1}DX, \text{ modulo } 2 \quad (4.16)$$

where  $X$  is the input sequence to the shift register and  $D^iX$  is the output at the  $i^{\text{th}}$  stage of the register. Considering that modulo 2 subtraction or addition are equivalent, equation (4.16) can be rewritten as follows:

$$p_nX = p_0D^nX + p_1D^{n-1}X + \dots + p_{n-1}DX, \text{ modulo } 2 \quad (4.17)$$

For maximum length binary sequences to be obtained,  $p_0$  and  $p_n$  have to be set to unity and the remaining coefficients in equation (4.17) are either 0 or 1. For the example shown in Figure 4.2, the characteristic equation is:

$$D^3 + D + 1 = 0, \text{ modulo } 2 \quad (4.18)$$

And the corresponding primitive polynomial is  $x^3 + x + 1$ , modulo 2.

## 4.5. Design and generation of MLPRS.

The theory behind the generation of multilevel pseudo random sequences (MLPRS) based on multilevel maximum length signals is well developed. As in binary pseudo random sequences, MLPRS are periodic, deterministic signals, and have an autocorrelation function similar to white noise [10]. MLPRS exist for the number of levels,  $q$ , equal to a prime or a power of a prime  $p(>1)$ , i.e. for  $q = 2, 3, 4, 5, 7, 8, 9, 11, 13, \dots$  (Zierler, 1959), [6, 11]. The relevant theory behind MLPRS is based on the algebra of finite fields [12, 13]. When  $q$  (the number of levels) is a prime, the digits of the sequence are the integers  $0, 1, \dots, (q - 1)$  and the sequence can be generated by a  $q$ -level,  $n$ -stage shift register with feedback to the first stage consisting of the modulo  $q$  sum of the outputs of the other stages multiplied by coefficients  $a_1, \dots, a_n$  which are also the integers  $0, 1, \dots, (q - 1)$ . The length of such a sequence  $\{x_r\}$  is  $q^n - 1$ , where  $n$  is an integer. After  $q^n - 1$  digits, the sequence repeats itself. MLPRS signals are generated in a similar manner that the binary ones using a shift register and modulo addition. The generator of such a sequence and an example of a 5-level sequence (fragment) are shown in Figure 4.3 (a) and (b), respectively. The algorithm of generation of the MLPRS signal is shown in appendix A. The initial state of the shift register

Improving the performance of micro-machined metal oxide gas sensors:  
 Optimization of the temperature modulation mode via pseudo-random sequences.

can be any combination of length  $n$  of the values  $0, 1, \dots, (q - 1)$ , exception made of  $n$  zeros. Each combination of these values (except  $n$  zeros) appears as the state of the register exactly once during a period of the MLPRS. The sequences can be generated by a  $q$ -level shift register with feedback to the first stage consisting of the modulo  $q$  sum of the outputs of the other stages multiplied by coefficients  $c_1, \dots, c_n$ , which are integers that lie in the range  $[0, q - 1]$ .

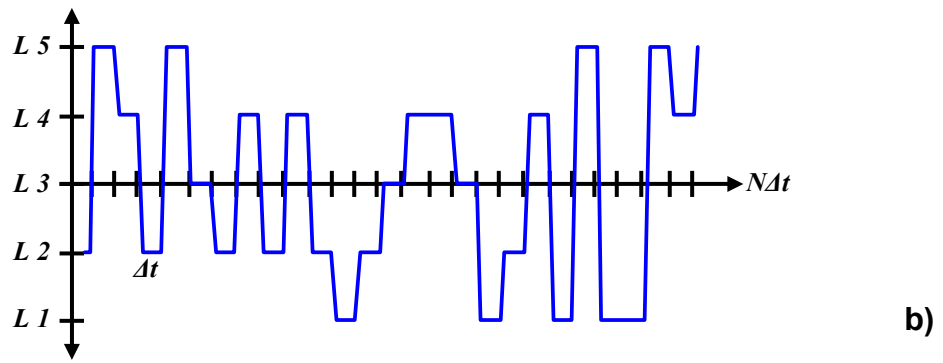
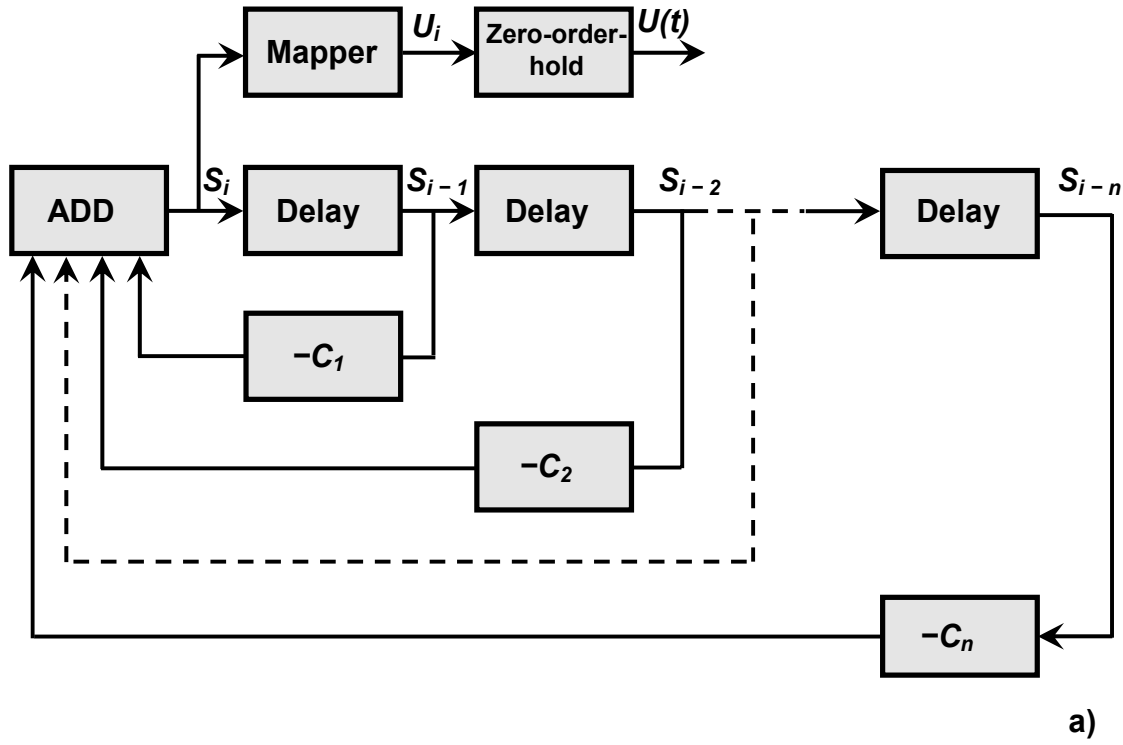


**Figure 4.3:** (a) A  $q$ -level pseudo-random maximum length sequence generator. (b) Fragment of a 5-level pseudo random sequence.



For ease of reference, the important properties of  $q$ -level maximum length signals are summarized below:

- Basic signals comprise the integer elements  $0, 1, 2, \dots, q - 1$ .
- Each cycle has  $(q^n - 1)$  digits, where  $n$  is an integer ( $n > 1$ ) corresponding to the number of stages in the equivalent  $q$ -level feedback shift register (FSR) generator.
- The number of zeros in each cycle is  $(q^{n-1} - 1)$ .
- The number of each of the non-zero elements in a cycle is  $q^{n-1}$ .
- Each cycle comprises  $(q - 1)$  sequential 'blocks' of digits of length  $(q^{n-1})/(q - 1)$  digits, and hence  $(q - 1)$  is always a factor of  $(q^n - 1)$  for all  $q$  and  $n$ .
- From any reference point in the cycle, the block comprising the subsequent  $(q^n - 1)/(q - 1)$  digits can be derived by multiplying (modulo  $q$ ) all digits in the preceding block of length  $(q^n - 1)/(q - 1)$  by a primitive element  $g$  of the Galois field of  $q$  elements  $GF(q)$ .

In a similar way to the binary case, the feedback configuration of the shift register is given by a primitive polynomial, modulo  $q$ . If  $\alpha_n x^n + \alpha_{n-1} x^{n-1} + \dots + \alpha_1 x + \alpha_0$  is primitive, modulo  $q$  (i.e. the polynomial is irreducible and thus, has no factors modulo  $q$ ), then the connections to the first stage are given by:

$$\alpha_0 X = -\alpha_1 DX - \dots - \alpha_{n-1} D^{n-1} X - \alpha_n D^n X, \quad \text{modulo } q \quad (4.19)$$

where  $X$  is the input sequence to the shift register,  $DX$  is the sequence at the output of the first stage of the register, so that  $D^n X$  is the sequence at the output of the last stage of the  $n$ -stage register.  $\alpha_0 = 1$  and the remaining coefficients  $\alpha_1, \dots, \alpha_n$  have integer values in the range 0 to  $q - 1$ .

Equation (4.19) can be rewritten as follows:

$$X = a_1 DX + \dots + a_{n-1} D^{n-1} X + a_n D^n X, \quad \text{modulo } q \quad (4.20)$$

where

$$a_i = (q - \alpha_i), \quad i = 1, 2, \dots, n \quad (4.21)$$

For example, the polynomial  $3x^4 + 4x^3 + 4x^2$  is primitive, modulo 5, and the feedback to the input of the four-stage, five-level shift register is given by:

$$X = D^2 + D^3 X + 2D^4 X, \quad \text{modulo } 5 \quad (4.22)$$

The sequence resulting from equation (4.22) has logic values 0, 1, 2, 3 and 4 and its period is  $5^4 - 1 = 624$ . Actually this is the MLPRS used in this thesis. A list of all irreducible polynomials modulo 3, 5 and 7 for different values of  $n$  can be found in [14]. More details on the properties of  $q$ -level maximum length signals can be found elsewhere [6].

Improving the performance of micro-machined metal oxide gas sensors:  
 Optimization of the temperature modulation mode via pseudo-random sequences.

Finally, the feedback connection (with modulo  $q$ ) for generating  $q$ -level  $m$ -sequences are given in Table 4.2, for  $q = 5$  and  $n = 2, 3, 4$  and  $5$  and for  $q = 7$  and  $n = 2, 3$ , and  $4$ , derived from the primitive polynomials listing of church in 1935 [14] and for  $n = 3$  and  $q = 11, 13, 19, 23, 29$ , and  $31$  (all prime numbers), based on the given by Everett in 1966 [4].

**Table 4.2:** Feedback configuration for some  $q$ -level  $m$ -sequences of length  $L = q^n - 1$ .

			Feedback coefficients				
$q$	$n$	$N$	$a_1$	$a_2$	$a_3$	$a_4$	$a_5$
5	2	24	1	3	-	-	-
5	3	124	0	1	2	-	-
5	4	624	0	1	1	2	-
5	5	3124	0	0	0	1	2
7	2	48	1	4	-	-	-
7	3	342	0	1	5	-	-
7	4	2400	0	1	1	4	-
11	3	1330	0	10	7	-	-
13	3	2196	0	12	7	-	-
17	3	4912	0	16	14	-	-
19	3	6858	0	18	15	-	-
23	3	12166	0	22	20	-	-
29	3	24388	0	28	18	-	-
31	3	29790	0	30	17	-	-

## 4.6. Pseudo Random Sequences (PRS) and systems identification.

The impulse response,  $h(t)$ , is the main descriptor of a linear invariant system. Among the different strategies to estimate impulse response, noise methods allow for exciting the system under study during enough time to supply it with the necessary energy to obtain a good estimate of  $h(t)$ . Exciting with white noise signals ensures a homogeneous distribution of the energy over a large frequency range. Periodic Pseudo-random sequences (PRS) signals, binary or multi-level, can potentially be employed as exciting signals for systems. Since PRS signals have a low crest factor (i.e. low peak-to-average factor) they minimize the risk of saturating the system under study. In practice, this means that the signals contain energy enough to obtain a good signal-to-noise ratio in a wide frequency range (i.e., measurement

with high dynamic range) and avoid sensor non-linearity caused by signals with high crest factors (e.g. impulsive signals). Furthermore, because the noise signal is deterministic, reproducible results would be obtained, provided that the conditions of the system under analysis remain unchanged.

The power spectrum envelope of either Binary or Multi Level PRS of maximum length is almost flat up to a frequency equal to  $0.45 \times f_c$ , where  $f_c$  is the frequency of the clock signal applied to the shift register used to generate the signal. The power spectrum is discrete and the separation between spectral lines (i.e. the spectral resolution) is  $f_c/L$ , where  $L$  is the length of the PRS signal. The power spectrum envelope is similar to the power spectrum of white noise up to the  $-3$  dB cut-off frequency:  $0.45 \times f_c$ . Figure 4.4 shows the power spectrum of a PRS signal. Therefore, pseudo-random sequences are routinely used to obtain an estimate of the impulse response of systems [15].

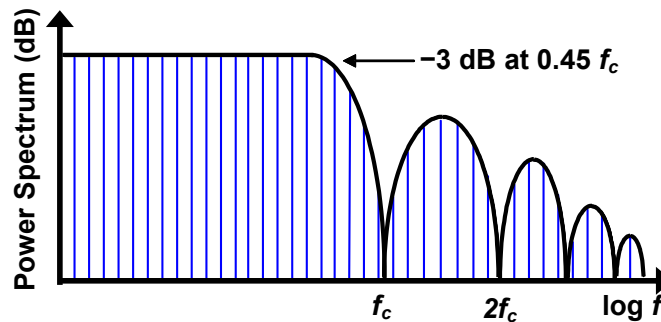


**Figure 4.4:** Discrete power spectrum of a PRS of maximum length signal. Spectral resolution is  $f_c/L$ , where  $f_c$  is the frequency of the clock signal applied to the shift register and  $L$  is the length of the sequence.

When the pseudo-random sequence is a maximum length signal, the impulse response estimate,  $\hat{h}(n)$ , can be obtained by computing the circular cross-correlation between the excitatory signal,  $x(n)$ , and the response signal,  $y(n)$  [15]. The circular cross-correlation of two sequences  $x$  and  $y$  in  $\Re L$  may be defined as:

$$\hat{h}(n) = \frac{1}{L} \sum_{l=0}^{L-1} y(l+n)x(l), \quad n = 0, 1, 2, \dots, L-1. \quad (4.23)$$

The cross-correlation is circular since  $l+n$  is interpreted modulo  $L$ , where  $L$  is the length of the sequence. In equation (4.23),  $L$  is a normalization factor that is optional. The circular cross-correlation between input and output sequences can readily be interpreted in terms of

Improving the performance of micro-machined metal oxide gas sensors:  
 Optimization of the temperature modulation mode via pseudo-random sequences.

$\hat{h}(n)$  because the autocorrelation function of the PRS of maximum length signal is of approximately impulsive form.

Most non-linear systems can be described by their Volterra functional expansion [16]:

$$y(t) = \int_0^{\infty} h_1(\lambda_1)u(t - \lambda_1)d\lambda_1 + \int_0^{\infty} \int_0^{\infty} h_2(\lambda_1, \lambda_2)u(t - \lambda_1)u(t - \lambda_2)d\lambda_1d\lambda_2 + \dots$$

$$+ \int_0^{\infty} \dots \int_0^{\infty} h_n(\lambda_1, \lambda_2, \dots, \lambda_n)u(t - \lambda_1)u(t - \lambda_2) \dots u(t - \lambda_n)d\lambda_1d\lambda_2 \dots d\lambda_n + \dots$$
(4.24)

where  $h_n(\lambda_1, \lambda_2, \dots, \lambda_n)$  is called the Volterra kernel of order  $n$  (the kernel of order 1 accounts for the linear dynamics).

When the excitatory signal,  $x(n)$ , which is an PRS of maximum length signal, and the response signal,  $y(n)$ , are cross-correlated over an integer number of periods of the excitatory signal, contributions from even-order kernels disappear, which leaves the linear term and terms involving kernels of order 3, 5, etc. Since in most cases, higher order kernels have a small effect on the output (this effect diminishes rapidly when the order,  $n$ , increases), a better estimate of the linear kernel is obtained by removing the effects of the second order kernel. This property is advantageous to better study the dynamics of temperature modulated metal oxide gas sensors.

In other words, signals based on multi-level maximum length pseudo random sequences (i.e. with a number of levels higher than 2) are preferred to binary signals because the former provide a better estimate than the latter signals of the linear dynamics of a system with non-linearity, which is normally the case with gas sensors.

## 4.7. Gas/sensor systems identification.

PRS of maximum length signals can be of help to systematically study the effects of the frequencies used to modulate the working temperature of metal oxide gas sensors. When either binary or multi-level PRS signal voltage is applied to the heating element of a micro-hotplate gas sensor, its working temperature is modulated in a wide frequency range. If this sensor is in the presence of a gas diluted in air, the impulse response of the sensor-gas pair can be estimated from the circular cross-correlation of the PRS temperature-modulating signal  $x(t)$  and the sensor response sequence  $y(t)$ . Because metal oxide sensors change their resistance in the presence of gases, the sensor response sequence is the resistance transient of the temperature-modulated sensor. By using spectral analysis on the impulse response

estimate,  $\hat{h}(t)$ , important information about the modulation frequencies that are useful to discriminate between different gases and to estimate gas concentration is obtained in a systematic way. This process is illustrated in Figure 4.5.

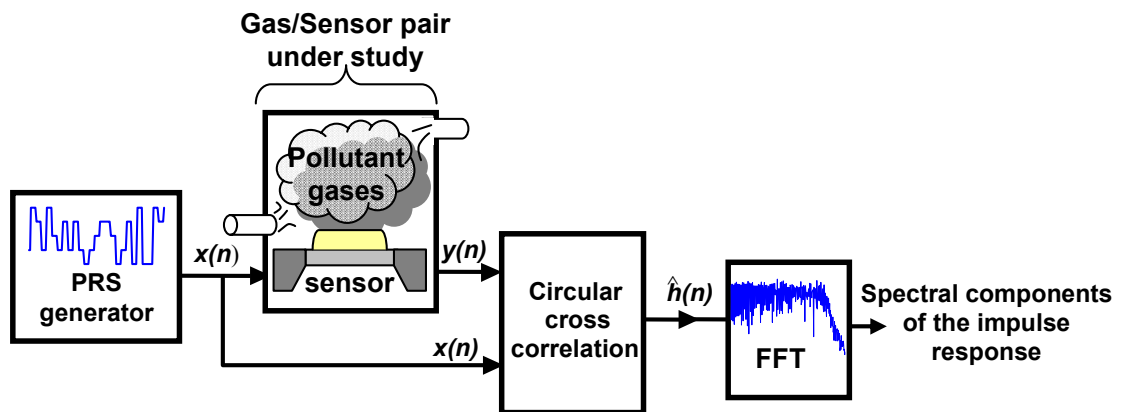


**Figure 4.5:** Study of the sensor/gas system using MLPRS signals. The MLPRS voltage signal,  $x(n)$ , is input to the heating element of a micro-hotplate gas sensor. The transient of the sensor conductance (i.e. the response in the presence of gases),  $y(n)$ , is recorded. An estimate of the impulse response,  $\hat{h}(t)$ , can be found via the circular cross-correlation of  $x(n)$  and  $y(n)$ . Finally, by performing the FFT of  $\hat{h}(t)$ , the spectral components of the impulse response estimate are found.

PRS of maximum length signals have a characteristic that make them especially suitable for the study of metal oxide gas sensors: Since their energy is distributed over  $L$  pulses of small amplitude, such signals have a low crest factor (i.e. low peak-to-average factor). In practice, this means that the signals contain energy enough to obtain a good signal-to-noise ratio in a wide frequency range (i.e. measurement with high dynamic range) and avoid sensor non-linearities caused by signals with high crest factors (e.g. impulsive signals).

By choosing the clock frequency ( $f_c$ ) used to generate the maximum length based PRS signal and the length ( $L$ ) of the sequence, the frequency range of modulating frequencies under study and the resolution are set. The range of modulating frequencies that are systematically studied is [from the D.C. to  $0.45 \times f_c$ ], which corresponds to the frequency range where the power spectrum of the PRS signals is approximately flat (e.g. white noise-like, see Figure 4.4). The resolution is ( $f_c/L$ ), which corresponds to the spectral resolution of the PRS power spectrum. The higher the clock frequency is, the wider the range of modulating frequencies studied is. If the clock frequency is increased, the length of the PRS signal should be increased too, for the spectral resolution not to degrade.

## Improving the performance of micro-machined metal oxide gas sensors: Optimization of the temperature modulation mode via pseudo-random sequences.

Once the impulse response for each gas-sensor pair was estimated, a simple variable selection procedure was implemented to select among the spectral components (i.e. to identify the optimal temperature-modulating frequencies). This process was described in Chapter 3 - Section 3.4.

## 4.8. Conclusions.

In this chapter signals, systems, and how they can be identified, were described from a general point of view. A signal was defined as any time-varying physical phenomenon, which is intended to convey information. Some general examples of signals were given: the human voice, a dog bark, a lion's roar, smoke signals, drums, sign language, Morse code, traffic signals, the voltages on telephone wires, the electric fields emanating from radio or television transmitters, and variations of light intensity in an optical fiber on a telephone or computer network.

On the other hand when one or more excitation signals are applied at one or more inputs of something which produces one or more response signals at its outputs, this is a system. What this means is, a system is anything that performs a function. Mathematically, a signal is the actual physical phenomenon which carries information, and the function is a mathematical description of the signal. In signals and systems, analyzing the characteristics of individual signals is, of course, important, but often the relationships between signals are just as important.

Once systems and signals had been explained in section 4.2, this chapter continued as follows: Section 4.3 reviewed the ways to obtain the impulse response of a system. Correlation, autocorrelation and cross correlation of system inputs and outputs were reviewed. In section 4.4 the generation of maximum length based pseudo random sequences (PRS) signals either binary or multilevel were presented. In section 4.5 these types of signals were presented as a good alternative to study and identify linear systems or to identify the linear dynamics of non-linear systems.

Finally, as was previously mentioned, in this particular case a gas-sensor pair could be considered as a system. The excitation signal input to the heating element and the pollutant gas to be measured are the inputs of the system, and the modulation of the sensor operating temperature and the sensor response to the pollutants are the outputs of the system. From this point of view, in section 4.6 a description of how gas-sensor pairs can be analyzed was introduced. Pseudo Random Sequences (PRS) signals will be used to identify, optimize and select the best frequencies to modulate the working temperature of a micro-hotplate gas sensor. This is shown in the next chapters.

## References.

- [1] M. J. Roberts, "Signals and Systems Analysis using transform methods and MATLAB", Mc Graw Hill, Tennessee, USA, 2004.
- [2] A.V. Openheim and K.W. Schafer, "Discrete-time signal processing", Englewood Cliffs, Prentice Hall, N.J., U.S.A., 1989.
- [3] H.A. Barker, "Choice of pseudorandom binary signals for system identification", Electron. Lett., vol. 3, pp. 524-526, 1967.
- [4] D. Everett, "Periodic digital sequences with pseudonoise properties", GEC Jnl. Sci. Technol., vol. 33, pp. 115-126, 1966.
- [5] K. Godfrey, "Correlation methods", Automatica, vol. 16, pp. 527-534, 1980.
- [6] K. Godfrey, "Perturbation signals for system identification", Prentice Hall, UK, 1993.
- [7] E: J. Watson, "Primitive polynomials (modulo 2)", Mathematics of Computing, vol. 16, pp. 368-369, 1962.
- [8] W. Stahnke, "Primitive polynomials", Math Comput., vol. 27, pp. 977-980, 1973.
- [9] P. A. N. Briggs, P. H. Hammond, M. T. G. Hughes, G. O. Plumb, "Correlation analysis of process dynamics using pseudo-random binary test perturbation", Proc. Inst. Mech. Engrs., vol. 179, Part 3H, pp. 37-51, 1965.
- [10] A. Vergara, E. Llobet, J. Brezmes, X. Vilanova, P. Ivanov, I. Gràcia, C. Cané, X. Correig, "Optimized temperature modulation of micro-hotplate gas sensors through pseudorandom binary sequences", IEEE Sensors Journal, vol. 5, pp. 1369-1378, 2005.
- [11] N. Zierler, "Linear recurring sequences", J. Soc. Ind. Appl. Msth., vol. 7, pp. 31-48, 1959.
- [12] Albert, A.A., "Fundamental Concepts of Higher Algebra", University of Chicago Press, Chicago, USA, 1956.
- [13] Barker, H. A., Int. J. Math. Educ. Sci. Technol., vol. 17, pp. 473-485, 1986.
- [14] R. Church, Ann. Math., vol. 36, pp. 198-209.
- [15] L. Ljung, "System Identification: Theory for the User", Englewood Cliffs, New Jersey: Prentice Hall, Chapters 6 and 8 to 11, 1987.

Improving the performance of micro-machined metal oxide gas sensors:  
Optimization of the temperature modulation mode via pseudo-random sequences.

- [16] V. Volterra, "*Theory of Functionals and of Integro-differential equations*", New York,  
Dover, 1930.



---

# 5.

# Experimental

---

<b>5. EXPERIMENTAL</b>	<b>109</b>
<b>5.1. Introduction.</b>	<b>110</b>
<b>5.2. Fabrication of the micro-hotplate gas sensors used in experiments.</b>	<b>111</b>
5.2.1. Micro-hotplate substrate fabrication.	111
5.2.2. Active layer deposition.	115
<b>5.3. Measurement system layout.</b>	<b>117</b>
<b>5.4. Description of the experiments performed.</b>	<b>123</b>
5.4.1. Experiment 1: PRBS signals to modulate the temperature operation of micro-hotplates gas sensors (preliminary study).	123
5.4.2. Experiment 2: Optimized temperature modulation of micro-hotplate gas sensors using Pseudo Random Binary Sequences (PRBS).	126
5.4.3. Experiment 3: Optimized Temperature Modulation of Metal Oxide Micro-Hotplate Gas Sensors through Multilevel Pseudo Random Sequences.	128
5.4.4. Experiment 4: Qualitative and quantitative gas mixture analysis using temperature-modulated micro-hotplate gas sensors: Selection and validation of the optimal modulating frequencies.	131
<b>5.5. Summary.</b>	<b>134</b>
<b>5.6. References.</b>	<b>136</b>

## Improving the performance of micro-machined metal oxide gas sensors: Optimization of the temperature modulation mode via pseudo-random sequences.

### 5.1. Introduction.

In this chapter, the micro-hotplate gas sensors used in this study, the measurement system layout and the experimental set-up including the pollutant gases measured are presented in detail.

The experiments presented here were performed using micro-hotplate gas sensors. The sensor substrates consisted of four-element integrated micro-hotplate arrays fabricated using Microsystems technology. Different active layer deposition techniques and sensitive materials were used. The gas sensitive materials used were tin oxide and tungsten oxide. The active layers were deposited onto microelectronic substrates by either sputtering or screen printing techniques. The sensors were encapsulated and placed in a chamber where measurements were performed by means of a continuous flow system. Neither the fabrication of the micro-hotplate substrates nor the deposition of active films were among the objectives and tasks of this thesis. The substrates were provided by the CNM (Dr. Cané) and the active films were deposited by Dr. Stankova (r.f. sputtering) and Dr. Ivanov (screen-printing).

In previous works, many authors have introduced different methods to modulate the operating temperature of micro-hotplate sensors. In the experiments performed here, we introduce a method, which is based on the use of pseudo-random maximum-length sequences (binary or multi-level), to modulate the working temperature of gas sensors. It allows modulating their working temperature and, additionally they enable studying and determining the optimal set of modulating frequencies to solve a given gas analysis problem. Once the optimal modulating frequencies are identified and selected, a multi-sinusoidal modulating signal can be synthesized and employed to modulate the sensor's operating temperature. These signals (i.e., either PRS or multi-sinusoidal) will be used in the different measurement data sets.

The selection of the gases to be measured was done considering those that present negative effects to the environment and human beings or are relevant in agro-food applications. For example  $\text{NO}_2$  and  $\text{NH}_3$  were chosen because they are atmospheric pollutants responsible for ambient degradation. Furthermore, acetaldehyde, ethylene, ammonia and their binary mixtures were chosen, since the first two are related to the quality of climacteric fruit during cold storage and the third one reveals the occurrence of a leak in the refrigeration system.

This chapter is distributed as follows: In section 5.2, the sensors used in this study are fully described. Therein, the substrate construction, characteristics of the sensors, and the

active layer deposition are detailed. In section 5.3, the measurement system layout used to perform the experiments and the experimental set-up is described in detail. Finally section 4 describes the different measurements performed during this study.

## **5.2. Fabrication of the micro-hotplate gas sensors used in experiments.**

In this section the design of the gas sensors used in this thesis is discussed. In the first stage, the design and fabrication of micro-hotplate silicon (Si) substrates for a metal oxide gas sensor is briefly described. The description includes the design of masks, the microelectronic processes used and the various elements that constitute the substrate. Actually, micro-hotplate substrates were implemented as alternative to the conventional substrates, used in gas sensors, because of the high power consumption of the latter. Low power consumption, fast heating/cooling and small dimensions are some of the principal features presented by this kind of substrates. It is important to remark that the micro-hotplate substrates used had been designed and fabricated by the National Center of Microelectronics (CNM) in Barcelona, Spain in the context of research projects of their own and, therefore, were readily available at the time of starting the works of this thesis.

In the following sub-sections, the different techniques used to deposit metal oxide layers on top of the micro-hotplate membranes are briefly described. Finally, the bonding and packaging are discussed too.

### **5.2.1. Micro-hotplate substrate fabrication.**

The substrates employed to fabricate the sensors used in this thesis were the micro-hotplates fabricated at the CNM (National Center of Microelectronics) in Bellaterra, Barcelona, Spain. An integrated sensor with an array of four microsensor elements was designed using finite element analysis [1] to achieve reduced power consumption, and constructed using microelectronic fabrication technology. The devices were fabricated on double-side polished p-type  $\langle 100 \rangle$  Si substrates 300  $\mu\text{m}$  thick [2-5].

In Figure 5.1, the technological processing steps for substrate fabrication are illustrated and the process needed to fabricate the micro-machined sensors, is summarized in the 9 following steps:

## Improving the performance of micro-machined metal oxide gas sensors:

### Optimization of the temperature modulation mode via pseudo-random sequences.

- 1) Deposition of the membrane layer. The dielectric membranes consisted of a  $0.3 \mu\text{m}$  thick  $\text{Si}_3\text{N}_4$  layer grown by LPCVD. Each chip had 4 membranes, the size of which was  $900 \times 900 \mu\text{m}^2$ .
- 2) Deposition and patterning of a  $\text{POCl}_3$ -doped polysilicon heating meander with a resistance of  $6 \Omega/\text{sq}$ . The temperature coefficient of resistivity (TCR) of polysilicon depends on the doping level which, for our devices, was  $6.79 \times 10^{-4}$ . The heater was also used as a temperature sensor.
- 3) Deposition of a  $0.8 \mu\text{m}$ -thick  $\text{SiO}_2$  layer to insulate the heater from the electrodes and the sensing film.
- 4) Opening of contacts for the heater bonding pads to be accessible.
- 5) Deposition of either parallel or interdigitated  $0.2 \mu\text{m}$ -thick Pt electrodes, patterned by lift-off. A thin layer (20 nm) of Ti was deposited prior to Pt to promote electrode adhesion. The electrode area was  $400 \times 400 \mu\text{m}^2$ . Figure 5.2 shows a planar view of the membrane with heater and electrode configuration. Two sensors have an electrode gap of  $50 \mu\text{m}$ , and the other two have a  $100 \mu\text{m}$  electrode gap.
- 6) Patterning of the backside etch mask.
- 7) Deposition of the sensing layer onto the electrode area (two different pastes with tin or tungsten oxides of different particle size were used; this led to active films with grain sizes of near  $50 \text{ nm}$  and  $0.4 \mu\text{m}$  respectively)
- 8) Backside silicon etching with KOH at  $70^\circ\text{C}$  to create the thermally-insulated membranes.
- 9) Wire bonding and packaging. Each chip was mounted on a TO-8 package. Figure 5.3 shows the encapsulated circuit on a TO-8 package and the schematic view of a  $\text{SnO}_2$  MHP gas sensor. Gold wires with a diameter of  $25 \mu\text{m}$  were used for standard ultrasonic wire bonding. To prevent the membranes from breaking due to air expansion in the cavity below the membranes when the device is heated, the chips were not glued directly to the surface of the metallic package but kept elevated by using two lateral silicon spacers.

Typically, the films are deposited after silicon has been etched away to produce the thermally-isolated structures (etching chemicals are usually too aggressive to properly maintain the integrity of pre-deposited films). Unlike previous studies reported in [6], our technological procedure enables the sensing layers to be deposited before the membranes have been etched. This prevents the membranes from being damaged during film deposition, which leads to gas sensor micro-systems with an excellent fabrication yield.

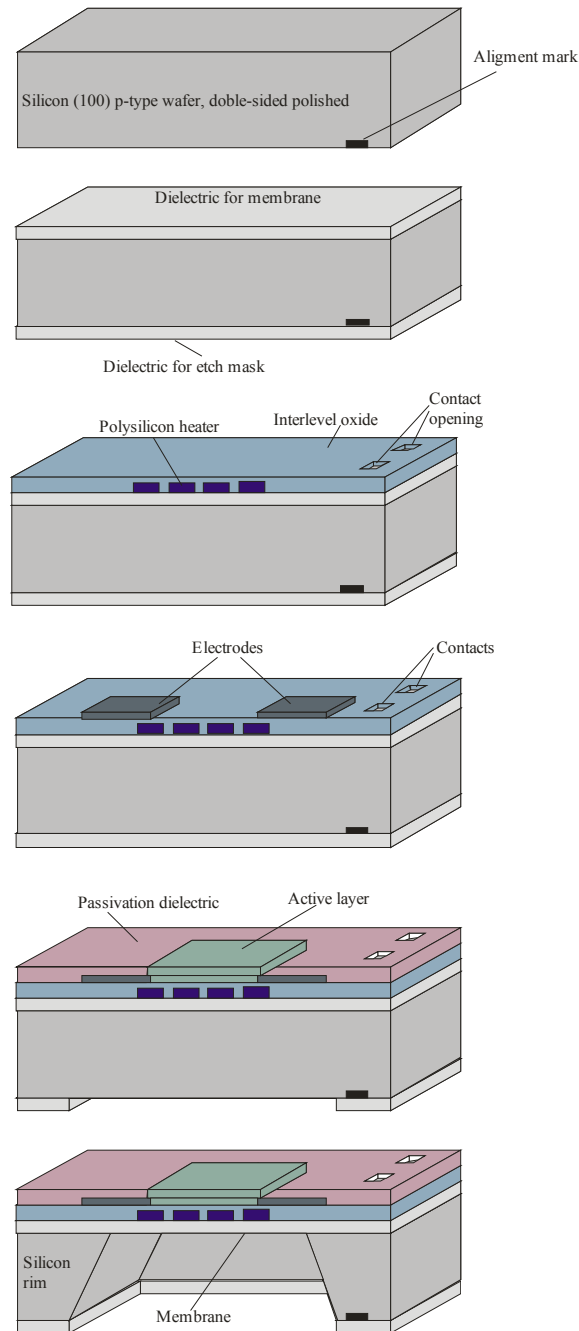


**Figure 5.1:** Technological processing steps for the fabrication of micro-sensors. Figure extracted from reference [2].

Improving the performance of micro-machined metal oxide gas sensors:  
Optimization of the temperature modulation mode via pseudo-random sequences.

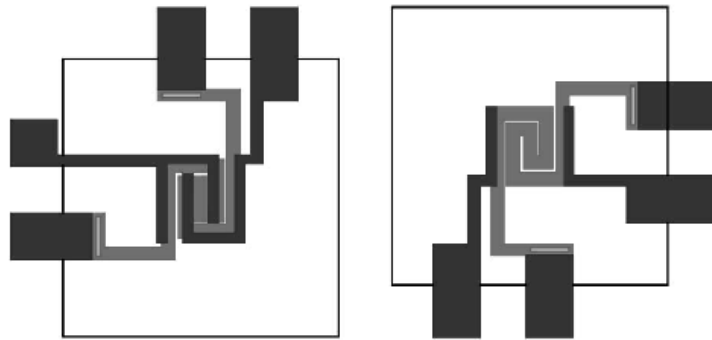


**Figure 5.2:** Planar view of the micro-machined gas sensor membrane; left: interdigitated electrodes; right: parallel electrodes. Figure extracted from [6].

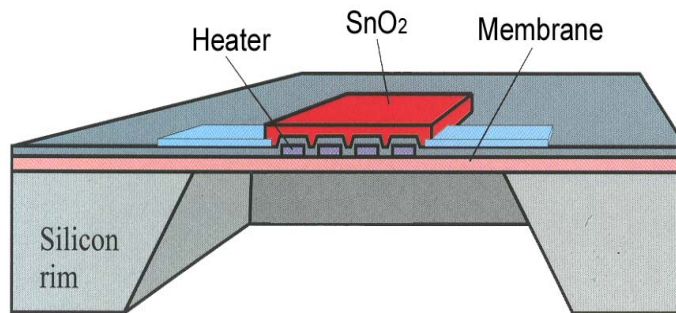
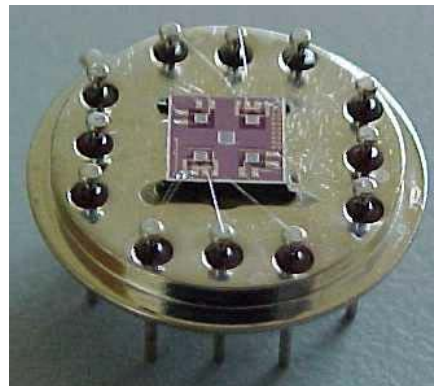


**Figure 5.3:** TO-8 package and structure of a micro-hotplate gas sensor (Top to bottom). Extracted from [6].

### 5.2.2. Active layer deposition.

The deposition techniques employed for coating the micro-hotplate gas sensors are briefly described in this sub-section. The active layers used in this thesis can be classified by their thickness, the sensitive materials used, the presence of additives (e.g., noble metals) and the deposition techniques. Two different techniques were applied for depositing the active layers. While r.f. magnetron sputtering was used to obtain thin active films, screen-printing was used to obtain thick films of tin or tungsten oxides (either pure or with noble metals added). The sputtered and screen-printed films were deposited by Dr. Stankova and Dr. Ivanov, respectively in the framework of their Doctoral Thesis at the URV. The main characteristics of the deposition techniques used are briefly described below.

As it is well known, thin solid films are fabricated by depositing individual atoms on a substrate and their thickness are typically less than 1  $\mu\text{m}$ . By varying the deposition process and modifying the film properties during deposition, a range of unusual properties can be obtained which are not found in bulk materials. The deposition process used was reactive r.f. magnetron sputtering using either tungsten or tin targets in the presence of an oxidizing atmosphere. The flexibility of the technique makes possible to find the process parameters (power, time, temperature, gas flow) which give the most appropriate layer stoichiometry and crystallinity. The target that was used is W of 99.95 % purity and had a diameter of 100 mm and a thickness of 0.125 inches. The target to substrate distance was fixed at 70 mm. The substrate temperature was kept constant during film deposition at room temperature. The sputtering atmosphere consisted of Ar-O<sub>2</sub> mixed gas (argon as carrier gas and oxygen as reactive gas) and its flow rate was controlled by separate gas flowmeters to tailor the Ar-O<sub>2</sub> gas percentage in the chamber. The pressure in the chamber during deposition was 0.5 Pa (5E-3 mbar). The r.f. forward input power was maintained at 200 W with zero reflected power [7]. Two deposition processes under different Ar-O<sub>2</sub> ratios were tested. In one case the flow of oxygen was 12 sccm and there was no Ar flow. In the other, all the parameters were the same except the gas composition, which was O<sub>2</sub> = 6 sccm, Ar = 6 sccm. The morphology of the films obtained in this latter case was better. In the case of the second sputtered material (tin dioxide), the process is consisted in a tin target with 99.99% purity. All conditions remained as for the deposition of tungsten oxide, exception made of the input power, which was maintained at 100 W. To define the active layer, an appropriate mask and a photolithographic process were used, followed by a lift-off. After deposition, all wafers were annealed in air for 2 h at 400°C.

On the other hand, a thick-film technique (screen-printing), which offers a route to small-scale devices and a cost that is likely to be lower than that of the thin-film equivalent, was

## Improving the performance of micro-machined metal oxide gas sensors: Optimization of the temperature modulation mode via pseudo-random sequences.

also used for depositing the active layer of our sensors. Good control over thickness and microstructure is possible and, although response time is likely to be longer than for a thin-film structure at the same temperature, the lifetime is also expected to be longer.

Screen-printing is an alternative deposition process that has been used for our sensors analyzed [8]. The deposition process for a thick-film circuit is essentially identical to that used for traditional silkscreen printing [8]. The main differences lie in the screen materials and the degree of sophistication of the printing machine. A typical thick-film screen consists of a finely woven mesh of stainless steel (nylon or polyester) mounted under tension on a metal frame. The mesh is coated with an ultra-violet (UV) sensitive emulsion onto which the circuit pattern can be formed photographically. The finished stencil has open mesh areas through which the desired pattern can be printed and is held in position at a distance of around 0.5 mm from the top surface of the substrate. The ink is placed on the opposite side of the screen and a squeegee traverses the screen under pressure, thereby bringing it into contact with the substrate and also forcing the ink through the open areas of the mesh. The required circuit pattern is thus left on the substrate. The next stage of the process is to dry the film and remove the organic solvents from the paste. This task can be performed in a conventional box oven but it is more common to use an infrared belt drier. After this stage, the dried film is relatively immune to smudging and the substrates can be handled. Sometimes it is permissible to screen print the next layer directly after the drying stage, but this really depends on the nature of the inks being deposited. The films themselves contain fine powders, which must be exposed to high temperatures if they are to form a solid, composite material. This is often referred to as sintering, and takes place in a belt furnace. Some of our thick-film inks contain glass. During the firing cycle, the glass melts and forms a mechanical key at the film-to-substrate interface. It also provides a suitable matrix for the active material of the film. The result is a fired composite film, which is firmly bonded to the substrate. The sensitive materials used were metal oxides as  $\text{SnO}_2$  and  $\text{WO}_3$ , which bind oxygen on their surface in a reversible way among other advantages.

The screen printed process consisted in the deposition of 5-  $\mu$ -thick  $\text{SnO}_2$  and  $\text{WO}_3$  nanopowder respectively. A printable paste was prepared by using an organic vehicle based on terpeneol. The paste was printed onto the semi-processed wafers by using a high-precision screen-printing machine that allows one-side mask alignment. Wafers were subsequently dried for 15 or 20 minutes (for the first and second material respectively) at 125°C and 150°C for the organic vehicle to be completely removed, and then fired for 1 h in a belt furnace at a single level of temperature, equal to 600°C or 650°C respectively. To obtain a better adhesion between the substrate and the active film, the wafer was heated to 60°C [6].



In the second batch of micro-machined sensors, we included the deposition of doping materials for the tungsten and for the tin oxide. There are two different types of deposition process. In the first case, the dopant is deposited simultaneously with the active layer. This leads to the homogenous distribution of the dopant in the active film. The second possibility was depositing the dopant after the active layer. Among the several doping materials used we have Pt, Au, Pd, Ag, Ti, where Pt, Au, and Pd were the final doping materials selected for our particular case.

### 5.3. Measurement system layout.

The layout of the test system employed is described in detail in this section. Basically, the principal components of the system are:

- 1) gas flow system
- 2) test chamber
- 3) electronic boards
- 4) power supply system
- 5) personal computer

In Figure 5.4 the general experimental set-up of the measurement system with its principal components is shown.

Since the species measured are often toxic or flammable gases, all the measurement system is kept under a forced air extraction system. Therefore, in the event of a leak from a calibrated bottle or from the measurement rig, the gases would be exhausted from the laboratory. Different calibrated bottles contain the different target species diluted in dry air (normally in the ppm range). High-purity dry air is used as carrier gas and to further dilute the concentration of analytes.

The first part of the continuous flow system, which is in fact used to convey the pollutant gases to the test chamber, is known as gas flow system. This is composed by a cabin where the gases on bottles under high pressure are stored, a gas transport system, and a mass flow system.

Between every bottle and the gas transport system there are “valves” (pressure regulators) which allow for obtaining a pressure drop from the very high pressures inside the calibrated gas bottles to near atmospheric pressures (i.e. from 200 bar to 2 bar). They must work perfectly because even the smallest flaw could lead to the occurrence of a leak of a toxic or flammable gas at very high pressure and, eventually, to explosions. Figure 5.5 illustrates the gas flow system components used.

Improving the performance of micro-machined metal oxide gas sensors:  
Optimization of the temperature modulation mode via pseudo-random sequences.

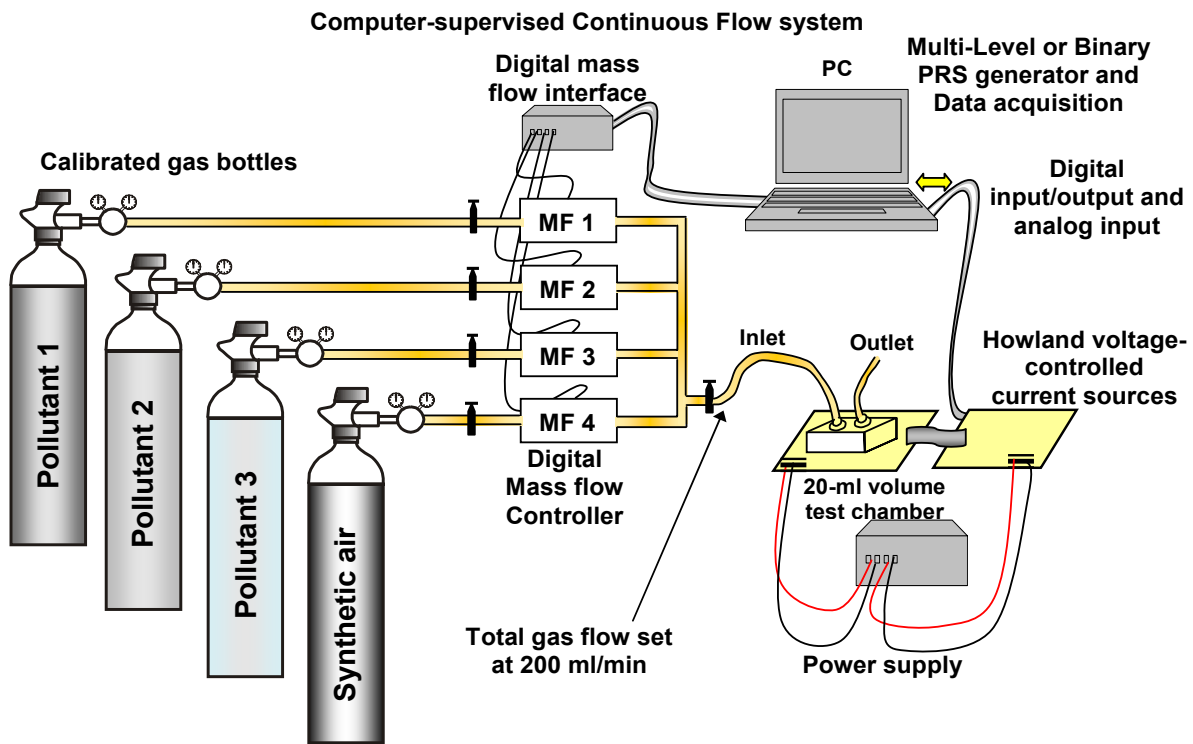


Figure 5.4: Experimental set-up: The sensors are studied in the presence of either single or binary mixtures of pollutant gases diluted at different concentrations in synthetic dry air.



Figure 5.5: Gas flow system: Gases stored in bottles under high pressure (left); Gas transport system and manual valves (center); Mass-flow controllers (right).

The gas transport system is made of different metallic pipes connected to several manual valves, which enable/disable the gases to flow. These pipes are connected to the mass flow system, which can create the gas mixtures desired.

The mass flow system is composed of 3 mass flow devices controlled by a desktop PC that works as a mass flow controller (Bronkhorst hi-tech 7.03.241). Each one of the mass flows is calibrated with synthetic air (this does not lead to significant errors since in the experiments performed the analytes measured are highly diluted in air). Nevertheless it implies that if any measurement would be made with a non-diluted analyte, the gas concentration would not be reliable (a new calibration would be needed). These devices incorporate mass sensors (MEM technology) which work in the following way: they have a silicon resistance exposed to the gas flow; when the flow changes, the temperature of the resistor is bound to change (according to a relation which depends on the calibration). Such temperature change is detected by monitoring the resistance values.

To get the desired concentration of a single or mixture of gas with high precision, three different mass flow devices are used. Every one of them has a 1% end-of-scale resolution. In order to reach the different gas concentrations desired (i.e., from a few ppm to higher concentrations) the 3 mass flow devices used have different maximum flow levels. Two of them (those labeled as MF2 and MF3) can also be combined between them to reach even higher concentration of a single pollutant gas. These levels are shown as follow:

- MF1: gas 1, maximum flow 400 sccm (cubic centimeters per minute). This is mass flow is intended for controlling the carrier gas.
- MF2: gas 1, maximum flow 100 sccm
- MF3: gas 2, maximum flow 15 sccm

After the mass flow system, there is a sensor, which controls the temperature and humidity of the mixture. In the experiments realized in this thesis the gases were kept at a moisture level of 10% R. H. (relative humidity) and at a temperature of  $30^{\circ}\text{C} \pm 1^{\circ}\text{C}$ . On the other hand, the pipes from the mass flow system to the sensor test chamber are covered with an insulating material, in order to prevent any possible condensation of analytes (especially moisture).

A total constant flow of 200 sccm (i.e. 200 ml per minute) was used. In order to obtain the desired gas concentration (depending of the analyte to be measured), while keeping constant the total flow, the set point of the different mass-flows had to be calculated using the formulae shown in Appendix A. The total flow is injected in a 20-ml volume test chamber. Two micro-arrays of metal oxide gas sensor (e.g., 2 integrated microarrays of 4

## Improving the performance of micro-machined metal oxide gas sensors: Optimization of the temperature modulation mode via pseudo-random sequences.

sensors each encapsulated in a TO-8 package), are placed into this chamber. Figure 5.6 (right) shows a close view of the test chamber where sensors are placed.

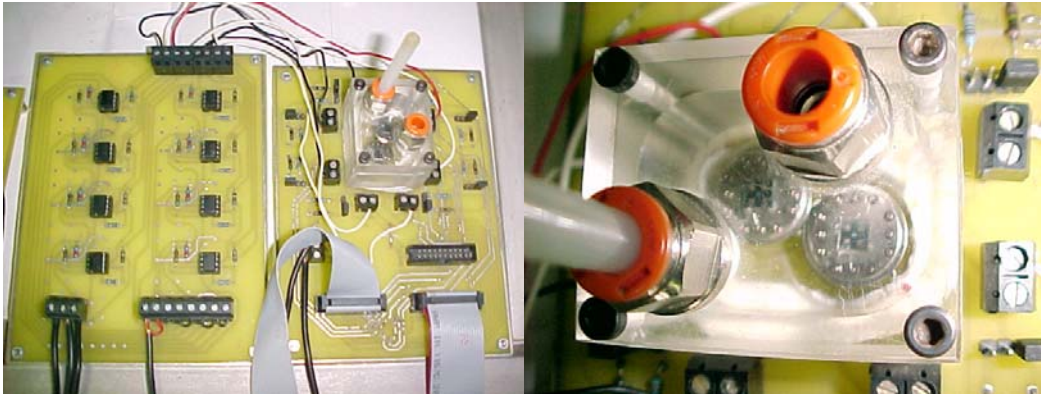


**Figure 5.6:** Experimental system: Howland voltage-controlled current sources (left); Close view of the gas chamber (right).

The test chamber is connected to an electronic board whose mission is twofold:

- To supply the gas sensors with the required operation voltages and currents.
- To acquire the dynamic responses of gas sensors and the voltage drop over their heating elements in order to monitor their temperature. Sensor resistances were acquired in a half-bridge configuration.

Both objectives are described in detail in the following paragraphs. However, a deeper description of how these electronic boards were constructed and their operation mode can be found in Appendix. In Figure 5.7 a schematic diagram of the circuits used to operate and to monitor the resistance of a sensor are shown.

The first function of this electronic board system is to supply the micro-hotplate gas sensors with the required operation voltage. As first step, by means of a 5 V voltage source, the voltage divider formed by the active film resistance ( $R_S$ ) and the load resistance ( $R_L$ ) of the measurement schematic board (used for data acquisition) is supplied with the required operation voltage(see Figure 5.7 (right)).

Additionally, the board injects the operation signal (i.e., a fixed current or a modulating signal current) to each polysilicon heating element (heater Resistance ( $R_h$ )) of each gas sensor. The  $R_h$  parameters (polysilicon temperature coefficient of resistivity  $\alpha$ ) and the current values are known (they are chosen when designing the experiment and kept independent of the  $R_h$  oscillating values thanks to the current source circuits), hence the estimating the temperature modulation range from the current modulation values is straightforward.

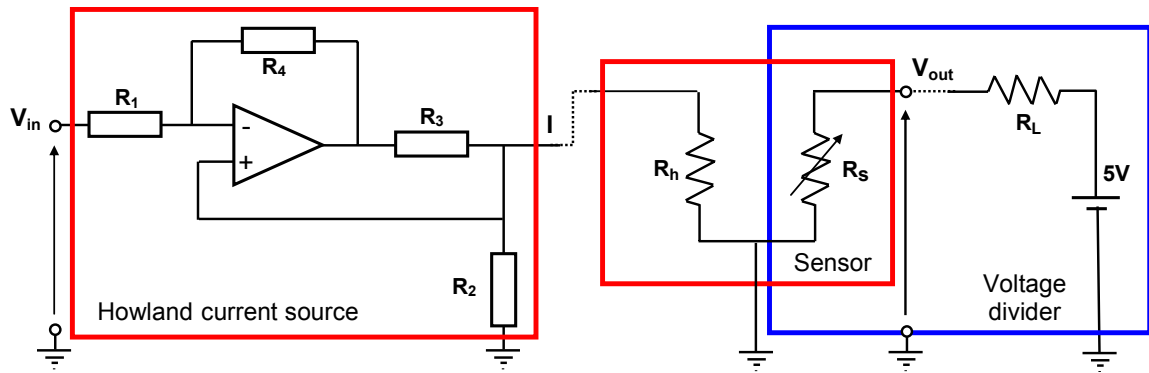


**Figure 5.7:** Experimental measurement schematic layout: Howland voltage-controlled current sources diagram (left); sensor representation and voltage divider (right remarked in red) employed for data acquisition (right remarked in blue).

The operation heater current is supplied by a Howland current source (see Figure 5.7 (left)). Such circuit receives the voltage signal from the PC (i.e., the fixed voltage or the modulating voltage signal) and converts it into a current signal. It is designed in a way that, receiving as input a voltage in the order of V, gives currents as outputs mA range.

On the other hand, the second main function of these electronic boards is to acquire the dynamic gas sensor response and the voltage drop over their heating elements (to monitor temperature). The voltage across  $R_s$  is measured and stored by the PC (the same PC that outputs the signal that is injected to the heater elements by means of the Howland current sources). The  $R_L$  in the voltage divider (see Figure 5.7 (right)) is a high precision resistance, with tolerance as low as 1%. Its precision is crucial since its value is directly connected to the measurement of the sensor response. The  $R_L$  in the scheme corresponds on the board to two possible values: 1 M $\Omega$  or 10 M $\Omega$  (there is a jumper connected to the two high precision load resistors and it is possible to switch manually to one or to the other according to our particular needs). Finally, it is important to remark that for each sensor there is one current source and one voltage divider.

These electronic boards are connected to the general power supply network and to the personal computer. The power supply system gets a high voltage signal from the general network (220 V AC). It generates an alternating signal and rectifies it to the desired level of voltage. It supplies the whole system and the electronic boards with the power needed. The personal computer, on the other side, has a fundamental role since it undertakes the following crucial functions:

- To generate the heaters' input signal (i.e., fixed signal or modulating signal) needed to keep fixed or to modulate the gas sensor operating temperature.

## Improving the performance of micro-machined metal oxide gas sensors: Optimization of the temperature modulation mode via pseudo-random sequences.

- To acquire and store the sensor responses for further processing

Here below the dynamic response data acquisition process is described. Figure 5.8 shows a block diagram layout where input/output data acquisition to/from the PC is done.

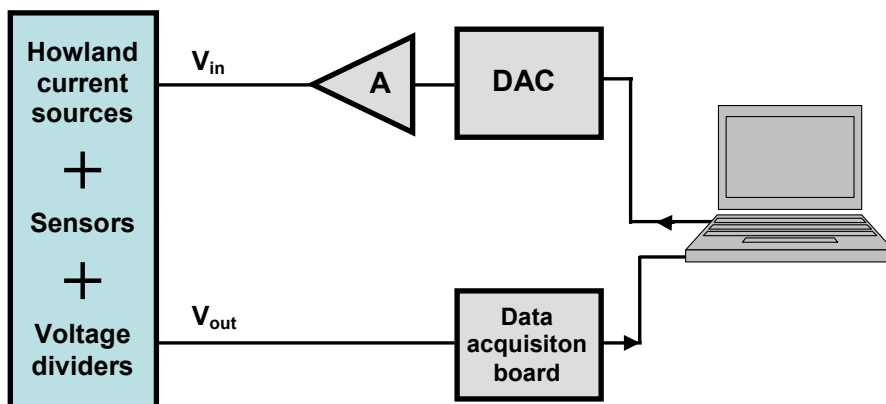


**Figure 5.8:** Block diagram layout of the input/output data acquisition.

Initially, both the modulating signal (i.e., Pseudo Random Maximum Length Sequences (Binaries or Multilevel), or sinusoidal modulating signals) and the fixed heater operating voltage (i.e., 6 V corresponding to a stable working temperature of 450°C) were generated in a written in house MATLAB program running on a PC platform. These signals, generated by the PC in digital form, are sent to a DAC (Digital to Analog Converter) which converts the binary words into voltage levels by means of a written in house LABVIEW program running on a PC platform. These voltage signals would be too low to drive the electronic board and thus they are first amplified by an operational amplifier and then sent to the Howland current sources. The sensor responses, i.e. the changes in the active film resistance  $R_s$ , are recorder by the PC by continuous measurements of the voltage  $V_{out}$ . For such aim the PC is provided with a data acquisition board (National Instruments, 6023E) which converts these analog voltage values in binary words understandable by the computer and vice versa. This board is directly connected to the PC bus. Both the voltage drop over the heating elements and the dynamic response of the gas sensors are acquired and stored in the PC by the data acquisition board in order to monitor operating temperature and to allow a subsequent step of data processing, respectively.

The different experiments performed will be described in the following sub-section of this chapter. The data processing and results will be detailed in chapters 6 and 7.

## 5.4. Description of the experiments performed.

The experimental set-up of the different experiments performed is described in detail in this sub-section. A total of 4 different experiments were performed aimed at systematically studying the frequencies to modulate the operating temperature of micro-hotplate gas sensors. A preliminary experiment was conducted to determine the frequency range of the thermal modulation to be considered in our studies. This was done by analyzing the thermal response of the sensor membranes. The second experiment is aimed at systematically studying the modulating frequencies of micro-hotplate gas sensors using pseudo random binary signals (PRBS). The discrimination among pollutant gases such as  $\text{NO}_2$ ,  $\text{NH}_3$  and their binary mixtures was envisaged. Third and fourth experiments deal with the optimization of the modulating frequencies using this time Multi-Level Pseudo Random Sequences (MLPRS). The validation of the optimization process is also considered. but. A detailed description of the different experiments is given in the following paragraphs.

### 5.4.1. Experiment 1: PRBS signals to modulate the temperature operation of micro-hotplates gas sensors (preliminary study).

The objectives of this experiment are twofold: On the one hand (preliminary experiment), the correct choice of the clock frequency and length of the sequence, essentials to study the appropriate frequency range with enough resolution. On the other hand, once the frequency range has been determined, to see whether it is possible, by studying the gas-sensor system in a systematic way using PRBS, to determine the most optimal frequencies to modulate the working temperature of the micro-hotplate gas sensors. The set-up of this experiment was then divided in the following steps:

In the first step, to determine the frequency range of the thermal modulation, the thermal response of the sensor membranes was studied. To do this, a stepwise current signal was applied to the heating element of either thin or thick film gas sensors. These current changes were applied three times to the heating elements. It was found that all membranes behaved as first-order systems, where the ones coated by screen-printing (thick film) presented a thermal response of around 19 ms while the thermal response of the membranes coated by sputtering (thin film) was of about 13 ms. Therefore, the cutoff frequency of the coated membranes was around 52 and 77 Hz respectively. Therefrom, the clock frequency used to generate the MLS signal ( $f_c$ ), was set to 250 Hz. This allowed the sensors to be tested for modulating frequencies raging from the D.C. up to 112.5 Hz. Once the  $f_c$  had been determined the length of the MLS signal was set to 65,535. Finally, a spectral resolution ( $f_c/L$ ) equal to 3.81 mHz

## Improving the performance of micro-machined metal oxide gas sensors: Optimization of the temperature modulation mode via pseudo-random sequences.

was obtained. Figure 5.9 shows the response of the heating element of a thin and thick film gas sensor (left to right) respectively to a stepwise voltage, where the thermal response change can be seen that is in the millisecond range.

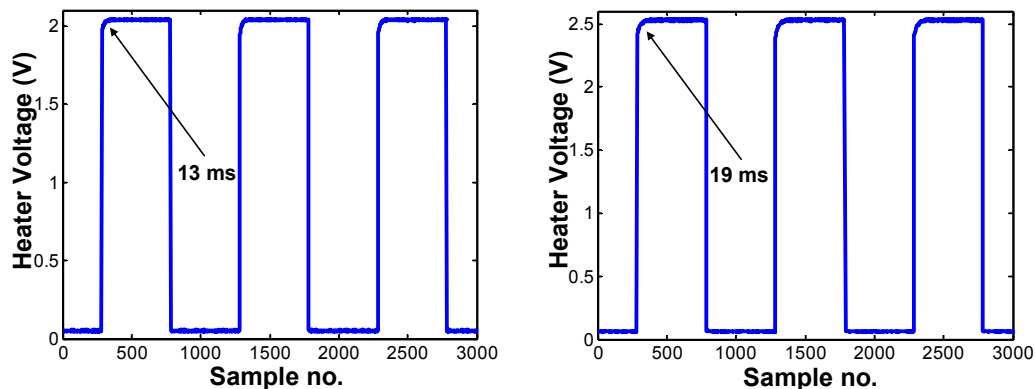


**Figure 5.9:** Response to a heater voltage stepwise applied to a micro-hotplate based gas sensor (thin and thick film (left to right)).

Once, the  $f_c$ , the length of the sequence, and the resolution have been determined, the second part of the experiment was performed. Vapors of synthetic air and  $\text{NO}_2$  diluted in synthetic air (at 3 different concentrations) were measured using the temperature-modulated micro-hotplate gas sensors. The measurements were performed at the Rovira i Virgili University, Tarragona (Spain) [9].

Six tungsten oxide (thin and thick film) micro-gas sensors were placed in the 20-ml volume test chamber shown in Figure 5.6. This chamber was connected to a continuous flow system. Three different concentrations of  $\text{NO}_2$  (2.5, 5 and 10 ppm) (i.e., pollutant gas to be measured) were obtained by computer-supervised mass-flow controllers. Therefrom, a PRBS current signal was injected to the polysilicon heating resistor of each micro-hotplate sensor. The high and low current levels were set to 6 mA and 5 mA, respectively. This resulted in a temperature variation of the micro-machined membranes equal to  $200^\circ\text{C}$ . The resistance of each sensing film (these resistances were measured in a half-bridge configuration) and also the voltage drop over of the heating elements (to monitor temperature) were then acquired and stored. During each measurement, 2.5 periods of the excitatory PRBS signal and corresponding sensor response signals (i.e. sensor resistance) were acquired and stored for further processing (see Figure 5.4).



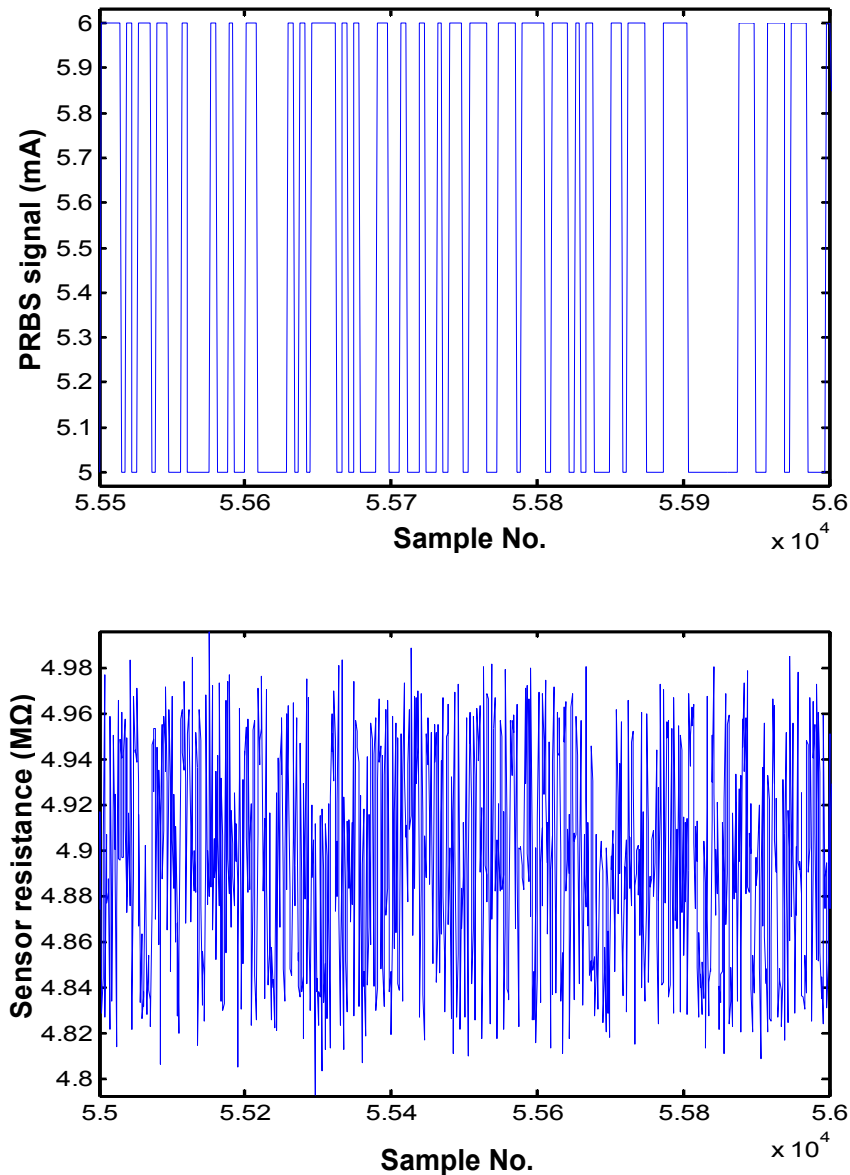


**Figure 5.10:** Small fragment of the PRBS temperature-modulating signal of length 65535 applied to the sensor heating element (top) and resulting resistance transient of a tungsten-oxide micro-hotplate sensor in the presence of 2.5 ppm of NO<sub>2</sub> (bottom). Figure extracted from [9].

Three different concentrations of NO<sub>2</sub> (2.5, 5 and 10 ppm) diluted in dry air were measured. These species were measured while modulating the working temperature of the

## Improving the performance of micro-machined metal oxide gas sensors: Optimization of the temperature modulation mode via pseudo-random sequences.

micro-hotplates by means of the PRBS signal. Each measurement of  $\text{NO}_2$  was replicated 6 times while dry air was repeated for 4 times. Every measurement took approximately 10 minutes to complete, which corresponded to the acquisition of 2.5 sequences of length 65535 generated with a clock frequency of 250 Hz. The sampling frequency was set to 1000 Hz. Finally, in Figure 5.10 the PRBS signal used to modulate sensor temperature and a typical transient response of a micro-hotplate gas sensor in the presence of 5 ppm of  $\text{NO}_2$  are shown.

### 5.4.2. Experiment 2: Optimized temperature modulation of micro-hotplate gas sensors using Pseudo Random Binary Sequences (PRBS).

A second experiment aimed to optimize the modulation frequencies of micro-hotplate gas sensors using PRBS signals was performed. The measurements were performed at the Universitat Rovira i Virgili, in Tarragona Spain, with 4  $\text{WO}_3$  micro-hotplate gas sensors placed in a 20-ml volume test chamber and connected to a continuous flow system set at 200 ml/min of total gas flow. (Figure 5.4) [10].

The generation/injection of the PRBS modulating signal to each gas sensor studied and the data acquisition process were the ones reported in experiment number 1.

In the previously described experiment, the clock frequency used to generate the PRBS signal,  $f_c$ , was set to 250 Hz. This allowed the sensors to be tested for modulating frequencies up to 112.5 Hz. Using an PRBS signal of length  $L = 65535$ , the spectral resolution was set near to 4 mHz. From this preliminary study, it was derived that the important modulating frequencies to discriminate and quantify gases lay in the range between 0 and 1 Hz. This result is not surprising, since the objective of the temperature modulation is to alter the kinetics of diffusion and reaction processes at the sensor surface and these kinetics are slow [11]. This explains why low-frequency temperature-modulating signals (i.e. in the mHz range) have been used with micro-hotplate gas sensors [12-15]. Therefore, in the study reported here, the clock frequency ( $f_c$ ) used to generate the PRBS signal was set to 2 Hz. This frequency allows the sensors to be tested at temperature-modulating frequencies that range from 0 up to near 1 Hz. The length of the sequence was set to 511, which resulted in a spectral resolution of 3.91 mHz.

In this experiment, three different concentrations of  $\text{NO}_2$  (0.5, 1, 2 ppm),  $\text{NH}_3$  (100, 500, 1000 ppm) and their binary mixtures (0.5 + 100, 1 + 500, 2 + 1000 ppm of  $\text{NO}_2$  and  $\text{NH}_3$ , respectively) diluted in dry air were measured. At first, the steady-state response (i.e. when the sensors were operated at a fixed temperature) was studied. Then, these species were measured while modulating the working temperature of the micro-hotplates. Each measurement was replicated 5 times. Every measurement took approximately 10 minutes to

complete, which corresponded to the acquisition of 2.5 sequences of length 511 generated with a clock frequency of 2 Hz. The sampling frequency was set to 10 Hz. Figure 5.11 shows the MLS signal used to modulate sensor temperature and a typical transient response of a micro-hotplate gas sensor in the presence of 2 ppm of  $\text{NO}_2$ .

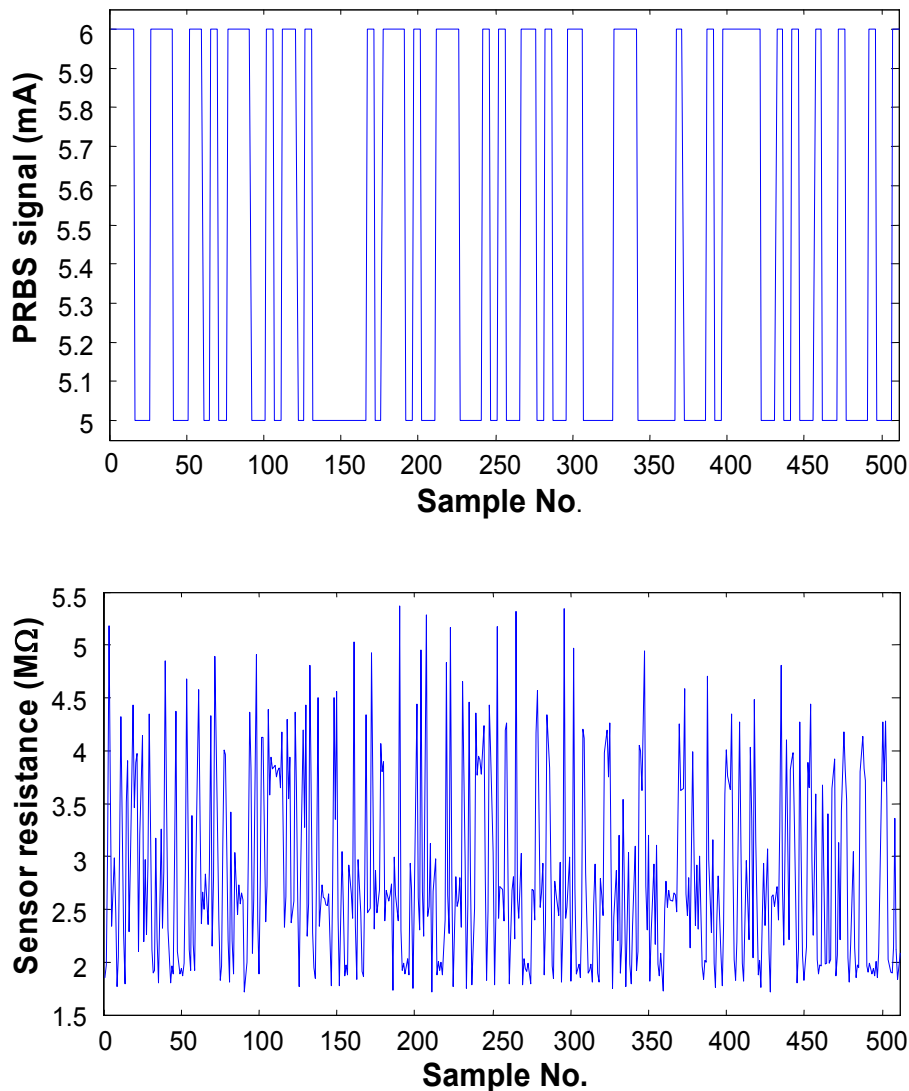


**Figure 5.11:** Temperature-modulating MLS sequence of length 511 applied to the sensor heating element (top) and resulting resistance transient of a tungsten-oxide micro-hotplate sensor in the presence of 2 ppm of  $\text{NO}_2$  (bottom). Figure extracted from [10].

Improving the performance of micro-machined metal oxide gas sensors:  
Optimization of the temperature modulation mode via pseudo-random sequences.

### 5.4.3. Experiment 3: Optimized Temperature Modulation of Metal Oxide Micro-Hotplate Gas Sensors through Multilevel Pseudo Random Sequences.

Experiments 1 and 2, we aimed at systematically selecting the modulation frequencies of micro-hotplate gas-sensors using pseudo-random binary sequences of maximum length (PRBS). In this experiment (*Experiment 3*), an evolved method to modulate the working temperature of metal oxide micro-hotplate gas sensors in a wide frequency range is presented, but this time based on the use of maximum length multilevel pseudo random sequences (MLPRS). One of the main reasons for considering multilevel signals instead of the binary ones is that the former can provide a better estimate than the latter of the linear dynamics of a process with non-linearities. And it is well known that temperature-modulated metal oxide gas sensors present non-linearity in their response.

The goals of this experiment are as follows:

- At first, to develop a system that allows us to select and identify, in a systematic way, the optimal set of modulating frequencies used to modulate the working temperature of the microhotplate gas sensors.
- Therefore, to synthesize a multi-sinusoidal signal (i.e., at the frequencies selected) aimed to modulate the working temperature of the gas sensors micro-array, validating then the gas-sensor system pair under study.
- Finally, the measurements generated in this experiment (i.e., the MLPRS or a multi-frequency sinusoidal signal), are used to introduce the DM and phase space as a feature extraction method when the working temperature of micro-hotplate gas sensors is modulated.

In this experiment, five tungsten oxide micro-hotplate gas sensors were placed in the 20-ml volume test chamber previously mentioned and connected to a continuous flow system. Concentrations of single gases and binary mixtures were once again obtained by computer-supervised mass-flow controllers. The MLPRS was generated by software written in MATLAB code. A written in house LABVIEW program running on a PC platform was used for controlling the data acquisition board (see Figure 5.4).

The missions for this acquisition board were: On the one hand, to inject a MLPRS current signal (high and low current level of 6 and 5 mA respectively divided in 5 levels) to the polysilicon heating resistor of each micro-hotplate gas sensor. This resulted in a maximum temperature variation of the micromachined membranes equal to 200°C. On the other hand, to acquire and store the resistance of each sensing film (these resistances were measured in a

half-bridge configuration) and the voltage drop over of the heating elements (to monitor temperature). During each measurement, 1 period of the excitatory MLPRS signal and corresponding sensor response signals (i.e. sensor resistance) were acquired and stored for further processing.

As was previously mentioned, reaction kinetics is slower than the thermal response of the membrane [11]. This explains why in the study reported here, the  $f_c$  used to generate the MLPRS signal was set to 2 Hz. This frequency allows the sensors to be tested under temperature-modulating frequencies ranging from 0 up to near 1 Hz. These modulating frequencies are far below the cut-off frequency of 52 Hz found for the screen-printed gas sensors. The length of the MLPRS signal in this experiment was set to 624, which resulted in a spectral resolution of 3.21 mHz. Finally, the number of levels of the pseudo random signal was set to 5.

In this experiment 3 different concentrations of  $\text{NO}_2$  (0.5, 1, 2 ppm),  $\text{NH}_3$  (100, 500, 1000 ppm) and their binary mixtures (0.5 + 100, 1 + 500, 2 + 1000 ppm of  $\text{NO}_2$  and  $\text{NH}_3$ , respectively) diluted in dry air were measured [16, 17]. Although ammonia can be detected at lower concentrations using these  $\text{WO}_3$ -based microsensors, the gas concentration levels were selected to get sensor responses with similar intensity when measuring either nitrogen dioxide or ammonia. At first, these species were measured while modulating the working temperature of the micro-hotplates with the 5-level PRS signal.

This study was aimed at identifying the set of modulating frequencies that were best suited at discriminating and quantifying the gases in this particular application. Each measurement was replicated 8 times, which gave a total of 72 measurements. Every measurement took approximately 5 minutes to complete, which corresponded to the acquisition of 1 sequence of length 624 generated with a clock frequency of 2 Hz. The sampling frequency was set to 10 Hz. Figure 5.12 shows the MLPRS signal used to modulate the temperature of the sensors and a typical transient response of a micro-hotplate gas sensor in the presence of 2 ppm of  $\text{NO}_2$ .

From the 8 replicate measurements available, 5 were selected to be part of the variable selection data matrices (there was one matrix per sensor). Therefore, these matrices gathered together 45 measurements (i.e. 9 different measurements  $\times$  5 replicates). The remaining 27 measurements integrated the validation data matrices. The processes of frequency selection and validation of this experiment will be discussed in chapter 7.

Improving the performance of micro-machined metal oxide gas sensors:  
Optimization of the temperature modulation mode via pseudo-random sequences.

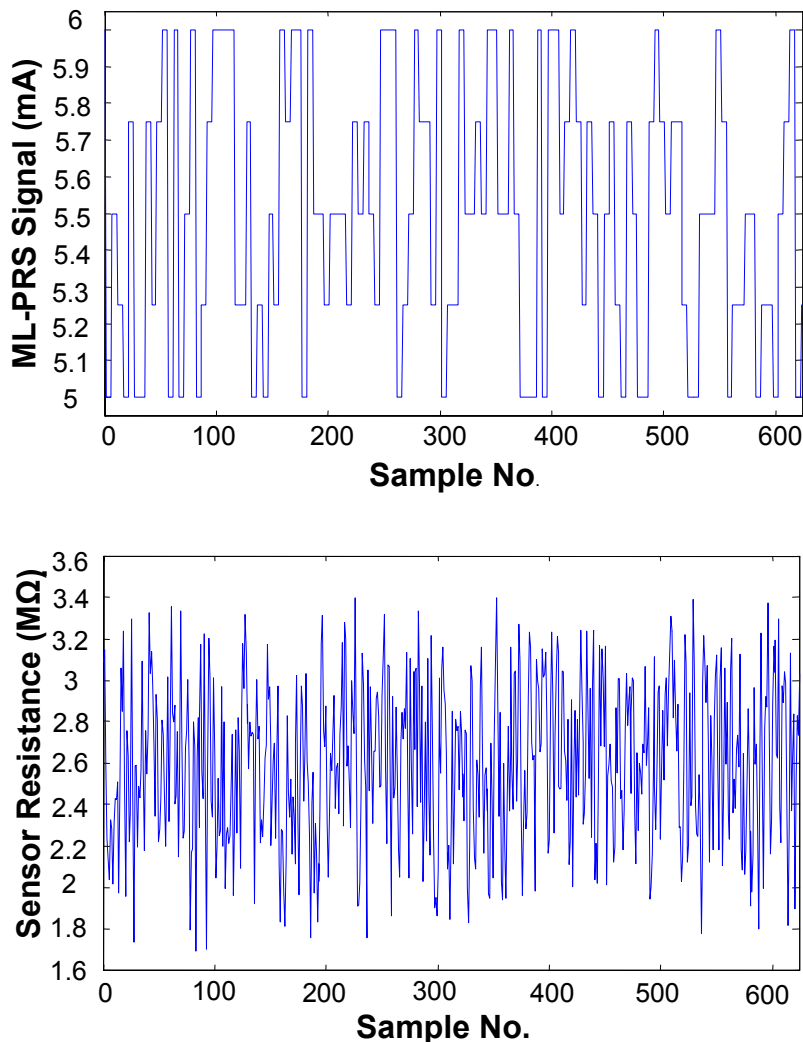


**Figure 5.12:** 5-level PRS applied to the heater element (top) and resulting resistance of a screen-printed  $\text{WO}_3$  micro-hotplate gas sensor in the presence of 2 ppm of  $\text{NO}_2$  (bottom). Figure extracted from [16].

In the second step, new measurements of the different species and concentrations studied were performed using the same sensors (5 replicate measurements per species and concentration, which gave a total of 45 new measurements) [16-18]. However, in this case the sensors had their operating temperature modulated by a signal resulting from the sum of a few sinusoids of identical amplitude, the frequencies of which had been identified previously (by the frequency selection and validation procedures) as the best for gas recognition. This study aims both at showing the actual operation of temperature modulated

sensors after their optimal modulation procedure had been studied and at estimating their performance in the gas analysis application considered.

The procedure of generating the multi-sinusoidal signal and the transient response of a gas sensor modulated by this kind of signals will be illustrated in chapter 7, while the measurement set-up procedure was the one reported above during the frequency selection step.

#### **5.4.4. Experiment 4: Qualitative and quantitative gas mixture analysis using temperature-modulated micro-hotplate gas sensors: Selection and validation of the optimal modulating frequencies.**

In this experiment a systematic method to determine which are the optimal temperature modulation frequencies to solve a given gas analysis problem has been introduced, discussed in detail and fully validated [19]. The optimization method is once again based on the use of multi-level pseudo-random binary sequences (MLPRS). Using this strategy, it is shown that the best temperature modulating frequencies to discriminate and quantify gases using an array of 4 metal oxide gas sensors are identified. The process is illustrated solving a practical application: the quantitative analysis of acetaldehyde, ethylene, ammonia and their binary mixtures. These species were chosen, since the first two are related to the quality of climacteric fruit during cold storage and the third one reveals the occurrence of a leak in the refrigeration system.

Two gas sensor micro-devices, fabricated in the same batch, were used in this study. The four active films in each micro-array consisted of Pd-doped, Pt-doped and Au-doped tin oxide (sensors 1,2 and 3, respectively), and Au-doped tungsten oxide (sensor 4). The first micro-array was used for selecting the optimal temperature modulation frequencies employing MLPRS signals and the second micro-array was used to validate the frequency selection process.

Measurement set-up: One of the two 4-element micro-arrays studied was placed in a 20-ml volume test chamber. This chamber was connected to a computer-supervised continuous flow system that allowed us to obtain, starting from calibrated gas bottles, the desired concentrations of the different gases and gas mixtures in a highly reproducible way. The carrier was dry air. The total gas flow was set to 200 ml/min and kept constant. Moisture level was kept at 10 % R.H. (measured at  $30^{\circ}\text{C} \pm 1^{\circ}\text{C}$ ) during the whole measurement process. In Figure 5.4 the experimental set-up is shown.

Initially (i.e., during the frequency optimization process) the response of the first micro-array was measured when the sensors' operating temperature was modulated using a 5-level

## Improving the performance of micro-machined metal oxide gas sensors: Optimization of the temperature modulation mode via pseudo-random sequences.

PRS. The MLPRS was generated by software written in MATLAB code. A written in house LABVIEW program running on a PC platform was used for controlling the data acquisition board (see Figure 5.4 and Figure 5.6). The mission of this board was twofold:

- To acquire the dynamic response of gas sensors and the voltage drop over their heating elements (to monitor temperature). Sensor resistance was acquired in a half-bridge configuration.
- Output an analog MLPRS signal to a set of four voltage-controlled current sources.

Each current source injected an MLPRS current signal to the polysilicon heating resistor of each micro-hotplate gas sensor. The higher and lower current levels were set to 8 mA and 7 mA, respectively. This resulted in a maximum temperature variation of the micro-machined membranes equal to 200°C. Since the number of levels of the pseudo random signal was set to 5, the current levels were 7, 7.25, 7.5, 7.75 and 8 mA. Additionally, the clock frequency ( $f_c$ ) used to generate the MLPRS signal was set at 2 Hz. This frequency allows for testing the gas/sensors system at temperature modulating frequencies that range from 0 up to near 1 Hz. These modulating frequencies are far below of the cut-off frequency of the metal oxide coated membranes, which is the inverse of their thermal response, (i.e.,  $1/19 \times 10^{-3} \text{ s}^{-1} = 52 \text{ Hz}$ ). The length of the MLPRS signal was set to 624, which resulted in a spectral resolution,  $f_c/L$ , of 3.21 mHz (see Figure 5.13 (top)). During each measurement, two periods of the excitatory MLPRS signal and the corresponding sensor response signals (i.e. sensor resistance) were acquired and stored for further processing.

In the second step (i.e., during the validation process) the response of the second micro-array was measured when the sensors' operating temperature was modulated using a multi-sinusoidal signal resulting from the sum of a few sinusoids of identical amplitude. The frequencies of these signals were a subset of those that had been identified in the first step as more advantageous for gas recognition and quantification. Once again, software written in MATLAB was in charge of generating the multi-sinusoidal signal and the set-up to modulate sensors' temperature and acquire their responses were identical to the one already described for MLPRS signals.

Databases: The first database was used for optimizing the temperature modulation of the sensors via a 5-level MLPRS. The following single gases and gas mixtures were measured using the first sensor micro-array:

- Acetaldehyde (10; 50 and 100 ppm)
- Ethylene (10; 50 and 100 ppm)
- Ammonia (25; 50 and 75 ppm)
- Acetaldehyde + Ethylene (10 + 10; 10 + 50; 10 + 100; 50 + 10; 50 + 50; 50 + 100; 100 + 10; 100 + 50; 100 + 100 ppm)



- Ethylene + Ammonia (10 + 25; 10 + 50; 10 + 75; 50 + 25; 50 + 50; 50 + 75; 100 + 25; 100 + 50; 100 + 75 ppm)
- Acetaldehyde + Ammonia (10 + 25; 10 + 50; 10 + 75; 50 + 25; 50 + 50; 50 + 75 ppm)

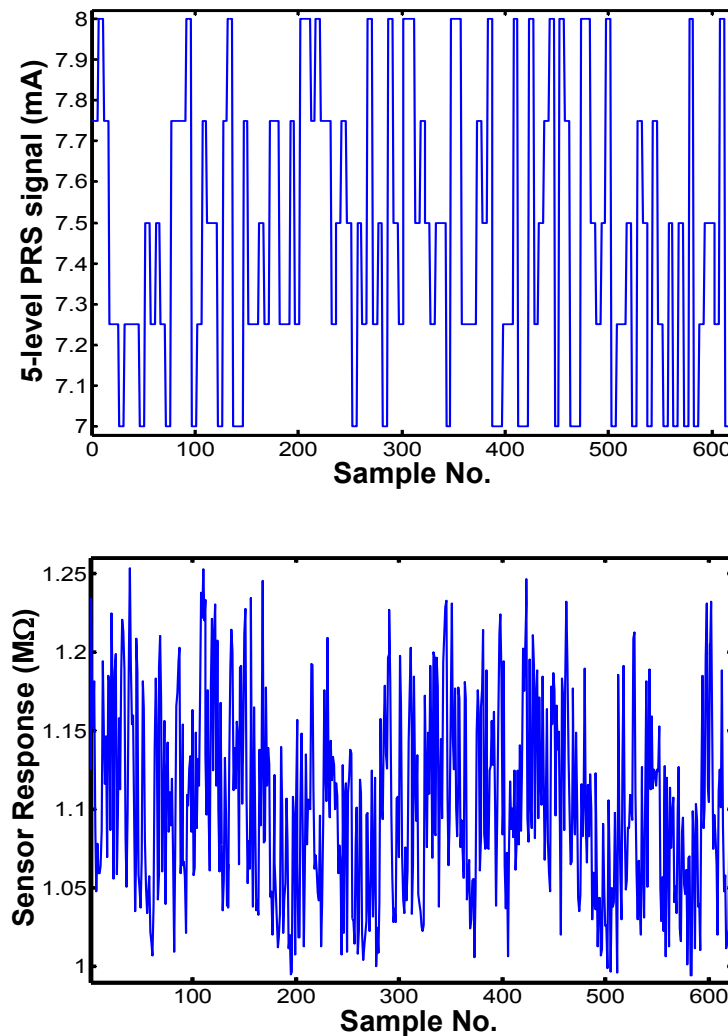


**Figure 5.13:** 5-level PRS applied to the sensors' heating element (top) and resulting resistance of a screen-printed  $\text{WO}_3$  micro-hotplate gas sensor in the presence of 50 ppm of Acetaldehyde (bottom).  
Figure extracted from [19].

Since each measurement was replicated 5 times (performed in a disordered way), this gave a total of 165 measurements in the first database. The measurement procedure consisted

## Improving the performance of micro-machined metal oxide gas sensors: Optimization of the temperature modulation mode via pseudo-random sequences.

in the following steps: First, the desired concentration of gas or gas mixture was injected by the continuous flow system into the chamber where the micro-sensors were kept at a stable working temperature of 450°C. This was done to measure the steady-state sensor response. Then the sensors' operating temperature was modulated using the MLPRS signal. After the sensors had been thermally modulated during five cycles of the MLPRS, the acquisition of 2 additional cycles started. This was done to ensure that reproducible response patterns were acquired during each measurement. The acquisition of these two cycles took 10.4 minutes to complete (i.e. 2 sequences of length 624 generated with a clock frequency of 2 Hz). The sampling frequency was set to 10 Hz. An example of the 5-level PRS signal used to modulate the temperature of the sensors and a typical transient response of a Au-doped WO<sub>3</sub> micro-hotplate gas sensor in the presence of Acetaldehyde 50 ppm are shown in Figure 5.13 (top to down respectively).

The second database was used for validating the frequency selection performed using the first database. A new set of measurements was run using the second micro-sensor array. The gases and concentrations measured were the ones reported for the first database. This time, a multi-sinusoidal signal was used to modulate the sensors' operating temperature. Once again, each measurement was replicated five times, which gave a total of 165 measurements available in the second database (performed in a disordered way). An equivalent procedure to the one reported before was employed to measure both the steady-state and the temperature-modulated response of the sensors.

## 5.5. Summary.

This chapter begins with a brief description of the micro-hotplate gas sensors used for this analysis. Basically two different kind of micro-gas sensor arrays were used: thick and thin film tungsten and tin oxide gas sensors. A brief description of how the substrate is fabricated and the active layers are deposited was given in Section 5.2.

The chapter continues with the description of the measurement system used to perform the different experiments. The measurement system is then fully detailed in section 5.3

The last sections of the chapter give information about the measurements performed, the experimental set-up, the different gases and concentrations measured in each experiment. In total there were a number of four experiments carried out.

*Experiment 1* is detailed in Section 5.4.1. Its aim was twofold: On th one hand (preliminary experiment) to determine the clock frequency and length of the sequence in order to study the appropriate range of modulating frequencies with enough resolution. On the other hand, to study a gas-sensor system in a systematic way, in order to determine the

optimal set of frequencies to modulate the working temperature of the micro-hotplate gas sensors using PRBS.  $\text{NO}_2$  at three different concentrations and single dry air were measured.

*Experiment 2* is detailed in Section 5.4.2. A second experiment aimed to optimize the modulation frequencies of micro-hotplates gas sensors using PRBS signals was performed. It was realized with  $\text{WO}_3$  based micro-hotplate gas sensors. The gases measured were nitrogen dioxide (at three different concentrations), ammonia (at three different concentrations) and binary mixtures nitrogen dioxide and ammonia.

*Experiment 3* is detailed in Section 5.4.3. The three objectives of this experiment were: At first, to develop a system that allows us to select and identify, in a systematic way, the optimal set of modulating frequencies used to modulate the working temperature of microhotplate gas sensors using MLPRS. Then, to synthesize a multi-sinusoidal signal (i.e., at the frequencies selected) to modulate the working temperature of the gas sensors micro-array, validating then the optimization process. Finally, the measurements generated in this experiment (i.e., the MLPRS or a multi-frequency sinusoidal signal), were processed with a novel DM and phase space feature extraction methods. The gases measured were, once again, those reported in experiment 2.

Finally *Experiment 4* is detailed in Section 5.4.4. This experiment further develops what was studied in *Experiment 3*. In this case the process optimization is illustrated by solving a practical application: the quantitative analysis of acetaldehyde, ethylene, ammonia and their binary mixtures. A multi-sinusoidal signal (i.e., at the frequencies selected) aimed to modulate the working temperature of the gas sensors micro-array was synthesized, and used to validate the whole process.

## 5.6. References.

- [1] A. Götz, I. Gràcia, C. Cané, E. Lora-Tamayo, M.C. Horrillo, J. Getino, C. García, J. Gutiérrez, “A micromachined solid state integrated gas sensor for the detection of aromatic hydrocarbons”, *Sensors and Actuator B*, vol. 48, pp. 483-487, 1997.
- [2] M.C. Horrillo, I. Sayago, L. Arés, J. Rodrigo, J. Gutiérrez, A. Götz, I. Gràcia, L. Fonseca, C. Cané, E. Lora-Tamayo, “Detection of low NO<sub>2</sub> concentrations with low power micromachined tin oxide gas sensors”, *Sensors Actuators B*, vol. 58, pp. 325-329, 1999.
- [3] D.G. Rickerby, N. Wächter, M.C. Horrillo, J. Gutiérrez, I. Gràcia, C. Cané, “Structural and dimensional control in micromachined integrated solid state gas sensors”, *Sensors Actuators B*, vol. 69, pp. 314-319, 2000.
- [4] I. Gràcia, J. Santander, C. Cané, M.C. Horrillo, I. Sagayo, J. Gutiérrez, “Results on the reliability of silicon micromachined structures for semiconductors gas sensors”, *Sensors and Actuators B*, vol. 77, pp. 409-415, 2001.
- [5] I. Jiménez, A. Cirera, A. Cornet, J. R. Morante, I. Gràcia, C. Cané, “Pulverisation method for active layer coating on Microsystems”, *Sensors and Actuators B*, vol. 84, pp. 78-82, 2002.
- [6] E. Llobet, P. Ivanov, X. Vilanova, J. Brezmes, J. Hubalek, K. Malysz, I. Gracia, C. Cané and X. Correig, “Screen-printed nanoparticle tin oxide films for high-yield sensor Microsystems”, *Sensors Actuators B*, vol. 96, pp. 94-104, 2003.
- [7] P. Ivanov, M. Stankova, E. Llobet, X. Vilanova, J. Brezmes, I. Gràcia, C. Cané, J. Calderer, and X. Correig, “Nanoparticle metal oxide films for micro-hotplate-based gas sensors systems”, *IEEE sensors journal*, vol. 5, pp. 798-809, 2005.
- [8] D. Vicenzi, A. Butturi, V. Guidi, M. Carotta, G. Martinelli, V. Guarnieri, S. Brida, B. Margesin, F. Giaocemozzi, M. Zen, D. Giusti, G. Soncini, A. Vasiliev, and A. Pisliakov, “Gas-sensing device implemented on a micromachined membrane: A combination of thick-film and very large scale integrated technologies,” *J. Vac. Sci. Technol. B*, vol. 18, pp. 2441–2445, 2000.

- [9] A. Vergara, E. Llobet, J. Brezmes, M. Stankova, P. Ivanov, X. Correig, I. Gràcia, C. Cané, X. Correig, "MLS based temperature modulation of micro-hotplates", Book of Abstracts of IEEE Sensors 2003, Toronto, Canada, pp.1255-1259, October 2003.
- [10] A. Vergara, E. Llobet, J. Brezmes, P. Ivanov, X. Vilanova I. Gràcia, C. Cané and X. Correig, "Optimized temperature modulation of micro-hotplate gas sensors through pseudorandom binary sequences", IEEE Sensor Journal, vol. 5, (6), pp. 2005 1369-1378, 2005.
- [11] P.T. Moseley, B.C. Tofield, Eds., "*Solid-state gas sensors*", The Adam Hilger series on sensors, Bristol, UK, 1987.
- [12] R. E. Cavicchi, J. S. Suehle, K.G. Kreider, M. Gaitan, P. Chaparala, "Optimized temperature-pulse sequences for the enhancement of chemically specific response patterns from micro-hotplates gas sensors", Sensors and Actuators B, vol. 33, pp. 142-146, 1996.
- [13] A. Heiling, N. Bârsan, U. Weimer, M. Schweizer-Berberich, J.W. Gardner and W. Gopel, "Gas identification by modulating temperatures of SnO<sub>2</sub>-based thick film sensors", Sensors and Actuators B, vol. 43, pp. 45-51, 1997.
- [14] E. Llobet, R. Ionescu, S. Al-Khalifa, J. Brezmes, X. Vilanova, X. Correig, N. Bârsan, J.W. Gardner, "Multicomponent gas mixture analysis using a single tin oxide sensor and dynamic pattern recognition", IEEE Sensors Journal, vol. 1, pp. 207-213, 2001.
- [15] E. Llobet, J. Brezmes, R. Ionescu, X. Vilanova, S.Al-Khalifa, J.W. Gardner, N. Barsan, X. Correig, "Wavelet transform fuzzy ARTMAP based pattern recognition for fast gas identification using a micro-hotplate gas sensor", Sensors Actuators B, vol. 83, pp. 238-244, 2002.
- [16] A. Vergara, E. Llobet, J. Brezmes, P. Ivanov, X. Vilanova I. Gràcia, C. Cané and X. Correig, "Optimised Temperature Modulation of Metal Oxide Micro-Hotplates Gas Sensors through Multi-Level pseudo random sequences", Sensors and Actuators B, vol. 111-112, pp. 271-280, 2005.
- [17] A. Vergara, E. Llobet, J. Brezmes, P. Ivanov, X. Vilanova I. Gràcia, C. Cané and X. Correig, "Optimised Temperature Modulation of Metal Oxide Micro-Hotplates Gas Sensors through Multi-Level PRS", Proceedings of the XVIII Eurosensors Conference, Rome, Italy, pp.614-615, September 2004.
- [18] A. Vergara, E. Llobet, J. Brezmes, X. Vilanova, M. Stankova, I. Gracia, C. Cane, X. Correig, "Optimized multi-frequency temperature modulation of micro-hotplate gas

Improving the performance of micro-machined metal oxide gas sensors:  
Optimization of the temperature modulation mode via pseudo-random sequences.

sensors”, Book of Abstracts of IEEE Sensors 2004, Vienna, Austria, pp. 1392 - 1395  
October 2004.

- [19] A. Vergara, E. Llobet, J. Brezmes, P. Ivanov, C. Cané, I. Gràcia, X. Vilanova, X. Correig, “Quantitative gas mixture analysis using temperature-modulated micro-hotplate gas sensors: Selection and validation of the optimal modulating frequencies”, *submitted to Analytical Chemistry*, 2006.

---

# 6.

# Gas analysis using PRBS

---

<b>6. GAS ANALYSIS USING PRBS</b>	<b>139</b>
<b>6.1. Introduction.</b>	<b>140</b>
<b>6.2. Analysis of the data from experiment 1: PRBS signals to modulate the temperature operation of micro-hotplates gas sensors (preliminary study).</b>	<b>141</b>
6.2.1. Estimation of the impulse response.	142
6.2.2. Variable selection procedure.	144
6.2.3. Qualitative and semi-quantitative analysis procedure.	145
<b>6.3. Analysis of the data from experiment 2: Optimized temperature modulation of micro-hotplate gas sensors using Pseudo Random Binary Sequences (PRBS).</b>	<b>147</b>
6.3.1. Steady-state response.	147
6.3.2. Estimation of the impulse response.	148
6.3.3. Variable selection procedure.	151
6.3.4. Qualitative gas analysis.	151
6.3.5. Semi-quantitative gas analysis.	154
<b>6.4. Conclusions.</b>	<b>155</b>
<b>6.5. References.</b>	<b>156</b>

## Improving the performance of micro-machined metal oxide gas sensors: Optimization of the temperature modulation mode via pseudo-random sequences.

### 6.1. Introduction.

Even if a great deal of work has been done with temperature-modulated micro-hotplate gas sensors, the selection of the modulating frequencies remains an obscure and non-systematic method. That is why here a method, borrowed from the field of system identification, is introduced for the first time to systematically study the effect of modulation frequencies in the discrimination and quantification ability of metal oxide based micro-hotplate gas sensors. Therefore, using maximum length pseudo-random binary sequences (PRBS) the optimal set of modulating frequencies can be determined for a given gas analysis application computing the impulse response of a pair sensor-gas system. This is computed by the circular cross-correlation of the PRBS temperature-modulating sequence and sensor response sequence. This method enables each sensor-gas system to be identified and to find, in a systematic way, those modulation frequencies that are important to discriminate between different gases and to estimate gas concentration. This is demonstrated by obtaining the impulse response of integrated micro-arrays of either sputtered or screen-printed  $WO_3$  in the presence of pollutant gases.

In this chapter, experiments 1 and 2 described in Chapter 5, are studied and fully analyzed. The analysis is divided as follows:

In section 6.2 the experiment 1, (preliminary study) was analyzed. The objectives of this analysis are twofold: firstly the thermal response of the gas sensor heating element is studied. This is aimed to obtain the cutoff frequency of the coated membranes and therefrom to determine the clock frequency ( $f_c$ ) and the length of the PRBS signal. With this, the frequency range under study is determined. Once the PRBS is generated and the frequency range is determined, the study and determination of the optimal modulating frequencies is done.

In section 6.3 the second experiment is analyzed. This consists in to systematically determine the optimal set of modulation frequencies of the micro-hotplate gas sensors. Pollutant gases as  $NO_2$ ,  $NH_3$  (at three different concentrations) and their binary mixtures are measured.

In both experiments the impulse response estimate is computed. Therefrom the module of the Fast Fourier Transform (FFT) of the impulse response estimate is calculated. By a variable selection method the set of the optimal spectral components are selected. These features (spectral components) extracted correspond to the frequencies that will be used in the qualitative and quantitative analysis of the gases studied. For this, statistical and neural network pattern recognition methods are used.



## 6.2. Analysis of the data from experiment 1: PRBS signals to modulate the temperature operation of micro-hotplates gas sensors (preliminary study).

In this section the analysis of the data from experiment 1 is carried out. The sensor used in the experiment was a tungsten oxide microhotplate gas sensor and NO<sub>2</sub> diluted in synthetic dry air (at three different concentrations) and dry air were the gases measured. The measurements were performed at the Universitat Rovira i Virgili, in Tarragona Spain, and the results of this analysis have been reported in [1].

As was mentioned earlier in the measurement set-up sub-section (in chapter 5), the objectives of this experiment are twofold:

- On the one hand (preliminary experiment) to determine the clock frequency and length of the sequence in order to study an appropriate modulation frequency range with enough resolution.
- On the other hand to study a gas-sensor system in a systematic way, in order to determine the optimal set of frequencies to modulate the working temperature of the micro-hotplate gas sensors.

To determine the frequency range of the thermal modulation, the thermal response of the sensor membranes was studied. A stepwise current signal was applied to the heating element of the gas sensors (i.e., sensor membranes were coated using either thin or thick film technology). Three replicate measurements were made for each one of the 4 different current impulses tested. The results on the thermal response of gas sensors are illustrated in Table 6.1. It was found that the membranes behaved as first-order systems, where the ones coated by screen-printing (thick film) presented a thermal response of around 19 ms while the thermal response of the membranes coated by sputtering (thin film) was of about 13 ms. Therefore, the cutoff frequency of the coated membranes was around 52 and 77 Hz respectively. Therefore, the clock frequency used to generate the PRBS signal ( $f_c$ ), was set to 250 Hz. This allowed the sensors to be tested for modulating frequencies ranging from the D.C. up to 112.5 Hz (i.e.,  $0.45 f_c$ ). Once the  $f_c$  had been determined, the length of the PRBS signal was set to 65,535. This implied that a spectral resolution ( $f_c/L$ ) equal to 3.81 mHz was obtained, which was judged to be convenient.

Once these parameters had been determined the PRBS was built in order to study, in the pre-established frequency range, the modulating frequencies. The thorough analysis of the gas sensors behavior in a wide range of modulating frequencies (i.e., from the D.C. up to

Improving the performance of micro-machined metal oxide gas sensors:  
 Optimization of the temperature modulation mode via pseudo-random sequences.

112.5 Hz) is needed to ensure that the set of frequency (or frequencies) selected are the optimal ones, for the specific application considered.

**Table 6.1:** Thermal response of the micro-hotplate coated membranes as a result of applying a stepwise change in the current applied to the membranes' heating element ( $\Delta I R_h$ ). Sensors 1, 2 and 3 are coated with a thick active film and sensors 4, 5 and 6 are coated with thin films.

Thermal response of the sensor membranes (ms)							
$\Delta I R_h$ (mA)↓	Sensor →	1	2	3	4	5	6
-2 → -6	Rep 1	21.7	20.4	19.6	13.3	11.8	13.2
	Rep 2	21.3	20.1	19.3	12.4	12.2	13.0
	Rep 3	21.3	20.4	19.2	13.1	11.7	13.0
	Aver (ms)	21.4	20.3	19.4	12.9	11.9	13.1
-3 → -6	Rep 1	22.6	19.8	19.5	12.6	13.4	13.4
	Rep 2	21.5	20.0	19.5	12.1	13.6	13.9
	Rep 3	21.7	21.4	19.9	13.0	12.5	12.9
	Aver	21.9	20.4	19.6	12.6	13.1	13.4
-4 → -6	Rep 1	20.5	19.2	18.5	12.7	13.3	13.2
	Rep 2	20.9	20.9	19.1	13.3	12.9	12.0
	Rep 3	20.6	19.6	19.0	13.0	11.9	12.2
	Aver	20.6	19.9	19.0	13.0	12.7	12.5
-5 → -6	Rep 1	20.3	20.2	20.5	14.2	14.3	13.4
	Rep 2	21.8	18.5	19.9	12.3	13.1	12.8
	Rep 3	20.3	21.0	18.5	12.7	13.3	12.9
	Aver	20.8	19.9	19.6	13.1	13.6	13.0

As was already mentioned in the experimental section, vapors of synthetic air and synthetic air + NO<sub>2</sub> (at 3 different concentrations) were measured using the temperature-modulated micro-hotplates. Figure 5.12 shows the temperature modulating pseudorandom signal used (in fact, a small portion of the PRBS signal is shown) and the typical response of a thermally modulated micro-hotplate gas sensor. The details of the sensor response analysis are discussed in the following sub-sections.

### 6.2.1. Estimation of the impulse response.

An estimate of the impulse response,  $\hat{h}(n)$ , of each sensor in the presence of the pollutant gas studied was computed through the circular cross-correlation of one period ( $L =$

65535 samples) of the PRBS signal,  $x(n)$ , and one period of the sensor response (i.e. resistance transient),  $y(n)$ .

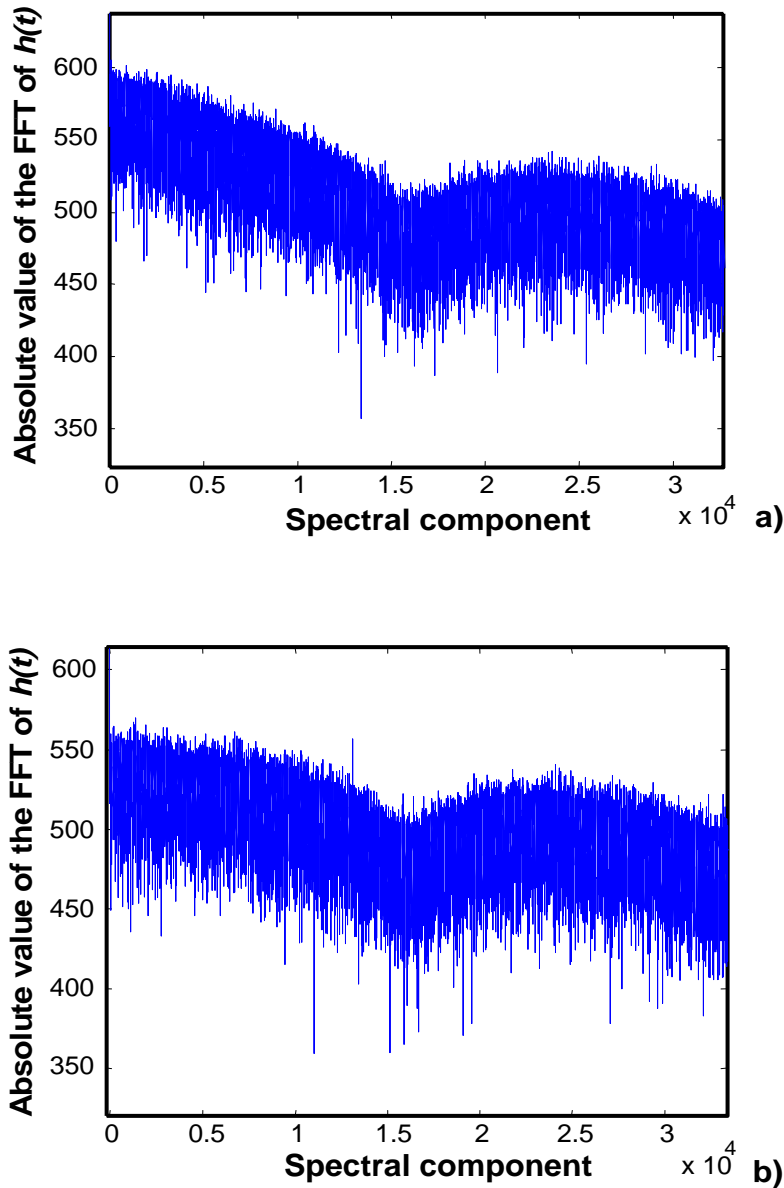


**Figure 6.1:** Module of the FFT of the impulse response estimate of a thick film tungsten oxide micro-hotplate sensor in: a)  $\text{NO}_2$  (10 ppm) and b) dry air.

## Improving the performance of micro-machined metal oxide gas sensors: Optimization of the temperature modulation mode via pseudo-random sequences.

Since the clock frequency of the PRBS sequence was set to  $f_c = 250$  Hz and the sampling rate of the acquisition system was set to 1 KHz, the sequences acquired had to be decimated by 5 before the cross-correlation was computed.

The module of the Fast Fourier Transform (FFT) of the impulse response estimate  $\hat{h}(n)$  was calculated and, stored for further processing. Figure 6.1 shows the module of the FFT of the impulse responses of a tungsten oxide micro-hotplate sensor in the presence of dry air (a) and 10 ppm of NO<sub>2</sub> diluted in dry air (b) where differences between these spectra when the sensor is in the presence of different gases can be seen.

In the next step, a variable selection method was implemented to identify those spectral components that carry important information for the discrimination and quantification of the pollutant gases studied. Spectral components can be related to a specific temperature-modulation frequency using the following expression:

$$f_m = \frac{SC_m \times f_c}{L} \quad (6.1)$$

where  $SC_m$  is the spectral component number and  $f_c/L$  is the spectral resolution. Therefore, by identifying a subset of spectral components, a subset of temperature modulating frequencies to correctly discriminate and semi-quantify the gases studied can be identified.

### 6.2.2. Variable selection procedure.

A simple variable selection procedure was implemented to select among the spectral components (i.e. the temperature-modulating frequencies) of the estimated impulse responses of the sensors.

A criterion was defined to rate the resolution power of each spectral component. For gas identification purposes, the measurements were grouped in as many categories as pollutant species are. In this case discrimination and semi-quantification of the pollutant gases were attempted at once (i.e., four categories were formed, which for one side NO<sub>2</sub> forms 3 categories (corresponding to their different concentration measured) and on the other side, dry air measurements is the fourth one). For each spectral component, intra-group and between-group variances were computed (see sub-section 3.4 in chapter 3). A figure of merit for the resolution power, ( $RP$ ), of a spectral component (i.e, the ratio between the inter-category variance and the intra-category variance) was calculated. Therefore, a small set of spectral components (i.e., those that have the higher figure of merit) were selected. These spectral components correspond to the temperature-modulating frequencies that lead to a better discrimination or quantification of the species studied (see Table 6.2).

### 6.2.3. Qualitative and semi-quantitative analysis procedure.

Six integrated micro-sensors were used in this study. These consisted of a nano-particle thick film tungsten oxide deposited onto either wide gap or narrow gap interdigitated electrodes (sensors labeled 1 to 3) and a thin film tungsten oxide deposited onto either wide gap or narrow gap interdigitated electrodes (sensors labeled 4 to 6).

**Table 6.2:** Frequencies selected (with high factor of merit for gas identification) for each of the different sensors studied and success rate in gas identification/semi-quantification using a fuzzy ARTMAP classifier. Sensors 1, 2 and 3 have thick film active layers and 4, 5 and 6 have thin film active layers.

Sensor no.	1	2	3	4	5	6
Frequencies selected (Hz)	0.9	0.9	0.168	0.3	0.1	0.1
	0.938	0.938	0.743	0.5	0.5	0.5
	0.942	0.942	0.9	0.6	0.6	0.6
	2.6	2.6	0.938	1.4	0.9	0.9
	3.5	3.5		30.1	1.8	1.8
			8.4	61.6		
		8.6				
Gas identification (%)	91	96	91	81.88	81.88	86.36

One matrix per sensor was formed, which contained as number of rows the number of measurements performed (i.e.22) and as number of columns the number of the spectral components selected. Therefore, every element in these matrices corresponded to the value of a selected spectral component of the impulse response estimate for a given gas-sensor pair. These matrices were used to build and validate fuzzy ARTMAP classifiers or PCA models to see whether it was possible to correctly identify the gases. A cross-validation of order one (i.e. a leave-one-out cross-validation) was implemented to estimate the success rates. Given  $n$  measurements, the classifiers were trained  $n$  times using  $n-1$  training vectors. The vector left out during the training phase (i.e. unseen by the fuzzy ARTMAP classifier) was then used for testing. The performance of a given classifier was estimated as the averaged performance over the  $n$  tests. More details about the building and validation of fuzzy ARTMAP classifiers can be found in [2, 3] and references therein. The discrimination/semi-quantification is possible even using a single micro-hotplate sensor. The method also allows for identifying frequencies that convey important information to semi-quantify the gases, at the same time that they are recognized. The discrimination/semi-quantification results of this analysis are summarized in Table 6.2. The success rate in gas

Improving the performance of micro-machined metal oxide gas sensors:  
 Optimization of the temperature modulation mode via pseudo-random sequences.

identification/semi-quantification (3 concentrations of NO<sub>2</sub> and dry air) was estimated to be near to 96% (leave-one-out cross-validation) even using a single sensor.

Through the selection of information from up to 7 modulating frequencies (case of sensor 2), the gas identification/semi-quantification rate was of 96%, and increased up to 100% when information from different sensors was combined (e.g., combining the information from sensors 1, 2 and 3). In Table 6.2 the modulation frequencies selected from the gas sensors studied are also shown. Since all the sensors studied are based on tungsten oxide, these frequencies might be characteristic of the interaction between tungsten oxide and the gases considered. The differences in the modulating frequencies selected for different sensors are due to their different electrode geometry, active layer thickness and sensing films with different microstructure. Although, the frequencies selected belong to the frequency range studied (i.e. from D.C. to 112.5 Hz), the more relevant frequencies (i.e. frequencies with higher figure of merit) are those ones whose value is low (i.e., in the mHz range). This occurs because it is known that the kinetics of diffusion and reaction processes at the sensor surface are significantly slower than the thermal response of the gas sensor heating element.

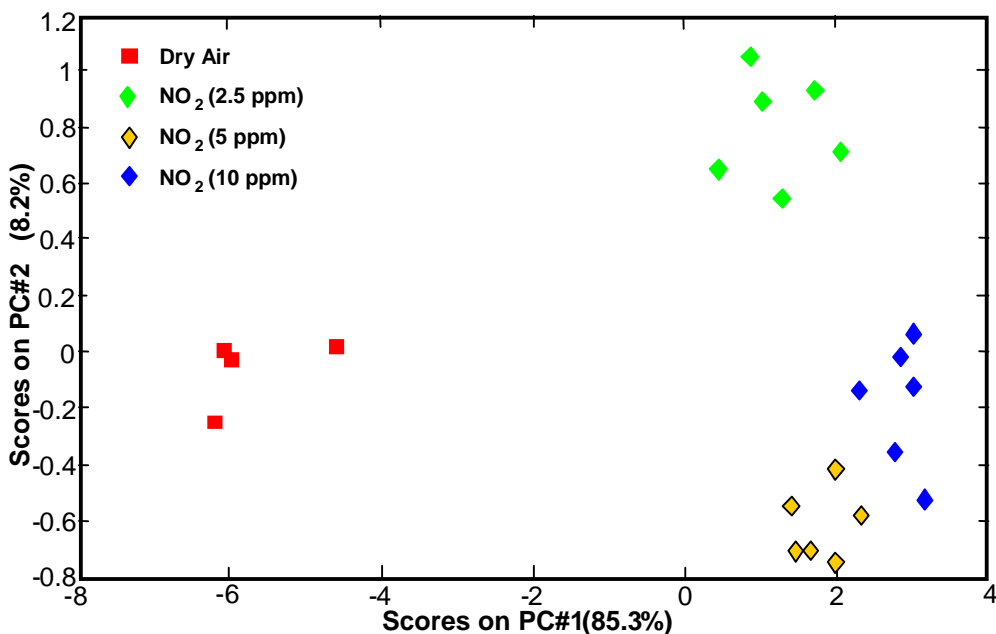


**Figure 6.2:** PCA discrimination between synthetic air and different concentrations of NO<sub>2</sub> using thick film gas sensors.

Finally, Figure 6.2 shows the results of a principal component analysis performed on a matrix resulting from the fusion of data from thick film gas sensors (sensors 1, 2 and 3). Data

were mean centered. The first two PCs captured more than 93.5% of data variance. There, we can see that NO<sub>2</sub> is discriminated from air, and the different measurements of NO<sub>2</sub> (at 2, 5, and 10 ppm) cluster together according to the three different concentrations measured. These results are in agreement with the ones from the fuzzy ARTMAP classifier.

### 6.3. Analysis of the data from experiment 2: Optimized temperature modulation of micro-hotplate gas sensors using Pseudo Random Binary Sequences (PRBS).

In this section the analysis of the data from experiment 2 is carried out. As was mentioned in the experimental section, this experiment was aimed at the optimization of the modulation frequencies of the micro-hotplates gas sensors using PRBS signals. The measurements were performed at the Universitat Rovira i Virgili, in Tarragona Spain, with 4 WO<sub>3</sub> micro-hotplate gas sensors. The gases measured were vapors of three different concentration of NO<sub>2</sub> (0.5, 1, 2 ppm), NH<sub>3</sub> (100, 500, 1000 ppm) and their binary mixtures (0.5 + 100, 1 + 500, 2 + 1000 ppm of NO<sub>2</sub> and NH<sub>3</sub>, respectively) diluted in synthetic dry air. The experimental set-up is fully described in chapter 5. The results of this analysis were published in [4]. The PRBS signal used to modulate sensor temperature and a typical transient response of micro-hotplate gas sensor in the presence of 2 ppm of NO<sub>2</sub> are shown in Figure 5.13. The analysis was conducted as follows: at first, the steady-state response (i.e. when the sensors were operated at a fixed temperature) was studied. Then, the transient response of the temperature modulated micro-hotplates was studied.

#### 6.3.1. Steady-state response.

The static response was defined as the normalized resistance change

$$\frac{\Delta R}{R_o} = \frac{R - R_o}{R_o} \quad (6.2)$$

where R<sub>o</sub> is the baseline resistance (i.e. in the presence of dry air) and R is the steady-state resistance of the sensor in the presence of a given gas. Table 6.3 summarizes the static responses of the four micro-hotplate sensors studied to NO<sub>2</sub> and NH<sub>3</sub> at two different operating temperatures. The static response to NO<sub>2</sub> is positive because tungsten oxide behaves as an n-type semiconductor (i.e. increases its resistance in the presence of an oxidizing species). On the other hand, the static response to NH<sub>3</sub> is negative since ammonia

Improving the performance of micro-machined metal oxide gas sensors:  
 Optimization of the temperature modulation mode via pseudo-random sequences.

is a reducing species. It is the oxidizing and reducing nature of  $\text{NO}_2$  and  $\text{NH}_3$ , respectively what makes especially difficult to discriminate and quantify mixtures of these species using the steady-state sensor response only [5, 6].

**Table 6.3:** Response ( $\Delta R/R_0$ ) of the micro-hotplate sensors to different concentrations of  $\text{NO}_2$  and  $\text{NH}_3$  at two operating temperatures. S1 and S3 are sensors with 100  $\mu\text{m}$  electrode spacing that are based on micro and nano-particle  $\text{WO}_3$ , respectively. S2 and S4 are sensors with 50  $\mu\text{m}$  electrode spacing that are based on micro and nano-particle  $\text{WO}_3$ , respectively.

Sensor	Working temperature ( $^{\circ}\text{C}$ )	$\text{NO}_2$ (ppm)			$\text{NH}_3$ (ppm)		
		0.5	1	2	100	500	1000
S1	200	2.13	3.00	4.26	-0.070	-0.787	-0.886
	400	0.01	0.70	1.68	-0.373	-0.849	-0.957
S2	200	3.37	5.35	5.29	-0.015	-0.749	-0.850
	400	0.31	1.65	2.22	-0.190	-0.796	-0.942
S3	200	2.51	3.88	5.95	-0.338	-0.809	-0.865
	400	0.13	1.07	2.54	-0.592	-0.909	-0.965
S4	200	3.45	6.74	7.30	-0.145	-0.776	-0.818
	400	0.33	2.23	3.25	-0.449	-0.880	-0.953

Once the steady state response had been analyzed, the transient response of the gas sensors caused by the modulation of their operating temperature was studied. The process to obtain the optimal modulation frequencies for a given sensor and target gases needs two steps:

- In the first step, an estimate of the impulse response of the sensor in the presence of each gas or mixture is computed. An estimate of the impulse response is obtained for every measurement and the spectral components of the impulse response are computed via the FFT (this step is described in sub-section 6.3.2).
- In the second step, it is necessary to select the subset of spectral components that carry important information to discriminate and/or quantify the target gases. This subset of spectral components is the set of optimal modulation frequencies (this step is described in sub-section 6.3.3).

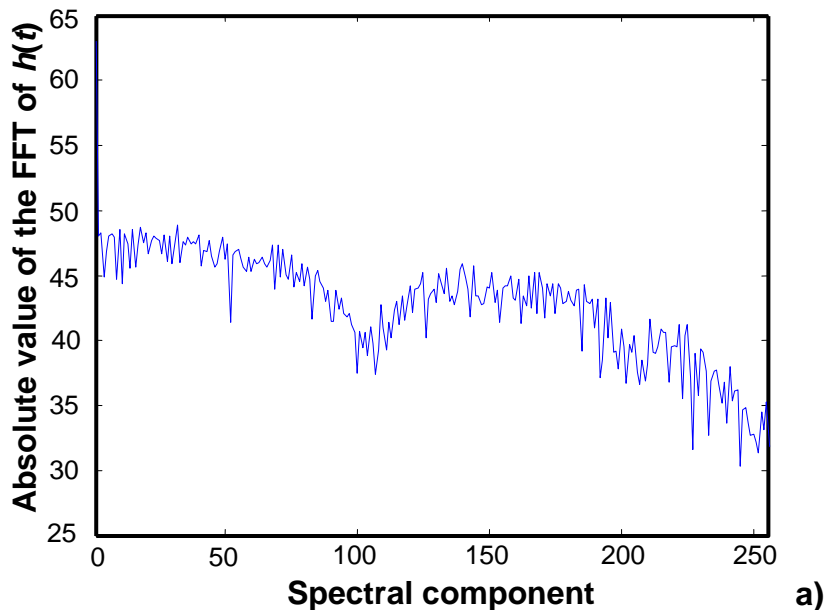
### 6.3.2. Estimation of the impulse response.

The database described in sub-section 5.4.2 in chapter 5 was used for this purpose. This database consisted of 45 measurements. An estimate of the impulse response,  $\hat{h}(n)$ , of each



sensor in the presence of the gases and gas mixtures studied was computed through the circular cross-correlation between one period ( $L = 511$  samples) of the PRBS signal,  $x(n)$ , and one period of the sensor response (i.e. resistance transient),  $y(n)$ . Since the clock frequency of the PRBS sequence was set to  $f_c = 2$  Hz and the sampling rate of the acquisition system was set to 10 Hz, the sequences had to be decimated by 5 before the cross-correlation was computed. The module of the Fast Fourier Transform (FFT) of the impulse response estimate was calculated and, stored for further processing. This was done to study which spectral components contain important information for the identification and quantification of gases. Figure 6.3 shows the module of the FFT of the impulse responses of a tungsten oxide micro-hotplate sensor in the presence of ammonia, nitrogen dioxide and an ammonia and nitrogen dioxide mixture. Figure 6.3 shows that differences exist between these spectra when the sensor is in the presence of different gases.

In the next step, a variable selection method was implemented to identify those spectral components that carry important information for the discrimination and quantification of the pollutant gases studied. The number of spectral components available is 255, which corresponds to half the length of the PRBS ( $L/2$ ). Two consecutive spectral components are separated by the spectral resolution,  $f_c/L$  (i.e.  $2/511$  Hz = 3.91 mHz). Spectral components can be related to a specific temperature-modulation frequency using the expression (6.1).



Improving the performance of micro-machined metal oxide gas sensors:  
Optimization of the temperature modulation mode via pseudo-random sequences.

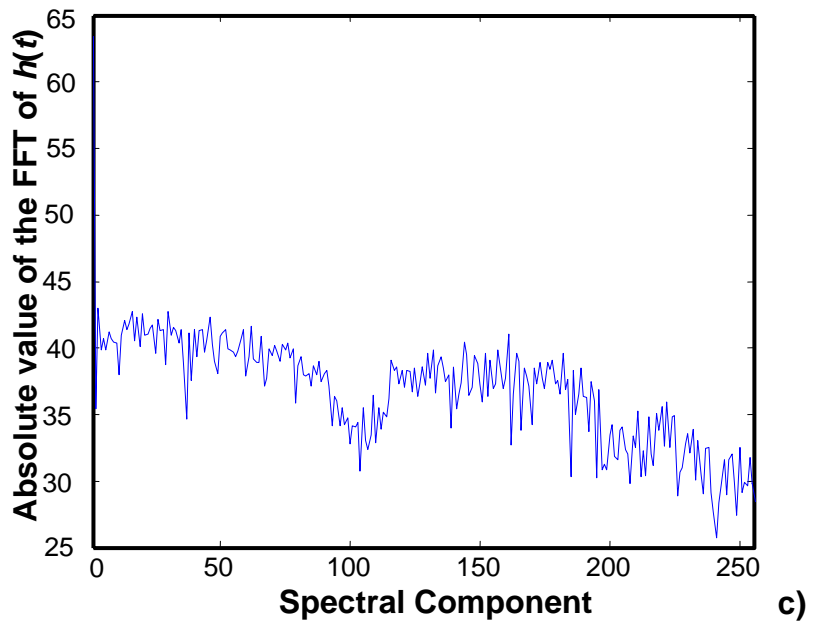
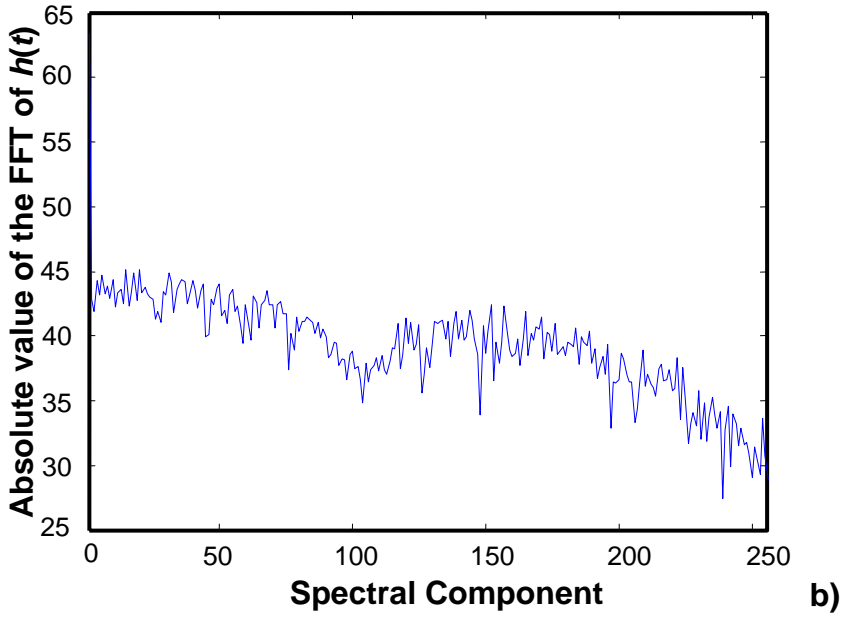


**Figure 6.3:** Module of the FFT of the impulse response estimate of a tungsten oxide micro-hotplate sensor in: a) NH<sub>3</sub> (1000 ppm), b) NO<sub>2</sub> (2 ppm ) and c) NH<sub>3</sub> (1000 ppm) + NO<sub>2</sub> (2 ppm).

Therefore, by identifying a subset of spectral components, a subset of temperature modulating frequencies to correctly discriminate and quantify the gases studied can be identified. The search technique used is discussed in the follow sub-section.

### 6.3.3. Variable selection procedure.

Once again, a simple variable selection procedure was implemented to select among the spectral components (i.e. the temperature-modulating frequencies) of the estimated impulse responses of the sensors.

For gas identification purposes, the measurements were grouped in 3 categories (i.e., ammonia, nitrogen dioxide and gas mixture). For quantification purposes, three specific models were built (one per species or mixture). Therefore, for every quantification model, the measurements were grouped in 3 categories (e.g. gas or gas mixture  $\times$  3 concentrations). For each spectral component, intra-group and between-group variances were computed (see sub-section 3.4 in chapter 3). A figure of merit for the resolution power, ( $RP$ ), of a spectral component (i.e, the ratio between the inter-category variance and the intra-category variance) was calculated. Therefore, a small set of spectral components (i.e., those that have the higher figure of merit) were selected. These spectral components correspond to the temperature-modulating frequencies that lead to a better discrimination or quantification of the gases studied.

### 6.3.4. Qualitative gas analysis.

Four integrated micro-sensors were used in this study. These consisted of a micro-particle tungsten oxide deposited onto either wide gap or narrow gap interdigitated electrodes (sensors labeled 1 and 2, respectively) and a nano-particle tungsten oxide deposited onto either wide gap or narrow gap interdigitated electrodes (sensors labeled 3 and 4, respectively).

In the first step, the selection of the optimal set of temperature-modulating frequencies to discriminate between the different gases and gas mixtures was envisaged. For every micro-sensor, those spectral components from the impulse response in the presence of the gases studied that had a high figure of merit (see eq. 3.20) were selected. Four matrices (one per sensor) were formed, which contained as number of rows the number of measurements performed (i.e. 45) and as number of columns the number of selected spectral components. Therefore, every element in these matrices corresponded to the value of a selected spectral component of the impulse response estimate for a given gas-sensor pair. These matrices were used to build and validate fuzzy ARTMAP classifiers to see whether it was possible to

Improving the performance of micro-machined metal oxide gas sensors:  
 Optimization of the temperature modulation mode via pseudo-random sequences.

correctly identify the gases. A cross-validation of order one (i.e. a leave-one-out cross-validation) was implemented to estimate the success rates. Given  $n$  measurements, the classifiers were trained  $n$  times using  $n-1$  training vectors. The vector left out during the training phase (i.e. unseen by the fuzzy ARTMAP classifier) was then used for testing. The performance of a given classifier was estimated as the averaged performance over the  $n$  tests. More details about the building and validation of fuzzy ARTMAP classifiers can be found in [2, 3] and references therein. The results of this analysis are summarized in Table 6.4. For each sensor studied, the success rates in gas identification are specified for  $\text{NH}_3$ ,  $\text{NO}_2$  and their mixtures. Finally, overall success rates are also given.

**Table 6.4:** Frequencies selected (with high factor of merit for gas identification) for the different sensors studied and success rate in gas identification using a fuzzy ARTMAP classifier.

Sensor no.	1	2	3	4
Frequencies selected (Hz)	0.919 0.938	0.188 0.403	0.168 0.399 0.743 0.797	0.188 0.328
$\text{NH}_3$ identification (%)	100	100	100	100
$\text{NO}_2$ identification (%)	86.67	80	93.33	73.33
$\text{NH}_3 + \text{NO}_2$ identification (%)	60	73.33	86.66	66.66
Overall success rate (%)	82.23	84.45	93.33	80

Through the selection of information from up to 4 modulating frequencies, the gas identification rate using a single sensor varied between 80 and 93.33%. For example, a 93.33% identification rate was reached with sensor 3 when the modulation frequencies of 168, 399, 743 and 797 mHz where used. While  $\text{NH}_3$  samples could be perfectly discriminated, confusions occurred between samples of  $\text{NO}_2$  and  $\text{NO}_2 + \text{NH}_3$  mixtures. Increasing the number of modulating frequencies used did not improve these results.

The gas identification rate of the fuzzy ARTMAP classifier increased up to 95.56% when information from different sensors was combined. For example, when sensors 1, 3 and 4 were combined, the modulating frequencies selected were 168, 188, 328, 399, 743, 797, 919 and 938 mHz. These results are shown in Table 6.5.

**Table 6.5:** Success rate in gas identification when the information from different sensors is combined using a fuzzy ARTMAP classifier.

Sensor no.	1-3-4	3-4	1-4	2-4
Identification success rate (%)	95.56	93.34	91.12	91.12

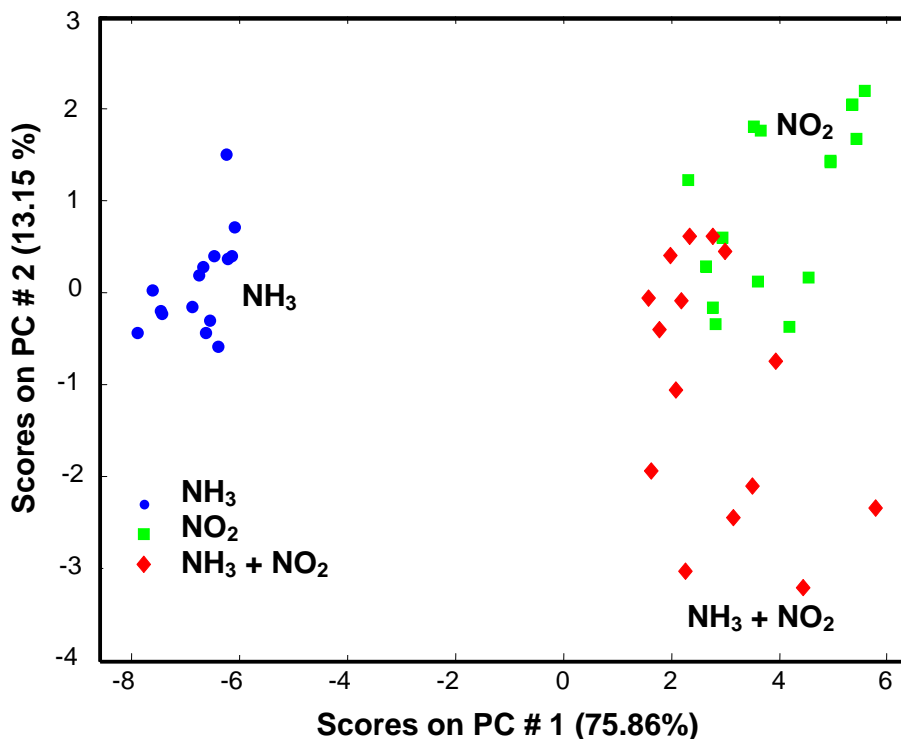


**Figure 6.4:** Results of a PCA performed by fusing information from sensors 1, 3 and 4. While NH<sub>3</sub> samples are well discriminated no matter their concentration, some overlapping exists between samples of the lowest NO<sub>2</sub> and NO<sub>2</sub>+NH<sub>3</sub> concentrations.

A principal component analysis (PCA) was performed on the data matrix resulting from the fusion of data from sensors 1, 3 and 4 (see Table 6.5). The score plot on the first two principal components is shown in Figure 6.4. The first two PCs captured more than 89% of data variance. While the cluster of ammonia samples is well apart from the other samples, some overlapping exists between the clusters for nitrogen dioxide and for the mixtures. These results are in agreement with the ones from the fuzzy ARTMAP classifier.

Improving the performance of micro-machined metal oxide gas sensors:  
 Optimization of the temperature modulation mode via pseudo-random sequences.

### 6.3.5. Semi-quantitative gas analysis.

In the second step the selection of the optimal set of temperature-modulating frequencies to quantify the different gases and gas mixtures was envisaged. By an equivalent procedure to the one described above, for every micro-sensor, the spectral components that had a high figure of merit for solving the quantification problem were selected to form the data matrices. Since specific quantification models were built (i.e. for NH<sub>3</sub>, NO<sub>2</sub> and their mixtures), for each micro-sensor 3 data matrices were formed. Once again, fuzzy ARTMAP classifiers were built and cross-validated (using the leave-one-out approach) to estimate the success rate in gas quantification.

**Table 6.6:** Frequencies selected (with high factor of merit for gas quantification) for the different sensors studied and success rate in gas quantification using a fuzzy ARTMAP classifier.

Gases		1	2	3	4
NH <sub>3</sub>	Frequencies selected (Hz)	0.950	0.070 0.188 0.234 0.789 0.950 0.993	0.188	0.789 0.950
	Quantification success rate (%)	100	100	87	100
	NO <sub>2</sub>	Frequencies selected (Hz)	0.445	0.797	0.797
	Quantification success rate (%)	93.33	100	93.33	100
NH <sub>3</sub> + NO <sub>2</sub>	Frequencies selected (Hz)	0.845	0.446 0.594 0.797 0.845	0.489 0.685	0.063 0.410 0.716 0.845
	Quantification success rate (%)	100	100	100	100

The results are summarized in Table 6.6, which shows that the concentration of the different gases and mixtures can be identified with a 100% success rate, even using a single sensor. For example, the gases and mixtures could be quantified by using sensor 1 and the following modulating frequencies: 445, 845 and 950 mHz. Increasing the number of modulating frequencies used beyond those reported in Table 6.6, did not improve the results.

Modulating the working temperature of metal oxide sensors results in a periodical heating and cooling of the gas sensitive surface, which alters the kinetics of the diffusion and reaction processes that characterize the gas-sensor interaction. From results shown in Table

6.6 it can be derived that, for a given gas, many sensors share some of the temperature-modulating frequencies selected. Since all the sensors studied are based on tungsten oxide, these frequencies might be characteristic of the interaction between tungsten oxide and the gas considered. Finally, the differences in the modulating frequencies selected for different sensors are due to their different electrode geometry and sensing films with different microstructure.

## 6.4. Conclusions.

In the last years, different authors have shown that more selectivity can be conferred to metal oxide gas sensors by modulating their operating temperature. However, the choice of the frequencies used to modulate the sensors' temperature for a given gas analysis application remained a non-systematic process.

In this chapter a method to systematically determine the optimal set of modulating frequencies to solve a given gas analysis application was introduced for the first time. Maximum-length Pseudo Random Sequences (PRBS) are used to modulate the working temperature of metal oxide gas sensors. Studying the transient response of the sensors, the modulating frequencies that should be used to discriminate and quantify gases are obtained in a systematic way.

The method was demonstrated by obtaining the impulse response of integrated micro-arrays of either sputtered or screen-printed  $\text{WO}_3$  in the presence of pollutant gases. It is shown that with this method it was possible to discriminate between three different types of gases. In this case we applied this method to discriminate and semi-quantify three different concentrations of  $\text{NO}_2$  and dry air (within experiment 1) with high accuracy and to discriminate and quantify between three different  $\text{NH}_3$ ,  $\text{NO}_2$  and their binary mixtures gas concentration diluted in synthetic dry air. Good results in the identification (95.55%) and quantification (100%) of the gases studied were reached (in experiment 2).

Finally, to determine the frequency range to be studied, the cutoff frequency of the membrane was determined. This was done studying the thermal response of the micro-sensor heating element. Therefrom the value of  $f_c$  and the length of the PRBS were determined and then the frequency resolution  $f_c/L$  was estimated.

For each gas-sensor pair, the modulating frequencies selected are related to characterize the interaction between the metal oxide layer and the gas (e.g. film microstructure, surface diffusion and reaction kinetics).

Improving the performance of micro-machined metal oxide gas sensors:  
Optimization of the temperature modulation mode via pseudo-random sequences.

## 6.5. References.

- [1] A. Vergara, E. Llobet, J. Brezmes, M. Stankova, P. Ivanov, X. Correig, I. Gràcia, C. Cané, X. Correig, “MLS based temperature modulation of micro-hotplates”, Book of Abstracts of IEEE Sensors 2003, Toronto, Canada, pp.1255-1259, October 2003.
- [2] G. Carpenter, S.Grossberg, N. Markuzon, J. Reynolds, and D. Rosen, “Fuzzy ARTMAP: A neural network architecture for incremental supervised learning of analog multidimensional maps”, IEEE Trans. Neural Nets., vol. 3, (5), pp. 698-713, 1992.
- [3] R. Ionescu, E. Llobet, X. Vilanova, J. Brezmes, J.E. Suerias, J. Calderer, X. Correig, “Quantitative analysis of NO<sub>2</sub> in the presence of CO using a single tungsten oxide semiconductor sensor and dynamic signal processing”, Analyst, vol. 127, pp. 1237-1246, 2002.
- [4] A. Vergara, E. Llobet, J. Brezmes, P. Ivanov, X. Vilanova I. Gràcia, C. Cané and X. Correig, “Optimized temperature modulation of micro-hotplate gas sensors through pseudorandom binary sequences”, IEEE Sensor Journal, vol. 5, (6), pp. 1369-1378, 2005.
- [5] E. Llobet, R. Ionescu, S. Al-Khalifa, J. Brezmes, X. Vilanova, X. Correig, N. Bârsan, J.W. Gardner, “Multicomponent gas mixture analysis using a single tin oxide sensor and dynamic pattern recognition”, IEEE Sensors Journal, vol. 1, pp. 207-213, 2001.



---

# 7.

# Gas analysis using MLPRS

---

<b>7. GAS ANALYSIS USING MLPRS</b>	<b>157</b>
<b>7.1. Introduction.</b>	<b>159</b>
<b>7.2. Analysis of the data from experiment 3: Optimized Temperature Modulation of Metal Oxide Micro-Hotplate Gas Sensors through Multilevel Pseudo Random Sequences (MLPRS).</b>	<b>160</b>
7.2.1. Estimation of the impulse response and selection of temperature modulating frequencies.	161
7.2.1.1. Estimation of the impulse response.	161
7.2.1.2. Variable selection procedure.	163
7.2.2. Optimization for qualitative gas analysis.	163
7.2.2.1. Identification of the best modulating frequencies.	164
7.2.2.2. Validation of the modulating frequencies.	164
7.2.3. Optimization for quantitative gas analysis.	165
7.2.4. Gas analysis using a sinusoidal temperature modulation.	167
7.2.5. Steady-state response.	170
7.2.6. Gas analysis of metal oxide gas sensors using dynamic moments combined with temperature modulation.	172
7.2.6.1. MLPRS temperature modulation database.	172
7.2.6.2. Multi-sinusoidal modulation database.	175

Improving the performance of micro-machined metal oxide gas sensors:  
Optimization of the temperature modulation mode via pseudo-random sequences.

<b>7.3. Analysis of the data from experiment 4: Qualitative and Quantitative gas mixture analysis using temperature-modulated micro-hotplate gas sensors: Selection and validation of the optimal modulating frequencies.</b>	<b>178</b>
7.3.1. Spectral analysis of the impulse response estimates.	179
7.3.2. Selection of the temperature-modulating frequencies.	181
7.3.3. Optimization for qualitative gas analysis.	181
7.3.4. Optimization for quantitative gas analysis.	184
7.3.5. Gas analysis using multi-sinusoidal temperature modulation.	187
7.3.6. Steady-state response.	193
<b>7.4. Conclusions.</b>	<b>194</b>
<b>7.5. References.</b>	<b>196</b>

## 7.1. Introduction.

In the works reported in chapter 6, a systematic method to choose the modulation frequencies of micro-hotplate gas-sensors based on pseudo-random binary sequences of maximum length was used. Since these signals have a flat power spectrum (i.e. like white noise) in a wide frequency range, an estimate of the impulse response of each gas-sensor pair can be computed by the cross-correlation of excitatory and response sequences. Studying the impulse response estimates, the set of modulating frequencies that are useful to discriminate between different gases and to estimate gas concentration, is obtained in a systematic way. In this chapter, an evolved method to modulate the working temperature of metal oxide micro-hotplate gas sensors in a wide frequency range is presented, but this time based on maximum length multilevel pseudo random sequences. One of the main reasons for considering multilevel signals instead of binary signals is that the former can provide a better estimate than the latter of the linear dynamics of a process with non-linearities. And it is well known that temperature-modulated metal oxide gas sensors present non-linearity in their response. The method described in this chapter enables each gas-sensor system to be identified and to find, in a systematic way, a reduced set of modulation frequencies that are important to discriminate between different gases and to estimate gas concentration. Its usefulness is demonstrated in two experiments in this chapter:

The first experiment is assessed by the analysis of different concentrations of ammonia and nitrogen dioxide using tungsten oxide based micro-hotplate gas sensors.

The second experiment further develops and fully validates the method for optimizing the choice of temperature modulating frequencies. The problem envisaged to illustrate the process is the building of calibration models for the analysis of acetaldehyde, ethylene, ammonia and their binary mixtures using metal oxide micro-hotplate gas sensors. These species were chosen, since the first two are related to the quality of climacteric fruit during cold storage and the third one reveals the occurrence of a leak in the refrigeration system.

In both experiments the impulse response estimate is computed. Therefrom the module of the Fast Fourier Transform (FFT) of the impulse response estimate is calculated. By a variable selection method the set of the optimal spectral components are selected. These features (spectral components) extracted corresponds to the frequencies that will be used in the qualitative and quantitative analysis of the gases studied. For this, both, linear statistical and neural networks pattern recognition methods are used.

Improving the performance of micro-machined metal oxide gas sensors:  
Optimization of the temperature modulation mode via pseudo-random sequences.

## **7.2. Analysis of the data from experiment 3: Optimized Temperature Modulation of Metal Oxide Micro-Hotplate Gas Sensors through Multilevel Pseudo Random Sequences (MLPRS).**

In this section the analysis of the data from *Experiment 3* is carried out. In this experiment, an evolved method, based on the use of multi-level maximum length pseudo random sequences (MLPRS), to select and determine the optimal set of frequencies used to modulate the working temperature of metal oxide micro-hotplate gas sensors in a wide frequency range is presented.

Vapors at three different concentrations of  $\text{NO}_2$  (0.5, 1, 2 ppm),  $\text{NH}_3$  (100, 500, 1000 ppm) and their binary mixtures (0.5 + 100, 1 + 500, 2 + 1000 ppm of  $\text{NO}_2$  and  $\text{NH}_3$ , respectively) diluted in dry air were measured by a continuous flow system. Measurements were performed at the Universitat Rovira i Virgili, in Tarragona Spain [1], using five tungsten oxide micro-hotplate gas sensors. The experimental set-up was described in chapter 5.

The gas analysis was as follows: At first, these species were qualitatively and quantitatively analyzed considering the transient response of the temperature modulation of the micro-hotplates through the MLPRS signal. Therefore, once the optimal set of modulating frequencies has been selected, new measurements of the different species and concentrations studied were performed using the same sensors. This time the sensors' temperature was modulated using a multi-frequency sinusoidal signal at the frequencies obtained during the optimization procedure. Finally, the databases generated (i.e., the ones generated using MLPRS signals or the multi-frequency sinusoidal signal), are used to introduce a novel feature extraction method to analyze them. The so-called Dynamic Moments (DM) and phase space (PS) as a feature extraction method combined with the characteristics given by the thermal modulation of the micro-sensors was introduced and compared with the results obtained using only the transient response of temperature modulation. Additionally, all results obtained were compared against the ones obtained when the traditional steady-state sensor response (i.e. when the sensors were operated at a fixed temperature) was used.

## 7.2.1. Estimation of the impulse response and selection of temperature modulating frequencies.

Five micro-sensors were used in this study. These consisted of a nano-particle tungsten oxide deposited onto either wide gap (sensors labeled 1 and 3) or narrow gap interdigitated electrodes (sensor labeled 2) and a nano-particle tungsten oxide deposited onto either wide gap or narrow gap interdigitated electrodes (sensors labeled 4 and 5, respectively). As was mentioned in the experimental section (see Chapter 5)  $\text{NO}_2$ ,  $\text{NH}_3$  and their binary mixtures at three different concentrations were measured while the sensors' temperature was modulated by a MLPRS signal. Each measurement was replicated 8 times (which gave a total of 72 measurements). Every measurement took approximately 5 minutes to complete, which corresponded to the acquisition of 1 sequence of length 624 generated with a clock frequency of 2 Hz. The sampling frequency was set to 10 Hz. The MLPRS signal used to modulate the temperature of the sensors and a typical transient response of a micro-hotplate gas sensor in the presence of 2 ppm of  $\text{NO}_2$  are shown in Figure 5.14.

Therefrom, the process to obtain the optimal modulation frequencies for a given sensor and target gases is performed. As already discussed, this process consists in two steps:

- In the first step, an estimate of the impulse response of the sensor in the presence of each gas or mixture has to be computed.
- In the second step, a variable selection method is implemented to identify those spectral components that carry important information for the discrimination and quantification of the pollutant gases studied.

### 7.2.1.1. Estimation of the impulse response.

For each measurement performed and gas sensor an impulse response estimate,  $\hat{h}(n)$ , was computed via the circular cross-correlation of the input MLPRS signal  $x(n)$  and the sensor response signal  $y(n)$ , (see sub-section 6.2.1 in chapter 6). Therefore, the absolute value of the fast Fourier transform (FFT) of the impulse response estimate  $\hat{h}(n)$  was calculated and stored for further processing. This was done to study which spectral components contain important information for the identification and quantification of gases. Figure 7.1 shows the absolute value of the spectral components within the impulse response estimates of a  $\text{WO}_3$  micro-hotplate gas sensor in the presence of the species analyzed. Therefrom, a method to identify these spectral components is implemented.

Improving the performance of micro-machined metal oxide gas sensors:  
Optimization of the temperature modulation mode via pseudo-random sequences.

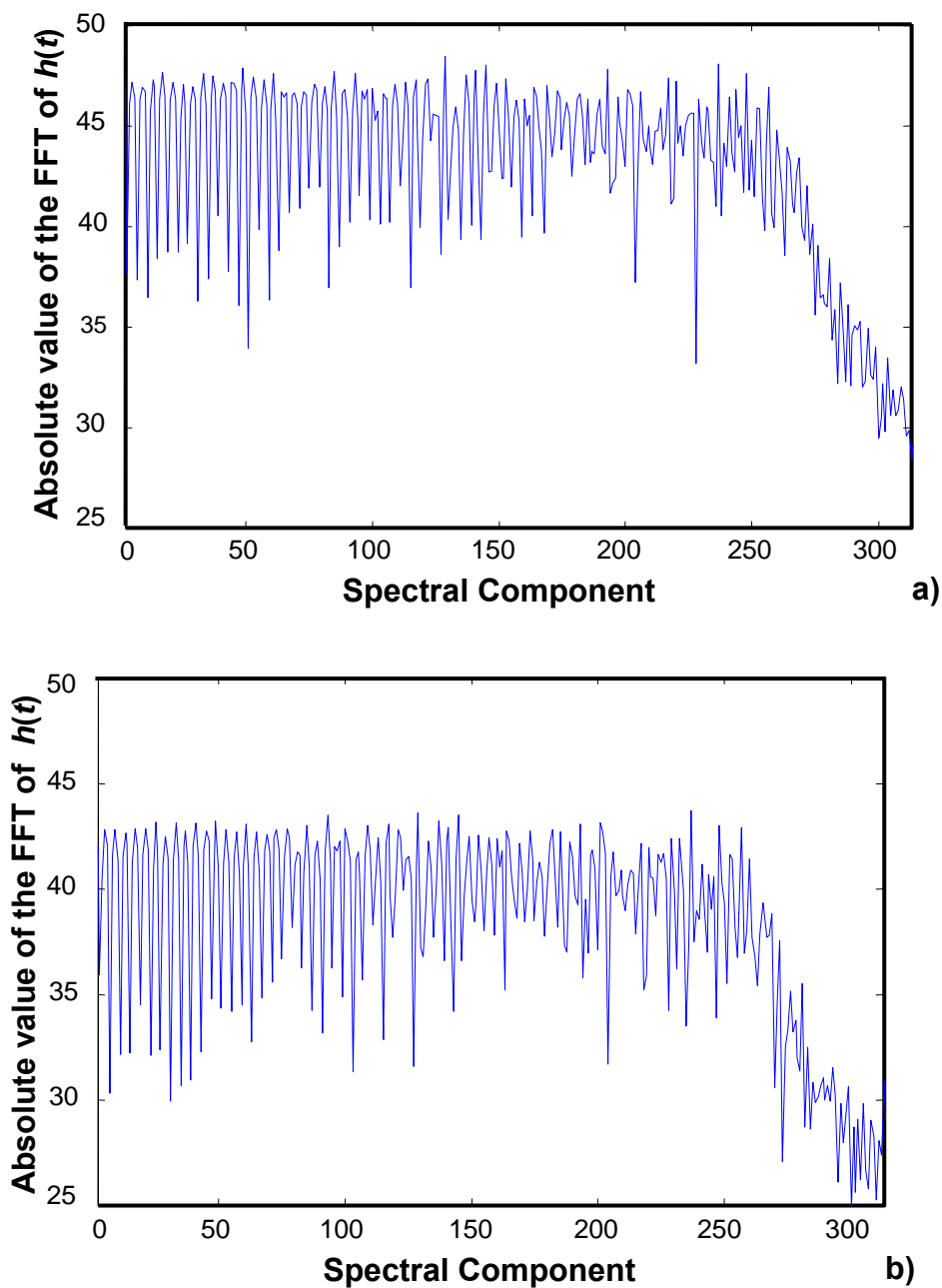


**Figure 7.1:** Absolute value of the FFT of  $h(t)$  for a temperature modulated, screen-printed  $\text{WO}_3$  micro-hotplate sensor in the presence of 1000 ppm  $\text{NH}_3$  (a) and 2 ppm  $\text{NO}_2$  (b).

### 7.2.1.2. Variable selection procedure.

In the next step, a variable selection method was implemented to identify those spectral components that carry important information for the discrimination and quantification of the pollutant gases studied. Before this variable selection method is implemented, 5 of the 8 replicate measurements available were selected to be part of the variable selection data matrices (there was one matrix per sensor). Therefore, these matrices gathered together 45 measurements (i.e. 9 different measurements  $\times$  5 replicates). The remaining 27 measurements integrated the validation data matrices.

Once the selection and validation matrices have been separated, the selection of the optimal set of temperature-modulating frequencies to discriminate between the different species and mixtures was envisaged. The number of spectral components available is 312, which corresponds to half the length of the MLPRS ( $L/2$ ). Two consecutive spectral components are separated by the spectral resolution,  $f_c/L$  (i.e.  $2/624$  Hz = 3.20 mHz). Spectral components can be related to a specific temperature-modulation frequency using the expression (6.1) shown in chapter 6 subsection 6.2.1.

For gas identification purposes, the measurements were grouped in three categories, (i.e., ammonia, nitrogen dioxide and gas mixture measurements). For quantification purposes, three specific models were built (one per species or mixture). Therefore, for every quantification model, the measurements were grouped in 3 categories (e.g. gas or gas mixture  $\times$  3 concentrations). And the process was conducted as already explained in subsection 3.4 in Chapter 3.

### 7.2.2. Optimization for qualitative gas analysis.

Once the spectral components with high figure of merit had been identified, five matrices (one per sensor) were formed. Every element in these matrices corresponded to the value of a selected spectral component of the impulse response estimate for a given gas-sensor pair. These matrices were used to build and validate fuzzy ARTMAP classifiers to see whether it was possible to correctly identify the gases. Details about the building and validation of fuzzy ARTMAP classifiers can be found in [2, 3] and references therein. A cross-validation of order one (i.e. a leave-one-out cross-validation) was implemented to estimate the success rates.

Improving the performance of micro-machined metal oxide gas sensors:  
 Optimization of the temperature modulation mode via pseudo-random sequences.

### 7.2.2.1. Identification of the best modulating frequencies.

Given the 45 measurements used in the variable selection step, the classifiers were trained 45 times using 44 training vectors. The vector left out during the training phase (i.e. unseen by the fuzzy ARTMAP classifier) was then used for testing. The performance of a given classifier was estimated as the averaged performance over the 45 tests. The results of this analysis are summarized in Table 7.1. Through the selection of information from up to 4 modulating frequencies, the gas identification rate using a single sensor varied between 77.78% and 97.78%. For example, a 97.78% identification rate was reached with sensor 1 when the modulation frequencies of 39, 538 and 827 mHz where used. While NH<sub>3</sub> samples could be perfectly discriminated, confusions occurred between samples of NO<sub>2</sub> and NO<sub>2</sub> + NH<sub>3</sub> mixtures. Increasing the number of modulating frequencies used did not improve these results.

**Table 7.1:** Frequencies selected (with high factor of merit for gas identification) for the different sensors studied and success rate in gas identification using a fuzzy ARTMAP classifier (results using a leave-one-out cross-validation on the variable selection data set).

Sensor no.	1	2	3	4	5
Frequencies selected (Hz)	0.039 0.538 0.827	0.0032 0.4807 0.5192 0.6987	0.173 0.429 0.814	0.397 0.743	0.141 0.144
Identification success rate (%)	97.78	84.45	77.78	80	80

### 7.2.2.2. Validation of the modulating frequencies.

A further validation of these results was envisaged as follows. For each sensor, a fuzzy ARTMAP classifier was trained using the 45 measurements available in the variable selection data set. Then, the 27 measurements in the validation data set —these measurements were not used to select the modulation frequencies and are completely new for the classifier— were input to the trained classifier, which produced a classification result. The spectral components input to the neural network classifier were those that had been selected previously (i.e., using the variable selection data set). The results of this validation are shown in Table 7.2. Exception made of sensor 2, the identification success rates obtained with the validation data set remain quite similar to the ones obtained with the variable selection data set. This proves that the variable selection process leads to the selection of the



modulating frequencies that help discriminating among the species considered. Identification performance remains high, e.g. 88.88% when sensor 1 was used.

**Table 7.2:** Success rate in gas identification by a fuzzy ARTMAP classifier (using the 27-measurement validation data set) for the different sensors studied and the frequencies selected previously (shown in **Table 7.1**).

Sensor no.	1	2	3	4	5
Identification success rate (%)	88.88	63	77.78	85.20	77.78

Considering the results globally, there was a small decrease in the identification performance when the validation data set was used. This is not surprising: using the same set of measurements to select among the different modulating frequencies and to estimate the performance of the classifier (i.e., using the variable selection data set only) leads to an optimistic estimate of the true identification success rate.

### 7.2.3. Optimization for quantitative gas analysis.

In the second step the selection of the optimal set of temperature-modulating frequencies to quantify the different gases and gas mixtures was envisaged. By an equivalent procedure to the one described above, for every microsensor, the spectral components that had a high figure of merit for solving the quantification problem were selected to form the data matrices. Once again, this procedure was conducted on the variable selection data set. Since specific quantification models were built (i.e. for  $\text{NH}_3$ ,  $\text{NO}_2$  and their mixtures), for each microsensor 3 data matrices were formed. Each matrix had 15 rows, which corresponded to 5 replicate measurements of a given species at 3 different concentrations. Once again, fuzzy ARTMAP classifiers were built and cross-validated (using the leave-one-out approach) to estimate the success rate in gas quantification. The results are summarized in Table 7.3, which shows that the concentration of the different gases and mixtures can be identified with a success rate near 90%, even using a single sensor. Increasing the number of modulating frequencies used beyond those reported in Table 7.3, did not improve results.

Using a similar procedure as the one described above, another estimate of the success rate in quantification was obtained by validating the fuzzy ARTMAP classifiers using measurements from the validation data set. The results of this validation are shown in Table 7.4. The values of the success in quantifying samples from the validation data set are significantly lower than the success rate estimated from the variable selection data set. This

Improving the performance of micro-machined metal oxide gas sensors:  
 Optimization of the temperature modulation mode via pseudo-random sequences.

can be due to the scarce number of measurements (15) that are available to train the neural networks for quantification.

**Table 7.3:** Frequencies selected (with high factor of merit for gas quantification) for the different sensors studied and success rate in gas quantification using a fuzzy ARTMAP classifier.

Gases		1	2	3	4	5
NH <sub>3</sub>	Frequencies selected (Hz)	0.051	0.006	0.019	0.012	0.108
		0.169	0.108	0.935	0.051	0.394
		0.394	0.974		0.394	0.471
		0.557	0.987		0.660	0.660
		0.660	0.996		0.820	0.900
		0.820	1.000		0.900	
		0.900			0.987	
	0.987			0.996		
Quantification success rate (%)	80	60	60	87	67	
NO <sub>2</sub>	Frequencies selected (Hz)	0.153	0.413	0.198	0.695	0.153
		0.897	0.592	0.884		0.192
	Quantification success rate (%)	80	93.33	80	87	73.33
NH <sub>3</sub> + NO <sub>2</sub>	Frequencies selected (Hz)	0.217	0.0032	0.035	0.791	0.269
			0.8717	0.044	0.942	0.791
			0.8910	0.637	0.977	
			0.9775	0.907	0.980	
			0.9807		0.983	
			0.9903		0.990	
					0.993	
	Quantification success rate (%)	93.33	93.33	73.33	66.66	93.33

**Table 7.4:** Success rate in gas quantification (%) by a fuzzy ARTMAP classifier (using the 27-measurement validation data set) for the different sensors studied and the frequencies selected previously (shown in **Table 7.3**).

Gases↓ Sensors→	1	2	3	4	5
NH <sub>3</sub>	67	56	45	45	45
NO <sub>2</sub>	45	56	78	45	45
NH <sub>3</sub> + NO <sub>2</sub>	45	67	56	56	56

## 7.2.4. Gas analysis using a sinusoidal temperature modulation.

This study aims both at showing the actual operation of temperature modulated sensors after their optimal modulation procedure had been studied and at estimating their performance in the gas analysis application considered. New measurements of the different species and concentrations studied were performed using the same sensors (5 replicate measurements per species and concentration, which gave a total of 45 new measurements). The sensors had their operating temperature modulated by a signal resulting from the sum of 5 sinusoids of identical amplitude. These frequencies corresponded, one per sensor, to the best modulating frequencies for gas recognition, identified by the frequency selection and validation procedures. In other words, a single modulating frequency is selected per sensor, the one that had a higher figure of merit for gas identification. The selected frequencies are 39,0 mHz (sensor 1), 480.7 mHz (sensor 2), 429.0 mHz (sensor 3), 743.0 mHz (sensor 4) and 141.0 mHz (sensor 5). The procedure of generating the multi-sinusoidal signal is illustrated in Figure 7.2, while in Figure 7.3 a fragment of this signal generated is shown.

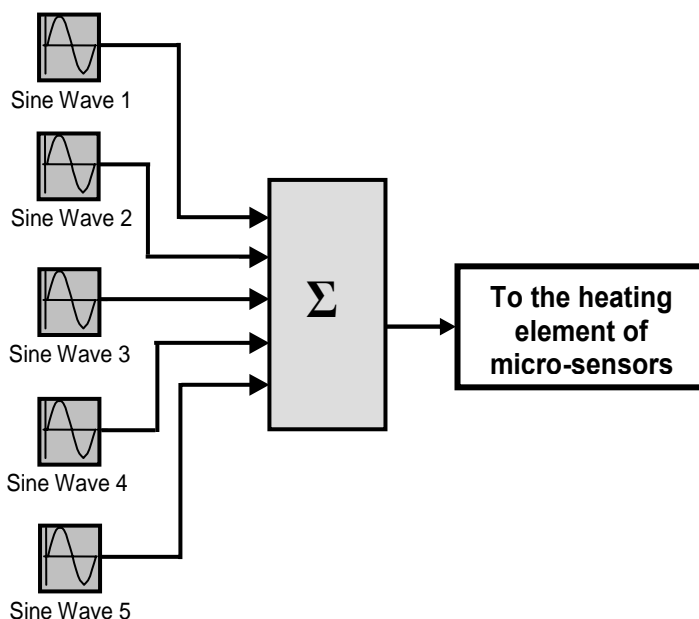


**Figure 7.2:** Set up used to generate a multi-sinusoidal signal, consisting of the sum of 5 sinusoids of identical amplitudes and different frequencies, that is applied to the heating element of the 5 micro-sensors studied.

### Improving the performance of micro-machined metal oxide gas sensors: Optimization of the temperature modulation mode via pseudo-random sequences.

The response signals of the temperature modulated microsensors in the presence of the different gases studied were obtained and processed as follows. The absolute value of the FFT was computed and the values of the d.c. component and the 5 harmonics corresponding to the modulating frequencies were extracted. Figure 7.4 shows the FFT spectra of the transient response of a sensor in the presence of  $\text{NH}_3$  (1000 ppm),  $\text{NO}_2$  (2 ppm) and a mixture (1000 ppm + 2 ppm) where different among the different species measured can be shown. Therefore, from each measurement, 6 features were extracted and used to build a fuzzy ARTMAP classifier aimed at discriminating between the different species measured. The classifier was cross-validated using a leave-one-out approach and results are summarized in Table 7.5. Despite the fact that the multi-sinusoidal signal contains one optimal frequency per sensor only, the gas identification rate remains high and peaks at 84.45% when sensor number 2 is used. The success rate in identification can be further improved by using the information from more than one sensor to build the fuzzy ARTMAP classifier. For example when sensors 2 and 5 are used, the success rate increases to 93.33%. These results (summarized in Table 7.6) prove the correct identification of the modulating frequencies that are relevant for the gas analysis application considered.

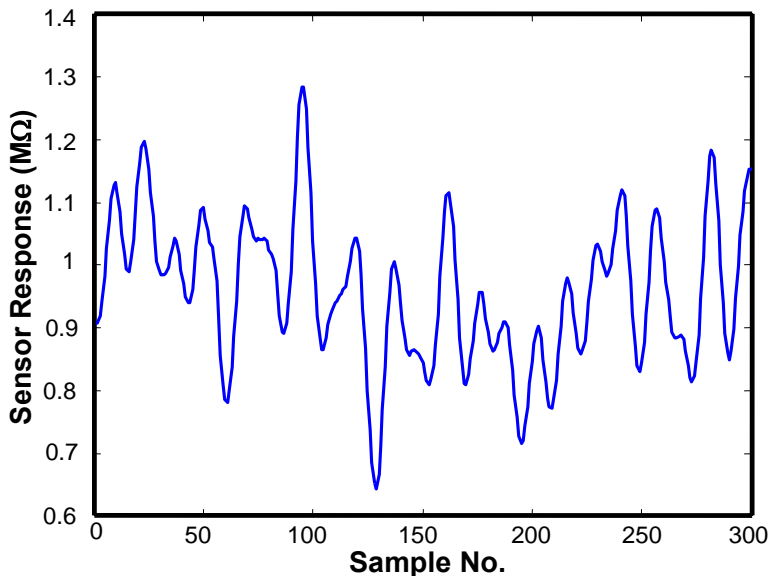
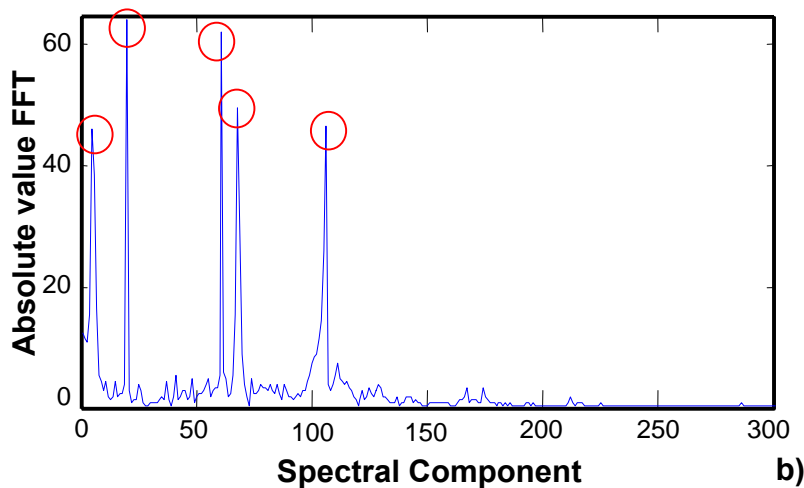
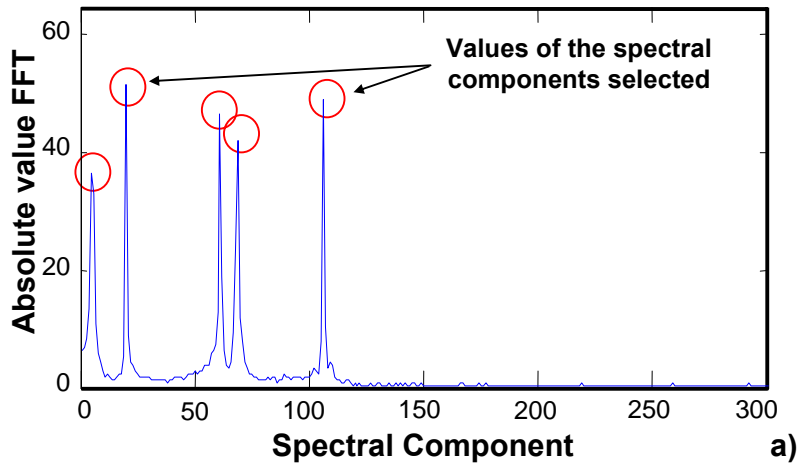


**Figure 7.3:** Response of a  $\text{WO}_3$  micro-hotplate sensor in the presence 1000 ppm of  $\text{NH}_3$  when its operating temperature is modulated using the sum of 5 sinusoidal signals.

**Table 7.5:** Success rate in gas identification using a fuzzy ARTMAP classifier when the sensor working temperature is modulated by a sum of 5 sinusoidal signals.

Sensor no.	1	2	3	4	5
Frequencies previously selected (Hz)	0.039	0.4807	0.429	0.743	0.141
Identification success rate (%)	68.88	84.45	66.67	64.44	73.33



Improving the performance of micro-machined metal oxide gas sensors:  
 Optimization of the temperature modulation mode via pseudo-random sequences.

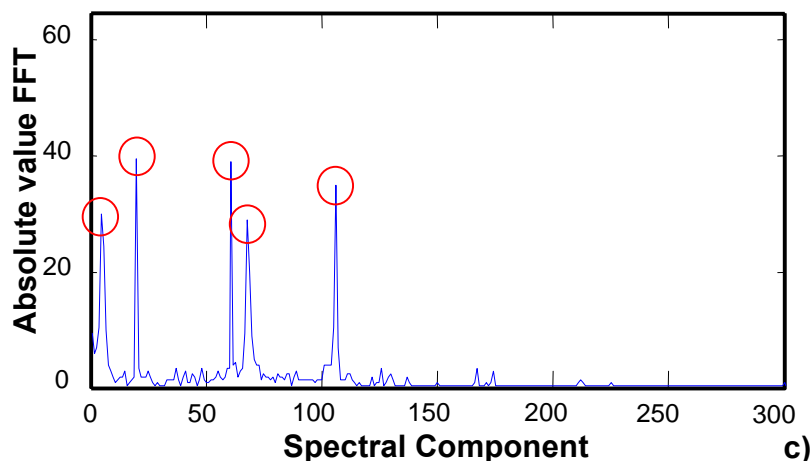


**Figure 7.4:** FFT (absolute value) of the transient response of a temperature-modulated WO<sub>3</sub> micro-hotplate sensor in the presence of (a) 1000 ppm NH<sub>3</sub>; (b) 2 ppm NO<sub>2</sub>; and (c) 1000 + 2 ppm of NH<sub>3</sub> + NO<sub>2</sub>. The temperature is modulated using a 5-frequency multi-sinusoidal signal.

**Table 7.6:** Success rate in gas identification using a fuzzy ARTMAP classifier when the sensor working temperature is modulated by a sum of 5 sinusoidal signals. The information from different sensors is combined at the input of the classifier.

Sensor no.	1-2	2-3	2-4	2-5	All
Identification success rate (%)	86.67	86.67	88.88	93.33	93.33

### 7.2.5. Steady-state response.

To better assess the improvement in gas identification and quantification obtained by modulating the operating temperature of the sensors, the ML-PRS and multi-sinusoidal modulation methods were compared against a simpler method based on the sensors' static response. Identification and quantification tasks were attempted using the steady-state value of the normalized resistance change,  $\Delta R / R_o$ , experienced by the 5 sensors in the presence of different gases and gas mixtures. The static response was defined as the normalized resistance change

$$\frac{\Delta R}{R_o} = \frac{R - R_o}{R_o} \quad (7.1)$$

where  $R_0$  is the baseline resistance (i.e. in the presence of dry air) and  $R$  is the steady-state resistance of the sensor in the presence of a given gas. Figure 7.5 shows a typical response of a micro-hotplate gas sensor to 1000 ppm of  $\text{NH}_3$  when it was operated in steady state mode.

Remembering that, for every measurement, the steady-state response was stored before acquiring the transient response due to temperature modulation, a database with 45 steady-state measurements was available to perform this analysis (see chapter 5). Table 7.7 summarizes the results for the different methods envisaged, including the simpler one that used the static sensor response and a fuzzy ARTMAP classifier. The table clearly shows that temperature-modulated methods outperform the use of static information.

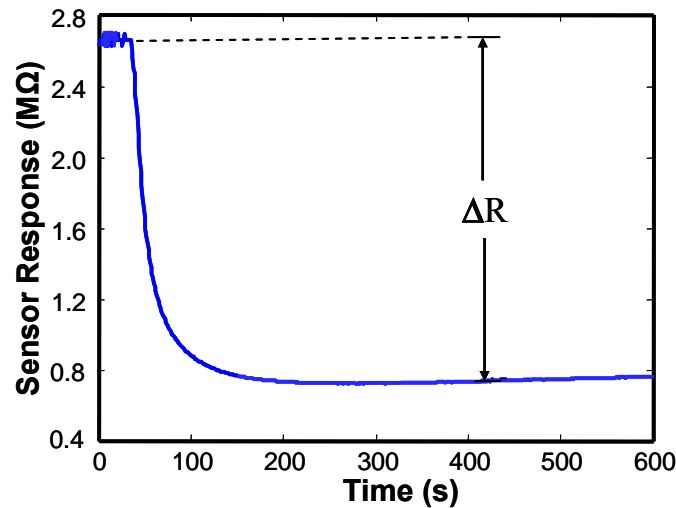


**Figure 7.5:** Typical steady state mode response of a tungsten oxide micro-hotplate sensor to ammonia (1000 ppm).

**Table 7.7:** Success rate in gas identification and quantification using a fuzzy ARTMAP classifier. The MLPRS method uses the frequencies defined in **Table 7.1** and **Table 7.3** for gas identification and quantification, respectively. The 5-sinusoidal signals method employs the frequencies defined in **Table 7.5**. Finally, the steady-state method employs the resistance change ( $\Delta R$ ) of the 5 sensors studied. These results were obtained using a leave-one-out cross-validation on the complete set.

	Temperature modulation by MLPRS	Temperature modulation by 5-sinusoidals	Steady-state
Identification success rate (%)	98	93	84
Quantification success rate (%)	84	77	52

## 7.2.6. Gas analysis of metal oxide gas sensors using dynamic moments combined with temperature modulation.

Additionally, in this sub-section we introduce the Dynamic Moments (DM) as an alternative feature extraction method applied when the working temperature of micro-hotplate gas sensors is modulated by means of either a Multi-Level Pseudo Random Sequence (MLPRS) or a multi-frequency sinusoidal signal (e.g. 5-frequency sinusoidal signal) (see sub-section 7.2.3 and 7.2.4). The performance of DM as feature extractor from metal oxide gas sensors has been evaluated discriminating two pollutant gases and their binary mixtures obtained from the database performed in *Experiment 3* (i.e., transient response of gas sensors when their working temperature was modulated by means of either MLPRS (optimization process) or a 5-multisinusoidal signal (validation process)). The qualitative gas analysis results obtained by combining thermal modulation with the DM feature extraction are compared against the ones obtained when classical feature extraction methods (e.g. the FFT) were used [4].

### 7.2.6.1. MLPRS temperature modulation database.

As mentioned in section 7.2.1.1 an estimate of the impulse response for each gas-microsensor system was calculated via the circular cross-correlation of the temperature modulating sequence and the sensor response signal. The spectral components of the impulse response were obtained by computing the FFT (see Figure 7.1) and those that were important for gas identification were then selected by a process described in section 7.2.1.2. Once the spectral components were selected, one matrix per sensor was formed, which contained as number of rows the number of measurements performed (i.e. 45 measurements) and as number of columns the number of selected spectral components. Each matrix was used to build and validate either fuzzy ARTMAP or PLS-DA classifiers to see whether it was possible to correctly identify the gases.

Alternatively, for every measurement performed, a small fragment of the response signal was taken (see Figure 7.6 (a)) and had its characteristic features extracted by the Dynamic Moments technique. The duration of the fragments was 1.1 s, which represented 0.35 % of the total length of the response signals. Measurements were aligned to ensure that the response fragments analysed corresponded always to the same fragment of the temperature modulating MLPRS sequence (i.e. the one that caused the highest response change). Figure 7.7 shows typical trajectories in the phase space of a MLPRS temperature-modulated micro-hotplate sensor in the presence of the gases studied. As this figure shows, the shape of these



trajectories is gas-dependent. The DM method is applied to extract characteristic features from these trajectories in the phase space.

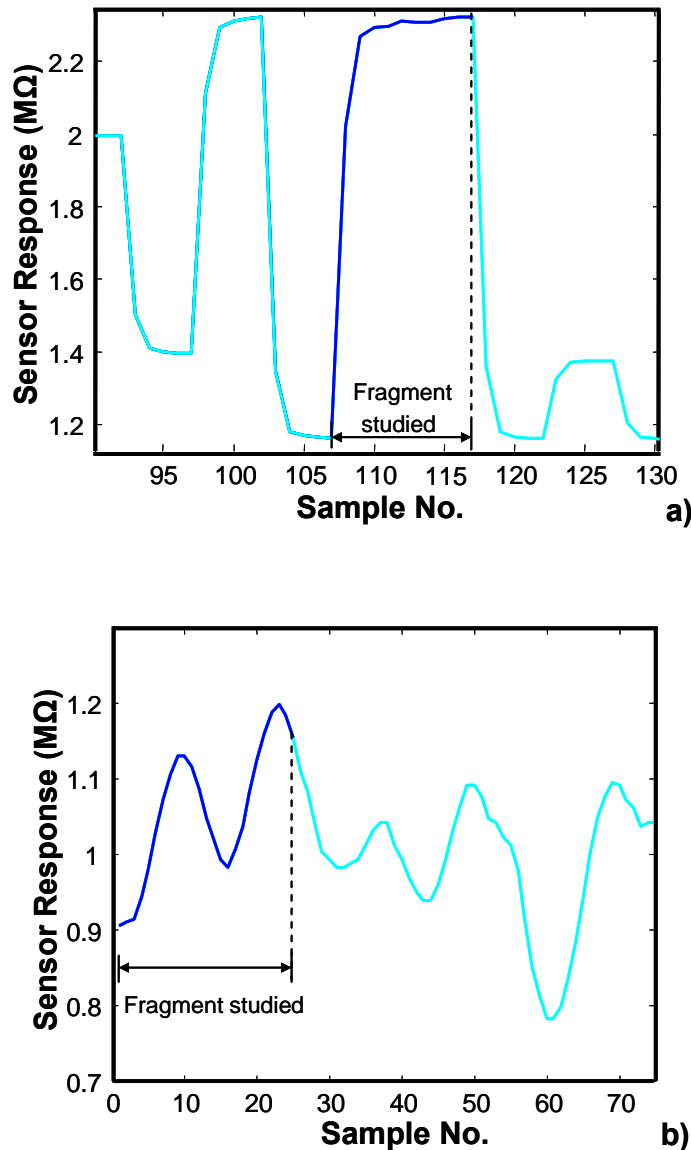


**Figure 7.6:** Fragments of the response signals used. The fragments in bold are those used to compute the dynamic moments: (a) Response to a thermal modulation by means of a MLPRS signal; (b) Response to a thermal modulation by means of a multi-sinusoidal signal.

Improving the performance of micro-machined metal oxide gas sensors:  
 Optimization of the temperature modulation mode via pseudo-random sequences.

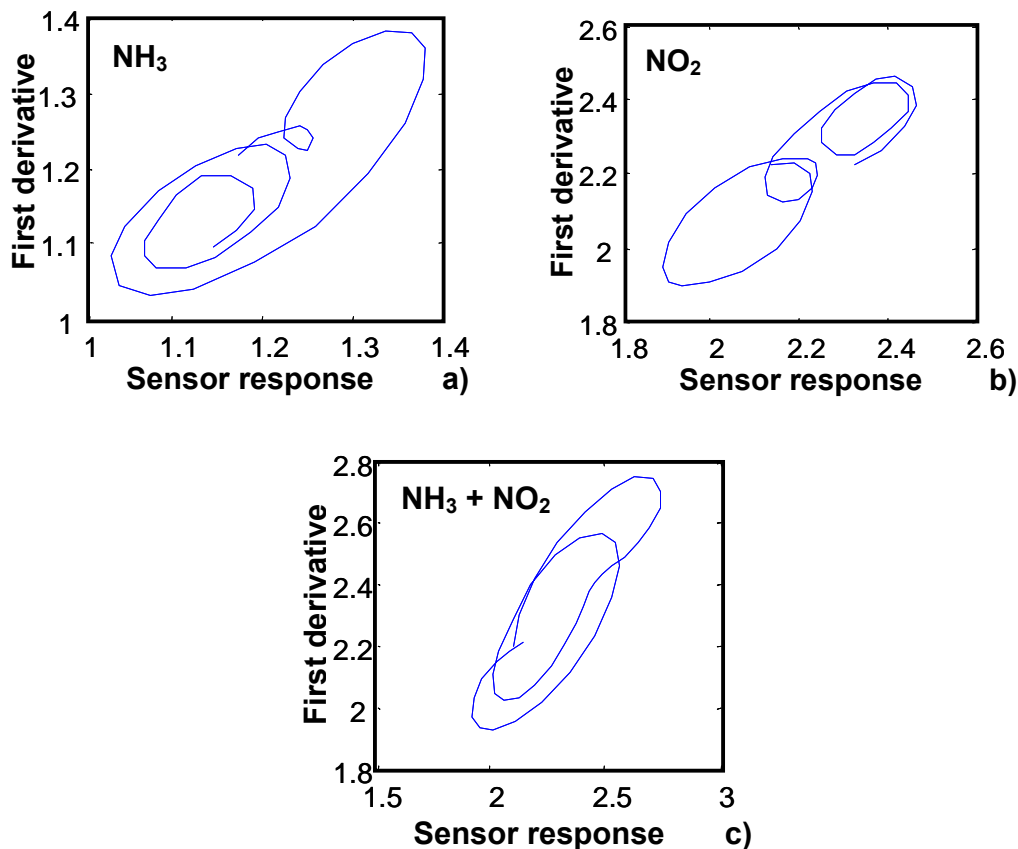


**Figure 7.7:** Typical response of a tungsten oxide micro-hotplate sensor to ammonia (500 ppm), nitrogen dioxide (1 ppm) and ammonia + nitrogen dioxide (500 + 1 ppm) in the phase space domain. The first derivative of the sensor response for  $\tau_L = 3$  ms (*y-axis*) is plotted versus the sensor response (*x-axis*).

Initially, different dynamic moments at different time lags were computed.  $MD3_Y$  at  $\tau_L = 1$  and 3 ms was selected to build PLS-DA classifiers. The success rate in gas identification was 93.3%. The number of latent variables was set to 6. It is important to mention that the measurements used to select the dynamic moments were different than those employed to validate the PLS-DA models (performance estimation was based on a leave-one-out approach). Table 7.8 shows the confusion matrix. While  $NH_3$  samples could be perfectly discriminated, confusions occurred between samples of  $NO_2$  and  $NO_2 + NH_3$  mixtures. If  $MD2$  for  $\tau_L = 1$  and 2 ms,  $MD3_X$  and  $MD3_Y$  at  $\tau_L = 1$  and 3 ms are used simultaneously in the PLS-DA classifiers, the success rate in classification increases to 95.6%. The number of

latent variables was set to 9. Increasing the length of the response signal used to compute the dynamic moments did not improve results.

Table 7.9 summarizes the results obtained using the dynamic moments and compares them with the results obtained using the selection of spectral components as described in sub-section 7.2.3. Table 7.9 also shows that the DM method obtains a similar gas identification performance while dramatically reduces measurement time, since a very small fragment of the sensor response transient is needed.

**Table 7.8:** Confusion matrix and success rate in gas identification using a 4-element microsensor array. The sensors' operating temperature was modulated by a MLPRS signal and just one dynamic moment (MD3<sub>Y</sub>) was input to PLS-DA models.

		Predicted as		
		NH <sub>3</sub>	NO <sub>2</sub>	NH <sub>3</sub> + NO <sub>2</sub>
Actual	NH <sub>3</sub>	15	0	0
	NO <sub>2</sub>	0	14	1
	NH <sub>3</sub> + NO <sub>2</sub>	0	2	13
Success Rate		93.3 %		

**Table 7.9:** Comparison among the different feature extraction and classification methods used for the identification of gases and gas mixtures (MLPRS temperature modulation).

Processing Method used	Success rate gas discrimination	Fragment of the response signal used
MD3 <sub>Y</sub> and PLS-DA	93.3%	0.35 % (1.1 s)
MD2, MD3 <sub>X</sub> , MD3 <sub>Y</sub> and PLS-DA	95.6 %	0.35 % (1.1 s)
Cross-correlation and NN	98 %	100 % (312 s)
Cross-correlation and PLS-DA	95.6 %	100 % (312 s)

### 7.2.6.2. Multi-sinusoidal modulation database.

In this experiment the sensor operating temperature was modulated using a multi-sinusoidal signal. This signal was synthesized adding 5 sinusoidal signals, the frequencies of which had been found to be important for discriminating among the gases and gas mixtures studied in the experiment of sub-section 7.2.3.

In the first step, the response signals of the temperature-modulated microsensors (see Figure 7.3) were processed as follows. The absolute value of the FFT was computed and the values of the d.c. component and the 5 harmonics corresponding to the modulating

Improving the performance of micro-machined metal oxide gas sensors:  
 Optimization of the temperature modulation mode via pseudo-random sequences.

frequencies were extracted (see Figure 7.4). Therefore, from each measurement, 6 features were extracted and used to build either a fuzzy ARTMAP or a PLS-DA classifier aimed at discriminating between the different species measured. The classifiers were cross-validated using a leave-one-out approach.

In the second step, the DM method was employed to extract features from the sensor responses. The method was implemented at different time lags ( $\tau_L$ ) and the use of response fragments with different lengths was considered. Finally, a small fragment of the sensor response signal was selected (i.e. 2.5 s of the response, which is about 1.8 % of its total length). The fragment of the response signal selected is shown in Figure 7.6 (b).

The dynamic moments used to build PLS-DA classifiers were MD2 and MD3<sub>V</sub> at the time lags  $\tau_L = 1$  and 3 ms. The success rate in gas and gas mixture identification was 95.6% (estimated by leave-one-out cross-validation). PLS-DA models used 5 latent variables. Table 7.10 shows the confusion matrix of this analysis: While NH<sub>3</sub> samples could be perfectly discriminated, confusions occurred between samples of NO<sub>2</sub> and NO<sub>2</sub> + NH<sub>3</sub> mixtures. Increasing the length of the response signal fragment used to calculate the dynamic moments did not improve these results.

Figure 7.8 shows the scores plot of the two first latent variables (LV) of a PLS-DA model built using the DM features. The first two LV captured more than 99.92% of data variance. As this figure shows, the cluster of ammonia samples is well apart from the other ones, while some overlapping exists between the clusters for nitrogen dioxide and for nitrogen dioxide and ammonia mixtures. These results illustrate the errors shown in the confusion matrix (Table 7.10).

**Table 7.10:** Confusion matrix and success rate in gas identification using a 4-element microsensor array. The sensors' operating temperature was modulated by a multi-sinusoidal signal and different dynamic moments (MD2 and MD3<sub>V</sub>) were input to PLS-DA models.

		Predicted as		
		NH <sub>3</sub>	NO <sub>2</sub>	NH <sub>3</sub> + NO <sub>2</sub>
Actual	NH <sub>3</sub>	15	0	0
	NO <sub>2</sub>	1	13	1
	NH <sub>3</sub> + NO <sub>2</sub>	0	0	15
Success Rate		95.6 %		

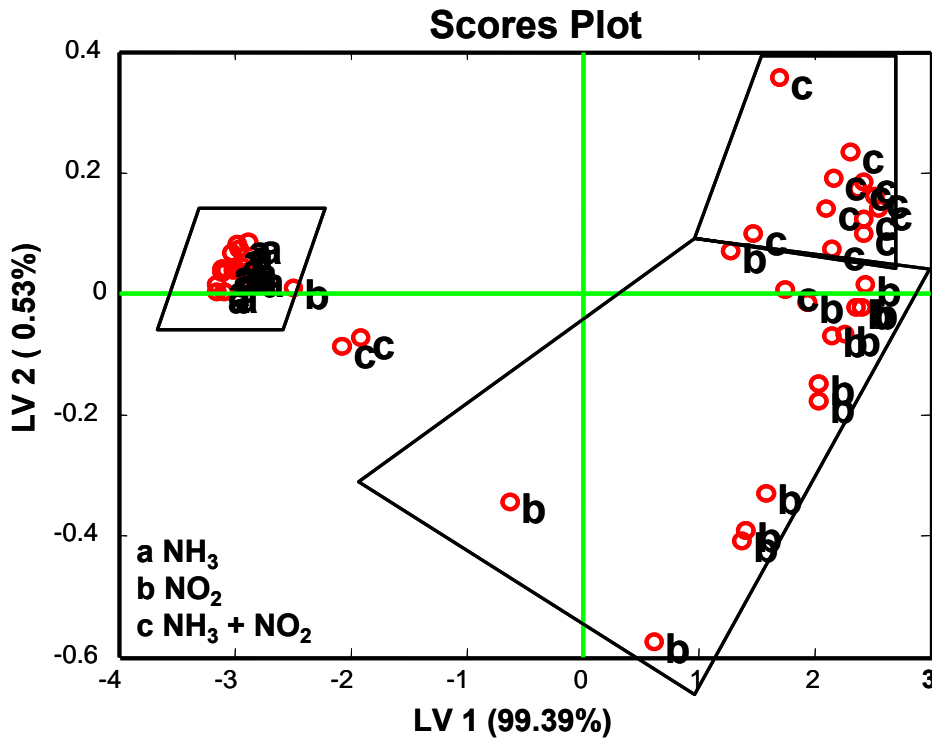


**Figure 7.8:** Thermal modulation by a sum of 5 sinusoidal signals: Scores plot of the first two latent variables of the PLS-DA model calculated using the MD2 and MD3<sub>γ</sub> dynamic moments as input features.

Table 7.11 summarizes the results obtained using the dynamic moments and compares them with the results obtained employing the features extracted from the whole response signal using the FFT. Table 7.11 also shows that the DM method obtains a slightly better gas identification performance while dramatically reduces measurement time.

**Table 7.11:** Comparison among the different feature extraction and classification methods used for the identification of gases and gas mixtures (multi-sinusoidal temperature modulation).

Processing Method used	Success rate gas discrimination	Fragment of the response signal used
DM and PLS-DA	95.6 %	1.8 % (2.5 s)
FFT and PLS-DA	91.0 %	100 % (142 s)
FFT and NN.	93.3 %	100 % (142 s)

### Improving the performance of micro-machined metal oxide gas sensors: Optimization of the temperature modulation mode via pseudo-random sequences.

## 7.3. Analysis of the data from experiment 4: Qualitative and Quantitative gas mixture analysis using temperature-modulated micro-hotplate gas sensors: Selection and validation of the optimal modulating frequencies.

In the previous experiments, we introduced a method borrowed from the field of system identification, to systematically study the effect of modulation frequencies in the discrimination and quantification ability of metal oxide gas sensors. This method is based on the use of pseudo-random maximum-length sequences to modulate the working temperature of gas sensors. It allows an optimal set of modulating frequencies to be determined for a given gas analysis problem.

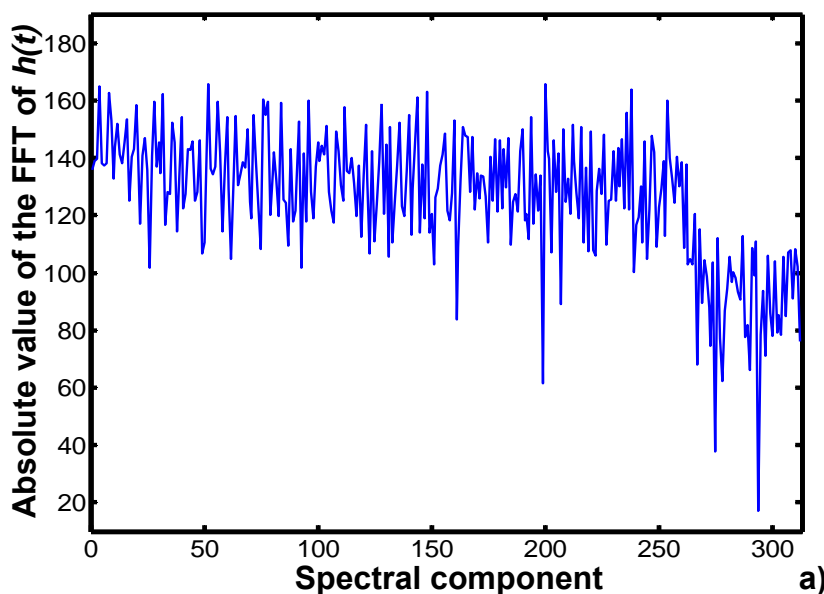
In this section the analysis of the data from *Experiment 4* is carried out. In this experiment, we further develop and fully validate the method for optimizing the choice of temperature modulating frequencies. The problem envisaged to illustrate the process is the building of calibration models for the analysis of acetaldehyde, ethylene, ammonia and their binary mixtures using metal oxide micro-hotplate gas sensors. These species were chosen, since the first two are related to the quality of climacteric fruit during cold storage and the third one reveals the occurrence of a leak in the refrigeration system. The results of this analysis were reported in [5].

The organization of this sub-section is as follows: The optimization process is applied to find a reduced set of modulation frequencies to discriminate among the different gases or mixtures and to estimate their concentration (sub-sections 7.3.1 to 7.3.4). The process of frequency selection is fully validated by running new measurements using different micro-hotplate sensors (same type than the ones used for frequency selection). During these measurements, the working temperature of the new sensors is modulated using a multi-sinusoidal signal. The temperature-modulating signal is made up of some of the frequencies found to be optimal in the frequency-selection step (sub-section 7.3.5). This ensures that an honest and accurate validation of the optimization process is possible. To do so, identification and calibration models are built based on the multi-sinusoidal temperature modulation and their performance is once again compared against the one of models based on the static sensor response (7.3.6).

### 7.3.1. Spectral analysis of the impulse response estimates.

The first database described in sub-section 5.4.4 (consisting of 165 measurements) was used for this purpose. For each measurement, an estimate of the impulse response,  $\hat{h}(n)$ , was computed by means of the circular cross-correlation between one period of the input MLPRS signal,  $x(n)$ , and one period of the sensor response signal (i.e. resistance transient),  $y(n)$ . The absolute value of the FFT of the impulse response estimates was calculated. This was done to study which spectral components contain important information for the identification and quantification of gases. Figure 7.9 shows the absolute value of the FFT of the impulse response estimates for a Au-doped,  $\text{WO}_3$  micro-hotplate in the presence of Acetaldehyde, Ethylene and Ammonia (the concentration of these species was 50 ppm). The number of spectral components available is 312, which corresponds to half the length of the MLPRS ( $L/2$ ). Two consecutive spectral components are separated by the spectral resolution,  $f_c/L$  (i.e.  $2/624 \text{ Hz} = 3.20 \text{ mHz}$ ). Each spectral component can be related back to a specific temperature-modulation frequency using expression (6.1) shown in subsection 6.2.1 of chapter 6 (see Figure 7.9).

Once again, a simple search method was implemented to find a reduced set of spectral components that better helped either in the discrimination of the gases and gas mixtures or in gas quantification. The search technique used is discussed below.



Improving the performance of micro-machined metal oxide gas sensors:  
Optimization of the temperature modulation mode via pseudo-random sequences.

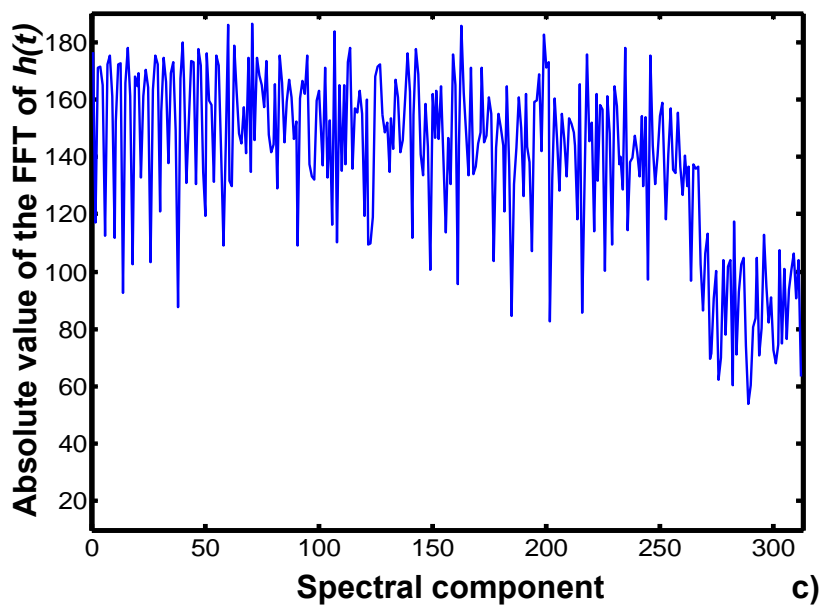
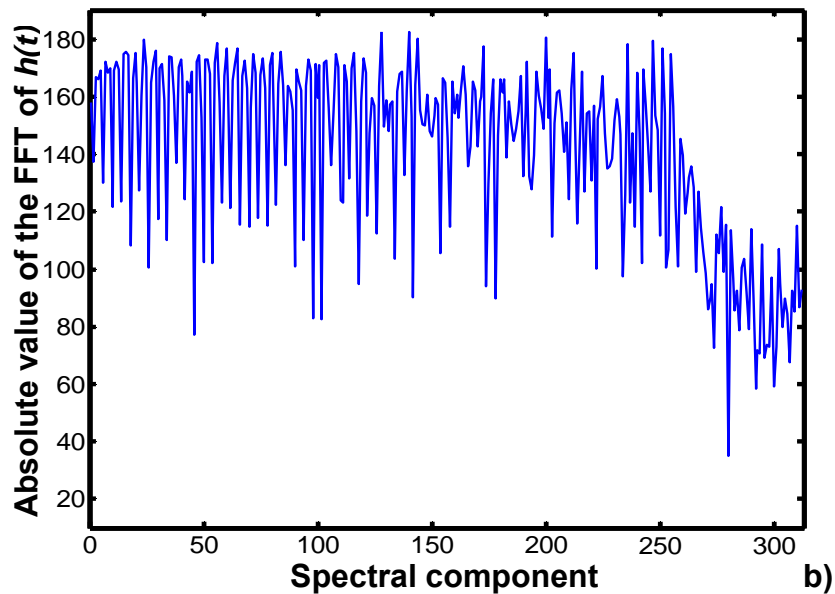


**Figure 7.9:** Absolute value of the FFT of  $h(t)$  for a temperature modulated,  $\text{WO}_3$  micro-hotplate sensor in the presence of (a) 50 ppm Acetaldehyde; (b) 50 ppm Ethylene; (c) and 50 ppm of Ammonia.



### 7.3.2. Selection of the temperature-modulating frequencies.

The one simple and univariate search of spectral components method shown in sub-section 7.2.1.2., was implemented as follows.

For discrimination purposes, measurements were grouped in 6 classes, three corresponding to the single species and three for gas mixtures. On the other hand for quantification model, the measurements were grouped in 3 categories (i.e., 3 concentrations). Once again for each spectral component, intra-category and between-category variances were computed, and then the parameter defined to rank the discriminating power of a given spectral component was computed (see eq. 3.20 in sub-section 3.4 of chapter 3).

### 7.3.3. Optimization for qualitative gas analysis.

The optimization was conducted on the first micro-sensor array. The number of measurements available in this database was 165 (5 replicate measurements for each gas, gas mixture and concentration). The objective here was to identify an optimal set of temperature-modulating frequencies to discriminate among the gases and gas mixtures, regardless their concentration.

The process of frequency selection was performed using a 5-fold validation approach. Selection data sets were formed by using 4 out of the 5 replicates available per measurement (there were 132 measurements in each of the 5 selection data sets). Their corresponding validation data sets were formed by the replicate left out (there were 33 measurements in each of the 5 corresponding validation data sets). Therefore, each sensor within the micro-array had 5 frequency selection matrices (132 rows or measurements  $\times$  312 columns or spectral components) and 5 validation matrices (33 rows  $\times$  312 columns). The process described in sub-section 7.3.2 was used with each frequency selection matrix in order to rank spectral components according to their usefulness to discriminate among gases and gas mixtures (6-category classification).

For each sensor and selection set, the best five spectral components were selected. Table 7.12 shows the frequencies corresponding to these components. Two conclusions can be derived from the frequencies selected:

- Considering each micro-sensor separately: A very high consistency exists among the frequencies selected over the five selection folds. Sensor 1 shows a higher variability than sensors 2, 3 and 4. Furthermore, differences arise generally in the fourth and fifth frequencies (i.e. those among the frequencies selected that had the lower value of the parameter used to rank them).

## Improving the performance of micro-machined metal oxide gas sensors: Optimization of the temperature modulation mode via pseudo-random sequences.

- Considering the 4 sensors studied together: There are a high number of coincidences in the values of the modulating frequencies selected. This is not surprising, since 3 out of 4 sensors are based on the same gas-sensitive material (tin oxide), even though in each sensor, a different noble metal catalyst was used.

Fuzzy ARTMAP classifiers were built and validated to see whether it was possible to correctly identify the different gases and gas mixtures using the spectral components that had been selected. This process was repeated for the 5 folds available. Leave-one-out cross-validation was the approach implemented to estimate the success rate in identification. Each fold comprised 165 measurements, (132 had been used in the frequency selection step and 33 had been left out). Fuzzy ARTMAP classifiers were trained 165 times using 164 training vectors. The vector left out during the training phase (i.e. unseen by the classifier) was then used for testing. The performance of a given classifier was estimated as the averaged performance over the 165 tests. More details about the building and validation of fuzzy ARTMAP classifiers can be found in [2, 3] and references therein.

Classifiers were built and validated using the information of 1 sensor, 2 sensors (2 and 3) and 3 sensors (2, 3 and 4). Therefore, the dimension of the vectors input to the fuzzy ARTMAP was 5, 10 and 15, respectively, since the values of 5 spectral components were used per sensor. The cross-validation results are shown in Table 7.12. This table shows that combining the information from sensors 2, 3 and 4 leads to success rates in gas identification that range between 84.3% and 89.7%, depending on the fold considered. The average of the success rate over the 5 folds is 87.3%. Increasing beyond 5 the number of spectral components used per sensor did not improve these results.

Table 7.13 shows the confusion matrix that integrates the identification results for the 5 folds when the information from sensors 2, 3 and 4 was used. A clear distinction is made between measurements that had participated in the frequency selection process and those that had not. Table 7.13 shows that most of the samples misclassified belong to gas mixtures. The success rate in gas identification (averaged for the 5 folds), estimated using measurements that took part in the selection of spectral components exclusively, is 89.4%. On the other hand, the success rate estimated using measurements that were left out (i.e. were not used in the selection of spectral components) is 80%. The latter success rate is similar to the former one (it decreases, but not substantially). This proves that the variable selection process is not over-trained and that it leads to the selection of those modulating frequencies that help discriminating among the species considered.

**Table 7.12:** Results of the 5-Fold selection and validation process for gas identification. A fuzzy ARTMAP classifier and a leave-one-out cross-validation were used to estimate performance.

Sample No. left out ↓	Sensors→	1	2	3	4	2, 3	2, 3, 4
Sample 1	Frequencies selected (mHz)	96.2	12.8	12.8	12.8	-	-
		121.8	25.6	25.6	38.4		
		134.6	76.9	38.4	198.7		
		144.2	102.6	64.1	464.7		
		198.7	115.4	76.9	618.6		
	Identification success rate (%)	42.4	63.0	61.8	51.5	84.2	89.7
Sample 2	Frequencies selected (mHz)	12.8	12.8	12.8	12.8	-	-
		25.6	25.6	25.6	25.6		
		38.4	115.4	38.4	38.4		
		185.9	153.8	64.1	185.9		
		198.7	192.3	76.9	198.7		
	Identification success rate (%)	42.4	55.7	61.2	47.3	80.6	84.3
Sample 3	Frequencies selected (mHz)	3.2	12.8	12.8	12.8	-	-
		12.8	25.6	25.6	25.6		
		25.6	76.9	38.4	38.4		
		38.4	89.7	64.1	134.6		
		134.6	102.6	76.9	618.6		
	Identification success rate (%)	52.7	63.6	61.2	51.5	80.6	85.5
Sample 4	Frequencies selected (mHz)	12.8	12.8	12.8	12.8	-	-
		28.8	25.6	25.6	25.6		
		121.8	76.9	38.4	38.4		
		134.6	102.6	64.1	198.7		
		198.7	115.4	76.9	451.9		
	Identification success rate (%)	50.9	73.3	60.0	55.1	83.0	89.7
Sample 5	Frequencies selected (mHz)	3.2	12.8	12.8	12.8	-	-
		22.4	25.6	25.6	25.6		
		25.6	76.9	38.4	38.4		
		28.8	102.6	76.9	134.6		
		134.6	192.3	89.7	618.6		
	Identification success rate (%)	52.7	64.8	57.5	55.1	81.2	87.3

Improving the performance of micro-machined metal oxide gas sensors:  
 Optimization of the temperature modulation mode via pseudo-random sequences.

**Table 7.13:** Confusion matrix (leave-one-out cross-validation results) for the fuzzy ARTMAP classifiers applied to the identification of gases and gas mixtures (adding up the results of the 5 different folds). Bold face is used for correct identifications, plain face is used for misclassified samples from the frequency selection data sets and Italics is used for misclassified samples from the validation sets.

		Real category					
		1	2	3	4	5	6
Predicted as	1	<b>72</b>		<i>1</i>	2	1	
	2	<i>1</i>	<b>75</b>				
	3			<b>74</b>			
	4				<b>189</b>	23+10	17+11
	5	2			26+4	<b>191</b>	2
	6				4		<b>120</b>

### 7.3.4. Optimization for quantitative gas analysis.

In the second step the selection of the optimal set of temperature-modulating frequencies to quantify the different gases and gas mixtures was envisaged. Once again, this optimization was conducted on the first micro-sensor array. Since specific quantification models were sought for every gas or gas mixture, the database (165 measurements, i.e. 5 replicate measurements for each gas, gas mixture and concentration) was split in 6 databases. The first 3 databases were for single gases (15 measurements in each) and the second 3 databases were for gas mixtures (45, 45 and 30 measurements for Acetaldehyde + Ethylene, Ethylene + Ammonia and Acetaldehyde + Ammonia, respectively). The process of frequency selection was performed using a 5-fold validation approach. Selection data sets were formed by using 4 out of the 5 replicates available per measurement. There were 12 measurements in the selection data sets of single gases and 36, 36 and 24 measurements in the selection data sets of gas mixtures. Their corresponding validation data sets were formed by the replicates left out. The process described in sub-section 7.3.2 was, once again, used with each frequency selection matrix in order to rank spectral components according to their usefulness to quantify the gases. Only sensors 2, 3 and 4 were studied (since sensor 1 was discarded in the qualitative analysis). For each sensor and selection set, the best five spectral components were selected. Table 7.14 summarizes the results of the selection process. The frequencies shown in Table 7.14 correspond to those that appeared selected more times over the five selection folds.

PLS calibration models that used the values of the spectral components selected from sensors 2, 3 and 4 were built and validated. Data were mean centered. PLS is a linear and

supervised multivariate calibration method that attempts to find factors, which capture as much variance as possible in the predictor block  $X$ -matrix (spectral components for sensors 2, 3 and 4), under the constraint of being correlated with the predicted block  $Y$ -matrix (gas or gas mixture concentrations) [6].

**Table 7.14:** Frequencies selected to build specific quantitative models. The number of times a frequency is selected over the 5 folds is shown in parenthesis.

Gases/mixture models↓	Sensors→	2	3	4
Acetaldehyde	Frequencies selected (mHz)	339.7 (3)	6.4 (3)	339.7 (2)
		496.8 (4)	224.4 (5)	676.3 (3)
		612.2 (5)	339.7 (5)	698.7 (5)
		804.5 (5)	785.3 (4)	804.5 (5)
		996.8 (2)	887.8 (3)	887.8 (4)
Ethylene	Frequencies selected (mHz)	12.8 (2)	22.4 (4)	41.7 (3)
		51.3 (5)	25.6 (5)	179.5 (2)
		60.9 (4)	28.8 (5)	195.5 (3)
		73.7 (5)	67.3 (5)	208.3 (4)
		734.0 (2)	734.0 (2)	339.7 (3)
Ammonia	Frequencies selected (mHz)	256.4 (4)	450.1 (4)	185.9 (3)
		500.0 (4)	500.0 (4)	250.0 (3)
		564.1 (3)	680.0 (5)	330.1 (3)
		698.7 (3)	685.9 (3)	403.8 (4)
		705.1 (4)	894.2 (3)	685.9 (5)
Ethylene + Acetaldehyde	Frequencies selected (mHz)	12.8 (4)	3.2 (4)	3.2 (5)
		25.6 (4)	378.2 (3)	9.6 (5)
		128.2 (3)	496.8 (5)	12.8 (5)
		551.3 (3)	641.0 (5)	16.02 (5)
		910.2 (4)	846.1 (3)	38.5 (3)
Ethylene + Ammonia	Frequencies selected (mHz)	51.3 (5)	38.5 (5)	92.9 (3)
		112.2 (2)	310.9 (2)	253.2 (5)
		121.8 (2)	419.9 (5)	368.6 (3)
		298.1 (5)	682.7 (3)	419.9 (5)
		689.1 (4)	717.9 (3)	987.2 (3)
Acetaldehyde + Ammonia	Frequencies selected (mHz)	92.9 (3)	272.4 (5)	317.3 (4)
		352.6 (3)	294.9 (2)	349.4 (2)
		419.9 (4)	342.9 (3)	419.9 (5)
		557.7 (3)	403.9 (2)	544.9 (4)
		695.5 (3)	846.2 (4)	689.1 (2)

Improving the performance of micro-machined metal oxide gas sensors:  
 Optimization of the temperature modulation mode via pseudo-random sequences.

The process used to build and validate the specific PLS calibration models was as follows. The number of latent variables (LV) to be used in each model was determined using the measurements in the selection data sets. Leave-one-out cross-validations were performed with these measurements and the root mean square error of cross validation (RMSECV) versus the number of latent variables was computed, according to the definition:

$$RMSECV = \sqrt{\frac{\sum_{i=1}^n (Y_i - y_i)^2}{n}} \quad (7.2)$$

where  $Y_i$  is the actual concentration value and  $y_i$  the model prediction. The number of LV selected was the value after the first sharp decrease in RMSECV.

**Table 7.15:** Validation results for the specific PLS calibration models (the selected spectral components from sensors 2, 3 and 4, were used as input data). Number of LV used, slope (m) and correlation coefficient (r) of the linear regression between real and predicted concentrations and root mean square of cross-validation (RMSECV).

Gas/gas mixture models ↓	Cross-validation results			
	LV#	m	r	RMSECV
Acetaldehyde	6	0.75	0.71	28.8
Ethylene	4	0.87	0.94	12.9
Ammonia	6	0.97	0.98	4.8
Ethylene + Acetaldehyde	17	0.6	0.65	31.8
		0.91	0.92	14.3
Ethylene + Ammonia	18	0.82	0.87	18.8
		0.92	0.94	7.2
Acetaldehyde + Ammonia	18	0.98	0.99	2.9
		0.98	0.97	5.3

Once the number of LV had been determined, PLS models were built (one for each gas or gas mixture) using the measurements in the selection data sets. These calibration models were validated using the measurements that had been left out, i.e. those that belonged to the validation data sets. Since 5 different selection and validation sets were available (5-fold selection), this process was repeated 5 times. Table 7.15 summarizes the quantification results for each gas/mixture model. These results are exclusively for validation measurements. In addition to the RMSECV, the table also shows the slopes and the correlation coefficients of the linear regressions between actual and predicted concentrations.

The closer to one are slopes and correlation coefficients, the better the calibration PLS models are.

Table 7.15 shows that the concentration of ammonia (either as a single gas or in mixtures) can be predicted accurately. On the other hand, the estimation of the concentrations of acetaldehyde (as a single gas) and ethylene (in ethylene + acetaldehyde mixtures) is poor. Finally, the performance of the remaining calibration models is fair.

Once the processes for determining the optimal frequencies for gas identification and quantification have been conducted, the final validation can be envisaged. This consists in selecting a reduced set of optimal frequencies, synthesize a multi-sinusoidal temperature-modulating signal, run a new set of measurements and build and validate identification and calibration models.

### 7.3.5. Gas analysis using multi-sinusoidal temperature modulation.

The six frequencies selected to synthesize the multi-sinusoidal signal were taken from the results for sensors 2, 3 and 4. These frequencies are shown in Table 7.16. The first three frequencies selected correspond to those that are more important for gas identification (i.e. were ranked with a high score in the selection process). The last three frequencies are representative of the ones used for quantification.

**Table 7.16:** Temperature modulation frequencies selected after the qualitative and quantitative gas analysis using MLPRS signals.

Final selection of frequencies (mHz)	12.8	25.6	38.5	92.9	339.7	682.7
--------------------------------------	------	------	------	------	-------	-------

The objectives of this study were the following:

- To show a practical application of temperature modulated sensors after the modulation process has been optimized. In other words, MLPRS are used to determine the optimal temperature-modulating frequencies. Following this optimization, a much simpler multi-sinusoidal signal (using optimal frequencies) would be used in a practical application.
- To validate the whole optimization process by performing a new set of measurements using a different micro-sensor array. This second micro-array belongs to the same fabrication batch of the array employed to perform the optimization.

To assess the performance of the temperature-modulated micro-sensors in qualitative and quantitative gas analysis.

### Improving the performance of micro-machined metal oxide gas sensors: Optimization of the temperature modulation mode via pseudo-random sequences.

The new measurement database consisted of 165 measurements (5 replicate measurements per gas, gas mixture and concentration) (see sub-section 5.4.4). The sensors had their operating temperature modulated by a signal resulting from the sum of 6 sinusoids of identical amplitude, the frequencies of which are those reported in Table 7.16). The amplitude of the resulting multi-sinusoidal signal (a current signal) was equal to 2 mA. The procedure of generating this signal is illustrated in Figure 7.10. Figure 7.11 shows a segment of the multi-sinusoidal signal applied to the heater of the second micro-sensor array (a) and a typical sensor response (b).

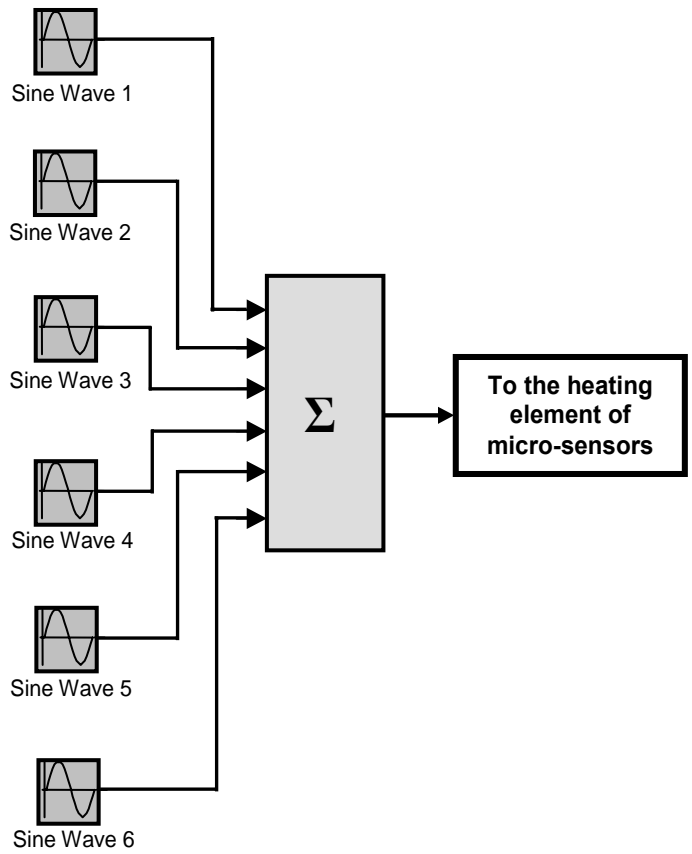


**Figure 7.10:** Set up used to generate a multi-sinusoidal signal, which consists of the sum of 6 sinusoids of identical amplitudes and different frequencies. The signal is applied to the heating element of the micro-sensors studied.



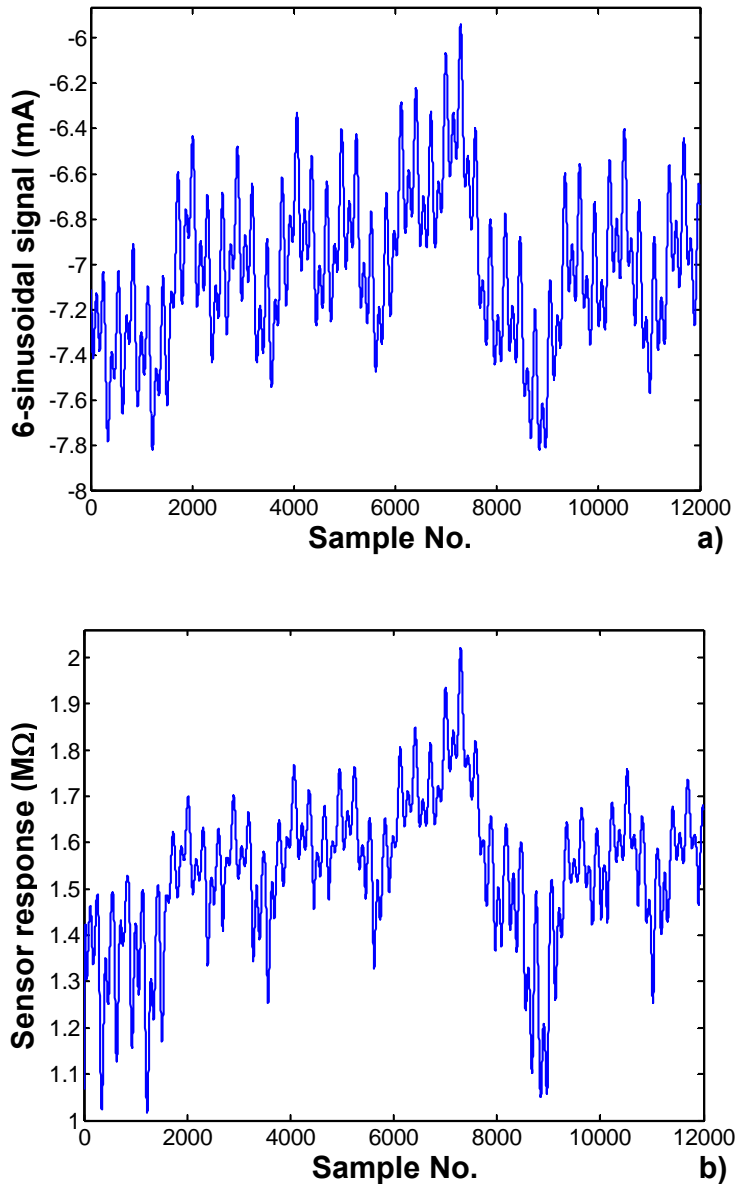


**Figure 7.11:** (a) Fragment of the multi-sinusoidal signal applied to the heating element of the micro-hotplate sensors. (b) Response of a temperature-modulated  $\text{WO}_3$  micro-hotplate in the presence of acetaldehyde 50 ppm.

The response signals of the temperature-modulated micro-sensors in the presence of the different gases studied were obtained and processed as follows. The absolute value of the

Improving the performance of micro-machined metal oxide gas sensors:  
 Optimization of the temperature modulation mode via pseudo-random sequences.

FFT was computed and the values of the 6 harmonics corresponding to the modulating frequencies were extracted. These were the 6 features used to build identification and quantification models. Figure 7.12 shows the FFT spectra of the transient response of a sensor in the presence of acetaldehyde, ethylene and ammonia. The peaks in these plots correspond to the temperature-modulating frequencies.

In the first step the identification of the gases and gas mixtures was envisaged. A fuzzy ARTMAP classifier was built and validated (using the leave-one-out approach) to discriminate among the different species (i.e. 6-category classification). The results of the identification process are shown in Table 7.17). A very high success rate in discrimination is reached, even using a single sensor. When the information from sensors 2, 3 and 4 was combined, gases and gas mixtures could be identified with a 100% success rate. This process was repeated using an additional feature, the d.c. component of the absolute value of the FFT. Adding this feature, which accounts for the mean value of transient signals (prone to be affected by drift), results in a slight degradation of the identification rate (see Table 7.17). These results prove that the modulating frequencies that are important for discriminating among the gases studied have been correctly identified.

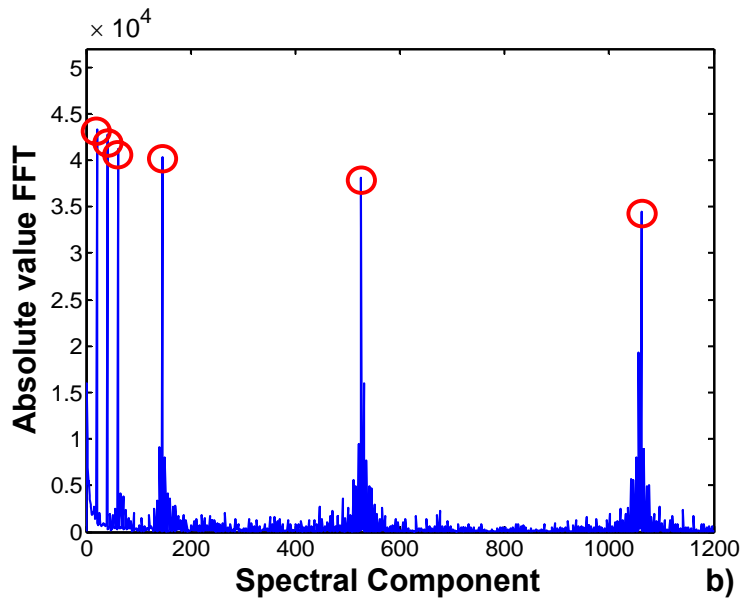
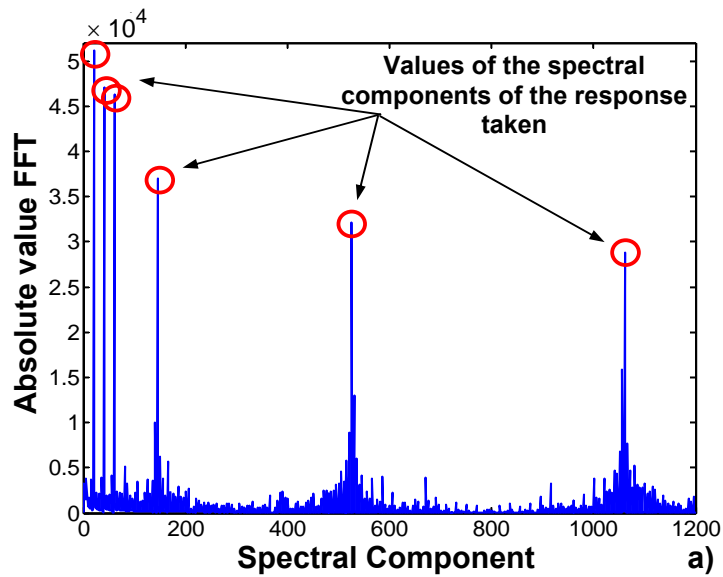
**Table 7.17:** Success rate in gas identification estimated by leave-one-out cross-validation using a fuzzy ARTMAP classifier when the sensor working temperature is modulated by a sum of 6 sinusoidal signals.

Identification success rate ↓	Sensors→	2	3	4	2,3,4
Using 6 harmonics (%)		98.20	97.00	96.36	100
Using 6 harmonics + d.c. (%)		96.36	92.69	95.20	100

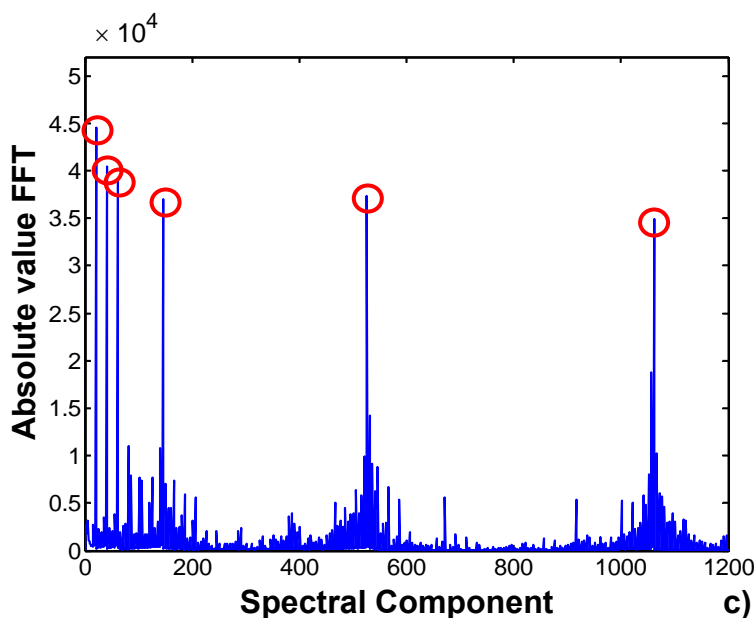
In the second step the building of PLS calibration models was envisaged. Like when MLPRS signals were used, specific calibration models for every gas or gas mixture were built and validated. The process employed to determine the number of latent variables to be used and the validation procedures are identical to the ones described for the MLPRS case.

Table 7.18 summarizes the validation results for the different PLS models built. These results show that the concentration of the different gases can be accurately estimated. This proves the usefulness of the optimization process conducted to identify the modulating frequencies that were important for gas quantification.

The fact that the frequency optimization process was conducted on a different micro-sensor array than the one used for validation, proves that this process is consistent and robust.



Improving the performance of micro-machined metal oxide gas sensors:  
 Optimization of the temperature modulation mode via pseudo-random sequences.



**Figure 7.12:** FFT (absolute value) of the transient response of a temperature-modulated  $\text{WO}_3$  micro-hotplate sensor in the presence of (a) 50 ppm Acetaldehyde; (b) 50 ppm Ethylene; and 50 ppm of Ammonia (c). The temperature is modulated using a 6-frequency multi-sinusoidal signal.

**Table 7.18:** Validation results for the specific PLS calibration models. The harmonics of the FFT corresponding to the 6 frequencies of the multi-sinusoidal temperature-modulating signal were used as input data (information from sensors 2, 3 and 4 was used). Number of LV used, slope ( $m$ ) and correlation coefficient ( $r$ ) of the linear regression between real and predicted concentrations and root mean square error of cross-validation ( $RMSECV$ ).

Gases/mixture models ↓	Cross-validation results on training phase			
	LV#	$m$	$r$	RMSECV
Acetaldehyde	5	0.999	0.999	0.92
Ethylene	10	0.954	0.978	0.61
Ammonia	6	0.999	0.998	0.99
Ethylene + Acetaldehyde	9	0.936	0.945	12.13
		0.959	0.980	7.29
Ethylene + Ammonia	5	0.952	0.973	8.52
		0.981	0.985	3.58
Acetaldehyde + Ammonia	6	0.982	0.990	2.81
		0.968	0.985	3.57

### 7.3.6. Steady-state response.

The gas identification and quantification problem was re-considered using the steady-state sensor response, which is the traditional way to operate gas sensors. Identification and quantification tasks were attempted using the steady-state value of the normalized resistance change,  $(R/R_o)$ , experienced by the sensors in the presence of gases or gas mixtures. The static

normalized resistance change was defined as  $\frac{\Delta R}{R_o} = \frac{R - R_o}{R_o}$ , where  $R_o$  is the baseline

resistance (i.e. in the presence of dry air) and  $R$  is the steady-state resistance of the sensor in the presence of a given gas or gas mixture.

This study is of help to better assess the improvement in gas identification and quantification obtained by an optimized modulation of the sensors' operating temperature.

Remembering that, for every measurement, the steady-state response was stored before acquiring the transient response due to temperature modulation, a database with 165 steady-state measurements was available to perform this analysis (see sub-section 5.4.4).

Initially, the identification of gases was attempted. A fuzzy ARTMAP classifier, which used as inputs the steady-state response of the sensors within the array was built and validated using the leave-one-out approach. Gases and gas mixtures could be identified with a 81% success rate, which is significantly worse than the identification rate reached when transient information was used (e.g. 100% when using multi-sinusoidal temperature modulation). Table 7.19 shows a comparison of these results.

**Table 7.19:** Comparative success rates in gas and gas mixture identification using fuzzy ARTMAP classifiers (leave-one-out cross-validation) together with temperature modulation or steady-state methods.

	MLPRS	Multi-sinusoidal	Steady-state
Identification success rate (%)	87.3	100	81

The building of PLS calibration models was also envisaged. Like in previous cases, specific calibration models for every gas or gas mixture were built and validated. The process employed to determine the number of latent variables to be used and the validation procedures are identical to the ones described above. Table 7.20 summarizes the validation results for the different PLS models built. These results show that the concentration of the different gases can not be accurately estimated when using the steady-state sensor response only.

Improving the performance of micro-machined metal oxide gas sensors:  
 Optimization of the temperature modulation mode via pseudo-random sequences.

Therefore, these results prove that optimizing the temperature-modulation frequencies of metal oxide gas sensors is essential if quantitative gas analysis is to be performed.

**Table 7.20:** Validation results for the specific PLS calibration models. The steady-state sensor response was used. Number of LV used, slope ( $m$ ) and correlation coefficient ( $r$ ) of the linear regression between real and predicted concentrations and root mean square error of cross-validation ( $RMSECV$ ).

Gases/mixture models ↓	Cross-validation results on training phase			
	LV#	m	r	RMSECV
Acetaldehyde	3	0.9	0.9	8.2
Ethylene	3	0.86	0.89	16.2
Ammonia	3	0.93	0.91	6.36
Ethylene + Acetaldehyde	2	0.22	0.44	33.05
		0.86	0.92	14.0
Ethylene + Ammonia	3	0.81	0.89	16.60
		0.83	0.90	8.86
Acetaldehyde + Ammonia	3	0.82	0.88	9.17
		0.37	0.57	16.81

## 7.4. Conclusions.

A systematic method to determine which are the optimal temperature modulation frequencies to solve a given gas analysis problem has been discussed in detail, illustrated with a practical application and fully validated in two experiments within this chapter.

The optimization method is based on the use of multi-level pseudo-random sequences to modulate the working temperature of metal oxide gas sensors instead of the PRBS signals used in the previous chapter. One of the main reasons for considering multilevel signals instead of binary signals is that the former can provide a better estimate than the latter of the linear dynamics of a process with non-linearities. And it is well known that temperature-modulated metal oxide gas sensors present non-linearity in their response. Using this strategy, it has been shown that the best temperature modulating frequencies to discriminate and quantify gases using an array of 4 metal oxide gas sensors could be identified.

The consistency and robustness of the optimization method has been demonstrated in two experiments, which are described in chapter 5.

On the one hand, the method was applied to integrated arrays of tungsten oxide microhotplate gas sensors in the presence of ammonia, nitrogen dioxide and their binary mixtures at 3 different concentrations. It was shown that it was possible to find the modulating frequencies obtaining good results in the identification (93.33%) of the gases studied. A semi-quantitative analysis of the gases was possible too.

On the other hand, using this strategy, it has been shown that the best temperature modulating frequencies to discriminate and quantify gases (acetaldehyde, ethylene, ammonia and their binary mixtures) using an array of 4 metal oxide gas sensors could be identified.

In both cases a completely independent validation procedure was performed. The optimization process was conducted using multi-sinusoidal modulating signal (at frequencies extracted during frequency selection process). The same micro-sensor array for the former experiment was used while a different sensor array in the case of the second one was used. The validation process implied the use of a new set of measurements. This new set of measurements was based on a temperature-modulating multi-sinusoidal signal, the frequencies of which were a reduced set of the optimal ones. Using this database, it was shown that the different gases and gas mixtures could be perfectly discriminated and semi-quantified using a fuzzy ARTMAP classifier. After the identification process, the gases could be accurately quantified (*Experiment 4*) using specific PLS calibration models. Furthermore, the qualitative and quantitative results obtained using temperature-modulated sensors with optimized modulating frequencies compare very favorably with the results when the steady-state sensor response is used.

Summarizing, the method for selecting the optimal modulating frequencies has been shown to be consistent and effective. The method is illustrated with the quantitative analysis of three species and their binary mixtures (related to the conservation of climacteric fruit) using an array of metal oxide gas micro-sensors. However, the method applies generally and can be used in any gas analysis problem or extended to other type of sensors (e.g. conducting polymer sensors).

Additionally, exclusively for *Experiment 3*, phase space methods combined with temperature-modulated metal oxide gas sensors were introduced for the first time in the analysis and evaluation of gas sensor responses. In this case, good results were obtained not only ameliorating the discrimination rate, but also dramatically reducing the time needed to perform measurements.

Improving the performance of micro-machined metal oxide gas sensors:  
Optimization of the temperature modulation mode via pseudo-random sequences.

## 7.5. References.

- [1] A. Vergara, E. Llobet, J. Brezmes, P. Ivanov, X. Vilanova I. Gràcia, C. Cané and X. Correig, "Optimised Temperature Modulation of Metal Oxide Micro-Hotplates Gas Sensors through Multi-Level pseudo random sequences", *Sensors and Actuators B*, vol. 111-112, pp. 271-280, 2005.
- [2] G. Carpenter, S. Grossberg, N. Markuzon, J. Reynolds, and D. Rosen, "Fuzzy ARTMAP: A neural network architecture for incremental supervised learning of analog multidimensional maps", *IEEE Trans. Neural Nets.*, vol. 3, (5), pp. 698-713, 1992.
- [3] R. Ionescu, E. Llobet, X. Vilanova, J. Brezmes, J.E. Suerias, J. Calderer, X. Correig, "Quantitative analysis of NO<sub>2</sub> in the presence of CO using a single tungsten oxide semiconductor sensor and dynamic signal processing", *Analyst*, vol. 127, pp. 1237-1246, 2002.
- [4] A. Vergara, E. Llobet, E. Martinelli, C. Di Natale, A. D'Amico, X. Correig, "Feature extraction of metal oxide gas sensors using dynamic moments", *submitted* to *Sensors and Actuators B*, 2006.
- [5] A. Vergara, E. Llobet, J. Brezmes, P. Ivanov, C. Cané, I. Gràcia, X. Vilanova, X. Correig, "Quantitative gas mixture analysis using temperature-modulated micro-hotplate gas sensors: Selection and validation of the optimal modulating frequencies", *submitted* to *Analytical Chemistry*, 2006.
- [6] P. Geladi, B.R. Kowalski, "Partial least squares regression: a tutorial", *Anal. Chim Acta*, vol. 185, pp. 1-17, 1986.



---

# 8.

# Conclusions

---

<b>8. CONCLUSIONS</b> .....	<b>197</b>
<b>8.1. Conclusions.</b> .....	<b>198</b>

## Improving the performance of micro-machined metal oxide gas sensors: Optimization of the temperature modulation mode via pseudo-random sequences.

### 8.1. Conclusions.

In the last years, the lack of reproducibility, stability and selectivity have been considered as one of the major problems in gas sensing systems based on metal oxide gas sensors devices. Thermal modulation of metal oxide gas sensors has been one of the most used methods to enhance sensor selectivity and counteracting these shortcomings. Nevertheless, the selection of the frequencies used to modulate the working temperature had remained until now, an empirical process.

In this doctoral thesis we developed a systematic method to determine which are the optimal temperature modulation frequencies to solve a given gas analysis problem. This method, which is borrowed from the field of system identification, has been developed and introduced for the first time in the area of gas sensors. The method has been discussed in detail, illustrated with a practical application and fully validated in this field.

The method consists of studying the sensor response to gases when their operating temperature is modulated via maximum-length pseudo-random sequences (either binary or multi-level). Such signals share some properties with white noise and, therefore, can be of help to estimate the linear response of a system with non-linearity (e.g., the impulse response of a sensor-gas system).

The optimization process is conducted by selecting among the spectral components of the impulse response estimates, the few that better help either discriminating or quantifying the target gases of a given gas analysis application. In this case in particular those spectral components were computed via the Fast Fourier Transform (FFT). Since spectral components are directly related to modulating frequencies, the selection of spectral components results in the determination of the optimal temperature modulating frequencies. The pattern recognition algorithms used range from linear, (i.e., unsupervised as Principal component analysis (PCA), or supervised as partial least squares (PLS) and PLS-DA), to artificial neural networks such as the fuzzy ARTMAP neural networks.

In the first experiments, pseudo-random binary signals (PRBS) were employed to modulate the working temperature of micro-machined metal oxide gas sensors in a frequency range from 0 up to 112.5 Hz. The upper frequency is slightly higher than the cutoff frequency of the sensor membranes. The outcome of this initial study was that the important modulating frequencies were in the range between 0 and 1 Hz. This is understandable, since the kinetics of reaction and adsorption processes taking place at the sensor surface are slow and if these are to be altered by the thermal modulation, low frequency modulating signals need to be devised. This explains why low-frequency

temperature-modulating signals (i.e. in the mHz range) have been used with micro-hotplate gas sensors, even though the thermal response of their membranes is much faster (typically, near 100 Hz). So from this point of view the temperature modulating frequency range under study was reduced to range from 0 up to near 1 Hz.

In the experiments that followed the first ones, an evolved method to determine the optimal temperature modulating frequencies for micro-hotplate gas sensors was introduced, which was based on the use of maximum length multilevel pseudo-random sequences (MLPRS). Multilevel signals were considered instead of the binary ones because the former can provide a better estimate than the latter of the linear dynamics of a process with non-linearity. And it is well known that temperature-modulated metal oxide gas sensors present non-linearity in their response.

These systematic studies were fully validated by synthesizing multi-sinusoidal signals at the optimal frequencies previously identified using pseudo-random sequences. When the sensors had their operating temperatures modulated by a signal with a frequency content that corresponded to the optimal, the gases and gas mixtures considered could be perfectly discriminated and the building of accurate calibration models to predict gas concentration (after identification process) was found to be possible. In some cases, the validation process was conducted on sensors that had not been used for optimization purposes (e.g. a different sensor array from the same fabrication batch). Furthermore, the qualitative and quantitative results obtained using temperature-modulated sensors with optimized modulating frequencies compare very favorably with the results when the steady-state sensor response is used.

Additionally, in this doctoral thesis, a novel feature extraction method called Dynamic Moments (DM) and Phase Space (PS) combined with temperature-modulated metal oxide gas sensors were introduced and tested for the first time in the analysis and evaluation of gas sensor responses. In this case, good results were obtained not only in the discrimination rate, but also dramatically reducing the time needed to perform measurements.

The main conclusion that can be drawn from this thesis is that an optimized thermal modulation of their working temperature can significantly increase the selectivity of metal oxide sensors. Therefore, the systematic optimization process to implement the selection of modulating frequencies developed permits to ensure a significant increase in performance for metal oxide based multisensor systems. The simplicity of the methods implemented makes them suitable for the development of low-cost gas analysers and hand-held e-noses. The method applies generally and can be used in any gas analysis problem or extended to other type of sensors (e.g. conducting polymer sensors). Finally, we can envisage that for each gas-sensor pair, the modulating frequencies selected could be related to characterize the

**Improving the performance of micro-machined metal oxide gas sensors:**

**Optimization of the temperature modulation mode via pseudo-random sequences.**

interaction between the metal oxide layer and the gas (e.g. film microstructure, surface diffusion and reaction kinetics).

The scientific contributions of this thesis are collected in four journal papers and thirteen conference proceedings.

---

# 9.

## Annex: List of Publications

---

<b>9. ANEX: LIST OF PUBLICATIONS</b> .....	<b>201</b>
<b>9.1. Publications directly derived from this doctoral thesis.</b> .....	<b>202</b>
<b>9.2. Others related publications.</b> .....	<b>202</b>
<b>9.3. Conferences.</b> .....	<b>203</b>

Improving the performance of micro-machined metal oxide gas sensors:  
Optimization of the temperature modulation mode via pseudo-random sequences.

## 9.1. Publications directly derived from this doctoral thesis.

- [1] **A. Vergara**, E. Llobet, J. Brezmes, P. Ivanov, X. Vilanova I. Gràcia, C. Cané and X. Correig, “Optimized temperature modulation of micro-hotplate gas sensors through pseudorandom binary sequences”, *IEEE Sensor Journal*, vol. 5, (6), pp. 1369-1378, 2005.
- [2] **A. Vergara**, E. Llobet, J. Brezmes, P. Ivanov, X. Vilanova I. Gràcia, C. Cané and X. Correig, “Optimised Temperature Modulation of Metal Oxide Micro-Hotplates Gas Sensors through Multi-Level pseudo random sequences”, *Sensors and Actuators B*, vol. 111-112, pp. 271-280, 2005.
- [3] **A. Vergara**, E. Llobet, E. Martinelli, C. Di Natale, A. D’Amico, X. Correig, “Feature extraction of metal oxide gas sensors using dynamic moments”, *Sensors and Actuators B*, *in press* 2006.
- [4] **A. Vergara**, E. Llobet, J. Brezmes, P. Ivanov, C. Cané, I. Gràcia, X. Vilanova, X. Correig, “Quantitative gas mixture analysis using temperature-modulated micro-hotplate gas sensors: Selection and validation of the optimal modulating frequencies”, *submitted to Sensors and Actuators B*, 2006.
- [5] **A. Vergara**, E. Martinelli, E. Llobet, C. Di Natale, A. D’Amico, “An alternative global feature extraction of temperature modulated  $\mu$ -hotplate gas sensors array using an Energy Vector approach”, in preparation to be submitted to *Sensors and Actuators B*, 2006.

## 9.2. Others related publications.

- [6] M. Vinaixa, **A Vergara**, C. Duran, E. Llobet, C. Badia, J. Brezmes, X. Vilanova and X. Correig, “Fast detection of rancidity in potato crisps using e-noses based on mass spectrometry or gas sensors”, *Sensors and Actuators B*, vol. 106, pp. 67-75, 2005.
- [7] P. Ivanov, E. Llobet, **A. Vergara**, M. Stankova, X. Vilanova, J. Hubalek, I. Gracia, C. Cané, X. Correig, “Towards a micro-system for monitoring ethylene in warehouses”, *Sensors and Actuators B*, vol. 111-112, pp. 63-70, 2005.

- [8] P. Ivanov, E. Llobet, F. Blanco, **A. Vergara**, J. Brezmes, X. Vilanova, I. Gracia, C. Cané, X. Correig, “On the effects of the materials and the noble metal doping to NO<sub>2</sub> detection”, *Sensors and Actuators B, in press*, 2006.
- [9] **A. Vergara**, E. Martinelli, E. Llobet, C. Di Natale, “Landscaping Report, CoE Software”, Network of Excellence on General Olfaction and Sensing Projects on a European Level (GOSPEL), [www.gospel-network.org](http://www.gospel-network.org), 2006.

### 9.3. Conferences.

- [10] **A. Vergara**, E. Llobet, J. Brezmes, “Identificación de sensores de gases mediante secuencias pseudo-aleatorias”, Book of Abstracts of SAAEI 2003 CD Version, Vigo Spain, 2003.
- [11] **A. Vergara**, E. Llobet, J. Brezmes, M. Stankova, P. Ivanov, X. Correig, I. Gràcia, C. Cané, X. Correig, “MLS based temperature modulation of micro-hotplates”, Book of Abstracts of IEEE Sensors 2003, Toronto, Canada, pp. 1255-1259, October 2003.
- [12] M. Vinaixa, C. Duran, **A Vergara**, E. Llobet, C. Badia, J. Brezmes, X. Vilanova, X. Correig, “Fast detection of rancidity in potato crisps using e-noses based on MS or gas sensors”, Book of abstracts ISOEN 2003, Riga, Latvia, pp. 105-108, 2003.
- [13] **A. Vergara**, E. Llobet, J. Correa, “MLS-based temperature modulation of micro-hotplates”, Poster in the 1st Nano-electronic and photonic systems workshop, Book of abstracts ISBN: 84-8424-023-1, Tarragona Spain, pp. 30 - 31, 2003.
- [14] **A. Vergara**, E. Llobet, J. Brezmes, P. Ivanov, X. Vilanova I. Gràcia, C. Cané and X. Correig, “Optimised temperature modulation of metal oxide micro-hotplate gas sensors through multi-level PRS”, Proceedings of the XVIII Eurosensors Conference, pp. 614-615, Rome, Italy, September 2004.
- [15] P. Ivanov, E. Llobet, M. Stankova, **A. Vergara**, X. Vilanova, J. Hubalek, I. Gracia, C. Cané, X. Correig, “Towards a microsystem for monitoring ethylene in warehouses”, Proceedings of the XVIII Eurosensors Conference, pp. 604-605, Rome, Italy, September 2004.
- [16] **A. Vergara**, E. Llobet, J. Brezmes, M. Stankova, X. Vilanova I. Gràcia, C. Cané and X. Correig, “Optimized multi-frequency temperature modulation of micro-hotplate gas sensors”, Book of Abstracts of IEEE Sensors 2004, Vienna, Austria, October 2004.

Improving the performance of micro-machined metal oxide gas sensors:  
Optimization of the temperature modulation mode via pseudo-random sequences.

- [17] E. Llobet, **A. Vergara**, J. Brezmes, R. Ionescu, "Temperature modulated gas sensors: Selection of modulating frequencies through noise methods", Proceedings of SPIE Vol. 5472, SPIE Noise and Information in Nanoelectronics, Sensors and Standards II, pp. 152-162, Maspalomas, Gran Canaria Spain, 2004.
- [18] **A. Vergara**, E. Martinelli, E. Llobet, C. Di Natale, A. D'Amico, "Feature extraction of metal oxide gas sensor through dynamic moments", Proceedings of ISOEN 2005, ISOEN 2005 11th International Symposium on Olfaction and Electronic Nose, pp. 40 - 42, Barcelona, Spain, 2005.
- [19] P. Ivanov, E. Llobet, F. Blanco, **A. Vergara**, J. Brezmes, X. Vilanova, I. Gracia, C. Cané, X. Correig, "On the effects of the materials and the noble metal doping to NO<sub>2</sub> detection", Proceedings of the 19th European Conference on Solid-State Transducers Eurosensors XIX, Barcelona Spain, pp. 604-605, 2005.
- [20] **A. Vergara**, E. Llobet, "MLS - Contribution to the selection of temperature modulation frequencies for metal oxide micro-hotplates gas sensors using MLPRS", Poster in the 3th Nano-electronic and photonic systems workshop, Book of abstracts ISBN: 84-8424-023-1, Tarragona Spain, pp 35 - 36, 2005.
- [21] **A. Vergara**, E. Llobet, J.L. Ramírez, P. Ivanov, L. Fonseca, S. Zampolli, A. Scorzoni, T. Becker, S. Marco, J. Wöllenstein, "An RFID reader with onboard sensing capability for monitoring fruit quality", Eurosensors XX, Göteborg, 2006, to be presented.
- [22] **A. Vergara**, E. Martinelli, A. D'Amico, E. Llobet, C. Di Natale, "Feature extraction of thermally modulated  $\mu$ -hotplate gas sensors: the energy matrix approach", Eurosensors XX, Göteborg, 2006, to be presented.



---

# Appendix

---

<b>APPENDIX</b>	<b>205</b>
<b>A.1. Introduction.</b>	<b>206</b>
<b>A.2. Continuous flow system: calculating flow values.</b>	<b>206</b>
A.2.1. Example of a calculation.	208
<b>A.3. Electronic board system construction.</b>	<b>209</b>
<b>A.4. Generation algorithm of the modulating signals.</b>	<b>215</b>
A.4.1. Generation algorithm of the PRBS modulating signal.	215
A.4.2. Generation algorithm of the MLPRS modulating signal.	216
A.4.3. Generation code of the multi-sinusoidal modulating signal.	217
<b>A.5. References.</b>	<b>220</b>

## Improving the performance of micro-machined metal oxide gas sensors: Optimization of the temperature modulation mode via pseudo-random sequences.

### **A.1. Introduction.**

The objective of this appendix is to add some important details that were skipped in the previous chapters. Most of its content is related to the experimental set-up described in Chapter 5. Therefore, the complete set of formulae employed to find the set points of the mass-flow controllers in order to obtain the desired concentrations of simple gases and gas mixtures is reviewed in the first section of this appendix. Additionally, the architecture and the PCB diagrams of the voltage-controlled current sources (Howland circuits) used to modulate the operating temperature of the sensors and of the data acquisition boards employed are given in the second section of this appendix. Finally, the algorithms implemented to generate the binary or multi-level pseudo-random signals and the multi-sinusoidal signals are introduced in the last section of this appendix.

### **A.2. Continuous flow system: calculating flow values.**

As was mentioned in chapter 5, the first part of the continuous flow system is known as gas flow system. This is composed by a cabin where the gases are stored under high pressure in calibrated bottles, a gas transport system, and a mass flow system. Between every bottle and the gas transport system there are valves which allow switching from very high pressures to regular atmosphere pressure (i.e. from 200 b to 2 b) (see figure 5.7).

Furthermore, the gas transport system was made of different metallic tubes connected to several manual “valves” (pressure regulators), which enable the gases to flow. These tubes are connected to the mass flow system which creates the desired concentrations of gases and gas mixtures.

To get the desired concentration of a single gas or a mixture of gases with high precision, three different mass flow devices (Bronkhorst hi-tech 7.03.241) are used. These devices are controlled by a desktop PC that works as a mass flow controller. Each one of the mass flow meters is calibrated with synthetic air (this does not lead to significant errors since in the experiments performed the analytes measured are highly diluted in air). These devices incorporate mass sensors (MEM technology) which work in the following way: they have a silicon resistance exposed to the gas flow; when the flow changes, the temperature of the resistor is bound to change (according to a relation which depends on the calibration). Such temperature change is detected by monitoring the resistance values. Every mass flow meter has a 1% resolution. In order to reach the different gas concentrations desired (i.e., from

some ppm to high concentrations) the 3 mass flow devices used have different maximum flow levels. Two of them (those labeled as MF2 and MF3) can also be combined between them to reach even higher concentration of a single pollutant gas. These levels are shown as follow:

- MF1: gas 1, maximum flow 400 sccm (standard cubic centimeters per minute)
- MF2: gas 1, maximum flow 100 sccm
- MF3: gas 2, maximum flow 15 sccm

The test chamber where sensors are placed has a volume of 20 ml. We want to keep a constant flow of 200 sccm (i.e. 200 ml per minute) (see figure 5.8). In order to obtain the gas/gas mixtures concentrations and keep constant the total flow, we give a list of formulae that have been used to regulate the mass flow devices (values expressed in sccm) for each type of analyte. These formulae are expressed as follows:

**1. Calculating the flow values (in sccm) obtained from each bottle according to their level of analyte dilution:**

$$\begin{aligned} sccm's\_GAS1 &= ((\%1MF\_2 \times 100) + (\%1MF\_3 \times 15)) \times \%1Dilution\_bottle\_1 \\ sccm's\_GAS2 &= (\%1MF\_3 \times 15) \times \%1Dilution\_bottle\_2 \end{aligned} \quad (A.1)$$

where:

- $\%1MF\_i$  ( $i=1, \dots, 3$ ) indicates the opening degree percentage selected by the mass flow controller;
- $\%1Dilution\_bottle\_1$  and  $\%1Dilution\_bottle\_2$  indicate the percentage values of analyte dilution in the gas bottles we are using.

**2. Calculating the opening degree of MF1 (synthetic air):**

$$MF\_1 = \frac{(200 - (sccm1 \times MF\_2 + sccm2 \times MF\_3)) \times 100}{200} \quad (A.2)$$

where:

$sccm_i \cdot MF\_i$  ( $i=1 \dots 3$ ) is the resulting product of the maxim sccm flow value (in percentage) times the opening degree of the corresponding mass flow device (absolute value).

**3. Determining the mixture gas final flow:**

$$\begin{aligned} sccm's\_bottle1 &= (\%1MF\_2 \times 100) + (\%1MF\_3 \times 15) \\ sccm's\_bottle2 &= (\%1MF\_3 \times 15) \end{aligned} \quad (A.3)$$

$$Total\_flow = sccm's\_bottle1 + sccm's\_bottle2 + (MF\_1 \times 200) \quad (A.4)$$

Improving the performance of micro-machined metal oxide gas sensors:  
 Optimization of the temperature modulation mode via pseudo-random sequences.

**4. Calculating the ppm concentrations for both gases:**

$$[c]_{GAS1} = \frac{sccm's\_GAS1}{Total\_Flow} \times 1 \cdot 10^6 \quad \text{and} \quad [c]_{GAS2} = \frac{sccm's\_GAS2}{Total\_Flow} \times 1 \cdot 10^6 \quad (A.5)$$

**A.2.1. Example of a calculation.**

What follows is an example of the way these formulae have been used. Let us consider that the values below are the given data to work with:

$$Dilution\_bottle\_1(Ethylene) = 0.02\%$$

$$Dilution\_bottle\_2(Ammonia) = 0.1\%$$

$$C\_gas1 = 50\text{ ppm} \quad ; \quad C\_gas2 = 50\text{ ppm} \quad ;$$

$$sccm1 = 100 \quad ; \quad sccm2 = 15$$

The results are the following.

As the desired concentrations (in ppm) of the pollutant gases are given, then from equation A.5 then, the concentrations (in sccm) can be estimated:

$$1. \quad sccm's\_GAS1 = \frac{50.0\text{ ppm}}{1 \cdot 10^6} \cdot 200 = 0.01\text{ sccm}$$

$$sccm's\_GAS2 = \frac{50.0\text{ ppm}}{1 \cdot 10^6} \cdot 200 = 0.01\text{ sccm}$$

therefore, knowing the flow values (in sccm) of each specie, the opening degree percentage from each mass flow controller and pollutant gas bottle according to their level of analyte dilution can be calculated (see eq. A.1):

$$2. \quad \%MF\_2 = 100 \times \frac{0.02}{(100 \times 0.01)} = 0.5 = 50\%$$

$$\%MF\_3 = 100 \times \frac{0.01}{(0.1 \times 15)} = 0.666 = 66.6\%$$

Once the opening degree percentage from each mass flow controller has been estimated, the opening degree percentage from the mass flow controller 1 is calculated (see eq. A.2):

$$3. \quad MF\_1 = \frac{(200 - ((1 \times 50) + (0.15 \times 66.6))) \times 100}{200} = 70.005\%$$

Finally, determining the mixture gas final flow is done (see eqs. A.3 and A.4):

$$sccm's\_bottle1 = (0.5 \times 100) = 50$$

$$4. \quad sccm's\_bottle2 = (0.666 \times 15) = 9.99$$

$$Total\_Flow = 50 + 9.99 + (70.005 \times 2) = 200$$

### A.3. Electronic board system construction.

The test chamber, where sensors are placed when measuring (see figure 5.8), is connected to different electronic boards the missions of which are as follows:

- To supply the gas sensors with the required operation voltages, for feeding both the sensor heating resistors and the voltage dividers employed to acquire the resistance of the sensors. (Howland voltage-controlled current sources electronic board).
- To acquire the dynamic responses of gas sensors and the voltage drop over their heating elements in order to monitor their temperature. Sensor resistances were acquired in a half-bridge configuration. (Sensor conditioning and voltage divider electronic board).

Each sensor can be conveniently represented by the following model (Figure A.1):

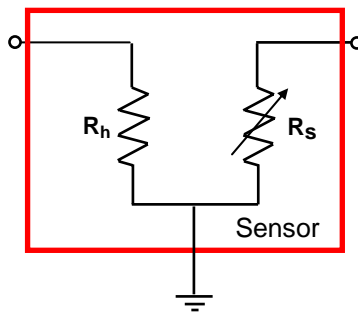


**Figure A.1:** Schematic diagram of a micro-hotplate gas sensor.

The sensor conditioning electronic board supplies the voltage divider between the active film resistance ( $R_s$ ) of each gas sensor and its corresponding load resistance ( $R_L$ ) with the required operation voltage (5V) (see figure 5.9 (right)). Load resistances are placed in this electronic board. Additionally, this board injects the operation signal (i.e., a fixed current or a modulating current) to the polysilicon heating element (heater Resistance ( $R_h$ )) of each gas sensor, supplied from the output of the **current voltage-controlled source** electronic board. The  $R_h$  parameters (polysilicon thermal coefficient  $\alpha$ ) and the current values are known (they are chosen when designing the experiment and kept independent of the  $R_h$  oscillating values

Improving the performance of micro-machined metal oxide gas sensors:  
 Optimization of the temperature modulation mode via pseudo-random sequences.

thanks to the current source circuits, hence the switch from the current modulation values to the temperature modulation values is obvious. Since:

$$R(T_0) = R(1 + \alpha\Delta T) \tag{A.6}$$

then,

$$\frac{R(T) - R(T_0)}{R(T_0)} = \alpha(T - T_0) = \alpha\Delta T \tag{A.7}$$

where R(T) is calculated by dividing the measured tension across it by the known current value.

The modulated or fixed operation current injected to the polysilicon heating resistance of each micro-sensor is supplied by a Howland voltage-controlled current source. Such circuit receives the exciting voltage signal (from the PC) and converts it in a current signal. It is designed in a way that, receiving as input voltages in the order of a few Volt, gives as output currents in the order of a few mA (i.e. the transconductance of the device is 10<sup>-3</sup> Ω<sup>-1</sup>).

The input signal to the Howland voltage-controlled current source comes from the PC and it is an operation signal (e.g., it could be a fixed voltage, a PRS modulating signal (either binary or multilevel), and/or a multi-sinusoidal modulated signal). It is important to remark that the output current is not a function of the loading resistance (R<sub>h</sub>). So from Figure A. 2 we can deduce:

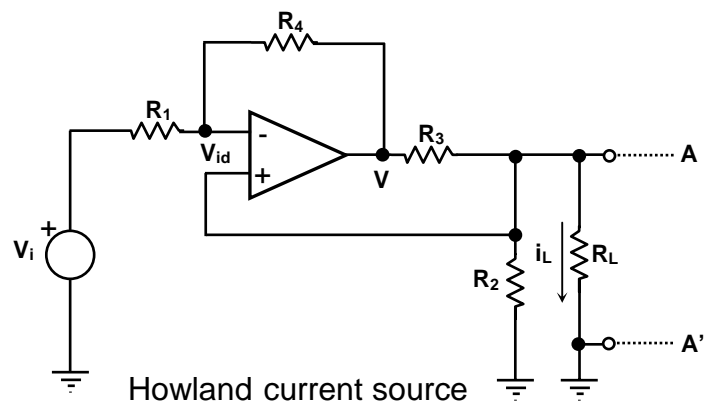


**Figure A. 2:** Schematic diagram of a Howland voltage-controlled current source.

Therefore, short-circuiting the terminals A-A', obtaining then the Norton circuit equivalent, we have the following scheme:

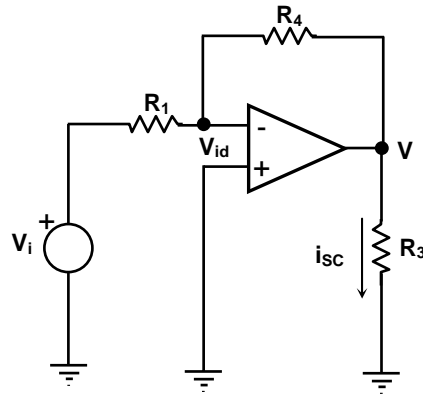


**Figure A.3:** Circuit employed to find the short-circuit current.

where the short circuit current ( $i_{SC}$ ) is given by:

$$i_{SC} = -\frac{R_4}{R_1 R_3} V_i \quad (\text{A.8})$$

therefore, from Figure A. 2 if we connect a voltage generator instead of the  $R_L$ , the equivalent resistance of the circuit ( $R_{eq}$ ) can be calculated as follows:

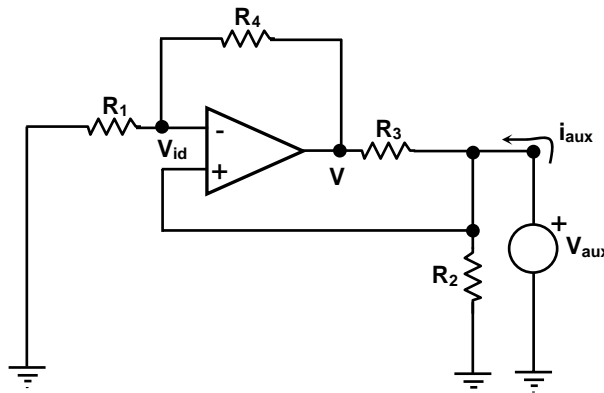


**Figure A.4:** Howland current source connected to a voltage generator in stead of the  $R_L$

Firstly, the current aux  $i_{aux}$  of the circuit is given by:

$$i_{aux} = \frac{V_{aux}}{R_2} + \frac{V_{aux} - V_{aux}(1 + R_4 / R_1)}{R_3} = V_{aux} \left( \frac{1}{R_2} - \frac{R_4}{R_1 R_3} \right) \quad (\text{A.9})$$

from eq. A-9 we obtain that the  $R_{eq}$  is:

Improving the performance of micro-machined metal oxide gas sensors:  
 Optimization of the temperature modulation mode via pseudo-random sequences.

$$R_{eq} = \frac{V_{aux}}{i_{aux}} = \frac{R_1 R_2 R_3}{R_1 R_3 - R_2 R_4} \quad (\text{A.10})$$

In this particular case, as the relation  $R_1 R_3 = R_2 R_4$  exists, the previous circuit then behaves as an ideal current voltage-controlled source, where the  $R_{eq} \rightarrow \infty$ . Its Norton equivalent model is as follows:

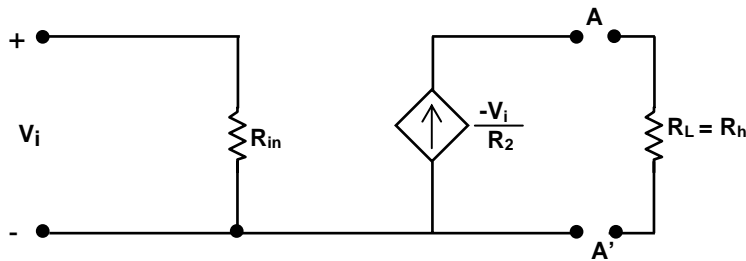


**Figure A.5:** Norton equivalent model of the Howland voltage-controlled current source where  $R_{eq} \rightarrow \infty$ . Then the current value at the output of the circuit is equivalent to the input voltage control but divided by 1000.

Where  $R_L$  is the resistance of the heating element of the sensor  $R_h$ .

So, the excitation current in range of mA corresponds to the  $V_i$  value but divided by 1000. The fact that these current levels are sufficient to successfully excite the operating temperature of these gas sensors is an immediate consequence of the low power consumption that has been achieved with micromachining technology. Low thermal inertia means low current levels (hence low power consumption) and fast time responses.

The voltage across  $R_S$  is measured and stored by the PC (see Figure 5.7 of chapter 5). The load resistance  $R_L$  in the voltage divider is a high precision resistance, with a tolerance as low as 1%. Its precision is crucial since its value is directly connected to the measurement of the sensor response: we obviously need good resolution in the measurement of  $R_S$  and thus we need the value of load resistances to be precise enough:

$$\frac{V_{DD} - V_{out}}{R_L} = \frac{V_{out}}{R_S} \quad (\text{A.11})$$

The load resistance  $R_L$  in the scheme corresponds on the board to two possible values: there is a jumper connected to two high precision load resistors (of 1 M $\Omega$  or 10 M $\Omega$ ) and it is possible to switch manually to one or to the other according to our particular needs (i.e. the resistance of the sensing film). However, usually the 1 M $\Omega$  resistance is enough.



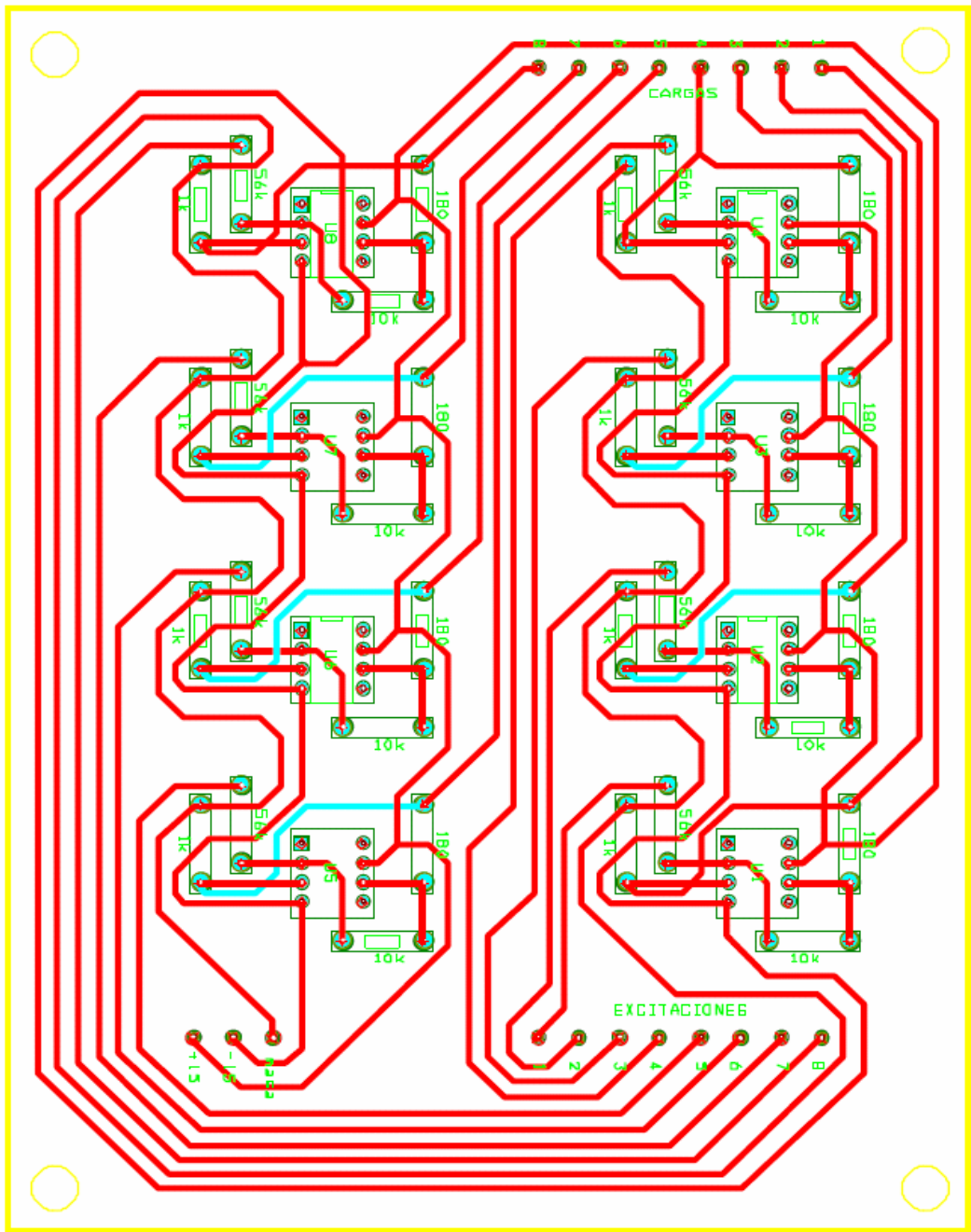


**Figure A.6:** Schematic layout of the Howland voltage - controlled current source board.

Improving the performance of micro-machined metal oxide gas sensors:  
Optimization of the temperature modulation mode via pseudo-random sequences.

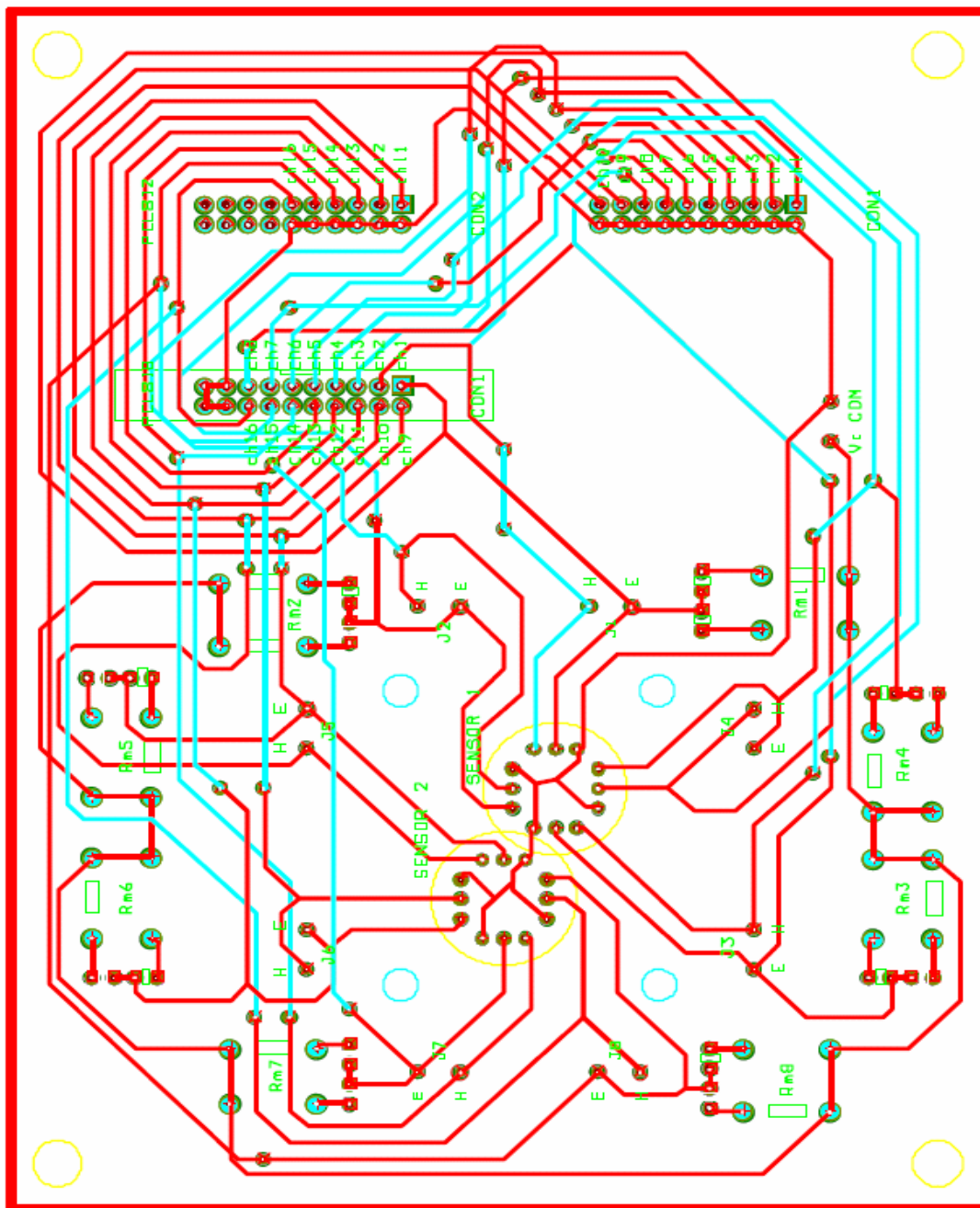


**Figure A.7:** Schematic layout of the sensor conditioning and voltage divider electronic board.

For each sensor there is one current source and one voltage divider. Therefore on the actual sensor conditioning board we have 8 times replicated the basic block shown in Figure A. 2. We show in Figure A.6 the layout of the Howland voltage-controlled current sources electronic board. Figure A.7 shows the layout of the sensor conditioning and voltage-divider electronic board.

## A.4. Generation algorithm of the modulating signals.

Within this appendix, the algorithms used to generate the pseudo-random sequences (binary or multi-level signals) and the multi-frequency sinusoidal signal used to modulate the working temperature of the micro-hotplate gas sensor are presented.

### A.4.1. Generation algorithm of the PRBS modulating signal.

One of the most useful types of periodic signal for process identification is the pseudo-random binary sequence (PRBS) [1-4]. The properties of these signals were introduced and discussed in chapter 4, specifically in section 4.4. As was mentioned there a PRBS of length  $L$  is generated by an  $n$ -stage shift register with an OR-exclusive logic gate feedback to the first stage. The XOR gate performs a modulo 2 addition. Such a circuit goes through a set of states and eventually repeats itself after  $2^n-1$  clock pulses. An example of shift register circuit that generates a sequence of length  $L=7$  was presented in Figure 4.2, where it is seen that the shift register can be started with any binary number excepted 0, 0, 0 (which would give a sequence of length unity).

As was mentioned in chapter 4 and 5 a written-in-house MATLAB program running on a PC platform was in charge of generating the PRBS. The algorithm for the generation, in MATLAB environment, of the PRBS from order 3 up to order 18 is presented as follows:

```
% PRBS signal generator.  
if exist('N') ~= 1; N= 9; end;  
if N == 18; taps=[0 0 0 0 0 0 0 0 0 1 0 0 0 0 0 0 1]; end;  
if N == 17; taps=[0 0 0 0 0 0 0 0 0 0 0 0 0 1 0 0 1]; end;  
if N == 16; taps=[0 0 0 1 0 0 0 0 0 0 0 0 1 0 1 1]; end;  
if N == 15; taps=[0 0 0 0 0 0 0 0 0 0 0 0 1 1]; end;  
if N == 14; taps=[0 0 0 1 0 0 0 1 0 0 0 0 1 1]; end;  
if N == 13; taps=[0 0 0 0 0 0 0 0 1 1 0 1 1]; end;  
if N == 12; taps=[0 0 0 0 0 1 0 1 0 0 1 1]; end;  
if N == 11; taps=[0 0 0 0 0 0 0 0 1 0 1]; end;  
if N == 10; taps=[0 0 0 0 0 0 1 0 0 1]; end;
```

## Improving the performance of micro-machined metal oxide gas sensors: Optimization of the temperature modulation mode via pseudo-random sequences.

```

if N == 9; taps=[0 0 0 0 1 0 0 0 1]; end;
if N == 8; taps=[0 0 0 1 1 1 0 1]; end;
if N == 7; taps=[0 0 0 1 0 0 1]; end;
if N == 6; taps=[0 0 0 0 1 1]; end;
if N == 5; taps=[0 0 1 0 1]; end;
if N == 4; taps=[0 0 1 1]; end;
if N == 3; taps=[0 1 1]; end;
M = 2^N-1;
m = [zeros(1,N-1) 1];
%m = ones(1,N);
regout = zeros(1,M);
for ind = 1:M
    buf = mod(sum(taps.*m),2);
    m(2:N) = m(1:N-1);
    m(1)=buf;
    regout(ind) = m(N);
end
    
```

Where “ $N$ ” is the length of the PRBS signal, “ $taps$ ” is the feedback shift register configuration (i.e., shift registers values according to their length) of the binary  $m$ -sequences, “ $m$ ” is the vector of combinations of “0” and “1” such the modulo 2 sum starts. The variable “ $buf$ ” is the modulo 2 sum between the product of the initial combination vector and the configuration of the shift registers of the  $m$ -sequences. Finally “ $ragout$ ” is the output vector with the PRBS signal combination. For example for a PRBS signal of length 511 (i.e.,  $2^9-1 = 511$ ) the feedback shift register configuration is [0 0 0 0 1 0 0 0 1] according to a primitive binary polynomial (modulo 2). A list of primitive polynomials can be found in [1, 4]. This example is the PRBS signal used in *Experiment 2*.

### A.4.2. Generation algorithm of the MLPRS modulating signal.

The theory behind the generation of multilevel pseudo random sequences (MLPRS) based on multilevel maximum length signals is well developed and presents similar characteristics than the binary ones. Remembering what in chapter 4 was discussed, MLPRS exist for the number of levels,  $q$ , equal to a prime or a power of a prime  $p(>1)$ , i.e. for  $q = 2, 3, 4, 5, 7, 8, 9, 11, 13, \dots$  (Zierler, 1959), [4, 5]. The length  $L$  of such a sequence  $\{x_r\}$  is  $q^n-1$ , where  $n$  is an integer. After  $q^n-1$  digits, the sequence repeats itself. MLPRS signals are generated in a similar manner than the binary ones using a shift register and modulo addition. The generator of such a sequence and an example of a 5-level sequence (fragment) were shown in chapter 4, specifically in Figure 4.3 (a) and (b). Once again, the MATLAB

environment was used to generate a code, which can synthesize the MLPRS signal. The MATLAB code to generate an MLPRS signal of  $q = 5$  levels and order  $n = 4$  is presented as follows:

```
%MLPRS signal Generation
%v is the shift register Start and  $L=(q^n)-1$  where  $n = 4$ 
%c are the values of the multiplied by coefficients [4]
v=[1 0 0 0];
C=[0 1 1 2];
for i=1:624,
    Vo=v(1)*C(1)+v(2)*C(2)+v(3)*C(3)+v(4)*C(4);
    Vo=mod(Vo,5);
    v(4)=v(3);
    v(3)=v(2);
    v1(i)=v(2);
    v(2)=v(1);
    v(1)=Vo;
    output(i)=Vo;
    output1=v1;
end
```

Where “ $v$ ” is the vector of initial values of the shift registers, “ $C$ ” is the feedback shift register configuration for some  $q$ -level  $m$ -sequence of length  $N=q^n-1$ . “ $Vo$ ” is the modulo  $q$  sum of the shift registers. Finally the MLPRS signal is in the variable labeled as “ $output$ ”. The feedback shift registers connection table (with modulo  $q$ ) for generating  $q$ -level  $m$ -sequences are given in the primitive polynomials listing of Church in 1935 [6].

### A.4.3. Generation code of the multi-sinusoidal modulating signal.

In the last step of this Appendix, the generation of the multi-sinusoidal modulating signal is presented. Once the optimal modulating frequencies for discrimination and quantification have been selected, these frequencies are taken to synthesize the multi-frequency sinusoidal modulating signal. This multi-frequency signal is generated by a sum of the different sinusoidal signals at different frequencies. Figure 7.10 in chapter 7 shows an example of the procedure of generating this signal at 6 different frequencies. As in the case of generating the pseudorandom sequences, this signal is generated in a MATLAB code that at the same time it calls to a SIMULINK code which in charges of generating the signals.

The SIMULINK code used for the generation of the multi-sinusoidal signal is shown in Figure A. 8.

Improving the performance of micro-machined metal oxide gas sensors:  
Optimization of the temperature modulation mode via pseudo-random sequences.

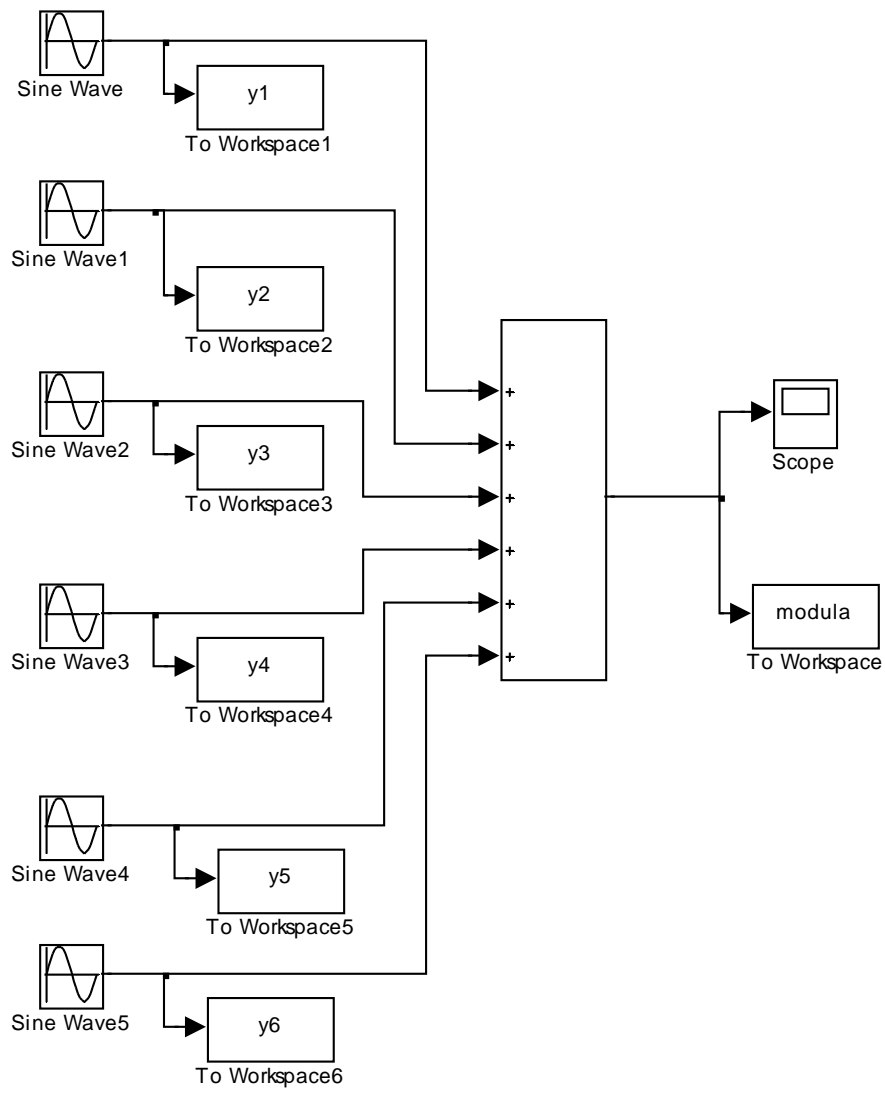


**Figure A. 8:** SIMULINK code of a schematic for the generation of a multi-sinusoidal signal.

Finally the MATLAB code that is used to call the SIMULIK code previously shown is as follows:

```
%sinusoidal signal generation code;
function [vector_digi,vector_modificado] = conv_sin_out_dig
(valor_max,valor_min,nombre_fichero_txt)
    sim('genera_seno_prfi')
    vector=modula; %"modula" are the output variables from simulink
    maximo=max(vector);%maximum range of the vector
    minimo=min(vector);%minimum range of the vector
    rango=maximo-minimo;
    rango_deseado=valor_max-valor_min;
    relacion_rango=rango/rango_deseado;
    continua=(valor_max + valor_min)/2;
    h = waitbar(0,'Digitalizando la señal...');
    for i=1:length(vector),
        vector_digi(i)=vector(i)/relacion_rango;
        vector_digi(i)=vector_digi(i)+continua;
        vector_modificado(i)=vector_digi(i);
        vector_digi(i)=256-(256*vector_digi(i)/10);
        vector_digi(i)=round(vector_digi(i));
        waitbar(i/(length(vector)),h)
    end
    close(h)
    dlmwrite(nombre_fichero_txt,vector_digi,'\n')%the file is saved in format ".txt"
```

Improving the performance of micro-machined metal oxide gas sensors:  
Optimization of the temperature modulation mode via pseudo-random sequences.

## A.5. References.

- [1] H.A. Barker, "Choice of pseudorandom binary signals for system identification", *Electron. Lett.*, vol. 3, pp 524-526, 1967.
- [2] D. Everett, "Periodic digital sequences with pseudonoise properties", *GEC Jnl. Sci. Technol.*, vol. 33, pp. 115-126, 1966.
- [3] K. Godfrey, "*Correlation methods, Automatica*", vol. 16, pp. 527-534, 1980.
- [4] K. Godfrey, "*Perturbation signals for system identification*", Prentice Hall, UK, 1993.
- [5] N. Zierler, "Linear recurring sequences", *J. Soc. Ind. Appl. Msth.* 7 (1959), 31-48, 1959.
- [6] R. Church, *Ann. Math.*, vol. 36, pp. 198-209